THE UNIVERSITY OF HULL

An investigation into the mechanisms of tissue factor-mediated apoptosis in endothelial cells

Thesis submitted to the University of Hull towards the degree of

Doctor of Philosophy

by

Azza Mostafa Elkeeb

June 2014

Abstract

Cells are known to express and release tissue factor (TF) following activation. In addition, endothelial cells are capable of acquiring TF carried by circulating microvesicles. Accumulation of TF in the endothelium contributes to chronic pathological conditions including cardiovascular disease. The aim of this study was to investigate the mechanisms that regulate the release of TF within microvesicles. In addition, the effects of accumulation of TF on the mediators of cell proliferation and apoptosis were examined and the underlying mechanisms explored. Throughout this study, endothelial cells were transfected to express TF or, alternatively, incubated with TF-containing microvesicles to permit accumulation of TF within cells. Activation of PAR2 receptor in TF-bearing cells resulted in prolonged activation of p38 which was enhanced by preventing the phosphorylation of Ser253 within the cytoplasmic domain of TF through Ala-substitution. Moreover, the inhibition of p38α resulted in decreased Ser258 phosphorylation and increased TF release as microvesicles. Expression of wild-type TF or Asp253-substituted TF induced cell proliferation via a mechanism that involves the up-regulation of Cyclin D1. In contrast, increased cellular apoptosis was observed in cells expressing Ala253-substituted TF, but only following cell activation. The level of p53 protein, p53-phosphorylation at Ser33, p53 nuclear localisation and transcriptional activity, but not p53 mRNA, were increased in cells expressing the wild-type and Ala253-substituted TF. These observations were reversed by inhibition of p38α using either SB202190 or siRNA-mediated suppression. The expression of bax and p21 mRNA and Bax protein was also increased in cells expressing Ala253-substituted TF, but not in cells expressing wild-type TF. Inhibition of transcriptional activity of p53 with pifthrin-α or inhibition of p38α suppressed the expression of bax. These data suggest that the activation of endothelial cells expressing TF prolongs p38α activation which in turn phosphorylates TF at Ser258 and terminates TF release within microvesicles. This leads to the accumulation of TF within cells and can induce cell apoptosis. The mechanism of apoptosis is mediated via the activation of p38α which in turn phosphorylates p53 at Ser33 and stabilises p53 within the nucleus. This study has shown a mechanism associating increases in circulating TF-containing microvesicles with endothelial depletion and the progression of vascular disease.

Acknowledgments

I would like to thank my supervisor Dr Camille Ettelaie for her supervision, support and encouragement during the course of my PhD. I would also like to thank Dr Mary Collier for her unconditional help and advice. I will always be grateful to you for your support. Many thanks to Clover for her help in flow cytometry. My special thanks go to my parents for their continuous support, encouragement and inspiration throughout my PhD. Your thoughts kept me strong and resolute in the achievement of my goals. I would like to thank my husband Mohamed whose support and encouragement has taught me to be relentless throughout the years of studying for a PhD. I am very thankful to all my friends especially, Sana and Nkichi for their support and believe in me. I also appreciate my children, Noor, Hashim, Anas and Mayar who were always by my side and have grown up to be wonderful and understanding in this time. They never complained when I had to spend countless hours to focus on my work. You all make this achievement worth the while. To Mayar especially, who was born in the second year of my studies, your gentle and loving demeanor was always a source of comfort to me.

Publications and presentations

Parts of this work have been published as:

Elkeeb A, Collier MEW, Ettelaie C. (2010) The activation of p38 MAPK by the phosphorylation of the cytoplasmic domain of TF. Presented at the Northern biology Group meeting. University of Hull, UK.

Ettelaie C, Elkeeb A, Maraveyas A, Collier MEW. (2012) p38α phosphorylates serine 258 within the cytoplasmic domain of tissue factor and prevents its incorporation into cell-derived microparticles. *Biochimica et Biophysica Acta Cell Research.* **1833** (3):613-621.

Ettelaie C, Elkeeb A, Maraveyas A, Collier MEW. (2013) The retention and release of tissue factor by endothelial cells results in the differential activation of p38-MAPK and influences the fate of the cells. Presented at congress of the international society on thrombosis and haemostasis. Amsterdam, The Netherlands.

ElKeeb A, Collier MEW, Maraveyas A, Ettelaie C. (2015) Accumulation of tissue factor in activated coronary artery endothelial cells causes cell apoptosis, mediated through p38 and p53 activation. *Thrombosis and Haemostasis.* 114

To my parents

Thank you for believing in me and making me what I am today

Table of Contents

Investigation of the mechanism of TF-mediated cellular apoptosis

List of figures

List of Tables

List of Symbols and Abbreviations

°C	Degrees centigrade
µ	Micro
%	Percentage
α	Alpha
β	Beta
γ	Gamma
δ	Theta
aa	Amino acid
ABP-280	Actin binding protein-280
Ala	Alanine
Apaf-1	Apoptotic protease activating factor-1
Asp	Aspartate
ATF2	Activating transcription factor
ATP	Adenosine triphosphate
Bax	Bcl-2 associated X protein
BCL-2	B-cell CLL/lymphoma 2
Bid	BH3 interacting domain death agonist
BSA	Bovine serum albumin
Ca^{+2}	Calcium
CHAPS	3-[(Cholamidopropyl)-dimethylammonio]-1-propanesulfonate
CHOP	C/EBP homologous protein
Ct	Threshold cycle
DAPI	4′,6-Diamidino-2-phenylindole dihydrochloride
DMEM	Dulbecco's modified Eagle's medium

DMSO	Dimethyl sulfoxide
DNA	Deoxyribonucleic acid
dNTP	Deoxynucleotide triphosphate
DTT	Dithiothreitol
EC	Endothelial cells
EDTA	Ethylenediaminetetraacetic acid
EGF	Epidermal growth factor
EGFP	Enhanced green fluorescent protein
ELISA	Enzyme-linked immunosorbent assay
ERK1/2	Extracellular signal-regulated kinases 1/2
FACS	Fluorescence-activated cell sorting
FCS	Foetal calf serum
FICT	Fluorescein isothiocynate
FVII	Factor VII
FVIIa	Activated Factor VII
FX	Factor X
FXa	Activated Factor X
g	Gram
g	Gravity
GAPDH	Glyceraldehyd-3-phosphate dehydrogenase
GFP	Green fluorescent protein
GTP	Guanosine-5'-triphosphate
Glu	Glutamine
H	Hour
HCAEC	Human coronary artery endothelial cells

HEPES	(4-(2-hydroxyethyl)-1-piperazineethanesulfonic acid
HRP	Horseradish peroxidase
IgG	Immunoglobulin G
IL	Interleukin
JNK	c-Jun N-Terminal Kinase
L	Litre
LB	Luria bertani medium
Log	Logarithm
M	Molar
m	Milli
MAPK	Mitogen-activated protein kinase
MAPKAPK	MAPK-activated protein kinase
MEK	Mitogen-activated protein kinase kinase
MDA	Melanoma differentiation associated
MDM2	Murine double minute 2
mRNA	Messenger ribonucleic acid
MVs	Microvesicles
NaCl	Sodium chloride
ng	Nanograms
NO	Nitric oxide
p	pico
p21	Protein 21
p38	Protein 38
p53	Protein 53
PAR	Protease activated receptor

PAR2-AP	Protease activated receptor2-agonist peptide
PBS	Phosphate buffered saline
PCR	Polymerase chain reaction
PD98059	ERK1/2 pathway inhibitor
PDK	Proline directed protein kinase
PKCα	Protein kinase Cα
PS	Phosphatidylserine
PT	Prothromin time
RNA	Ribonuclic acid
RNase	Ribonuclease
rpm	Revolutions per minute
RT-PCR	Reverse transcription-polymerase chain reaction
s	Second
SB202190	p38 inhibitor
SD	Standard deviation
SAPK	Stress-activated protein kinase
SDS-PAGE	Sodium dodecyl sulphate polyacrylamide gel electrophoresis
Ser	Serine
SSC	Saline Sodium Citrate
TAD1	Transactivating domain 1
TAD2	Transactivating domain 2
TBE	Tris borate-EDTA
TBST	Tris-buffered saline tween-20
TdT	Terminal deoxynucleotidyl Transferase
TEMED	N,N,N',N'-Tetramethylethylenediamine

TF	Tissue factor
TFPIs	Tissue factor pathway inhibitors
Thr	Threonine
TMP	3,3’,5,5’ Tetramethylbenzidine
TNF	Tumour necrosis factor
Tyr	Tyrosine
U	Unit
UV	Ultra violet
V	Volt
v/v	Volume to volume
w/v	Weight to volume

CHAPTER 1

GENERAL INTRODUCTION

1. General introduction

Elevated levels of tissue factor (TF) associated microvesicles originating from endothelial cells have been found in various disease states and may contribute to hypercoagulable states (Simak et al., 2006; Hussein et al., 2008; Jung et al., 2009; Sabatier et al., 2009). In addition to its role as the principal initiator of the coagulation, TF is known to be capable of initiating intracellular signalling pathways. It has been shown that signalling arising from TF is involved in various biological conditions such as inflammation (Cunningham et al., 1999), tumour angiogenesis, metastasis (Mueller & Ruf, 1998; Bromberg et al., 1995; Siegbahn, 2004) and progression of cardiovascular diseases (Taubman et al., 1997). This has moved the focus from whether or not TF induces thrombosis to the underlying mechanisms by which TF contributes to these biological conditions. Conceivably, the answer to this question will be of the greatest therapeutic value.

1.1. Tissue factor

1.1.1. The role of TF in haemostasis and coagulation

TF has a principal role in haemostasis as the main initiator of extrinsic blood coagulation cascade. The coagulation cascade is composed of two separate pathways: intrinsic and extrinsic pathways which lead to the activation of a common pathway (Fig 1.1). Activation of the intrinsic pathway by exposure to a negatively charged surface such as collagen leads to factor X activation by FIXa in the presence of FVIIIa. The extrinsic pathway is activated upon disruption of the endothelial barrier which allows the binding of circulating coagulation factor VII (FVII) to the extracellular domain of TF. This results in the activation of FVII to FVIIa. This TF:FVIIa complex is capable of activating both circulating factor IX (FIX) and factor X (FX).

Figure 1.1. Coagulation cascade pathways

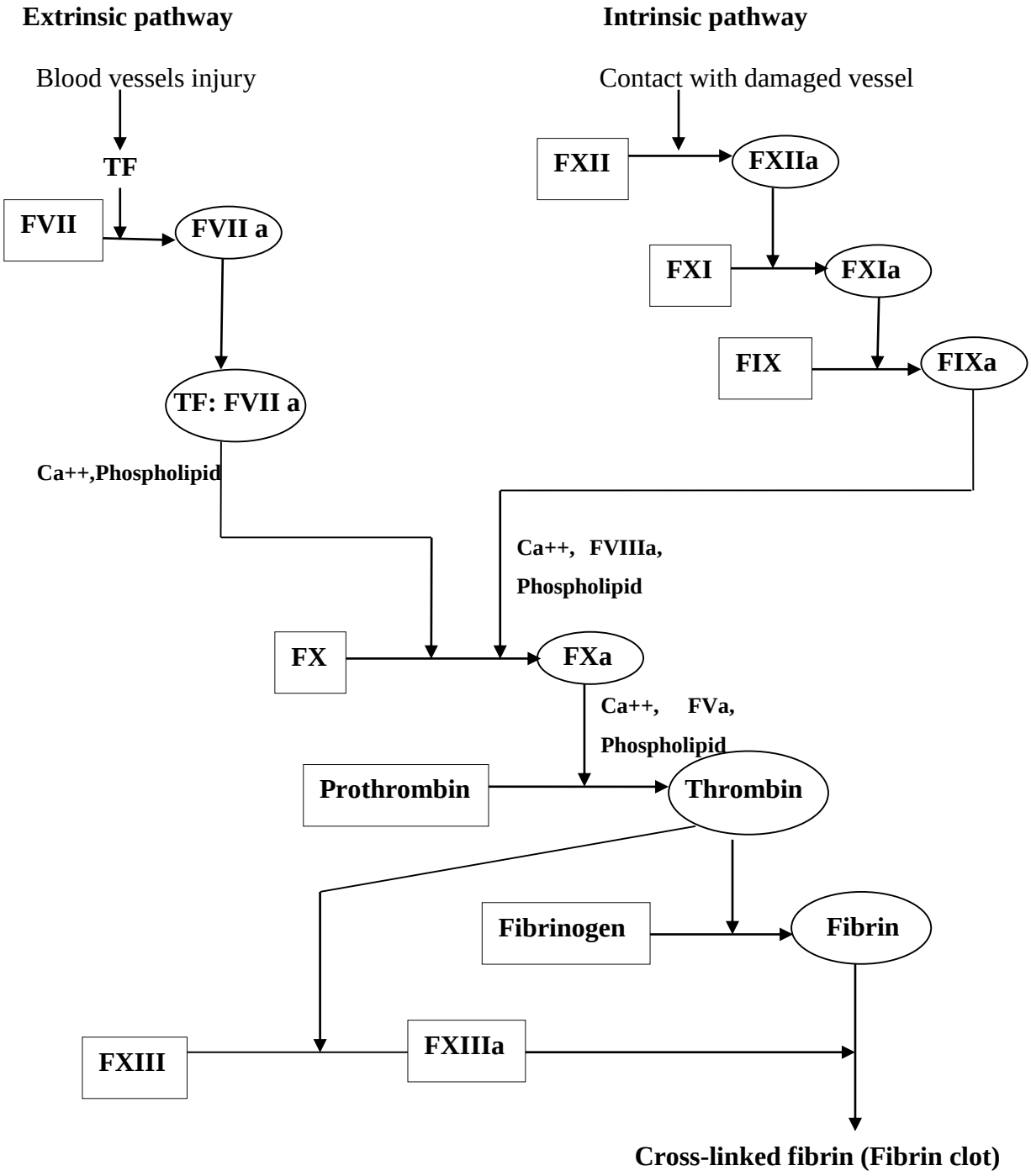

The coagulation cascade is composed of two separate pathways (extrinsic and intrinsic). Tissue factor (TF) and FVIIa represent the extrinsic pathway. FXIIa, FXIa, FIXa, and FVIIIa are members of the intrinsic pathway. Both pathways lead to the activation of FXa and the common pathway ultimately results in the formation of a fibrin clot. (Adapted from Mackman, 2009)

Generation of FXa promotes proteolytic conversion of prothrombin to thrombin. As a result, thrombin digests fibrinogen to fibrin monomers that polymerise to produce the fibrin clot (Fig 1.1). Usually, the cell surface TF exhibits a low procoagulant activity. To become procoagulantly active, TF requires the presence of negatively charged phospholipids on the outer side of the cell membrane (Paborsky et al., 1991).

TF is constitutively expressed in the intima and adventitia of the vascular wall and other extra-vascular cells, forming a haemostatic envelope which is separated from the bloodstream by the vascular endothelium. Generally circulating blood cells and vascular endothelial cells do not constitutively express TF under normal physiological conditions (Drake et al., 1989), although TF can be expressed by these cells when stimulated by cytokines or inflammatory mediators (Nawroth & Stern, 1986; Noguchi et al., 1989; Parry & Mackman, 1995; Mackman, 1996; Mechtcheriakova et al., 2001; Funderburg et al., 2010). The expression of TF is mediated by the activation of intracellular signalling kinases (ERK1/2 and p38) (Lopez-Pedrera et al., 2006; Oku et al., 2013).

1.1.2. Tissue factor structure and biochemistry

Tissue factor (TF), also known as coagulation factor III, thromboplastin or CD142, is a 47 kDa transmembrane glycoprotein and a member of the cytokine-receptor superfamily. The human TF molecule is a single chain that consists of 263 amino acids arranged in three domains: 219-amino-acid extracellular, 23-amino-acid transmembrane segment and a 21-amino-acid cytoplasmic tail (Morrissey et al., 1987) (Fig 1.2). TF is known to show a large degree of structural similarity to the proteins of the class II cytokine receptor family, particularly the interferon γ receptor (Bazan, 1990).

Figure 1.2. Schematic representation of the TF structural domains

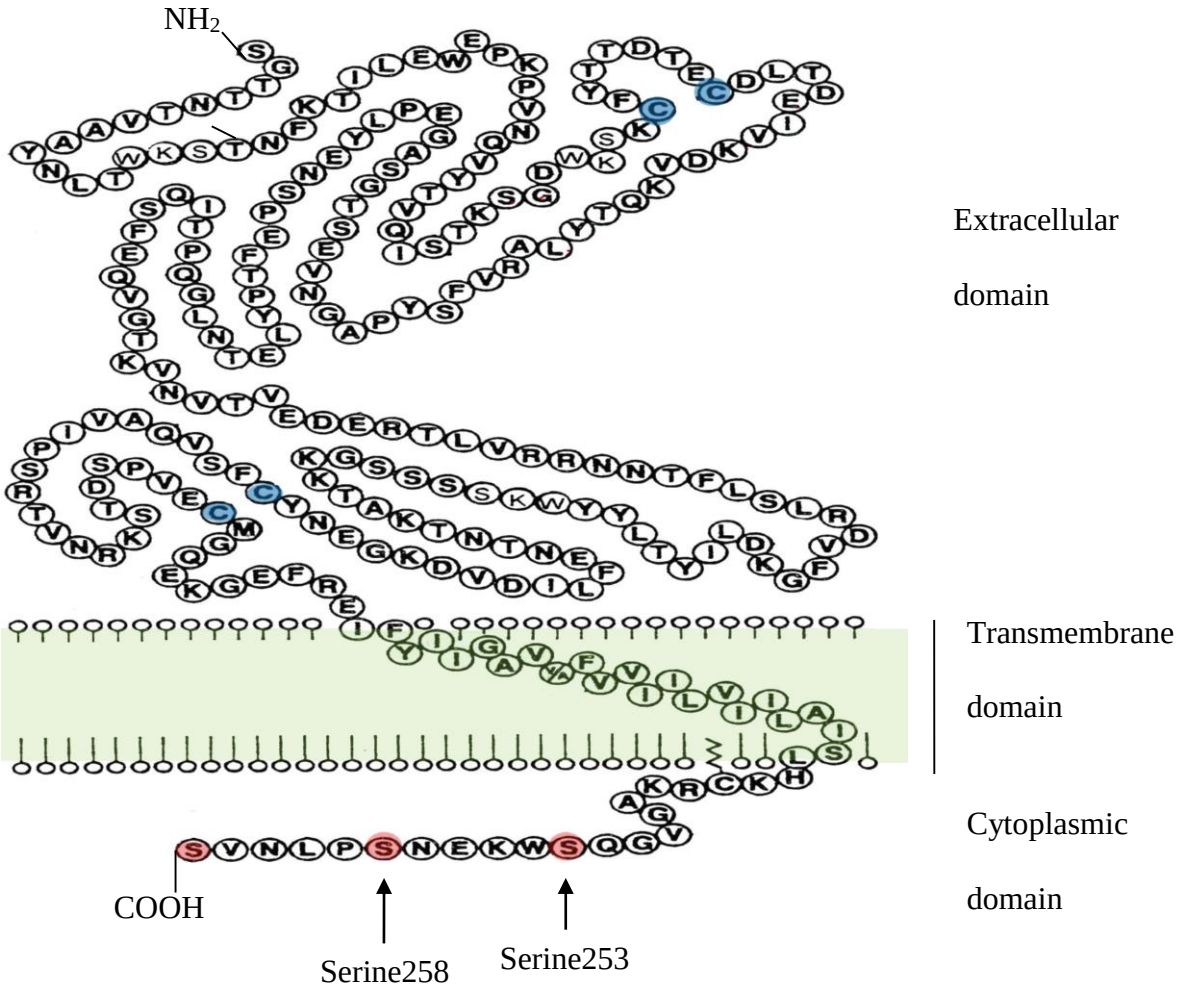

TF is a membrane-bound glycoprotein single polypeptide chain that consists of a large extracellular domain, a transmembrane and a short cytoplasmic domain. There are two disulfide bonds (Cys49-Cys57 and Cys186-Cys209 shown in blue) in the extracellular domain. There are three serine residues (Ser253, Ser258 and Ser263 shown in red) in the cytoplasmic domain for undergoing phosphorylation. (Adapted and modified from Chu, 2011)

The extracellular domain of TF contains the factor VII/activated factor VII (FVIIa) binding site. The transmembrane domain plays a crucial role in anchoring the TF-FVIIa complex to the cell surface and also in the procoagulant activity of TF. In contrast to other cytokine receptors, TF has a short C-terminal cytoplasmic domain (Bazan, 1990). However, this domain contains two serines residues (Ser253 and Ser258) as potential phosphorylation sites (Zionchek et al., 1992).

In healthy individuals, TF is present in plasma at low levels (Albrecht et al., 1996). Aberrant expression of TF triggers intravascular thrombosis associated with various diseases, such as atherosclerosis and cancer and contributes to thrombosis associated with these diseases (Annex et al., 1995; Tremoli et al., 1999; Rickles et al., 2003). TF is found in circulation located on blood cells, platelets and as microvesicles (Muller et al., 2003; Butenas et al., 2005). In addition to full-length TF, an alternative spliced form of TF has been detected, although its coagulation activity remains undetermined (Bogdanov et al., 2003).

1.1.3. Non-haemostatic function of TF

TF is well known as the principal initiator of blood coagulation. However, TF has been shown to function as a cell signalling receptor. TF signalling has been involved in a number of physiological processes including angiogenesis (Abe et al., 1999; Pyo et al., 2004), cell migration (Siegbahn et al., 2005; Aberg & Siegbahn, 2013), and wound healing (Chen et al., 2005). Furthermore, signalling arising from TF has been implicated in pathological conditions such as inflammation (Ahamed et al., 2007), tumour metastasis (Mueller & Ruf, 1998; Bromberg et al., 1995) and progression of cardiovascular diseases (Taubman et al., 1997). These signalling mechanisms are mediated either by TF itself through its cytoplasmic domain (Ruf, 1999), or by TF-FVIIa complex through the activation of PAR1 and 2 (Hjortoe

et al., 2004). The activation of PAR2 by the TF:FVIIa complex and FXa has been shown to result in the induction of MAPK signalling pathways (Morris et al., 2006; Jiang et al., 2004) and to induce the expression of proinflammatory cytokines and growth factors (Hjortoe et al., 2004; Morris et al., 2006). In addition, the cytoplasmic domain of TF can control TF release into the bloodstream as microvesicles. One mediator of TF-microvesicle release involves the cellular signalling arising from the proteolytic activation of PAR2 (Burnier et al., 2009).

1.2. Endothelial cells

Endothelial cells form a single layer of cells, lining the blood vessels and separating blood from tissue (Galley & Webster, 2004). Endothelial cells regulate many processes including haemostasis, angiogenesis, inflammation and others. However, the main functions of endothelial cells are to maintain vessel tone and anticoagulant properties of the vessels. Endothelial cells contribute to the regulation of blood pressure and blood flow by releasing vasodilators such as nitric oxide and prostacyclin, as well as vasoconstrictors, including endothelin and platelet-activating factor. Under physiological conditions, the endothelium inhibits coagulation by synthesising and displaying anti-thrombogenic substances including TFPI, heparan sulphate proteoglycans and nitric oxide. These in turn prevent platelet adhesion and clot formation (Michiels, 2003). The activation of endothelial cells is induced by various agents including inflammatory cytokines (Bevilacqua et al., 1986; Combes et al., 1999). The endothelial cells respond to these agents by up-regulating the expression of various pro-inflammatory and pro-coagulant receptors and molecules (Mantovani & Dejana, 1989; Mesri et al., 1999). However, under pathological conditions endothelial cells are stimulated to express TF on the surface of the cells as well as release TF within microvesicles (Morel et al., 2004). TF-bearing microvesicles are capable of activating the

coagulation mechanism, resulting in the precipitation of a hypercoagulable state and an increased tendency to thrombosis (Morrissey, 2001). Endothelial cells express TF in response to cytokines such as tumor necrosis factor (TNF-α) (Steffel et al., 2005) and, interleukin 1β (Napoleone et al., 1997) or through the proteolytic activity of thrombin (Archipoff et al., 1991; Eto et al., 2002). Up-regulation of TF expression by endothelial cells has been found to be mediated by the activation of the MAPK p38, ERK and protein kinase C (PKC) (Mechtcheriakova et al., 2001). Therefore, the expression and release TF within microvesicles may be an indicator and mediator of disease condition.

1.3. Microvesicles

Microvesicles are small vesicles of less than 1 μm in diameter that are released from the plasma membrane of almost all types of cells upon stimulation and during apoptosis (Scholz et al., 2002; Jimenez et al., 2003). Microvesicles differ in number, size and antigenic composition depending on cellular origin. The procoagulant activity of microvesicles mainly arises from the presence of TF (Morel et al., 2004) (Fig 1.3). Circulating microvesicles have been detected at low levels in the blood of healthy individuals (Berckmans et al., 2001). However, elevated levels of microvesicles in various diseases including cardiovascular disease, sepsis and inflammation indicate their diagnostic potential (Morel et al., 2004; Morel et al., 2008; Amabile et al., 2011; Rautou et al., 2011; Habersberger et al., 2012). Microvesicles may be released from endothelial cells, platelets (Schloz et al., 2002), leukocytes (Rauch et al., 2000) and cancer

Figure 1.3. Cell membrane microvesicles

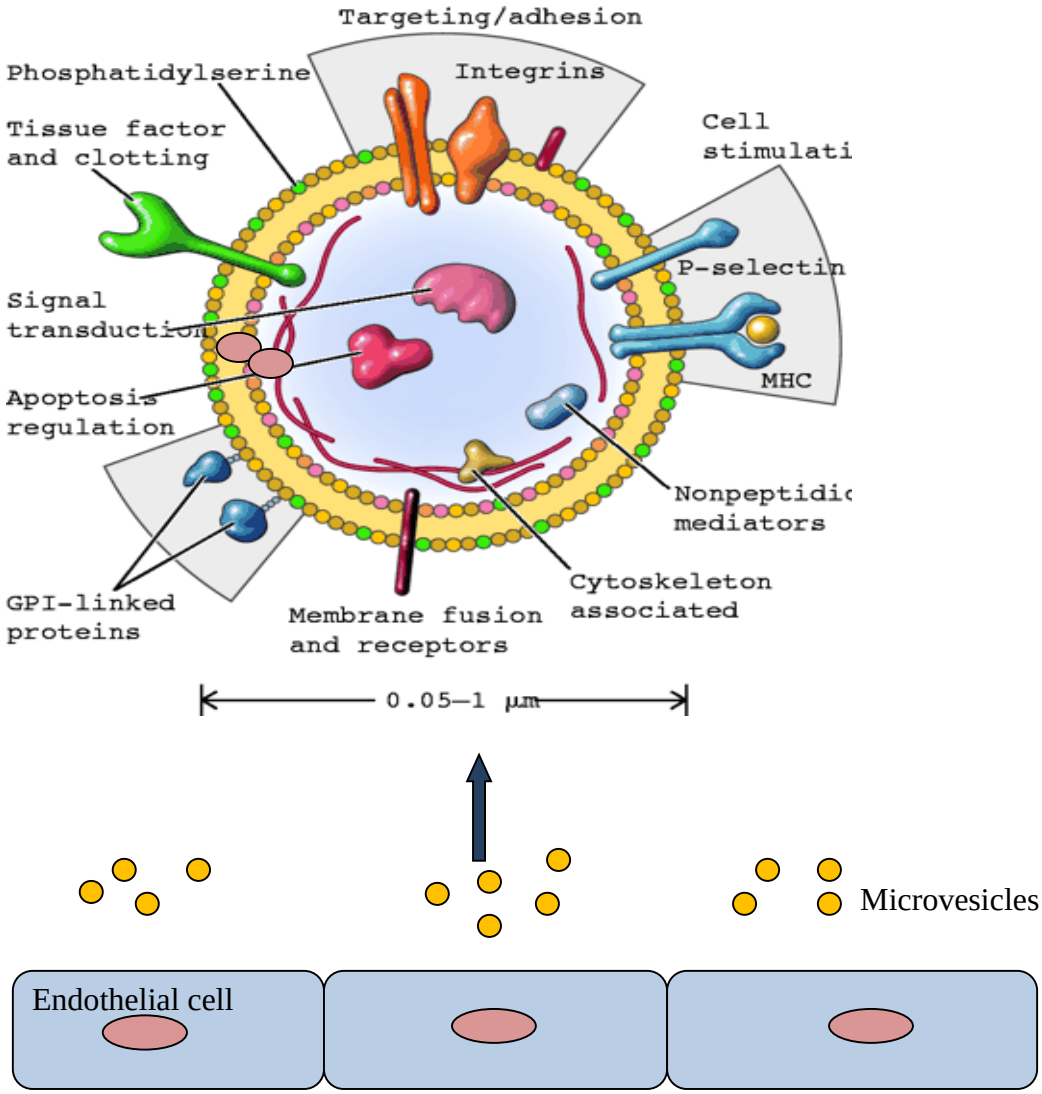

Membrane microvesicles are shed from the plasma membrane of stimulated cells. They are composed of a phospholipid bilayer and contain proteins, such as adhesion proteins derived from the activated cells, and tissue factor (TF). (Adapted from Hugel et al., 2005)

cells (Yu & Rak, 2004). Circulating microvesicles display a variety of activities. For example, they support cell-to-cell communication, transfer antigens and receptors to remote cells, and induce cell signals leading to vascular inflammation, endothelial dysfunction, leukocyte adhesion and thrombosis (Mesri et al., 1999; Mack et al., 2000; Deregibus et al., 2007). Endothelial cells release microvesicles in response to a variety of stimuli including cytokines such as tumour necrosis factor-α (TNF-α) and interleukin-1β (IL-1β) (Schecter et al., 2004; Shet, 2008; Peterson et al., 2008) and protease activated receptor (PAR2) (Vergnolle et al., 1999, Riewald & Ruf, 2003; Coughlin & Camerer, 2003). Specifically, high levels of circulating endothelial-derived microvesicles have been associated with many human diseases, particularly cardiovascular diseases (Simak et al., 2006; Jung et al., 2009; Sabatier et al., 2009).

1.3.1. Microvesicles formation

The cell membrane is characterised by its phospholipid asymmetry. Phosphatidylcholine and sphingomyelin are situated on the external membrane layer, whereas phosphatidylserine (PS) and phosphatidyl-ethanolamine are located on the inner side of the cell membrane. This asymmetry is maintained through the action of at least three lipid transporters (flippase, floppase, and scramblase). Flippase is an ATP-dependant enzyme that transports aminophospholipids from the outer to inner leaflet of the membrane. Floppase replaces some of these changed phospholipids to the outer layer. Scramblase is a non-specific transporter that permits the redistribution of the membrane lipids in a Ca^{2+}-dependent manner. However, this balance is disrupted once the cell is activated. This causes the exposure of negatively charged PS on the outer cell membrane surface

(Zwaal & Bevers, 1997). Cell activation or apoptosis also drives the budding of the cell membrane and microvesicle release. This is associated with changes in phospholipid asymmetry, cytoskeleton disruption, and increased cytosolic calcium (Fig 1.4).

1.4. Mitogen-activated protein kinases (MAPK) pathways

Eukaryotic cells respond to extracellular stimulation through a number of different intracellular signal transduction mechanisms. Protein kinases are key regulators in signal transduction and serve to orchestrate the activity of almost all cellular processes. The kinases direct the activity and overall function of many proteins by adding phosphate groups to specific amino acids, usually serine or threonine residues within the target protein substrate (Pearson et al., 2001).

Mitogen-activated protein kinases (MAPK) pathways are a family of conserved kinase cascades that are activated in response to various mitogens, stress factors and developmental signals. The MAPK signal transduction involves a cascade–like mechanism that forms a highly integrated network required for promoting important cellular functions including proliferation, differentiation and apoptosis (Kyriakis & Avruch, 2001). MAPK proteins are expressed in all cell types and have the same general structure, which consists of approximately 250 amino acids (Hanks & Hunter, 1995). Currently four MAPK pathways have been characterised and include more than 20 MAPK protein isoforms. These pathways include the extracellular-signal regulated kinase 1/2 (ERK1/2), c-Jun amino terminal kinase (JNK) (also known as stress- activated protein kinase 1 (SAPK1)); and p38 MAPK (Imajo et al., 2006; Cuevas & Rousseau,

Figure 1.4. Proposed mechanisms of microvesicle formation

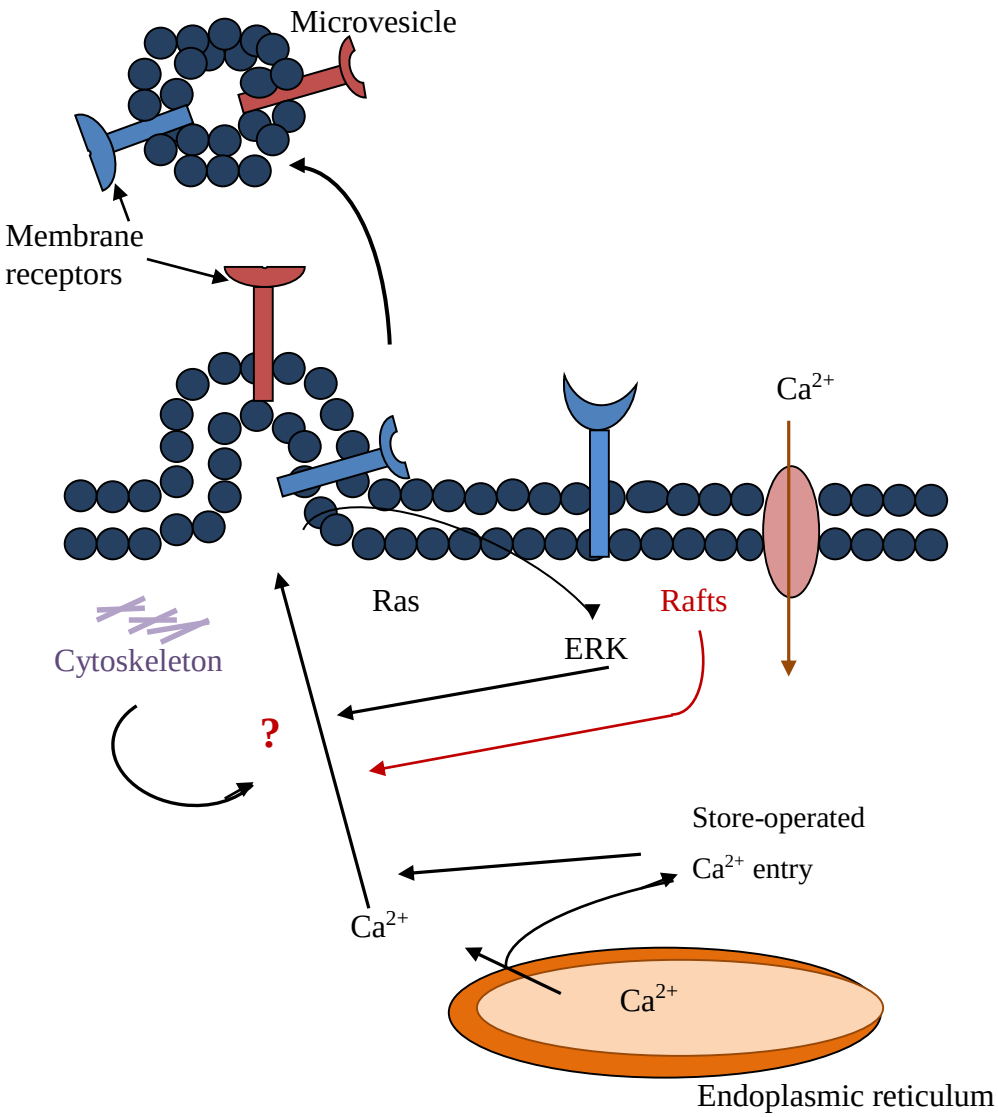

Signalling mechanisms alter the cytoskeleton conformation resulting in the budding of the membrane. Subsequently, microvesicles are formed by outward budding of the plasma membrane. (Adapted and modified from Freyssinet, 2003)

2007) (Fig 1.5). In addition, other less well characterised MAPK pathways such as the extracellular-regulated kinase 5 pathway (ERK5) have been suggested (Lee et al., 1995).

MAPK pathways are composed of at least three levels of protein kinases, which are phosphorylated in a canonical manner. The three levels are referred to as MAPK kinase kinase such as MEKK, MAPK kinase such as MEK or MKK, and MAPK such as ERK, JNK and p38 (Fig 1.5). MAPK pathways are activated by tyrosine kinases receptors and some G-protein coupled receptors (e.g. PAR2) (Lowes & Wong, 2002; Wang et al., 2006). Activation of MAPK requires phosphorylation on both Thr and Tyr residues by upstream kinases. Once activated, MAPK enzymes phosphorylate target substrates on specific Ser and Thr residues that are immediately followed by Proline (Pro). MAPK enzymes phosphorylate a variety of substrates which are localised either in the cytoplasm or in the nucleus. These substrates include transcription factors, translational regulators, MAPK-activated protein kinases (MAPKAP kinases), and phosphatases. These lead to gene expression, regulation of metabolism, cell cycle progression and cytoskeletal rearrangement in response to different extracellular stimuli.

The specific cellular outcome of MAPK activity depends on the intensity and duration of the activation. For example, strong activation of p38 can induce apoptosis, whereas lower p38 activation tends to be associated with cell survival (Dolado & Nebreda, 2008; Tormos et al., 2013). This explains the varied cellular outcomes of MAPK activation observed such as proliferation, apoptosis, differentiation and migration.

Figure 1.5. MAPK pathway

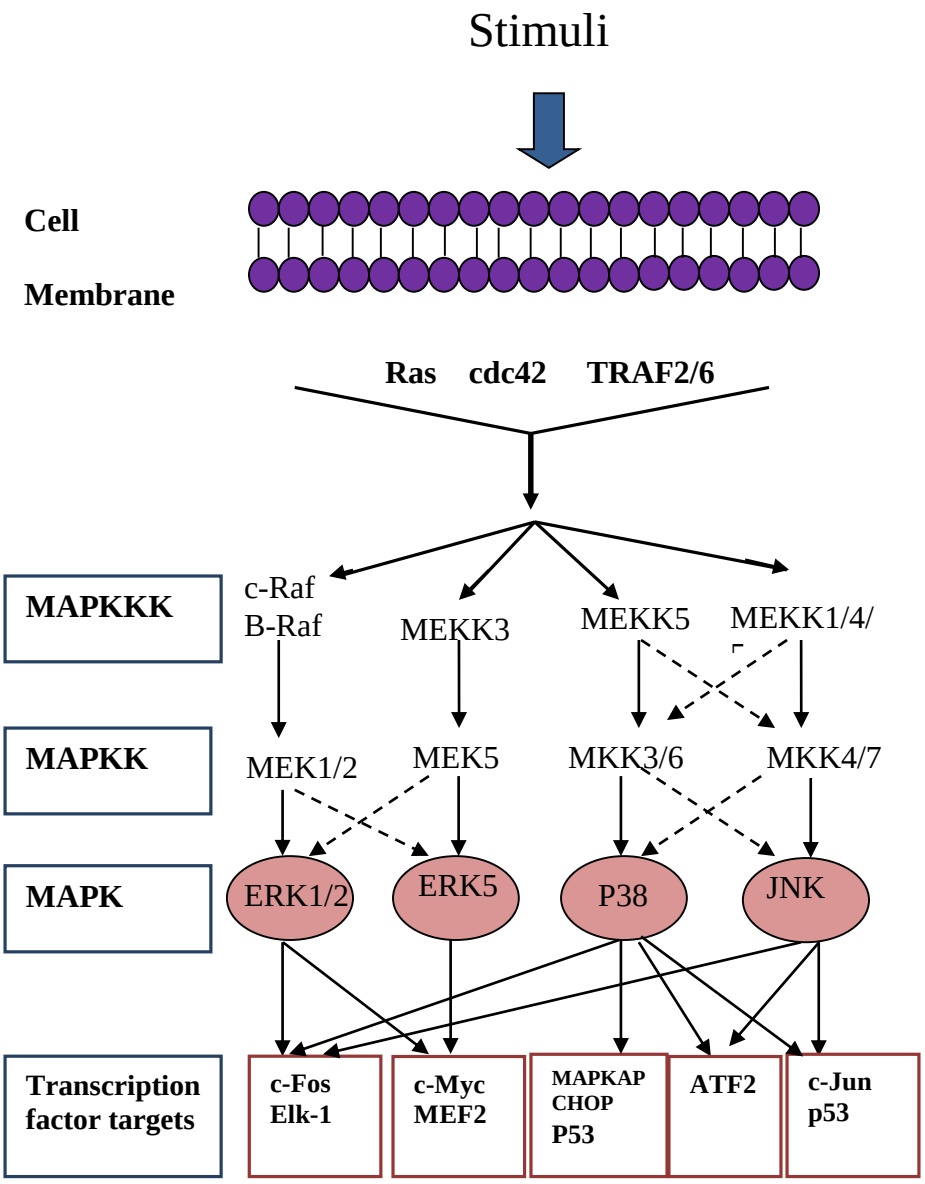

Four major MAPK pathways have been identified, including the extracellular signal-regulated kinase 1/2 (ERK1/2), ERK5 (BMK1), p38 MAPK, and c-Jun amino terminal kinase (JNK). Each MAPK pathway is composed of at least three main tiers, including MAPKKK, MAPKK, and MAPK. Each signalling cascade can be induced by sets of stimuli, such as stress, growth factors and cytokines. Following activation, site-specific phosphorylation of Ser, Thr, or Tyr residues on kinases at each tier results in signal amplification. This leads to the phosphorylation of transcription factors or other kinases that have direct roles in mediating cell proliferation, differentiation, apoptosis, and transcription. (Adapted and modified from Junttila & Westermarck, 2008)

1.4.1. The ERK 1/2 pathway

Extracellular signal-regulated kinases (ERK1/2), also known as p44/p42 (Shaul & Seger, 2007), are proline-directed Ser/Thr kinases (Tanoue et al., 2000). ERK2 represents the predominant form and is found in most cells (Behn-Krappa & Newton, 1999). The ERK1/2 pathway is strongly activated by growth factors and serum although osmotic stress and cytokines can also activate this pathway (Chen et al., 2001; Meloche & Pouyssegur, 2007). The ERK1/2 pathway has been implicated as a key regulator of cell proliferation and survival. ERK1 and ERK2 proteins share 70 % structural homology, with > 90 % homology in the kinase domains (Bolton et al., 1991). Activation of the ERK1/2 pathway is initiated through receptor-mediated activation of the small G-protein, Ras. Ras is activated through recruitment of SOS protein (son of sevenless), which is responsible for GDP/GTP exchange. Active Ras recruits and activates Raf kinases which consequently phosphorylate MEK1 and MEK2 dual-specificity kinases, which in turn phosphorylate ERK1/2 within a conserved Thr-Glu-Tyr (TEY) motif in their activation loop (Payne et al., 1991). Inactivation of ERK1/2 is mediated by phosphatases, including Ser/Thr protein phosphatase 2A (PP2A) (Alessi et al., 1995), Tyr phosphatase and dual-specificity phosphatases known as MAPK phosphatases (MKPs) (Sun et al., 1993). However, a study has shown that the amplitude and duration of signal propagation through the ERK1/2 pathway are controlled by Raf dephosphorylation as well as MEK1/2 phosphorylation and dephosphorylation (Hornberg et al., 2005). Upon activation, ERK1/2 phosphorylate numerous substrates in various cellular compartments, including cytoplasm, and nuclear substrates (e.g. SRC-1, Pax6, NF-AT, KlK-1, MEF2, c-Fos, cmyc, and STAT3) as well as cytoskeletal proteins (e.g. neurofilaments and paxillin) (Chen et al., 2001). Up-regulation of the ERK pathway has been shown in a relatively large number of tumours; therefore, the ERK pathway represents an attractive target for anti-cancer therapy (Montagut & Settleman, 2009). In addition, it has

been shown that the activation of ERK1/2 by exogenous lipidated TF increases endothelial cells proliferation (Collier & Ettelaie, 2010). This finding indicates that TF is capable of regulating MAPK signals.

1.4.2. The p38 MAP kinase signal transduction pathway

The p38 MAPK pathway is activated by a number of stimuli, including proinflammatory mediators such as tumour necrosis factor (TNF), interleukin-1β (IL-1β), lipopolysaccharide (LPS), and environmental stress including oxidative stress, UV irradiation and hypoxia (Chen et al., 2001). This pathway is composed of four p38 isoforms, p38α (Rouse et al., 1994), p38β (Jiang et al., 1996), p38γ (ERK6/SAPK3) (Lechner et al., 1996; Cuenda & Dorow, 1998), and p38δ (SAPK4) (Jiang et al., 1997). The p38 isoforms share 60 % of their amino acids structure but they are encoded by separate genes and have different tissue expression patterns. It has been found that p38α is expressed at significant levels in most cell types, whereas p38β is expressed mainly in the brain, p38γ is found in skeletal muscle and p38δ is detected in endocrine glands (Cuenda & Rousseau, 2007). The four isoforms also differ in their susceptibility to chemical inhibitors; for example, pyridinyl imidazoles can inhibit p38α and p38β but have no inhibitory effect on p38γ and p38δ (Cohen, 1997). All p38 isoforms are activated by upstream kinase MEK6 while MEK3 phosphorylates the p38α and p38β isoforms only. The activation of p38 is mediated through GTP-binding proteins such as Rac1, Rho and Rit (Zhang et al., 1995; Marinissen et al., 2001; Sakabe et al., 2002). Phospho-p38 activates transcription factors such as p53 (Bulavin & Fornace, 2004), ATF2, and CHOP, as well as other nuclear proteins (Zhu & Lobie, 2000). Consequently p38 regulates cellular responses including apoptosis and cell differentiation (Ono & Han, 2000). Furthermore, a number of studies have shown that the p38 pathway is capable of suppressing cell proliferation by inhibiting the ERK pathway (Aguirre-Ghiso et

al., 2003; Efimova et al., 2003; Junttila & Westermarck, 2008). p38 signalling is involved in promotion of inflammation by inducing the production of proinflammatory cytokines such as TNFα, IL-1 (Guan et al., 1998). This process is in turn regulated by several mechanisms that control the phosphorylation and dephosphorylation of the residues within the activation-loop of the p38 protein (Lee et al., 2003). Activation of p38 can induce the phosphorylation and transcription of a number of genes that control apoptosis. The tumour suppressor protein p53 is an important target for p38, which phosphorylates p53 protein at various sites including Ser33 (Kishi et al., 2001) and Ser46 (Sanchez-Prieto et al., 2000) in response to cellular stress (Appella & Anderson, 2001). Although a large number of *in vitro* studies have focused on the role of p38 MAPK in endothelial cell apoptosis (Grethe et al., 2004), anti-apoptotic functions of the p38 pathway have also been reported (Zechner et al., 1998; Park et al., 2002). Therefore, the final outcome of p38 activation may depend on other signalling mechanisms, the strength of the stimulus and duration of the signals (Cuadrado & Nebreda, 2010; Tormos et al., 2013). The p38 pathway is a mediator of enhanced cell migration initiated by the phosphorylation of the cytoplasmic domain of TF and the activation of GTPase Rac1 (Ott et al., 2005).

1.5. Protease-activated receptor 2

Protease-activated receptor 2 **(**PAR2) is a member of the G protein-coupled receptors family which includes PAR1-4. PAR2 acts as cell-surface mediators for extracellular proteases including trypsin and coagulation factor Xa (Riewald & Ruf, 2001; Camerer et al., 2000). Cell signalling through PAR2 is involved in diverse cellular processes, particularly during inflammation (Rothmeier & Ruf, 2012). Both TF and PAR2 expression are up-regulated during inflammatory response by endothelial cells (Nystedt et al., 1996). PAR2 signalling has been shown to induce the phosphorylation of the cytoplasmic domain of TF (Ahamed

& Ruf, 2004). Moreover, PAR2 activation initiates the activation of ERK1/2 and p38 (Kanke et al., 2001). The activation of PAR2 by proteases including trypsin and coagulation factor Xa leads to translocation of PKCα to the plasma membrane (Ahamed & Ruf, 2004). Recruitment of PKCα to the plasma membrane is thought to be involved in the release of microvesicles from the cell surface (Pilzer et al., 2005). PKCα also induces TF release by phosphorylating Ser253 within the cytoplasmic domain of TF (Collier & Ettelaie, 2011). Phosphorylation of Ser253 in turn enhances the subsequent Ser258 phosphorylation within TF (Dorfleutner & Ruf, 2003), which acts to terminate TF release (Collier & Ettelaie 2011). In addition, mutagenic alterations of Ser253 and Ser258 have shown the involvement of these serine residues in TF release (Collier & Ettelaie, 2011).

1.6. Aims

Increased expression and accumulation of TF in the endothelial cells contributes to chronic pathological conditions including cardiovascular disease. The aim of this investigation was to examine the mechanism that prevents the release of TF within microvesicles and leads to the accumulation of TF in the cell. This study investigates the role of accumulation of TF on coronary artery endothelial cells proliferation and apoptosis. An understanding of the mechanisms involved in endothelial cell apoptosis may help to elucidate the mechanism of the loss of endothelial cells and the progression of chronic disease. The main objectives of the study were as follows.

- To investigate the role of TF in the phosphorylation of MAPK proteins ERK1/2 and p38
- To identify the MAPK isoforms responsible for the phosphorylation of the cytoplasmic domain of TF and induction of termination of its release within microvesicles

- To investigate the influence of TF-mediated p38 phosphorylation on endothelial cell proliferation and apoptosis
- To investigate the mechanism of TF-mediated apoptosis and to examine the involvement of p53 in TF-mediated pro-apoptotic signalling

CHAPTER 2

MATERIALS AND METHODS

2.1. Materials

Abcam, Cambridge, UK

Mouse monoclonal anti-human ATF-2 (phospho T69-T71) HRP-conjugated antibody
Rabbit polyclonal anti-phospho-serine HRP-conjugated antibody
Rabbit anti-human tissue factor (phospho-S290) antibody

Active Motife, Rixensart, Belgium

Nuclear extraction kit
Phosphatase inhibitor solution
Crystal violet solution

Affinity Biologicals, Epsom, Surrey, UK

Sheep anti-human TF capture antibody
HRP-conjugated goat anti-human TF detecting antibody

Agilent Technologies, Wokingham, UK

Pathdetect p53-Luc *cis*-reporting plasmid

American diagnostic inc, Stamford, USA

Recombined human TF (non-lipidated)

AMS Biotechnology Limited, Abingdon, UK

HT Titer TACs ™ apoptosis assay kit

BACHEM, Bubendorf, Switzerland

Tumour necrosis factor-α (human)

BD Biosciences, Oxford, UK

Becton Dickinson FACSCalibur flow cytometer

CellQuest software version 3.3.

Falcon FACS tubes

pCMV-EGFP vector

BDH, Poole, UK

EDTA

Glycerol

Magnesium chloride

Sodium acetate

Sodium dodecyl sulphate (SDS)

Sodium hydroxide

Sodium carbonate anhydrous

Berthold Technologies Ltd, Redbourn, UK

Junior LB9509 luminometer

BioLegend, Cambridge, UK

Rabbit polyclonal anti-human CHOP antibody

Bioline Ltd, London, UK

Molecular grade agarose

Bio-Rad, Hemel Hempstead, Hertfordshire, UK

iCycler real-time thermal cycle

Nitrocellulose membrane

BMG lab Tech, Offenburg, Germany

POLAR star OPTIMA Plate reader

Calbiochem, Heidelberg, Germany

CHAPS (3-Cholamidopropyl-dimethylammonio-propane-sulfonate)

Carl Zeiss Ltd, Welwyn Garden City, UK

Zeiss LSM 710 confocal microscope

ZEN software

Dade Behring, Liederbach, Germany

Innovin recombinant human tissue factor reagent

Cell signalling technologies, Leiden, The Netherlands

Rabbit anti-human phospho-ERK1/2 antibody

Rabbit anti-human ERK1/2 antibody

Mouse monoclonal anti-human phospho-p38 antibody (28B10)

Rabbit anti-human p38 antibody

Eurofins MWG, Ebersberg, Germany

Bax-primers, β-actin primers, Cyclin D1 primers, p21 primers, p53 primers

Fisher Scientific, Leicestershire, UK

GeneRuler 1 kb DNA Ladder

Fisher scientific, Loughborough, Leicestershire, UK

Glycine

NaCl

Tris base

Flowgen Bioscience, Nottingham, UK

Horizontal electrophoresis tank

ProtoFlowGel (acrylamide: bisacrylamid)

ProtoFlowGel resolving buffer
ProtoFlowGel staking buffer

FMC corporation, Philadelphia, USA

SYBR Green I DNA stain

GeneTex, CA, USA

Rabbit anti-human GAPDH antibody

Greiner bio-one, Gloucestershire, UK

12-well culture plates, 24-well culture plates, 25 and 75 cm^2 tissue culture flasks

Hoefer, Inc, San Francisco, USA

TE 50X protein transfer tank

http://imagej.nih.gov/ij/

ImageJ program

http://www.ncbi.nlm.nih.gov/tools/primer-blast/

Base pair program

Hyphen BioMed/Quadratech Ltd, Epson, UK

Zymuphen microvesicle determination kit
Thrombin chromogenic substrate CS 01 (81)

Ibidi, Thistle Scientific, Glasgow, UK

µ-Dish 35 mm, high glass bottom

Insight Biotechnology, Middlesex, UK

Phospho-p53 (Ser33) polyclonal rabbit antibody

LGC-ATCC, Teddington, UK

MDA-MB-231 breast cancer cell line

Life Technology, Paisley, UK

Endothelial cell serum-free medium

Lipofectin reagent

Lipofectamine

HEPES buffer

Lonza, Basel, Switzerland

DMEM medium

Media Cybernetics, Bethesda, USA

Image-Pro plus version 5.1.2.

Milteny Biotech, Bisley, UK

Colloidal super-paramagnetic microbeads

MACS µ-column

Magnetic MACS separator

New England Biolabs, Hertfordshire, UK

Cyclin D1 mouse anti-human antibody (DCS6)

Mouse IgG antibody Isotype control

Rabbit anti-human phospho-p53 (Ser46) antibody

Novus Biologicals, Cambridge, UK

Mouse monoclonal anti-human CHOP/GADD153 antibody (9C8)

OriGene, Rockville, USA

pCMV-XL5-TF

Promega Corporation, Southampton, UK

DeadEnd fluorimetric TUNEL assay
GoTaq 1-Step RT-qPCR system
Luciferase assay substrate (Luciferine)
Luciferase cell culture lysis reagent (5X)
TMB stabilised substrate for horse radish peroxidase
Tris-borate EDTA (TBE) buffer (10X)
Western Blue stabilised substrate for alkaline phosphatase
Wizard Midipreps DNA purification system

PromoCell, Heidelberg, Germany

Accutase solution
Endothelial cell growth medium (MV2)
Endothelial cell growth supplement pack
Foetal calf serum (FCS)
Human coronary artery endothelial cells (HCAEC)

R & D Sytem, Abingdon, UK

Donkey anti-rabbit IgG-NL637 NorthernLights
Escherichia coli TB-1 strain
Pifithrin-α hydromide

Santa Cruz Biotechnology, Heidelberg, Germany

Control siRNA

Control siRNA (FITC Conjugate)

Goat anti-human GAPDH

Goat anti-mouse alkaline phosphatase-conjugated antibody

Goat anti-mouse horseradish peroxidase-conjugate antibody

Goat anti-rabbit alkaline phosphatase-conjugated antibody

Goat anti-rabbit horseradish peroxidase-conjugated antibody

Mouse monoclonal anti-human Bax antibody (2D2)

Mouse monoclonal anti-human TF antibody (10H10)

p38α siRNA

Rabbit anti-human p53 IgG antibody

Rabbit polyclonal anti-human tissue factor antibody

Scientific Laboratory Supplies Ltd, Hessle, UK

CO_2 incubator

Serotec Ltd., Oxford, UK

Mouse monoclonal anti-human p21

Sigma Chemical Company Ltd, Poole, UK

Ammonium persulfate

Antibiotic antimycotic solution (Penicillin − Streptomycin − Neomycin Solution) (100X)

Bovin serum albmin (BSA)

Bradford reagent

4′,6-Diamidino-2-phenylindole dihydrochloride (DAPI)

Formaldehyde solution

Donkey serum

Laemmli's lysis-buffer (2X)

LB broth medium

N,N,N',N'-tetramethylethylenediamine (TEMED)

PAR2-AP

Phosphate buffered saline (PBS)

Plasma Barium Sulfate Eluate CS 01 (81)

Protease inhibitor cocktail

TRI reagent

Triton-X 100

Trypsin/EDTA solution

Tween 20

Source Bioscience, Nottingham, UK

Mouse monoclonal anti-human GAPDH antibody (1D4B)

SPPSS Inc. Chicago, USA

Statistical Package for the Social Sciences

Syngene, Cambridge, UK

GeneSnap image capture system and GeneTtool analysis programme

TCS Cellworks, Claydon, UK

DMSO Freeze medium (2X)

Tocris Bioscience, Bristol, UK

PD98059 MEK inhibitor

SB202190 p38 inhibitor

UVP Ltd, Cambridge, UK

3UV-transilluminator

WPA, Cambridge, UK

UV-Visible spectrophotometer

Yorkshire Bioscience Ltd, York, UK

DNA molecular weight marker (100-10000 bp)
TF primers

2.2. Methods

2.2.1. Culture of human coronary artery endothelial cells (HCAEC)

Human coronary artery endothelial cells (HCAEC) were used throughout this study as a model for studying endothelial cells. All cells were cultured under sterile conditions and all reagents warmed to 37°C prior to use. Complete HCAEC medium was prepared by mixing MV2 base medium and 5 % (v/v) foetal calf serum (FCS) and contained epidermal growth factor (recombinant human) (5 ng/ml), basic fibroblast growth factor (recombinant human) (10 ng/ml), insulin-like growth factor (Long R3 IGF) (20 ng/ml), vascular endothelial growth factor 165 (0.5 ng/ml), ascorbic acid (1 µg/ml), and hydrocortisone (0.2 µg/ml). The cells were cultured in T25 (25 cm^2) flasks with complete MV2 medium, incubated at 37°C under 5 % CO_2 and supplemented every 2 days by replacing 2 or 3 ml of culture medium with fresh medium.

2.2.2. Culture of human breast cancer cell line

The human breast cancer cell line MDA-MB-231 was cultured in T75 (75 cm^2) flasks in DMEM medium supplemented with 10 % (v/v) FCS and 1 % (v/v) antibiotic (penicillin (5 unit/ml), streptomycin (5 µg/ml) and amphotericin (25 ng/ml)). Cells were incubated at 37°C under 5 % CO_2 and supplemented every 3 days by replacing 3 ml of culture medium with fresh medium.

2.2.3. Subculture, harvesting and counting of cells

Once the cells were 80 % confluent, the medium was removed from the flask and the cells washed with 5 ml of sterile phosphate buffered saline (PBS) (pH 7.2) to remove all trace of serum and to maintain the correct pH. The cells were then incubated at 37°C with 3 ml accutase enzyme solution for 2-3 min to detach the cells. The flask was then tapped to release the cells and cell suspension was then transferred to a 20 ml sterile tube and centrifuged at 400 *g* for 5 min at room temperature. The supernatant was carefully discarded without disturbing the pellet and the cells re-suspended in 3 ml of fresh medium and mixed. To determine the cell density, 20 µl of cell suspension was loaded onto a haemocytometer and the number of cells in 5 mm^2 squares counted. The density of cells per ml was then determined as the average number of cells counted per mm^2 multiplied by 10^4. This was taken to be the number of cells per ml and was then multiplied by the total volume of cell suspension to obtain the total number of cells.

2.2.4. Cryopreservation and recovery of cells

Cells were washed, detached, and pelleted as described in section 2.2.3. The cell pellet was re-suspended in 3 ml of pre-warmed DMSO freeze medium. The cells (10^6/ml) were mixed gently to ensure an even distribution and transferred to pre-labelled cryovials. The vials were placed in a freezing chamber surrounded with ethanol and frozen at -70°C overnight. The chamber allows the temperature to decrease gradually (-1°C/min) to retain optimal viability. Finally, the cryovials were transferred to liquid nitrogen for long-term storage. To start new cultures from frozen cells, cryovials containing the cells were quickly thawed in a 37°C water bath. Once defrosted, the cells were transferred to cell culture flasks containing pre-warmed medium at the required density.

2.2.5. Adaptation of HCAEC to serum-free medium

The culture medium contains FCS to allow the rapid propagation of the cells. However, studying the effects of TF on signalling pathways requires the absence of these factors from the culture medium. Therefore, HCAEC were cultured in serum-free medium to study the effect of the protein of interest. Cells were gradually adapted to serum-free medium by reducing the percentage of FCS in the culture medium from 5 % (v/v) to 2 % (v/v) and, finally, serum free over 2 days prior to experiments.

2.3. Bacterial cell culture and plasmid isolation

2.3.1. Isolation of plasmid DNA from bacteria using the Wizard Midiprep kit

LB broth medium was prepared by dissolving LB broth powder (10 g) in 400 ml of de-ionised water autoclaved. The Wizard plus Midipreps DNA Purification system was used to isolate plasmid DNA from bacterial cells as follows. Bacteria containing the DNA plasmid were incubated overnight in 100 ml LB medium at 37°C with gentle shaking. The medium was then divided between two 50 ml tubes. The bacterial cells were then pelleted by centrifugation at 2500 *g* for 15 min at 4°C. The bacterial pellet was re-suspended in 3 ml of re-suspension buffer provided by the kit (50 mM Tris pH 7.5, 10 mM EDTA, 100 μg/ml RNase A) and transferred to a 20 ml tube. 3 ml lysis buffer (0.2 M NaOH, 1 % SDS) was added and mixed by gently inverting the tube 4–6 times. Neutralising buffer (1.32 M potassium acetate pH 4.8) (4 ml) was added and after gentle mixing the lysate was centrifuged at 3000 *g* for 20 min to pellet the cell debris. The upper clear phase was transferred into a 15 ml tube and centrifuged for a further 15 min at 3000 *g*. 10 ml resin was added to the Midiprep column and the supernatant lysate was transferred carefully to the resin and mixed. The lysate was then cleared using a vacuum. The column was then washed with 20 ml washing buffer (80 mM potassium acetate, 8.3 mM Tris-HCl pH 7.5, 40 μM

EDTA, 55 % (v/v) ethanol) using a vacuum. The neck of the Midiprep column was cut off and the resin transferred to a 1.5 ml microcentrifuge tube. Any residual column wash was then removed by centrifuging the tube at 12,400 rpm for 3 min on a microcentrifuge. The neck of the Midiprep column was then transferred to a clean 1.5 ml microcentrifuge tube, and 300 µl of pre-heated DNase-free water was added to the column and incubated for 1 min. The tube was then centrifuged for 2 min at 12,400 rpm to elute the plasmid. The neck of the Midiprep column was removed and the eluted plasmid was then centrifuged for 5 min at 12,400 rpm to pellet out the resin fibres. The eluted plasmid was then transferred carefully into another clean 1.5 ml microcentrifuge tube.

2.3.2. Determining plasmid DNA concentration and purity

The concentration of plasmid DNA in each sample was determined by measuring the absorption of a 1-in-10 dilution of the DNA at 260 nm against the water blank in a quartz microcuvette. The concentration of DNA in µg/ml was calculated using the following formula (Doyle, 1996).

DNA concentration (µg/ml) = Absorption (260 nm) x 50 x dilution factor

DNA purity was determined by measuring the absorption at 260 nm and 280 nm and calculating the ratio A_{260}/A_{280}. Samples with a ratio of above 1.3 were considered of sufficient DNA purity and therefore suitable for further use.

2.3.3. Ethanol precipitation of DNA

DNA was precipitated by mixing DNA solution with sodium acetate (5 M) pH 5.2, and 100 % (v/v) ethanol at a ratio of 1:1:4 (v/v/v). The samples were incubated at -20°C for 30 min

and centrifuged at 13,400 rpm for 10 min in a microcentrifuge. The pellet was washed with 300 µl of 75 % (v/v) ice-cold ethanol and centrifuged for 10 min at 12,400 rpm, and the ethanol was removed. The precipitated DNA was then re-suspended in DNase-free water (150 µl) and the concentration measured.

2.3.4. Examination of plasmid DNA by agarose gel electrophoresis

The plasmid DNA was analysed by electrophoresis on a 0.5 % (w/v) agarose gel to ensure the purity of eluted DNA. A 0.5 % (w/v) gel was prepared by adding 0.25 g of agarose to 50 ml of TBE buffer (89 mM Tris, 89 mM boric acid, 2 mM EDTA, pH 8.3). The agarose-TBE mixture was heated in a microwave oven until dissolved and was then poured into a sealed gel tray. An appropriate comb was placed in the gel and it was allowed to solidify. The samples were prepared by adding 1 µl SYBR Green I to 10 µl of DNA sample and then mixed with 10 µl of loading buffer. Additionally, a DNA ladder was prepared by mixing 10 µl DNA marker and 1 µl of SYBR Green I. The samples along with the markers were then loaded into wells and electrophoresis was carried out at 100 V for approximately 1 h. The gel was then examined using a UV transilluminator and the bands were recorded using the GeneSnap program.

2.4. Transfection of HCAEC with plasmid DNA

2.4.1. Transfection using Lipofectin reagent

HCAEC (10^5/well) were seeded in 12-well plates in MV2 medium (2 ml) containing 2 % FCS and incubated overnight. The following day the medium was removed and the cells were washed with PBS. Endothelial cells serum-free medium (800 µl), supplemented with 20 ng/ml bFGF and 10 ng/ml EGF, was then added to each well. For each transfection, solution A was prepared by diluting 1 µg plasmid DNA in serum-free medium (100 µl).

Solution B was prepared by adding the Lipofectin reagent (7 µl) in serum-free medium (100 µl). The two solutions were allowed to stand at room temperature for 30 min and then mixed together and allowed to stand at room temperature for a further 15 min. The mixture was then added to the samples and incubated at 37°C. After 4-5 h, the medium was removed and replaced with complete medium (2 ml) and incubated at 37°C for 48 h.

2.4.2. Transfection using Lipofectamine

HCAEC (10^5/well) were seeded in 12-well plates in MV2 medium (2 ml) containing 2 % FCS and incubated overnight. The following day the medium was removed and the cells were washed with PBS. Endothelial cells serum-free medium (800 µl), supplemented with 20 ng/ml bFGF and 10 ng/ml EGF, was then added to each well. For each transfection, solution A was prepared by diluting 1 µg plasmid DNA in serum-free medium (100 µl). Solution B was prepared by adding the Lipofectamine reagent (10 µl) in serum-free medium (100 µl). The two solutions were allowed to stand at room temperature for 30 min and then mixed together and allowed to stand at room temperature for a further 15 min. The mixture was then added to the samples and incubated at 37°C. After 4-5 h, the medium was removed and replaced with complete medium (2 ml) and incubated at 37°C for 48 h.

2.4.3. Transfection using Metafectene

HCAEC (10^5/well) were seeded in 12-well plates in 1 ml complete MV2 medium (2 ml) and incubated overnight. The following day, solution A was prepared by diluting 1 µg plasmid DNA in serum-free medium (50 µl). Solution B was prepared by adding the Metafectene reagent (5 µl) in serum-free medium (50 µl). Solutions A and B were mixed together and allowed to stand at room temperature for 20 min. The mixture (100 µl) was

then added to the samples and incubated at 37°C. After 4-5 h, the medium was removed and replaced with complete medium (2 ml) and incubated at 37°C for 48 h.

2.5. Determination of transfection efficiency by flow cytometry

Transfection efficiency was determined by transfecting HCAEC with the pCMV-EGFP mammalian expression vector which encodes an enhanced green fluorescent protein (EGFP). The expression of green fluorescent protein was measured by flow cytometry. HCAEC (10^5/well) were transfected with 1 µg of the pCMV-EGFP as described in section 2.4. Un-transfected cells were used as a control. The cells were then harvested and centrifuged at 400 *g* for 15 min. The cells pellets were re-suspended in PBS (300 µl) and transferred to polypropylene FACS tubes. Cells were analysed on a Becton Dickinson a FACS-Calibur flow cytometer and 10,000 events were recorded for each sample. A gate was set to contain approximately 3 % of events from un-transfected cells. The percentage of the transfected cells and the mean cell fluorescence were determined using CellQuest software version 3.3.

2.6. Molecular biology techniques

2.6.1. Estimation of the protein concentration using the Bradford reagent

Cell samples were lysed in 100 µl of Laemmli's buffer (62.5 mM Tris-HcL pH 6.8, 10 % (w/v) glycerol, 5 % 2-mercaptoethanol, 2 % (w/v) SDS, 0.002 % (w/v) bromophenol blue) by repeated pipetting. The samples were boiled at 99°C for 5 min and diluted in de-ionised water for the Bradford protein estimation assay. In order to construct a standard curve for the assay, standards of known protein concentrations (0, 10, 50, 100, and 150 µg/ml) were prepared by serial dilutions of lipid-free BSA in de-ionised water. 10 µl of each standard or sample was diluted in 90 µl de-ionised water. Diluted samples and standards (100 µl) were

placed into individual 1 ml plastic cuvettes and 900 µl of diluted Bradford reagent (1:1 v/v) was added to each cuvette. Both samples and standards were left at room temperature for 10 min and the absorption of the samples and the standards were then recorded at 595 nm using a spectrophotometer. A standard curve was prepared using the absorption values of the standards against protein concentrations (Fig 2.1). The protein concentrations in the samples were then determined from the standard curve.

2.6.2. SDS-polyacrylamide gel electrophoresis (SDS-PAGE)

A 12 % (w/v) polyacrylamide resolving gel was made by mixing 4 ml acrylamide solution (30 % (w/v) acrylamide, 0.8 % (w/v) bisacrylamide), 2.6 ml resolving buffer (1.5 M Tris-HCl, pH 8.8 0.4 % (w/v) SDS), 3.3 ml de-ionised water and 10 % (w/v) ammonium persulphate (100 µl). The components were then mixed thoroughly and de-gassed for 2 min under a vacuum. 10 µl of N,N,N',N'-tetramethylethylenediamine (TEMED) was then added to begin polymerisation. The solution was poured in between the electrophoresis glass plates in a gel caster, covered with a layer of butanol and allowed to set for at least 1 h. Once set, the butanol was poured off and the 4 % (v/v) stacking gel was prepared by mixing 0.65 ml of acrylamide solution, 1.3 ml staking buffer (0.5 M Tris-HCl pH 6.8, 0.4 % (w/v) SDS), 3 ml de-ionised water, and 100 µl ammonium persulphate (10 % w/v). The solution was mixed and de-gassed under a vacuum for 2 min before the addition of 10 µl of TEMED. The solution was then poured on top of the resolving gel and a comb inserted. Once the stacking gel was set (about 1.5 h), the comb was removed. The gel was removed from the gel caster and placed in the electrophoresis tank.

Figure 2.1. Standard curve for Bradford assay

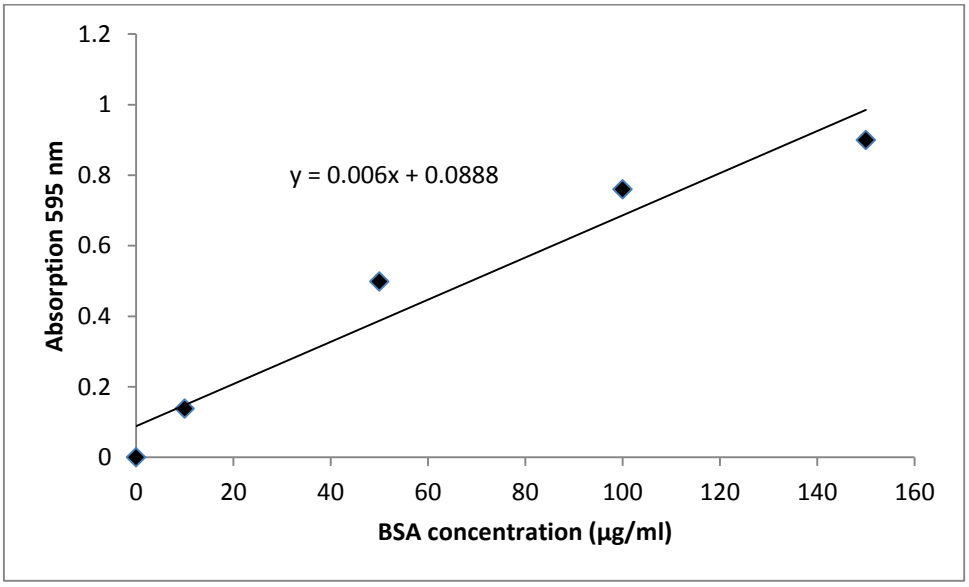

The standard curve was prepared by serially diluting the BSA in distilled water (0-150 µg/ml). 10 µl of each standard was diluted in 90 µl of distilled water. 100 µl of each diluted standard was placed in a separate plastic cuvette in duplicate and mixed with the diluted Bradford reagent (900 µl). After 10 min, the absorption was measured at 595 nm using a spectrophotometer.

Electrophoresis buffer (25 mM Tris-HCl pH 8.3, 192 mM glycine, 0.035 % (w/v) SDS) was poured into the electrophoresis tank and behind the gel. 5 µl of a set of molecular weight protein markers (10-260 kDa) was loaded into the first well, and the protein samples (20 µg) were loaded into the subsequent wells. Electrophoresis was carried out at 100 V to separate the proteins until the leading blue dye band had reached the bottom of the gel.

2.6.3. Western blot analysis

Following electrophoresis, proteins were transferred onto nitrocellulose membrane using a transfer system. The gel was placed in between blotting paper and nitrocellulose membrane soaked in transfer buffer (150 mM glycine, 20 mM Tris-HCl pH 8.3, 20 % (v/v) methanol) and placed in the transfer tank. Proteins were transferred at 16 mA overnight at 4°C. Following protein transfer, the nitrocellulose membranes were blocked with TBST (20 mM Tris–HCl pH 8.0, 150 mM NaCl, 0.05 % (v/v) Tween 20) (Batteiger et al., 1982) for 2 h at room temperature with gentle shaking. Membranes were incubated with primary antibody diluted in TBST overnight at 4°C. Membranes were then washed three times with TBST followed by incubation with an appropriate secondary antibody for 2 h at room temperature with gentle shaking. After three further washes with TBST, the membranes were washed in distilled water for 5 min and developed with either Western Blue stabilised substrate for alkaline phosphatase or 3,3',5,5'-tetramethylbenzidine (TMB)-stabilised substrate for HRP, and images were recorded using the GeneSnap image capture system. The bands were analysed using the ImageJ program.

2.7. Real-time reverse transcriptase-polymerase chain reaction (Real-time RT-PCR)

2.7.1. Isolation of total RNA from cells

The HCAEC (10^5/well) were harvested in 1.5 ml tubes and lysed by adding 200 µl of TRI reagent (concentrations are not disclosed by the manufacturer). The lysed cells were then incubated at room temperature for 5 min. Chloroform (40 µl) was added to each tube, and the tubes were vortexed for 15 s and allowed to stand for 10 min at room temperature. The samples were then centrifuged at 12,000 rpm for 15 min in a microcentrifuge to form two visible layers. The clear aqueous upper phase was carefully transferred to a fresh RNase-free 1.5 ml tube. The RNA was precipitated by adding isopropanol (100 µl) to each sample, mixed by vortexing and then incubated at -20°C for 1 h. The samples were then centrifuged at 12,000 rpm for 10 min in a microcentrifuge. The supernatant was removed and the RNA pellet washed with 75 % (v/v) ethanol (200 µl). The RNA pellet was re-suspended in RNase-free water (60 µl) and stored at -70°C until required. The concentration of RNA in the samples was determined by measuring the absorption of each sample at 260 nm on a spectrophotometer. The concentration of RNA was calculated as follows:

RNA concentration (µg/ml) = Absorption (260 nm) x 40 x dilution factor

The absorption at 260 & 280 nm was also determined and was used to determine the purity of RNA in each sample.

The volume of RNA that contains 0.1 µg RNA for real time RT-PCR was then calculated as follows:

The volume of RNA required (µl) = 0.1/RNA concentration x 1000

2.7.2. Primer design for real time RT-PCR

The full-length cDNA sequences for each gene to be analysed were downloaded from the Entrez nucleotides database on PubMed website. The optimal length of RT-PCR primers to

ensure specificity is between 18 and 22 bp long with a minimum GC content of 40-60 %. Primers were designed using the Base Pair program.

2.7.3. Real-time RT-PCR

Total RNA was isolated from HCAEC (10^5/well) using the TRI reagent system as in section 2.7.1. Each RNA sample was amplified with specific primers as well as with β-actin primers (housekeeping gene) as a reference. The primers were reconstituted in RNase-free water to give a final concentration of 100 nM. Appropriate volumes of each RNA solution were calculated to contain 0.1 µg RNA as described in section 2.7.1. This solution was then diluted in RNase-free water to a final volume of 8.6 µl and placed into six separate wells of a 96-well PCR plate. 1 µl of mixed forward and reverse primers (100 nM) for the target gene, or for β-actin, were each added to three of the wells. Single-step RT-PCR was carried out using the GoTaq® 1-Step RT-qPCR System to convert RNA to cDNA and then amplify the cDNA. For each RNA sample**,** RT-PCR mix (10 µl/well) and reverse transcriptase enzyme mix (0.4 µl/well) (provided by the kit) were added to the wells to make up the volume in each well to 20 µl. RT-PCR was carried out using an iCycler thermal cycler RT-PCR machine at temperatures shown in Table 2.1. Following the reaction, the data were analysed by automatically determining threshold cycle (Ct) numbers using the iQ software. The relative expression of each mRNA was then calculated using $2^{-\Delta\Delta CT}$ method (Livak et al., 2001). Each mRNA Ct value was normalised against its respective endogenous β-actin mRNA Ct value. The ΔΔCt was calculated as the difference between the normalised Ct values (ΔCt) of the treatment and the control samples.

Table 2.1. Real-time RT-PCR program

Number of cycles	Temperature	Time	Step
1x	48°C	30 (min)	Conversion of RNA to cDNA
	95°C	10 (min)	Degradation of RNA
40x	95°C	15 (sec)	Denaturation
	60°C	1 (min)	Primers annealing
1x	60-90°C Increase temp by 0.5°C		Dissociation Determining the melt temperature of the amplicons
Final hold	4°C		

2.8. Isolation of cell-derived microvesicles from cultured endothelial cells

Microvesicles were isolated from endothelial cells cultured in 12-well plates (~10^5/well). The cells were adapted to serum-free medium for 1.5 h prior to activation with PAR2-AP (20 μM) and incubated for 90 min to allow the microvesicles release. In some experiments, the cells were incubated with a range of p38 or ERK pathway inhibitors (SB202190 or PD98059 respectively) for 30 min prior to addition PAR2-AP (20 μM). The conditioned medium was then collected and cleared of cells and debris by centrifugation at 400 *g* for 10 min. The supernatant was then centrifuged at 100,000 *g* for 60 min at 20°C in a Beckman TL-100 ultracentrifuge using a TLA-100.2 rotor. The resultant pellets were re-suspended in 200 μl of PBS (pH 7.4) and used immediately in the experiments, or frozen at -70°C.

2.8.1. Estimation of microvesicle concentration by measuring thrombin generation

The concentration of microvesicle samples was determined by measuring the potential for thrombin generation using the Zymuphen Microvesicle Assay Kit according to the manufacturer's instructions. Samples of the isolated microvesicles (25 μl) were added to a 96-well plate in duplicate. The wells were then incubated with the supplied R1 solution (50 μl) containing bovine FXa, FVa and calcium. 25 μl of the supplied RII solution containing prothrombin was then added to each well and incubated for 10 min at 37°C. Finally, the wells were developed with the supplied RIII solution (50 μl) containing the thrombin chromogenic substrate CS 01 (81) (0.1 mM) for 10 min at 37°C. The reactions were terminated with 2 % (v/v) citric acid (50 μl) and the absorptions measured at 410 nm on a plate reader. The microvesicles standard was reconstituted with 2 ml of microvesicle-sample diluent (MVs-SD) to generate a solution of 2.8 nM. Five standard points were prepared by serially diluting the standard solution with distilled water to produce a range of 0-2.8 nM.

25 µl of each standard was added to the wells in duplicate. The assay was carried out alongside the sample as described above. The standard curve of microvesicles concentration against absorption at 410 nm was prepared (Fig 2.2). The absorption values from the unknown samples were then compared to the standard curve.

2.8.2. Measurement of microvesicles-associated TF antigen using Enzyme-Linked Immunosorbent Assay (ELISA)

Concentration of microvesicle-associated TF antigen isolated from conditioned media from the cells was determined using a TF-specific ELISA kit. 100 µl of sheep anti-human TF antibody (1.7 µl), diluted 1:50 (v/v) in capture buffer (15 mM Na_2CO_3 buffer, pH 9.6) was added in separate wells in the ELISA plate and incubated overnight at 4°C. The wells were then blocked using 150 mM of PBS pH 7.4, containing 1 % (w/v) bovine serum albumin (BSA) (200 µl) and incubated for 90 min at room temperature. The excess unbound antibody was then washed four times, each time with 200 µl wash buffer (PBS pH 7.4, 0.1 % (w/v) Tween 20). 100 µl/well of the microvesicle samples in sample buffer (100 mM HEPES, 10 mM NaCl, 40 ml H_2O, pH 7.2) were added to the wells and incubated for 1 h at room temperature. The wells were then washed four times, each time with wash buffer (200 µl), and incubated with 100 µl detecting antibody (HRP-conjugated goat anti-human TF antibody) diluted 1:100 in conjugate buffer (100 mM HEPES, 10 mM NaCl, 1 % (w/v) bovine serum albumin and 1 % (w/v) Tween 20, pH7.4) for 90 min at room temperature. Finally, the wells were washed four times with wash buffer (200 µl)

Figure 2.2. Standard curve for microvesicles concentration using Zymuphen Microvesicle Assay

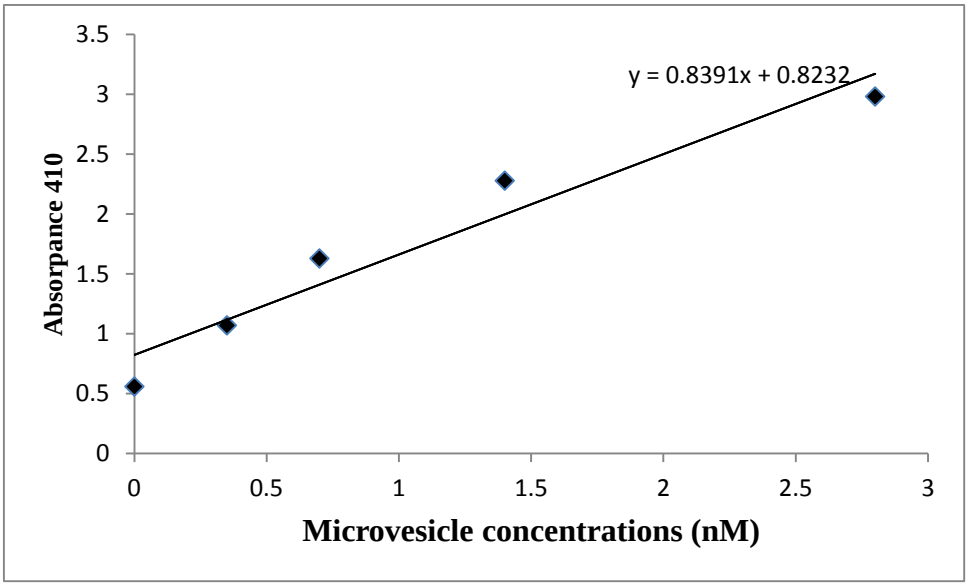

Serial dilutions of recombinant human TF protein were prepared to produce a range of 0-2.8 nM. 25 µl of each diluted sample was added to wells in triplicate and the assay carried out using the RI, RII and RIII. The absorption of the samples was measured at 410 nm and the standard curve constructed. Data were representative of one experiment in triplicate. The standard curve was prepared for each occasion.

and developed with 100 µl/well of TMB substrate for 5-15 min at room temperature until the colours developed. The reactions were terminated with 2 M sulphuric acid (50 µl) and the absorptions measured at 450 nm wavelength on a plate-reader. To prepare a standard curve, serial dilutions of recombinant human TF (25 mg/ml) were prepared in sample buffer. 100 µl of each standard was added to wells in duplicate to give final concentrations of 0, 6.25, 12.5, 25, 50 and 100 ng/ml of recombinant human TF (Fig 2.3). The ELISA was carried out alongside the sample as described above. A standard curve of TF concentration against absorption at 450 nm was prepared and the TF antigen values were determined. When necessary, the TF concentrations were normalised against the microvesicle densities.

2.9. TF activity assay

Cells ($10^{5)}$ were harvested and transferred into 1.5 ml microcentrifuge tubes. The cells were pelleted by centrifugation at 12,000 rpm for 5 min in the microcentrifuge. The cell pellets were washed with PBS (1 ml) and re-centrifuged at 12,000 rpm for 3 min. The cells were then re-suspended in 100 µl of PBS. 30 µl of cell suspensions were placed into a 96-well plate followed by the addition of 60 µl of Tris buffer (50 mM) and 30 µl of $CaCl_2$. Thrombin generation was initiated by the addition of 30 µl of plasma barium sulphate solution (10 mg/ml) and incubated for 10 min at 37°C. 100 µl of thrombin substrate (0.1 mM) was then added to each well and developed at 37°C for 20 min before measuring the absorption at 410 nm. To obtain a standard curve, the stock solution of Innovin recombinant human TF was reconstituted in distilled water (10 ml) and serial dilutions were prepared of 0.1, 0.5, 1, 5, 10 and 20 U/ml, where the stock solution of recombinant human TF was considered to have 1000 U/ml. The TF activity of each TF dilution was measured as above, converted to log values.

Figure 2.3. Standard curve for the TF ELISA

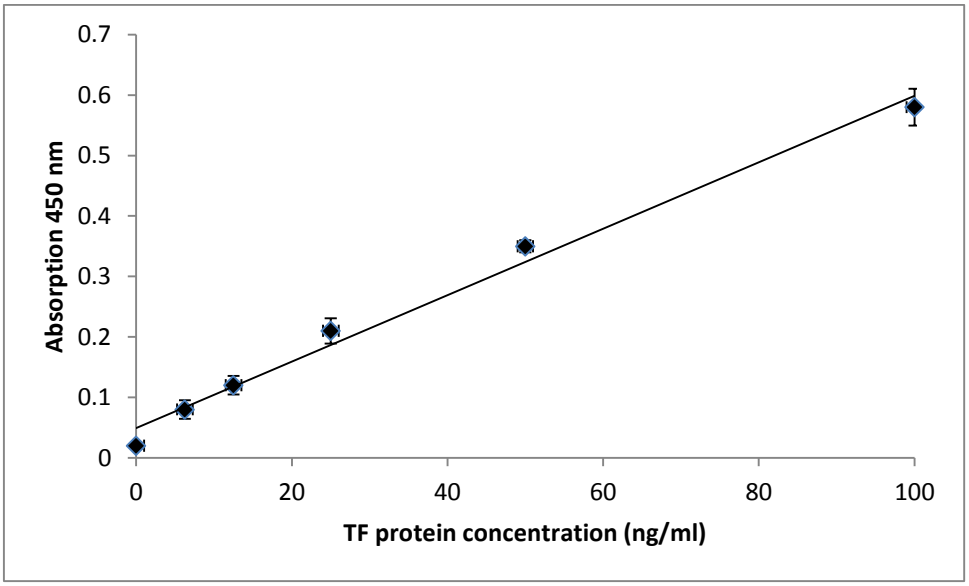

Serial dilutions of recombinant human TF protein (25 mg/ml) were prepared to give a range of concentrations (0-100 ng/ml). 100 µl of each diluted sample was added to a 96-well plate in triplicate and the ELISA carried out. The absorption of the samples was measured at 450 nm and the standard curve constructed. Data represent one experiment in triplicate.

.

From the standard curve, the concentration of TF expressed in unit per ml was determined using the following equation (Fig 2.4):

$$\text{Log (TF (U/ml))} = \frac{\text{absorption} - 550.41}{25.533}$$

2.10. Statistical analysis

All data represent the calculated mean values from the number of experiments stated in each figure legend ± the calculated standard error of the mean. Statistical analysis was carried out using the Statistical Package for the Social Sciences (SPSS). A One-Way ANOVA procedure was used for the analysis of variance of data against the control with Tukey's honestly significant difference test to highlight statistically significant differences.

Figure 2.4. Standard curve for the TF activity assay

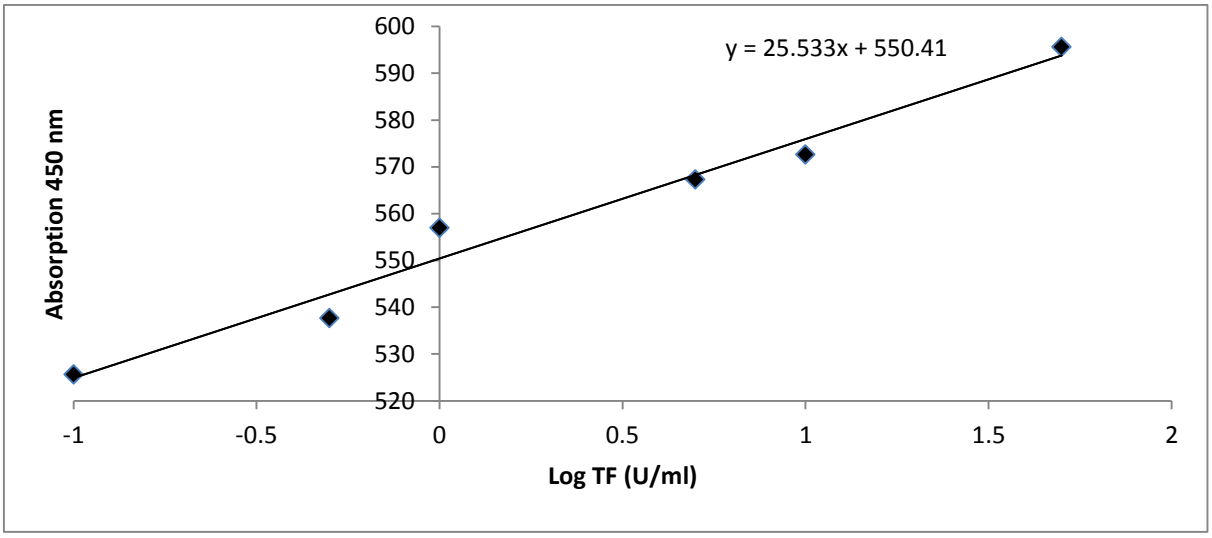

The standard curve was constructed by serial dilution of the recombinant human TF Innovin reagent (0-50 U/ml) in distilled water. 30 µl of each dilution was placed into a 96-well plate, with the addition of 60 µl of Tris buffer (50 mM) and 30 µl of $CaCl_2$. Thrombin generation was initiated by the addition of 30 µl of plasma barium sulphate solution (10 mg/ml) followed by incubation for 10 min at 37°C. Thrombin substrate (100 µl) was then added to each well and developed at 37°C for 20 min before the absorption was measured at 450 nm. The absorption of each sample was measured. Data represent one experiment in triplicate. The standard curve was prepared for each occasion.

CHAPTER 3

The influence of phosphorylation of cytoplasmic domain of TF on p38 phosphorylation and the release of TF as microvesicles

3.1. Introduction

3.1.1. TF signalling

It has long been recognised that the TF is of crucial importance for haemostasis. TF has also been identified as a cell signalling receptor involved in a number of physiological processes including angiogenesis (Abe et al., 1999), cell migration (Siegbahn et al., 2005) and wound healing (Chen et al., 2005). The signalling pathways arising from TF have been implicated in pathological conditions such as inflammation (Cunningham et al., 1999), tumour angiogenesis, metastasis (Mueller & Ruf, 1998; Bromberg et al., 1995) and progression of cardiovascular diseases (Taubman et al., 1997).

The extra-cellular domain of TF is responsible for the induction of coagulation and some TF-dependent cellular responses. Binding of FVIIa to TF results in the activation of several intracellular signalling pathways including all three MAPK pathways: ERK1/2 (Poulsen et al., 1998), p38, and JNK (Camerer et al., 1999). The activation of these pathways by the FVIIa:TF complex regulates the expression of a number of genes leading to a broad range of cellular responses, including cell survival and cytoskeletal rearrangement (Versteeg & Ruf, 2006). Moreover, binding of FVIIa to TF also activates PAR2 which has been shown to induce MAPK signalling (Morries et al., 2006; Jiang et al., 2004) (Fig 3.1). However, direct TF-mediated cell signalling can also occur via cytoplasmic domain of TF (Ruf, 1999). This protease-independent signalling, through the cytoplasmic domain of TF, has been demonstrated to be influenced and possibly regulated by PAR2 (Ahamed & Ruf, 2004). In addition, separate TF-mediated cell signalling has been demonstrated to include binding of TF to transmembrane receptors such as β1-integrin (Collier & Ettelaie, 2010).

Figure 3.1. TF signalling mechanisms

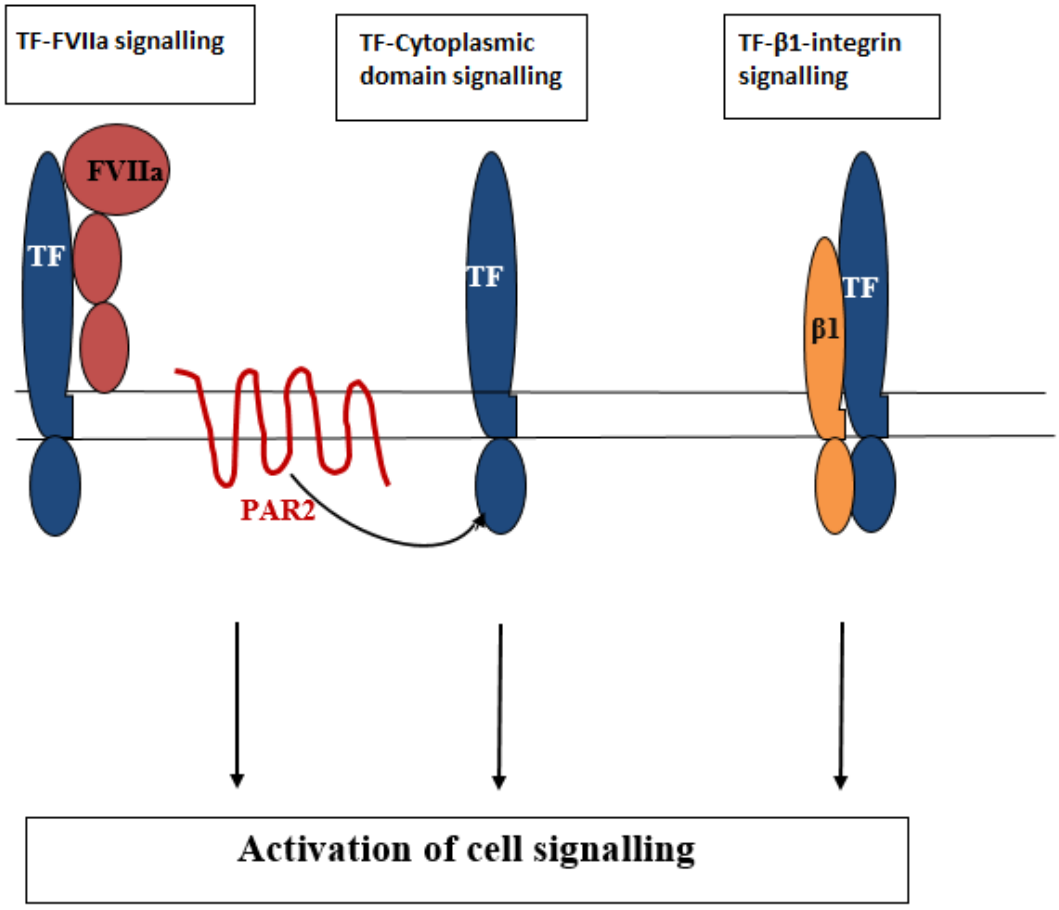

TF activates cell signalling through three main pathways. In the first mechanism, TF-mediated activation of FVIIa leads to activation of PAR2. The activation of PAR2 then leads to intracellular signalling pathways. TF can also signal directly through its cytoplasmic domain although the cytoplasmic domain of TF is influenced by PAR2. Finally, TF can bind to the β1-integrin, resulting in the activation of intracellular signalling pathways.

3.1.2. Cytoplasmic domain-dependent signalling

TF is known to show a large degree of structural similarity to the proteins of the class II cytokine receptor family, particularly the interferon γ receptor. However, the cytoplasmic domain of TF is short compared to other cytokine receptors, and it lacks the typical tyrosine kinase binding motifs (Bazan, 1990). However, involvement of the cytoplasmic domain in intracellular processes is suggested by the presence of two phosphorylation sites at Ser residues 253 and 258 (Zioncheck et al., 1992). Ser253 has been shown to be phosphorylated by protein kinase C (PKC) following activation of PAR2. Phosphorylation of the Ser253 leads to a conformational change and allows Ser258 phosphorylation by previously unknown proline-directed protein kinase (Ahamed & Ruf, 2004). Phosphorylation of these serine residues may lead to the formation of potential docking sites for important signalling proteins. In addition, it has been found that the cytoplasmic domain of TF is required for p38 MAPK activation (Ott et al., 2005). However, the mechanisms by which TF activates p38 remain unknown. The cytoplasmic domain of TF has also been shown to interact with actin-binding protein 280 (ABP-280) (Ott et al., 1998) which may result in cytoskeletal reorganisation (Ott et al., 2005).

The cytoplasmic domain of TF is not required for the procoagulant activity of TF (Mueller & Ruf, 1998). However**,** the cytoplasmic domain of TF has been implicated in inflammation (Ahamed et al., 2007), cell migration (Siegbahn et al., 2005), and angiogenesis (Abe et al., 1999), and it is essential for the release of TF as cell-derived microvesicles (Collier & Ettelaie, 2011).

3.1.3. Microvesicles-associated TF

Levels of circulating endothelial-derived microvesicles have been shown to be elevated in a variety of diseases, particularly in vascular diseases (Jimenez et al., 2005; Diamant et al., 2004; Nomura et al., 2008). TF-associated microvesicles represent a significant fraction of cell-derived microvesicles (Schecter et al., 2004) and account for a significant portion of circulating TF activity (Yu & Rak, 2004). The levels of TF-containing microvesicles have been found to be elevated in cardiovascular disease (Nieuwland et al., 1997; Shet et al., 2003). Moreover, TF-bearing microvesicles are thought to be key mediators of thrombosis (Ahn, 2005; Hron et al., 2007) as well as distant metastasis in lung cancer (Tseng et al., 2014). Cells release TF as cell-derived microvesicles in response to injury, trauma or as part of the inflammatory response (Nieuwland et al., 2000). The incorporation and release of TF within cell-derived microvesicles appear to be regulated by a mechanism that is dependent on the phosphorylation of the cytoplasmic domain of TF (Collier & Ettelaie, 2011). It has been shown that the phosphorylation of the cytoplasmic domain of TF at Ser253 by PKCα initiates the release of TF within microvesicles. In addition, phosphorylation of Ser253 by PKCα promotes the subsequent phosphorylation of Ser258 (Dorfleutner & Ruf, 2003). The phosphorylation of Ser258 in turn acts to terminate TF release (Collier & Ettelaie, 2011). Phosphorylation of Ser258 within the cytoplasmic domain of TF is thought to be mediated by an unknown proline-directed kinase (Mody & Carson, 1997).

It has been reported that the cytoplasmic domain of TF is capable of activating p38 (Ott et al., 2005; Ahamed et al., 2007) and suppressing ERK1/2 phosphorylation (Ahamed et al., 2007). The activation of p38 pathway in turn contributes to upregulation of TF expression in monocytes (Bohgaki et al., 2004; Lopez-Pedrera et al., 2006) and endothelial cells (Vega-Ostertag et al., 2005; Oku et al., 2013). This crosstalk-between TF and MAPK

suggests the possible involvement of MAPK in the phosphorylation of the cytoplasmic domain of TF and the subsequent regulation of TF incorporation and release within microvesicles.

3.1.4. Aims

The main objectives of this study were as follows.

• To assess the activation of ERK1/2 and p38 by measuring the phosphorylation state of these proteins in the presence or absence of TF

•To determine the role of the phosphorylation of the Ser residues (Ser253) within TF on the activation of ERK1/2 and p38 by using Asp253-substitution (to mimic phospho-serine) or Ala253-substitution (to prevent phosphorylation) of this residue

• To investigate the outcome of ERK1/2 and p38 activation and their contribution to the regulation of TF release as microvesicles, and also the termination of this process

• To identify the kinase responsible for the phosphorylation of Ser258 within the cytoplasmic domain of TF

3.2. Methods

3.2.1. Determination of transfection efficiency by flow cytometry

HCAEC (10^5/well) were transfected with 1 µg of the pCMV-EGFP using Lipofectin as described in the general methods section 2.4.1. A set of un-transfected cells was used as a control. The cells were then harvested and centrifuged at 400 *g* for 15 min. The cells were re-suspended in PBS (300 µl) and transferred to polypropylene FACS tubes, and 10,000 events were recorded for each test sample using a Becton Dickinson FACS-Calibur flow cytometer. A gate was set to contain approximately 3 % of events from the un-transfected cells. The percentage of the transfected cells and the mean cell fluorescence were determined using CellQuest software version 3.3.

3.2.2. Assessment of the expression of TF in transfected HCAEC

3.2.2.1. Measurement of TF mRNA expression in HCAEC by quantitative real-time RT-PCR

HCAEC (10^5/well) were seeded out into 12-well plates and transfected with pCMV-XL5-TF plasmid. The cells were then harvested at 24, 48 and 72 h and total RNA isolated using the TRI-reagent system as described in the general methods section 2.7.1. The purity and the concentration of each RNA sample were determined as described in the general methods section 2.7.1. Single-step RT-PCR was carried out in triplicate using 0.1 µg of RNA from each sample diluted in RNase-free water. Each RNA sample was analysed with specific TF primers (100 nM) as well as with β-actin primers (housekeeping gene) (100 nM) as a reference. For each test, Power SYBR Green RT-PCR mix (10 µl/well) and RT enzyme mix (0.16 µl/well) were added to each well and the volume made up to 20 µl. Following the RT step, PCR was carried out at melting temperatures of 90°C using the GoTaq® 1-Step RT-qPCR System on an iCycler thermal cycler.

The primers used were as follows:

TF-forward 5′-TACAGACAGCCCGGTAGAGTG-3′

TF-reverse 5′-GAGTTCTCCTTCCAGCTCTGC-3′

β-actin-forward 5′-TGATGGTGGGCATGGGTCAGA-3′

β-actin -reverse 5′-GTCGTCCCAGTTGGTGACGAT-3′

Following the reaction, the data were normalised against the respective β-actin quantities. A standard curve was prepared using the *in vitro*-transcribed TF mRNA (a gift from C. Ettelaie), and serial dilutions were prepared containing 0, 0.1, 0.5, 1, 5 and 10 ng of TF mRNA. A single-step RT-PCR was performed on each sample as above. The *in vitro*-transcribed TF mRNA concentrations were converted to log values and plotted against the threshold cycle (Ct). The exact TF mRNA quantities were then determined using the following equation obtained from the standard curve (Fig 3.2):

$$\text{Log (TF mRNA) (ng)} = \frac{\text{Ct} - 18.155}{-3.1159}$$

3.2.2.2. Determination of TF protein expression in transfected HCAEC by Western blot

HCAEC (10^5/well) were transfected with wild-type pCMV-XL5-TF plasmid or pCMV-EGFP and allowed to express the TF protein over 48 h. The cells were then lysed in Laemmli's buffer (100 µl). The protein concentrations were determined prior to analysis using Bradford protein estimation assay. Proteins were separated by 12 % (w/v) SDS-PAGE and transferred to nitrocellulose membranes as described before in sections 2.6.2 & 2.6.3. Membranes were probed using a rabbit antibody against human TF, followed by

Figure 3.2. Standard curve for TF concentrations

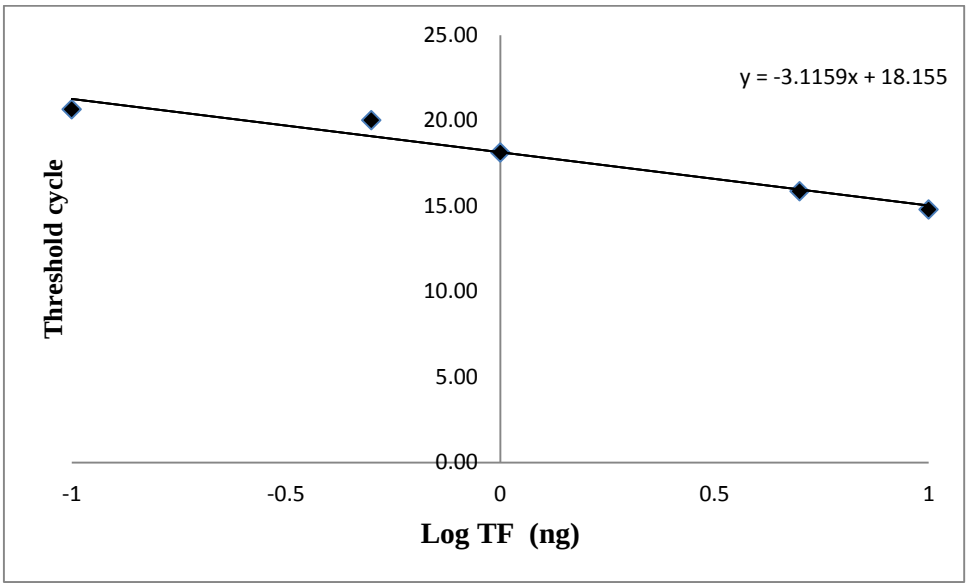

Serial dilutions of TF *in vitro*-transcribed TF mRNA ranging 0-10 ng were prepared in RNase free water. Single-step RT-PCR was performed on each dilution. The *in vitro*-transcribed TF mRNA concentrations were converted to log values and used to prepare a standard curve of TF mRNA concentrations against threshold cycle (Ct).

a goat anti-rabbit-HRP conjugated antibody diluted in TBST according to Table 3.1. Membranes were then developed with 3,3',5,5'-tetramethylbenzidine (TMB)-stabilised substrate for HRP and images were recorded using the GeneSnap image capture system. Membranes were then probed for GAPDH using mouse anti-human GAPDH antibody, followed by a goat anti-mouse alkaline phosphatase-conjugated antibody according to Table 3.1. The membranes were then developed with Western Blue stabilised substrate for alkaline phosphatase, images were recorded as above and TF was compared to GAPDH using the GeneTool software program.

3.2.3. Examination of the influence of TF on p38 and ERK1/2 phosphorylation

HCAEC (10^5/well) were transfected with wild-type pCMV-XL5-TF plasmid or pCMV-EGFP and allowed to express the TF protein over 48 h. The cells were then adapted to serum-free medium for 90 min, activated with PAR2-AP (20 µl) and harvested at intervals of up to 180 min. The cells were then washed with PBS/phosphatase inhibitor solutions and subsequently lysed in 100 µl of Laemmli's buffer. The protein concentration for each sample was then determined using Bradford protein estimation assay. Proteins were separated by 12 % (w/v) SDS-PAGE and transferred to nitrocellulose membranes. Membranes were probed using mouse antibody against human phospho-p38 (Thr180/Tyr182) according to Table 3.1 and incubated overnight at 4 °C, followed by a goat anti-mouse-HRP conjugated antibody (0.1 µg/ml final concentration) for 2 h at room temperature. Membranes were then developed with 3,3',5,5'-tetramethylbenzidine (TMB)-stabilised substrate for HRP and images were recorded using the GeneSnap image capture system. Membranes were then probed for total p38 using rabbit anti-human p38 antibody, followed by a goat anti-rabbit alkaline phosphatase-conjugated antibody, and developed

Table 3.1. Antibodies-TBST dilution for western blot

Primary antibodies	Dilution antibodies: TBST (v/v)	Secondary antibodies	Dilution antibodies: TBST (v/v)
Rabbit-anti-human phospho- ERK 1/2 (P-p44/42)	1:2000	Goat anti-rabbit HRP-conjugated antibody	1:5000
Rabbit anti-human ERK 1/2 (P-p44/42)	1:1000	Goat anti-rabbit alkaline phosphatase-conjugated antibody	1:5000
Mouse anti-human phospho-p38 (28B10)	1:2000	Goat anti-mouse-HRP-conjugated antibody	1:5000
Rabbit anti-human p38	1:2000	Goat anti-rabbit alkaline phosphatase-conjugated antibody	1:5000
Rabbit anti-human TF (Phospho-Ser 258)	1:3000	Goat anti-rabbit HRP-conjugated antibody	1:5000
Rabbit anti-human TF antibody (IgG)	1:1000	Goat anti-mouse alkaline phosphatase-conjugated antibody	1:5000
Rabbit anti-human Phospho-serin	1:1000	Goat anti-rabbit HRP-conjugated antibody	1:5000
Rabbit anti-human CHOP	1:1000	Goat anti-rabbit alkaline phosphatase-conjugated antibody	1:5000
Mouse-anti human phospho (T69-T71) ATF-2	1:1000	Goat anti-mouse HRP-conjugate antibody	1:5000
Mouse anti-human GAPDH (1D4B)	1:1000	Goat anti-rabbit alkaline phosphatase-conjugated antibody	1:5000
Mouse anti-human CHOP (9C8)	1:l000		

with Western Blue stabilised substrate for alkaline phosphatase. Images were recorded, and phospho-p38 was compared to total p38 using the GeneTool software program. Antibodies against phospho-ERK1/2 were also used and normalised against total ERK1/2 as above, using the GeneSnap image capture system and GeneTool software program.

3.2.4. Examination of the function of Ser253 within cytoplasmic domain of TF, on the phosphorylation of p38 and ERK

The influence of phosphorylation of Ser253 within the cytoplasmic domain of TF on p38 and ERK phosphorylation was explored by transfecting the HCAEC with (1µg) wild-type pCMV-XL5-TF, or the mutant forms of the plasmid (pCMV-XL5-TF_{Asp253} and pCMV-XL5-TF_{Ala253}). The cells were allowed to express TF for 48 h, and were then activated with PAR2-AP (20 µM). Samples were collected at 0, 40 and 120 min post-activation, and the phosphorylation state of p38 and ERK1/2 were examined as in section 3.2.3 by western blot.

3.2.5. Optimisation of concentration of p38 pathway inhibitor (SB202190) by measuring the phosphorylation of p38 substrates (CHOP and ATF-2) by western blot

It is known that SB202190 inhibits p38 kinase activity (Manthey et al., 1998). In order to determine the optimal concentration of this inhibitor to achieve maximal inhibition of the p38 pathway, HCAEC (10^5/well) were seeded out into 12-well plates and adapted to serum-free medium for 90 min. The cells were pre-incubated with a range of SB202190 concentrations (0-100 nM) for 30 min prior to activation with PAR2-AP (20 µM) and incubated for 40 min at 37°C. The effect of SB202190 on p38 activity was then examined by measuring the phosphorylation of known p38 substrates (CHOP and ATF-2). To analyse the phosphorylation of CHOP, Ser phosphorylation was examined by western blot using rabbit anti-phospho-serine antibody. The bands were recorded, and the CHOP protein band

was then identified using rabbit anti-CHOP antibody. The ratio of phospho-serine in the CHOP band was then determined. Phosphorylation of ATF-2 was also analysed by western blot using mouse anti-phospho-ATF-2 antibody.

3.2.6. Confirmation of inhibition of CHOP phosphorylation by p38 pathway inhibitor (SB202190) using immunoprecipitation and western blot

3.2.6.1. Optimisation of salt concentration for CHOP immunoprecipitation

Immunoprecipitation is a procedure for selectively purifying a protein from a mixture using an antibody against that specific protein. The precipitation is then carried out by a complex formation with an immunoglobulin-binding protein such as protein A or G immobilised onto beads such as agarose or magnetic beads. The immunoprecipitated samples are then analysed by SDS-PAGE and western blot. However, the affinity of protein A or G for an antibody is dependent on the salt concentration in the buffer. Therefore, to optimise the specificity of the immunoprecipitation three different concentrations of sodium chloride (NaCl) were used in the washing buffer.

HCAEC were cultured in 25 cm^2 flasks in MV medium. The cells were supplemented with fresh medium every two days. Once cells were about 80 % confluent, the culture medium was removed and the cells were washed three times with 10 ml ice-cold PBS. 2 ml lysis buffer (25 mM Tris-HCl pH 7.4, 150 mM NaCl, 2 mM EDTA, 0.5 % (w/v) CHAPS, 1 % (v/v) protease inhibitor cocktail) was directly added to each flask and the mixture was incubated on ice with gentle shaking for 15 min. The cell lysates were then divided between two 2 ml tubes and centrifuged at 12000 *g* for 15 min at 4°C in a microcentrfuge. The supernatants were carefully collected and transferred together to one tube. The protein concentrations were estimated using Bradford assay as described before in section 2.6.1. 1

ml aliquats of the supernatants were transferred into each of four 15 ml tubes. Mouse monoclonal anti-CHOP antibody (0.1 mg/ml) was added to three of the 15 ml tubes, and anti-mouse IgG was added to the final tube. All tubes were incubated for 1 h at 4°C before 75 µl of protein G attached to magnetic beads were added and incubated overnight at 4°C on a rotator. µ-MACS Column was attached to the magnet on the MACS Separator and washed once with 200 µl lysis buffer. Each of the labelled cell lysates was then loaded onto a separate column. The columns were washed four times with 200 µl washing buffer (25 mM Tris-HCl pH 7.4, 2 mM EDTA, 0.5 % (w/v) CHAPS) containing 150, 200 or 250 mM NaCl. The fifth wash was performed with 100 µl Tris-HCL pH7.4 (20 mM). The samples were then eluted by adding hot Laemmli's buffer (20 µl) and left for 5 min; then 60 µl hot Laemmli's buffer was added and the eluted samples were collected. 25 µl of each protein sample was then analysed by western blot using a rabbit anti-CHOP antibody followed by an alkaline phosphatase-conjugated antibody to detect CHOP protein according to Table 3.1.

3.2.6.2. Examination of the influence of p38 pathway inhibitor (SB202190) on CHOP phosphorylation by immunoprecipitation followed by western blot

HCAEC were cultured in two T25 flasks. Once cells reached 80 % confluence, the culture medium was replaced with serum-free medium and adapted for 90 min at 37°C. The cells were then incubated for 30 min in the presence of either SB202190 (30 nM) or DMSO as a control. The cells were then activated with PAR2-AP (20 µM) and incubated for a further 40 min. The cell lysates were prepared and CHOP protein was immunoprecipitated using 200 mM of NaCl in buffer. CHOP phosphorylation was then examined by western blot using a rabbit anti-phospho-serine HRP-conjugated antibody as described before in section 3.2.6.1 according to Table 3.1.

3.2.7. Optimisation of concentration of ERK1/2 pathway inhibitor (PD98059)

In order to optimise the concentration of PD98059, to inhibit Mek kinase activity (Dudley et al., 1995), HCAEC were treated with a range of PD98059 concentrations (0-50 µM) for 30 min. The cells were then incubated with PAR2-AP (20 µM) for 40 min at 37°C. Phosphorylation of ERK1/2 was measured at 40 min post-activation by western blot using an anti-phospho-ERK1/2 antibody and then normalised against the total ERK1/2 antigen, probed with an anti-ERK1/2 antibody according to Table 3.1.

3.2.8. Investigation of the influence of p38 pathway on the release of TF within cell–derived microvesicles

HCAEC (10^5/well) were seeded out into 12-well plates, transfected with wild-type TF plasmid and allowed to express the TF protein over 48 h. The cells were adapted to serum-free medium for 90 min. The cells were then pre-incubated with a range of concentrations of SB202190 (0-100 nM) for 30 min prior to activation with PAR2-AP (20 µM). The medium was removed at 90 and 120 min post-activation, and the microvesicles were isolated by ultracentrifugation and microvesicle density measured using a Zymuphen microvesicle determination kit as described in the general methods section 2.8.1. The TF activity was determined using TF activity assay as described in the general methods section 2.9. The concentrations of TF-associated microvesicles were determined using a TF-specific ELISA assay as in the general methods section 2.8.2.

3.2.9. Examination of the influence of ERK1/2 pathway on the release of TF within cell–derived microvesicles

HCAEC (10^5/well) were seeded out into 12-well plates, transfected with wild-type TF plasmid and allowed to express the TF protein over 48 h. The cells were then incubated with a range of concentrations of PD98059 (0-50 μM) for 30 min. The cells were then activated with PAR2-AP (20 μM). The medium was removed at 90 min post-activation, and the microvesicles were isolated by ultracentrifugation as described in section 2.8. Microvesicles-density was measured using a Zymuphen microvesicle determination kit as described in the general methods section 2.8.1. The TF activity was determined using TF activity assay as described in the general methods section 2.9. The concentrations of TF-associated microvesicles were determined using a TF-specific ELISA assay as in the general methods section 2.8.2.

3.2.10. Examination of the role of p38 on the phosphorylation of Ser258 within the cytoplasmic domain of TF

HCAEC (10^5/well) were seeded out into 12 well-plates, transfected with wild-type TF plasmid and allowed to express the TF protein over 48 h. The cells were adapted to serum-free medium and incubated with a range of SB202190 (0-100 nM) for 30 min before activation with PAR-AP (20 μM). The cells were then lysed in 100 μl of Laemmli's buffer at 120 min post-activation and the protein was separated by 12 % (w/v) SDS-PAGE. The phosphorylation of Ser258 was analysed by western blot as described in section 2.6.3 using a rabbit anti-TF (phospho-Ser258) antibody and then re-probed with a goat anti-rabbit HRP-conjugated antibody according to Table 3.1. Total TF protein was also analysed using a rabbit anti-human TF antibody, followed by a goat anti-rabbit alkaline phosphatase-conjugated antibody according to Table 3.1. The amounts of phospho-Ser258 and total TF antigen were then determined using the ImagJ program and the ratios were calculated.

3.3. Results

Transfection efficiency of HCAEC was measured using Lipofectin reagent, and was consistently 29.5 ± 1.5 % (Fig 3.3). In addition to Lipofectin, other transfection reagents were employed. These include Lipofectamine, FuGENE HD and Metafectene. However, the transfection efficiency using these reagents was deemed too low (data not shown). Consequently, all transfections were carried out using Lipofectin. The plasmids for wild-type or mutant forms of pCMV-XL5-TF were extracted from bacteria *E. coli* strain TB-1 using a midi-prep kit and analysed by agarose gel electrophoresis (Fig 3.4) as described in the general methods section 2.3. HCAEC (10^5) were transfected with pCMV-XL5-TF and permitted to over-express TF over 48 h. The expression of TF protein was confirmed by measuring TF mRNA using RT-PCR. Maximal TF mRNA expression was achieved at 48 h post-transfection (Fig 3.5). TF protein expression in cells transfected with either wild-type or mutant forms of TF plasmid was also detected by western blot analysis using pre-optimised rabbit anti-human TF antibody (Fig 3.6 & 3.7). This increase in TF expression was associated with an increase in TF activity as detected using TF chromogenic assay based on quantifying the activity of the generated thrombin as described in section 2.9.

Figure 3.3. Determination of plasmid transfection efficiency by flow cytometry

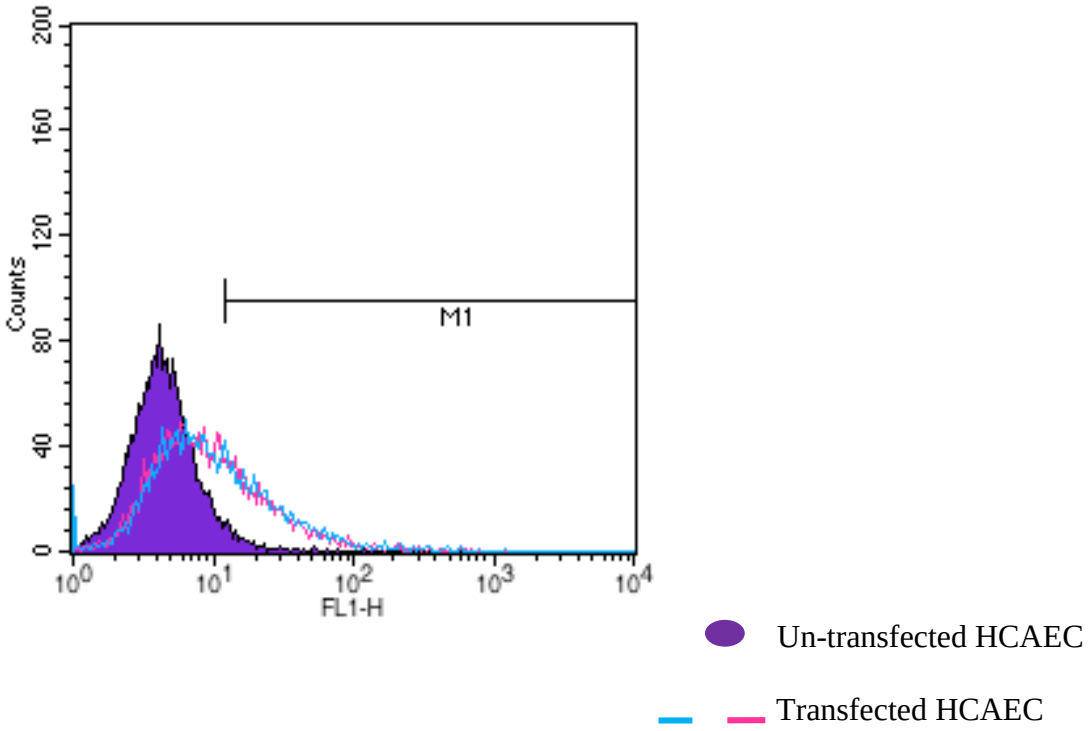

Two sets of HCAEC (10^5/well) were transfected with pCMV-EGFP plasmid and allowed to express the protein over 48 h. The analysis of transfected and un-transfected cells was carried out by flow cytometry. A gate (M1) was set to contain 3 % of the un-transfected sample (solid area); 28 % and 31 % of the pCMV-EGFP transfected cell samples (2 sets) were included in this region. Mean cell fluorescence intensity for the transfected cells samples was 13.7, and 14.6, and 5.09 for the un-transfected control cells. The data are representative of two independent experiments.

Figure 3.4. Analysis of isolated pCMV-XL5-TF plasmid

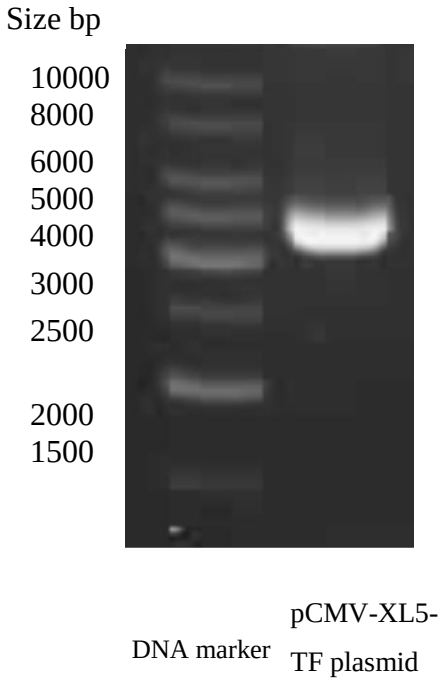

The plasmid DNA was extracted from *E. coli* strain TB-1 using a midi-prep kit and analysed by 0.5 % (w/v) agarose gel electrophoresis. A band representing pCMV-XL5-TF was observed at the expected size of approximately 4700 bp. The figure is representative of 11 experiments.

Figure 3.5. Assessment of expression of TF mRNA in HCAEC using real-time RT-PCR

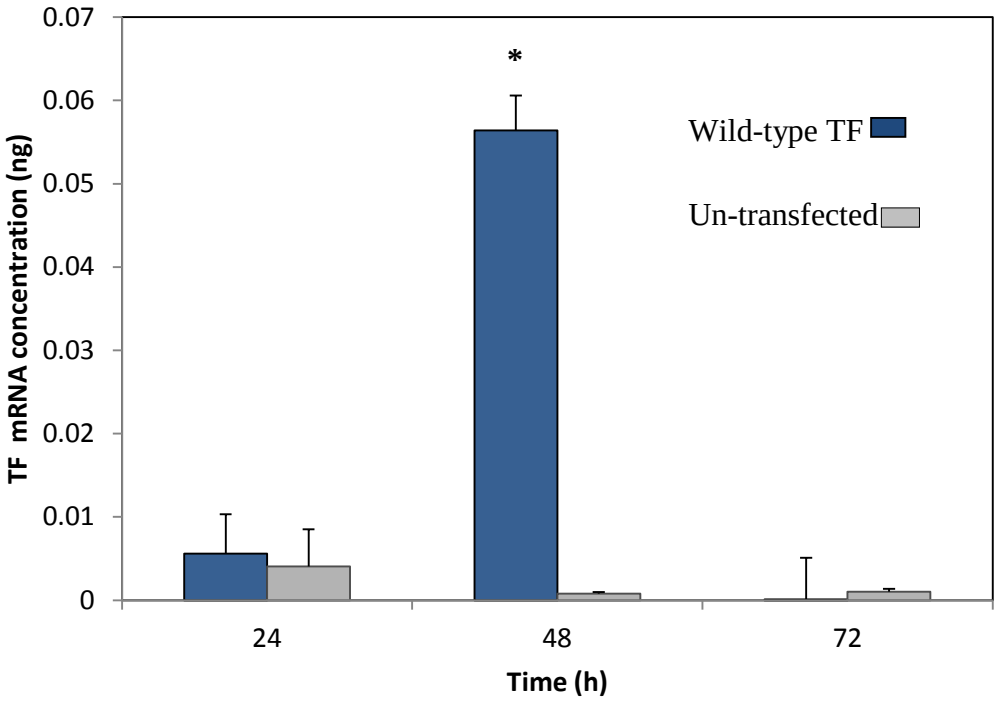

HCAEC (10^5) were transfected with wild-type TF plasmid or un-transfected and harvested at intervals of up to 72 h. Total RNA was isolated from the samples, and TF mRNA concentration was measured by the real-time RT-PCR. The data were normalised against the respective β-actin mRNA in each sample, and TF mRNA quantities determined from the standard curve were prepared using the *in vitro*-transcribed TF mRNA. (Data are representative of 3 independent experiments and expressed as means ± sd, *=P<0.05 vs. un-transfected cells)

Figure 3.6. Optimisation of concentration of rabbit anti-human TF antibody

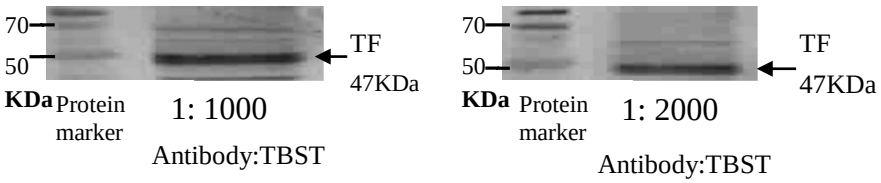

MDA-MB-231 breast cancer cell line was cultured in DMEM medium containing 10 % FCS until 80 % confluence. The cells were then lysed in Laemmli's buffer and two sets of protein samples were separated by 12 % (w/v) SDS/PAGE. After separation, the proteins were transferred onto nitrocellulose membrane. The membrane was then cut into two identical parts containing the sample and protein marker. Each membrane was probed with a rabbit anti-human TF antibody diluted in TBST at dilutions of 1:1000 or 1:2000 and incubated overnight. The membranes were incubated with anti-rabbit alkaline phosphatase-conjugated antibody for 2 h at room temperature, developed with a substrate for alkaline phosphatase and recorded using the GeneSnap program.

Figure 3.7. Assessment of expression of TF protein in transfected HCAEC by western blot

(A)

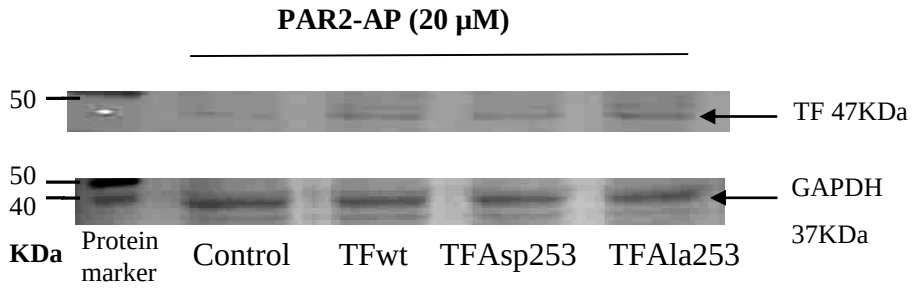

(B)

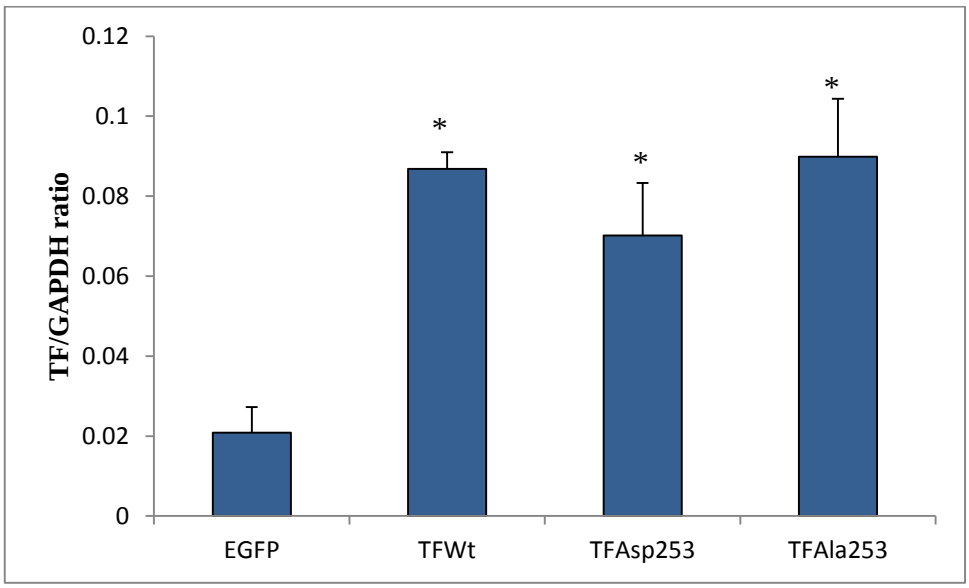

HCAEC (10^5/well) were transfected with 1 µg of wild-type pCMV-XL5-TF plasmid or alternatively, with pCMV-XL5-TF_{Asp235} or pCMV-XL5-TF_{Ala253} or with control plasmid (pCMV-EGFP). The cells were permitted to express TF over 48 h and then activated with PAR2-AP (20 µM). The cells were lysed following 90 min incubation and the proteins were examined by 12 % (w/v) SDS-PAGE. Proteins were transferred onto nitrocellulose membranes and probed for TF using a rabbit anti-human TF antibody and then re-probed for GAPDH using a mouse anti-GAPDH antibody (A). TF expression was compared to GAPDH (B) using the GeneTool program. (Data are representative of 3 independent experiments and expressed as means ± sd, *=P<0.05 vs. control sample)

3.3.1. Time-course analysis of the p38 and ERK1/2 phosphorylation following cellular PAR2 activation

In order to examine the phosphorylation states and duration of activation of p38 and ERK1/2, HCAEC were transfected to express wild-type TF for 48 h and then activated with PAR2-AP (20 µM). The cells were incubated for up to 180 min and analysed using western blot. Phosphorylation states of the p38 and ERK1/2 were examined by loading equal amounts of cell extract, as determined using the Bradford assay. The protein samples were separated by 12 % (w/v) SDS-PAGE. The proteins were transferred to nitrocellulose membrane and probed using antibodies against phospho-p38 (Thr180/Tyr182) and total p38. Analysis of p38 phosphorylation normalised against total p38 showed peak phosphorylation values at 40 and 120 min post-activation with PAR2-AP (Fig 3.8). In contrast, the second p38 phosphorylation peak (at 120 min) was not detectable in un-transfected cells following stimulation with PAR2-AP (Fig 3.9). Phospho-ERK1/2 was also detected using antibodies against phospho-ERK1/2 (Thr202/Tyr204) and normalised against total ERK1/2. Western blot analysis revealed a single ERK1/2 phosphorylation peak at 45 min post-activation with PAR2-AP (Fig 3.10).

3.3.2. Examination of the role of Ser253 within TF, on the phosphorylation of p38 and ERK

The function of phosphorylation of Ser253 within the cytoplasmic domain of TF, on the phosphorylation of p38 and ERK was explored by transfecting HCAEC with wild-type TF plasmid (1µg), or the mutant forms of the plasmid with Asp-substitution at residue 253 (to mimic phosphorylation), or Ala-substitution (to prevent phosphorylation of the residue). The phosphorylation state of p38 and ERK1/2 at 0, 40 and 120 min post activation with PAR2-AP was monitored by western blot. Analysis of the phosphorylation of p38 showed

Figure 3.8. Time-course of the phosphorylation of p38 in transfected HCAEC

(A)

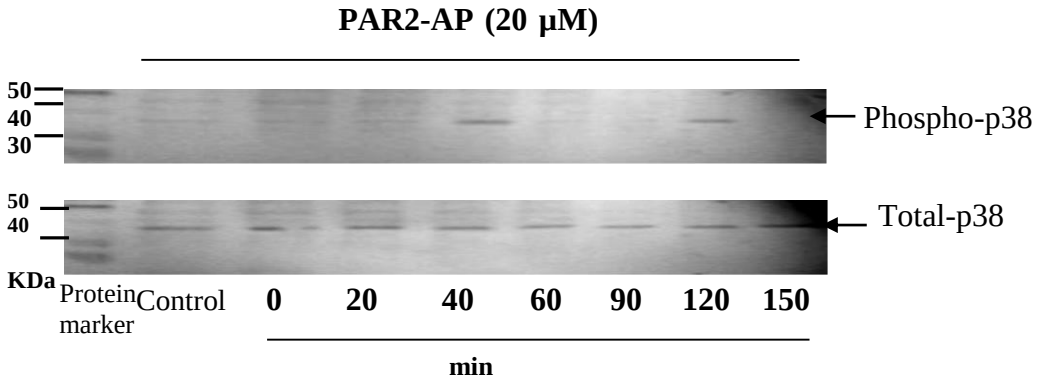

(B)

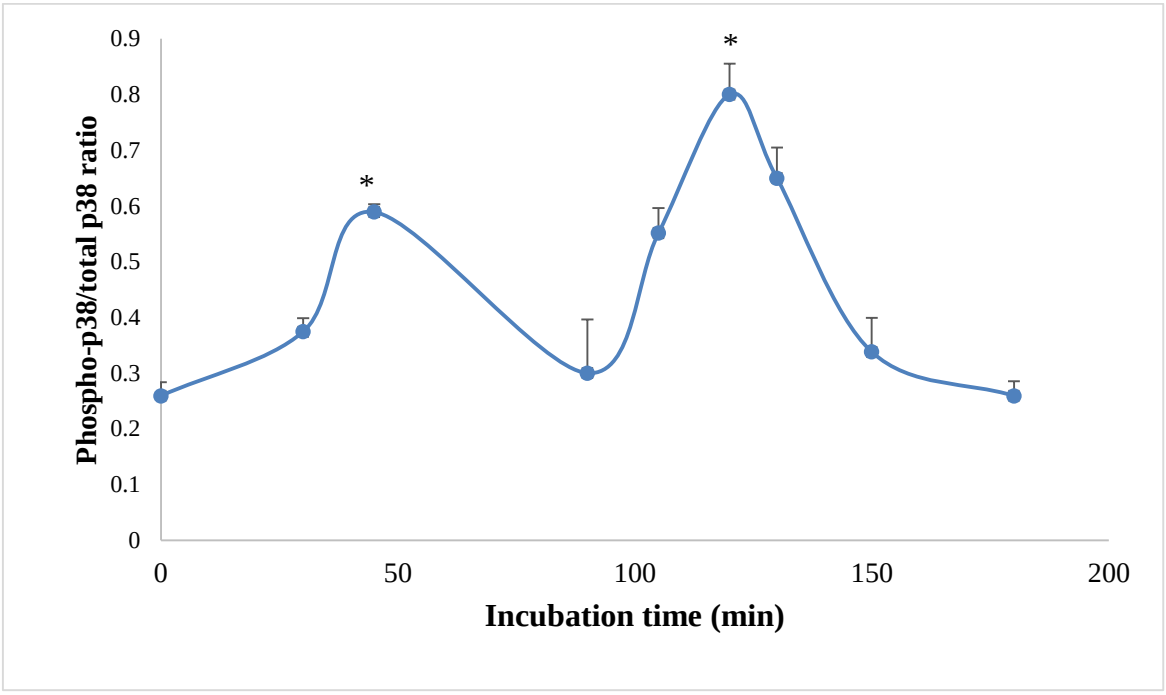

HCAEC (10^5/well) were transfected with wild-type pCMV-XL5-TF plasmid to express TF and allowed to express the TF protein over 48 h. Cells were activated with PAR2-AP (20 µM) and incubated as indicated on the graph. For each time point, cells were lysed and collected. The samples were then analysed by western blot (A) using a mouse anti-human phospho-p38 antibody and a rabbit anti-human total-p38 antibody. The ratio of phospho-p38/total p38 was then determined (B). (Data are representative of 4 independent experiments and expressed as means ± sd, *****=P<0.05 vs. untreated sample)

Figure 3.9. Time-course of the activation of p38 in un-transfected HCAEC

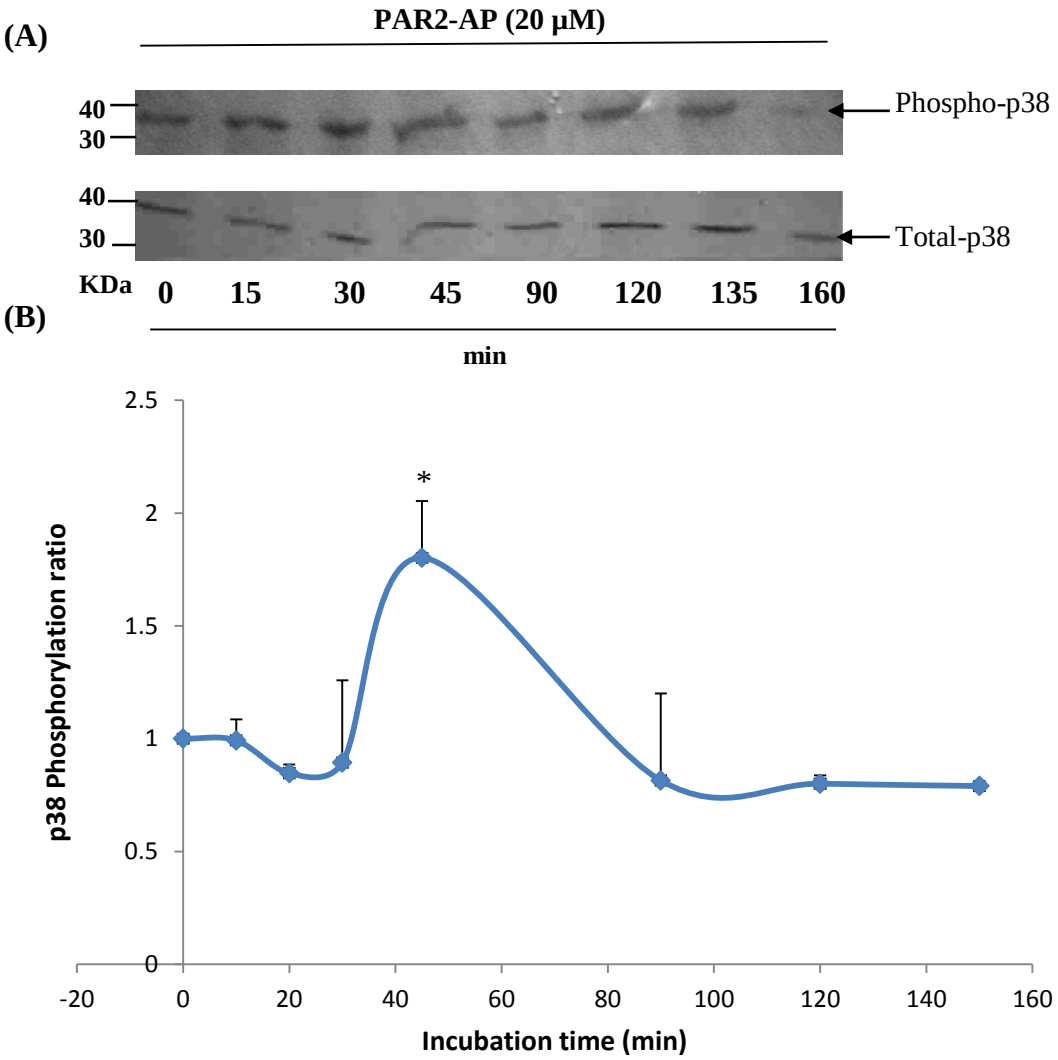

HCAEC (10^5/well) were activated with PAR2-AP (20 µM) and incubated for the indicated times. At each time point, cells were lysed and collected. The samples were then analysed by western blot (A) using a mouse anti-human phospho-p38 antibody and a rabbit anti-human total-p38 antibody. The ratio of phospho-p38/total p38 was then determined (B). Data represent the average of three independent experiments. (Data are representative of 3 independent experiments and expressed as means ± sd, *=P<0.05 vs. untreated sample)

Figure 3.10. Time course of the activation of ERK1/2.

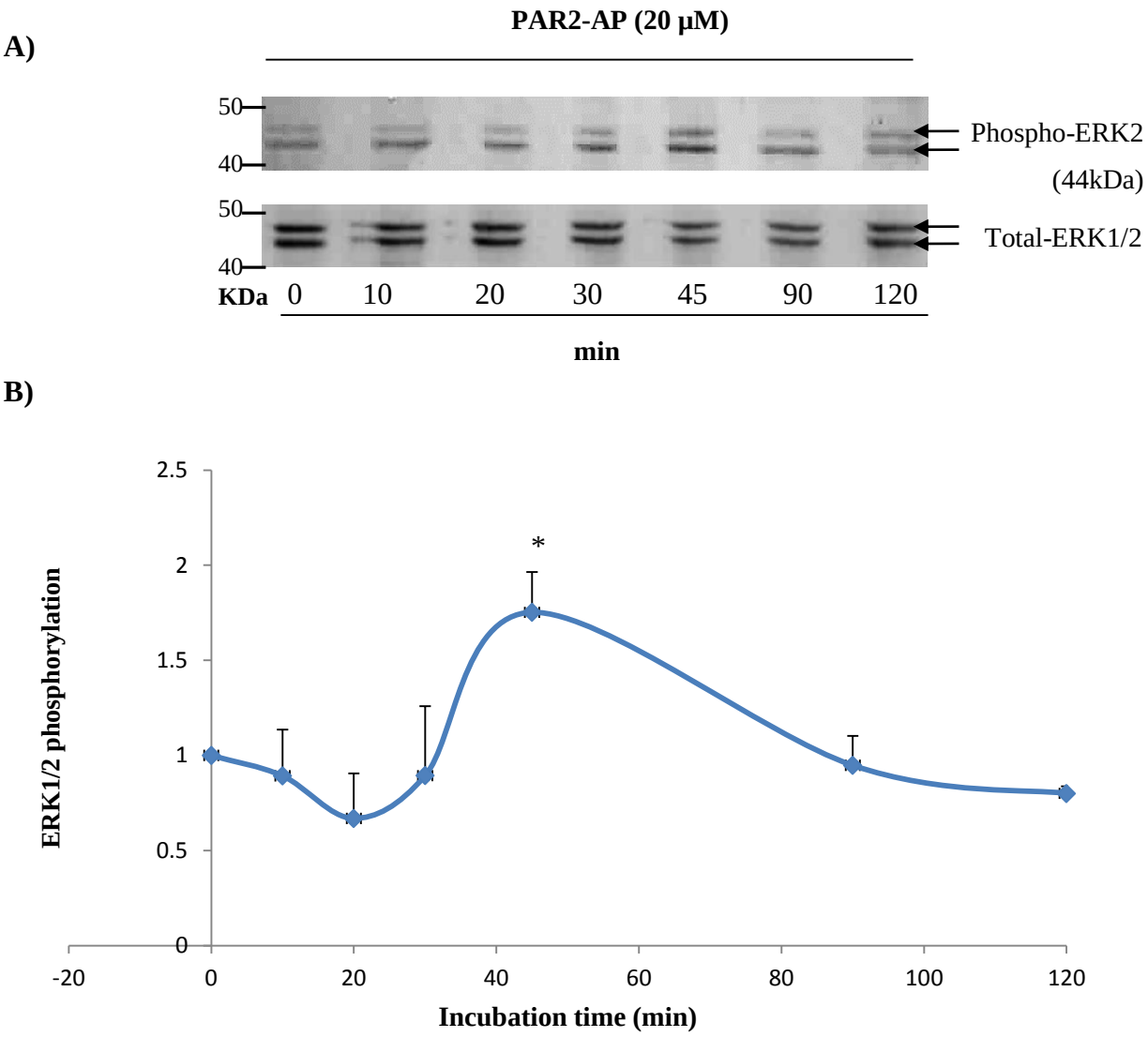

HCAEC (10^5/well) were transfected with wild-type pCMV-XL5-TF plasmid to express TF and allowed to express the TF protein over 48 h. Cells were activated with PAR2-AP (20 µM) and incubated as indicated on the graph. At each time point cells were lysed and collected. The samples were then analysed by western blot (A) using a rabbit anti-human phospho-ERK1/2 antibody and a rabbit anti-human total-ERK1/2 antibody. The ratio of phospho-ERK1/2 /total ERK1/2 was then determined (B). (Data are representative of 4 independent experiments and expressed as means ± sd, *=P<0.05 vs. untreated sample)

that Ala-substitution of Ser253 enhanced the level of p38 phosphorylation significantly at 120 min post-activation with PAR2-AP while Asp-substitution of Ser253 resulted in the reduction of p38 phosphorylation at this time point (Fig 3.11). In contrast, the phosphorylation of ERK1/2 was enhanced in cells expressing the Asp-substituted TF at 40 min while little alteration in ERK1/2 phosphorylation was observed in the cells expressing the Ala-substitution TF at the same time point (Fig 3.12).

3.3.3. Optimisation of concentration of p38 pathway inhibitor (SB202190)

SB202190 has been shown to inhibit p38 kinase activity specifically (Manthey et al., 1998). Therefore, in order to determine the optimal concentration of this inhibitor to achieve maximal inhibition of the p38 pathway, HCAEC were treated with a range of SB202190 concentrations (0-100 nM) for 30 min. The cells were then incubated with PAR2-AP for 40 min at 37°C to induce p38 activation. The effect of SB202190 on p38 activity was determined by measuring the phosphorylation of CHOP and ATF-2, which are known to be phosphorylated by p38 (Wang & Ron, 1996; Raingeaud et al., 1995). Treatment of HCAEC with SB202190 (0-100 nM) resulted in the inhibition of ATF-2 phosphorylation in a concentration-dependent manner (Fig 3.13). However, because ATF-2 can also be phosphorylated by JNK (MAPK) (Gupta et al., 1995) the experiment was discontinued. Treatment of HCAEC with SB202190 (30, 50 and 100 nM) resulted in 83.1 %, 65.9 % and 76.7 % decreases in CHOP phosphorylation respectively (Fig 3.14). However, complete inhibition was not achieved with any of the concentrations used.

Figure 3.11. Analysis of the phosphorylation of p38 in HCAEC transfected to express wild-type and mutant forms of TF

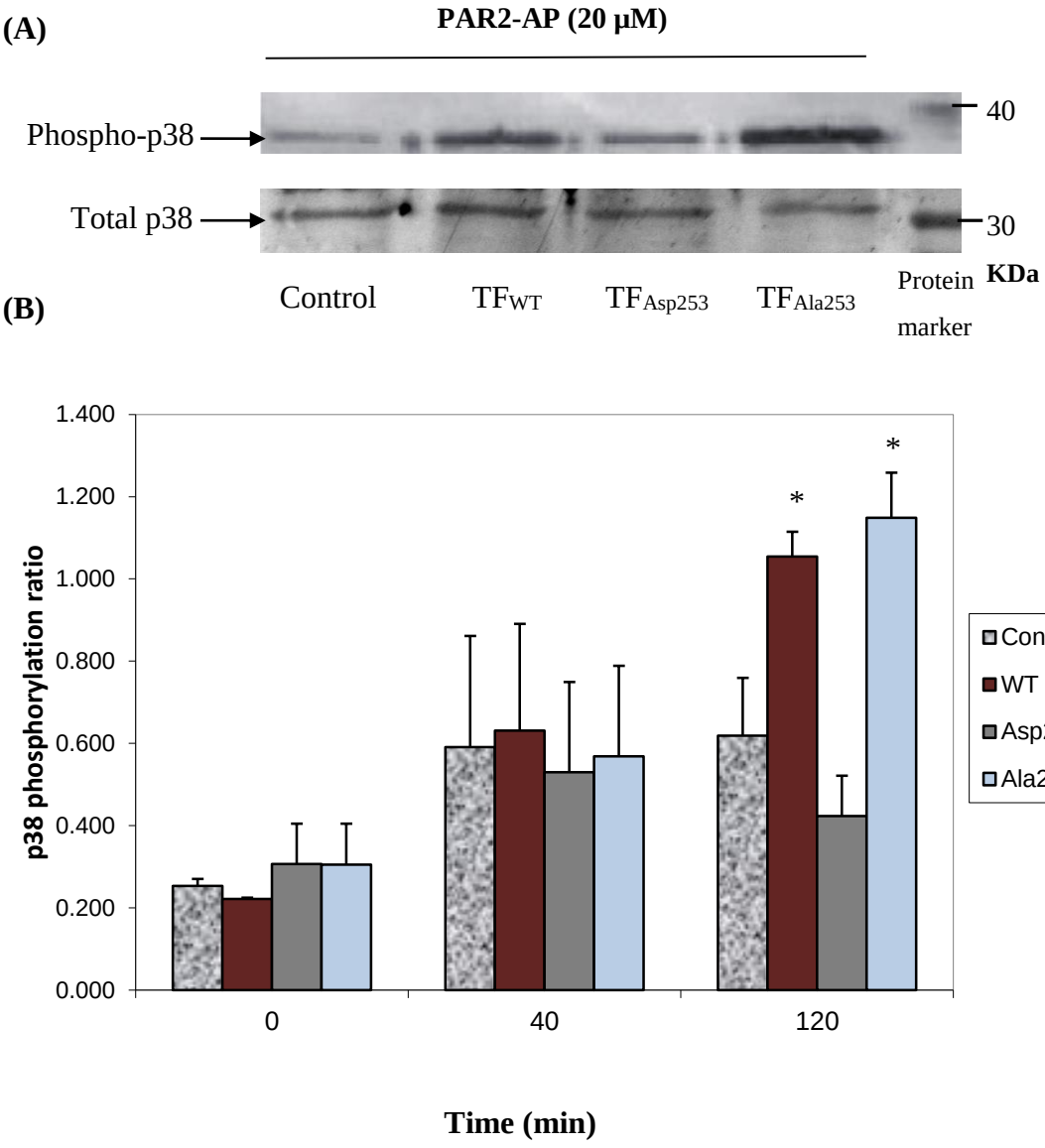

HCAEC (10^5/well) were transfected with wild-type pCMV-XL5-TF plasmid or, alternatively, with Ala- or Asp-substituted TF (at Ser 253). The cells were then activated with PAR2-AP (20 µM) and incubated for 0, 45 or 120 min. p38 phosphorylation was measured by western blot (A) using antibodies against phospho-p38 and then normalised against the respective total p38 (B). The gel illustrates the blot at 120 min post-activation. (Data are representative of 4 independent experiments and expressed as means ± sd, *=P<0.05 vs. untreated sample)

Figure 3.12. Analysis of the phosphorylation of ERK1/2 in HCAEC transfected to express wild-type and mutant forms of TF

(A)

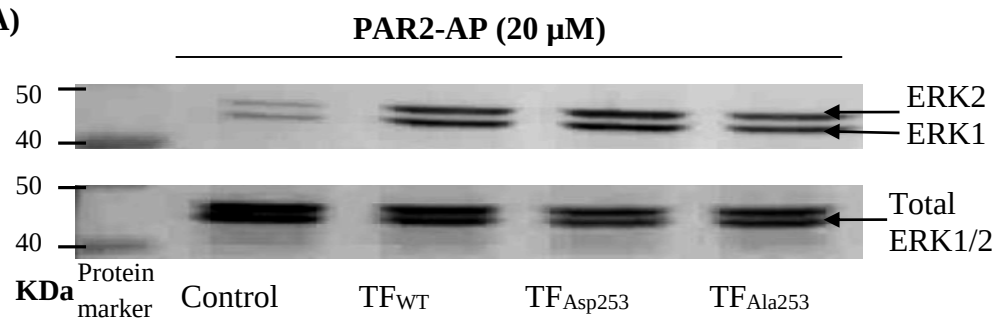

(B)

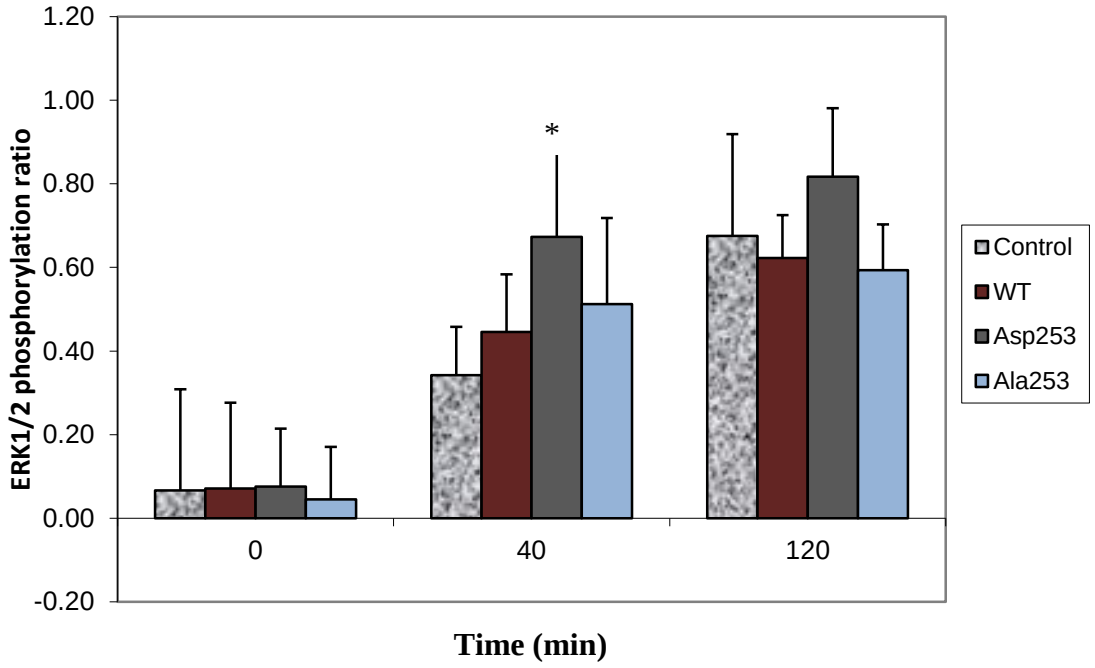

HCAEC (10^5/well) were transfected with wild-type pCMV-XL5-TF plasmid or alternatively, with Ala- or Asp-substituted TF (at Ser 253). The cells were then activated with PAR2-AP (20 µM) and incubated for 0, 45 or 120 min. ERK1/2 phosphorylation was measured by western blot (A) using antibodies against phospho-ERK1/2 and then normalised against the respective total ERK1/2 (B). The gel illustrates the blot at 40 min post-activation. (Data are representative of 3 independent experiments and expressed as means ± sd, *=P<0.05 vs. respective untreated sample)

Figure 3.13. Optimisation of the inhibition of p38 activity by SB202190 by measuring the phosphorylation of downstream substrates of p38 ATF-2

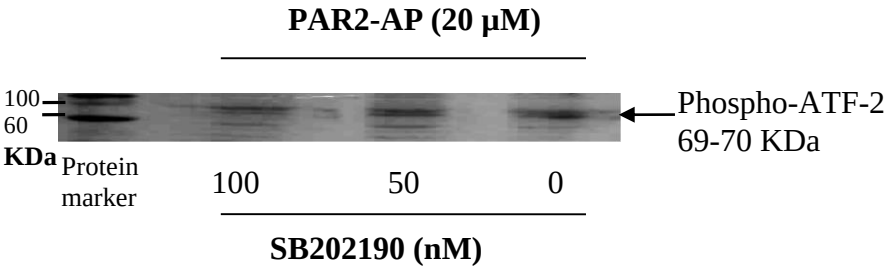

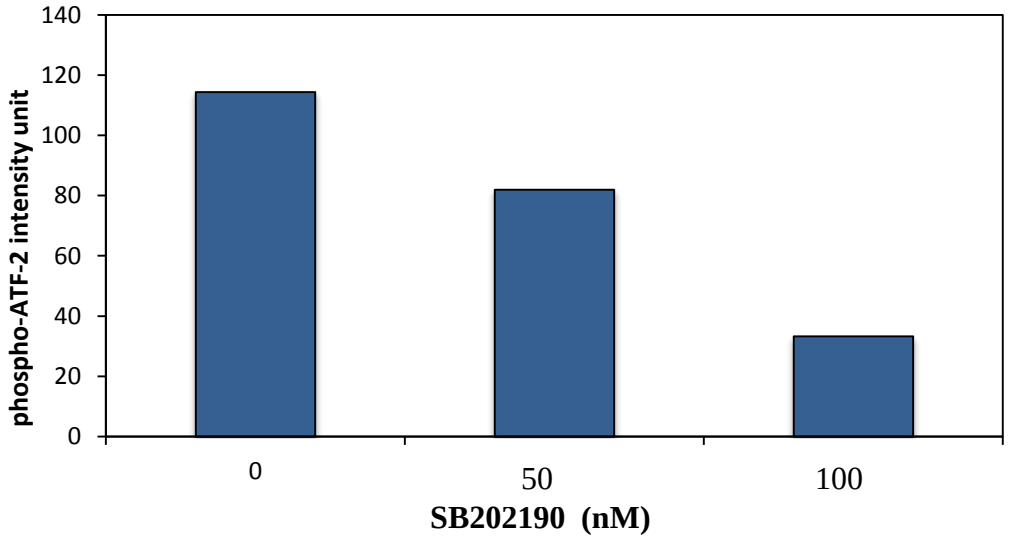

HCAEC (10^5/well) were seeded out into 12-well plates. The cells were pre-incubated with a range of SB202190 concentrations (0-100 nM) for 30 min prior to activation with PAR2-AP (20 µM) and incubated for a further 40 min. Phosphorylation of ATF-2 was analysed by western blot using an anti-phospho-ATF-2 antibody. The intensity of the bands were measured using the ImageJ program and blotted againsit SB202190 concentrations. ATF-2 can also be phosphorylated by other MAPK therefore, the experiment was discontinued (Data are representative of 1 experiment)

Figure 3.14. Optimisation of the inhibition of p38 activity by SB202190 by measuring the phosphorylation of downstream substrates of p38 CHOP

(A)

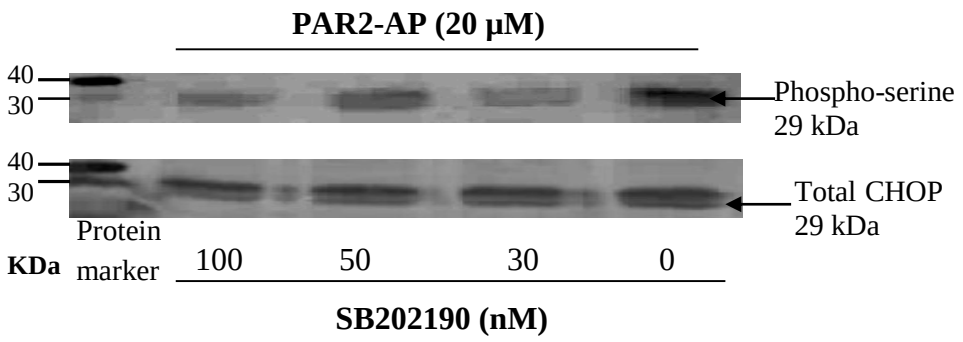

(B)

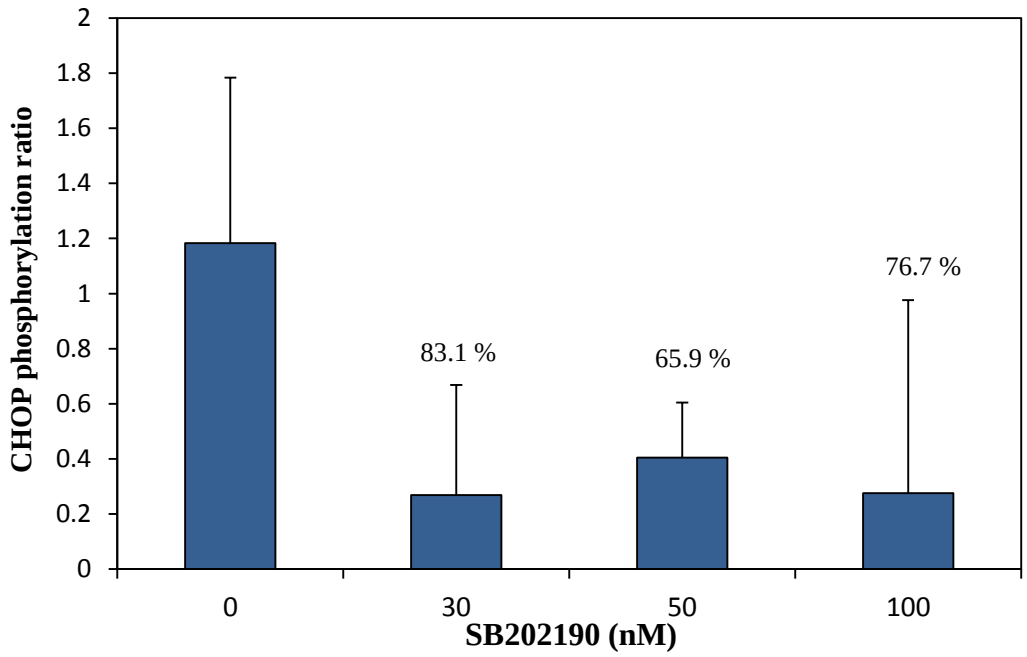

HCAEC (10^5/well) were seeded out into 12-well plates. The cells were pre-incubated with a range of SB202190 concentrations (0-100 nM) for 30 min prior to activation with PAR2-AP (20 µM) and incubated for 40 min. To analyse the phosphorylation of CHOP, Ser phosphorylation was examined by western blot (A) using an anti-phospho-serine antibody. The bands were recorded and the CHOP protein band was then identified using an anti-CHOP antibody. The ratio of phospho-serine in the CHOP band (B) was then determined. (Data are representative of 3 independent experiments and expressed as means ± sd)

To further confirm these data, CHOP was immunoprecipitated and then analysed by western blot to detect serine phosphorylation. The optimum salt concentration for CHOP immunoprecipitation was determined to be 200 mM (Fig 3.15). CHOP protein was targeted using a mouse anti-CHOP antibody and captured with protein G magnetic microbeads. The eluted protein was then separated by 12 % (w/v) SDS PAGE, and the level of CHOP phosphorylation was determined by western blot using a rabbit anti-phospho-serine antibody. Treatment of HCAEC with SB202190 (30 nM) showed the inhibition in CHOP phosphorylation in cells incubated with SB202190 compared to control cells (Fig 3.16).

3.3.4. The influence of p38 on the phosphorylation of Ser258 within the cytoplasmic domain of TF

To study the ability of p38 to phosphorylate TF at Ser258, HCAEC were transfected to over-express wild-type TF over 48 h. The cells were adapted to serum-free medium for 90 min. The cells were then incubated with a range of concentrations of SB202190 (0-100 nM) for 30 min before activation with PAR-AP (20 µM) for a further 120 min. The phosphorylation of TF at Ser258 was determined by western blot using antibody against phospho-TF at Ser258 according to Table 3.1, and the values of Ser258 phosphorylated TF were normalised against the total TF. Incubation of cells with increasing concentrations of p38 inhibitor (0-100 nM) resulted in decreased Ser258 phosphorylation (Fig 3.17).

Figure 3.15. Optimisation of the salt concentration for the immunoprecipitation of CHOP

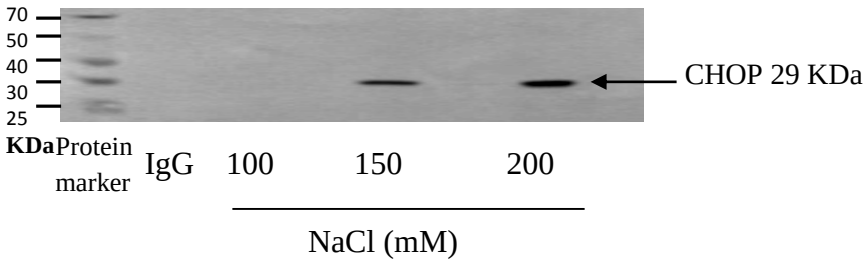

HCAEC were cultured in 25 cm^2 flasks. The cells were lysed in lysis buffer containing 25 mM Tris-HCl pH 7.4, 150 mM NaCl, 2 mM EDTA, 0.5 % (w/v) CHAPS, 1 % (v/v) protease inhibitor cocktail on ice. The cell lysates were then incubated with either anti- mouse IgG antibody or mouse anti-CHOP antibody for 1 h. The cell lyasates were then incubated with protein G magnetic-microbeads overnight at 4 °C. Cell lysates containing equal amounts of CHOP protein were loaded onto a separate µ-MACS column attached to a magnet on the MACS separator and washed with 200 µl washing buffer containing either 100, 150 or 200 mM NaCl. The samples were then eluted in hot Laemmli's buffer in a magnetic separator. Immunoprecipitated CHOP was detected by western blot using a rabbit anti-CHOP antibody. (The gel is representatives of one experiment)

Figure 3.16. Inhibition of the phosphorylation of CHOP by SB202190

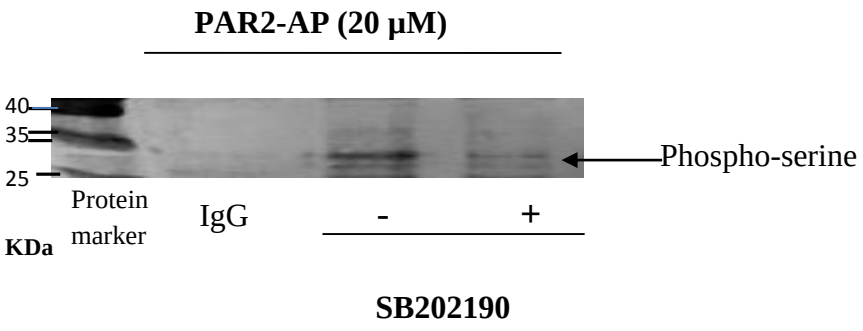

HCAEC were cultured in two 25 cm^2 flasks. The cells were incubated either with SB202190 (30 nM) or with an equivalent amount of DMSO as a control for 30 min. The cells were then incubated with PAR2-AP (20 µM) for 40 min. The cell lysates were prepared and CHOP protein was immunoprecipitated using mouse anti-CHOP antibody. CHOP phosphorylation was determined by western blot using a rabbit phospho-serine antibody. (The gel is representatives of 2 independent experiments)

Figure 3.17. Effect of SB202190 on Ser258-TF phosphorylation in HCAEC

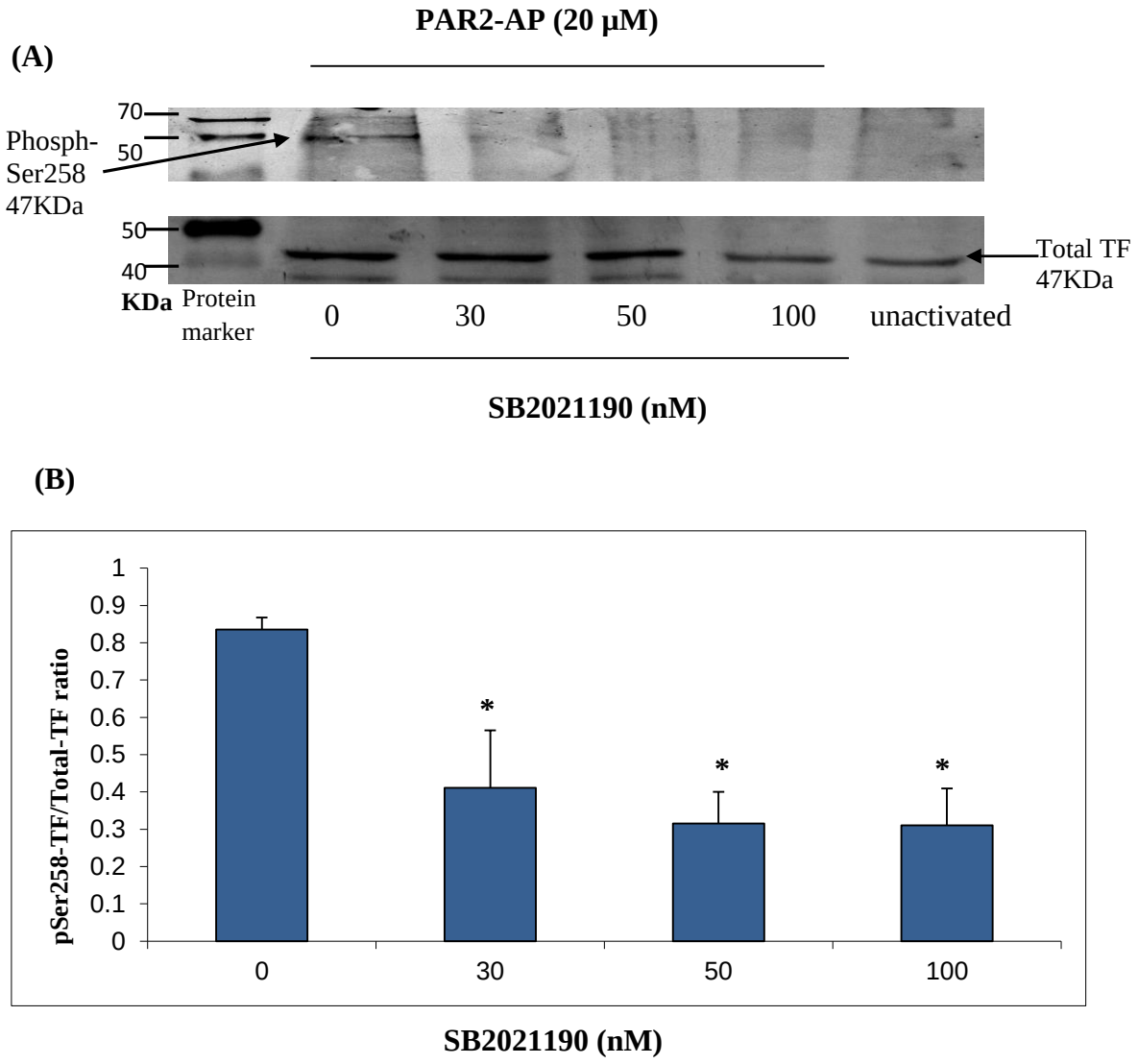

HCAEC (10^5/well) were seeded out into 12-well plates and transfected with wild-type pCMV-XL5-TF plasmid to express TF and allowed to express the TF over 48 h. Cells were then incubated with a range of SB202190 concentrations (0-100 nM) for 30 min prior to activation with PAR2-AP (20 µM). Cells were collected after 120 min incubation and assayed for Ser258 phosphorylation by western blot (A) using an anti-phospho-Ser258 antibody. Total TF antigen was then measured and the ratios of phospho-Ser258 to total TF antigen (B) were determined. (Data are representative of 3 independent experiments and expressed as means ± sd, *=P<0.05 vs. untreated sample)

3.3.5. The outcome of the inhibition of p38 pathway on the release of TF within cell-derived microvesicles

In order to examine the outcome of p38 inhibition on TF release within microvesicles, HCAEC were transfected to express wild-type TF. The cells were then incubated with a range of concentrations of SB202190 (0-100 nM) for 30 min prior to activation with PAR2-AP (20 µM). The microvesicles were isolated at 90 and 120 min following activation. The density of the released microvesicles was not significantly altered (Fig 3.18). TF release from cells was marginally reduced following incubation with SB202190 at 90 min. In contrast, the level of released TF was increased significantly at 120 min (Fig 3.19).

3.3.6. Optimisation of concentration of ERK1/2 pathway inhibitor (PD98059)

To optimise the concentration of PD98059, needed to inhibit Mek kinase activity (Dudley et al., 1995), HCAEC were treated with a range of PD98059 concentrations (0-50 µM) for 30 min. The cells were then incubated with PAR2-AP (20 µM) for 40 min at 37°C. The effect of PD98059 was examined by measuring the phosphorylation of ERK1/2. Incubation of the cells with PD98059 (0-50 µM) resulted in a significant inhibition in ERK1/2 phosphorylation at a concentration of 30 µM (88.9 %) (Fig 3.20).

3.3.7. The outcome of the inhibition of ERK1/2 pathway on the release of TF within cell–derived microvesicles

The influence of ERK1/2 activity on the release of TF within microvesicles was examined by inhibiting the ERK1/2 pathway prior to activation with PAR2-AP. HCAEC were transfected to express wild-type TF and incubated for 48 h to allow TF expression.

Figure 3.18. Effect of inhibition of the p38 pathway on microvesicles' release from HCAEC

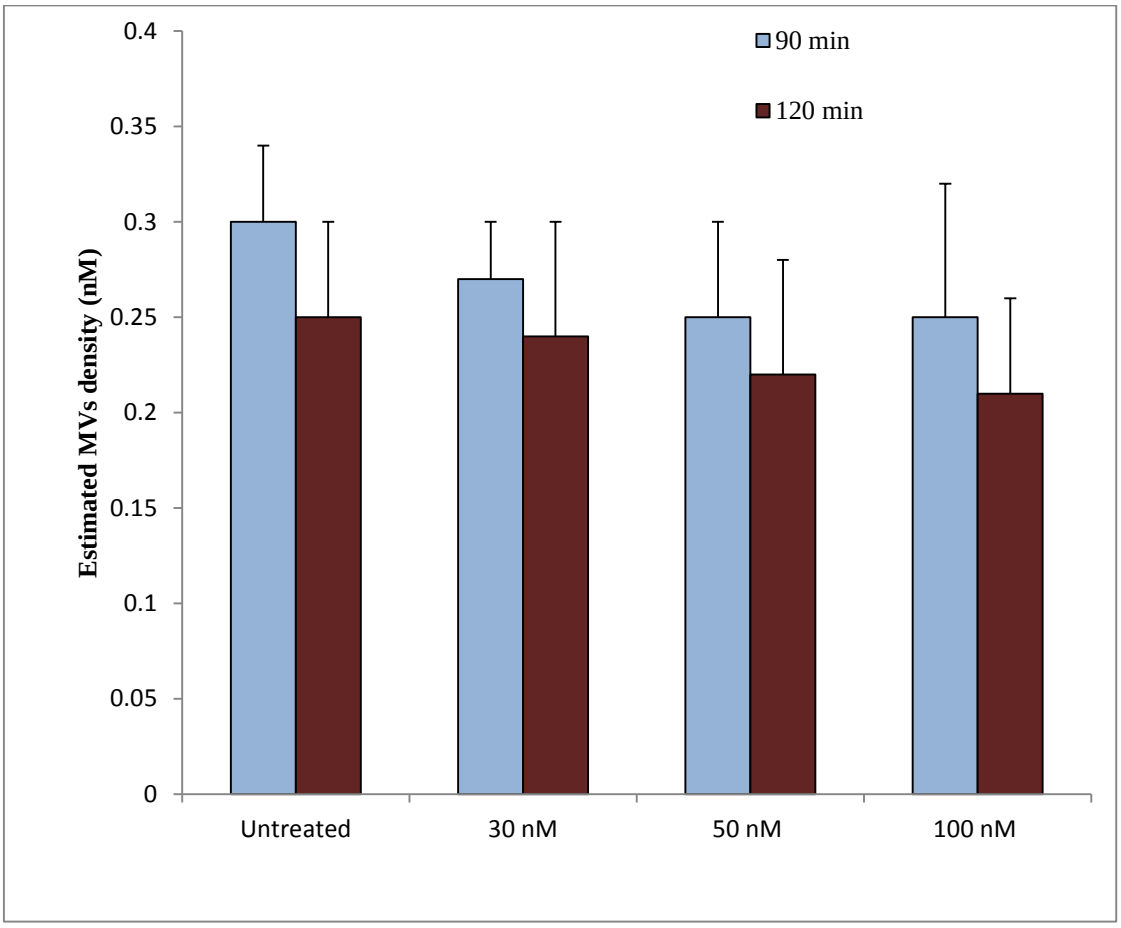

HCAEC (10^5/well) were seeded out into 12 well-plates and transfected with wild-type TF plasmid. The cells were pre-incubated with a range of SB202190 concentrations (0-100 nM) for 30 min prior to activation with PAR2-AP (20 µM). The medium was removed at 90 and 120 min post-activation, the microvesicles were isolated by ultracentrifugation and microvesicle density was measured using a Zymuphen microvesicle assay. (Data are representative of 3 independent experiments and expressed as means ± sd)

Figure 3.19. Effect of inhibition of the p38 pathway on TF release within microvesicles

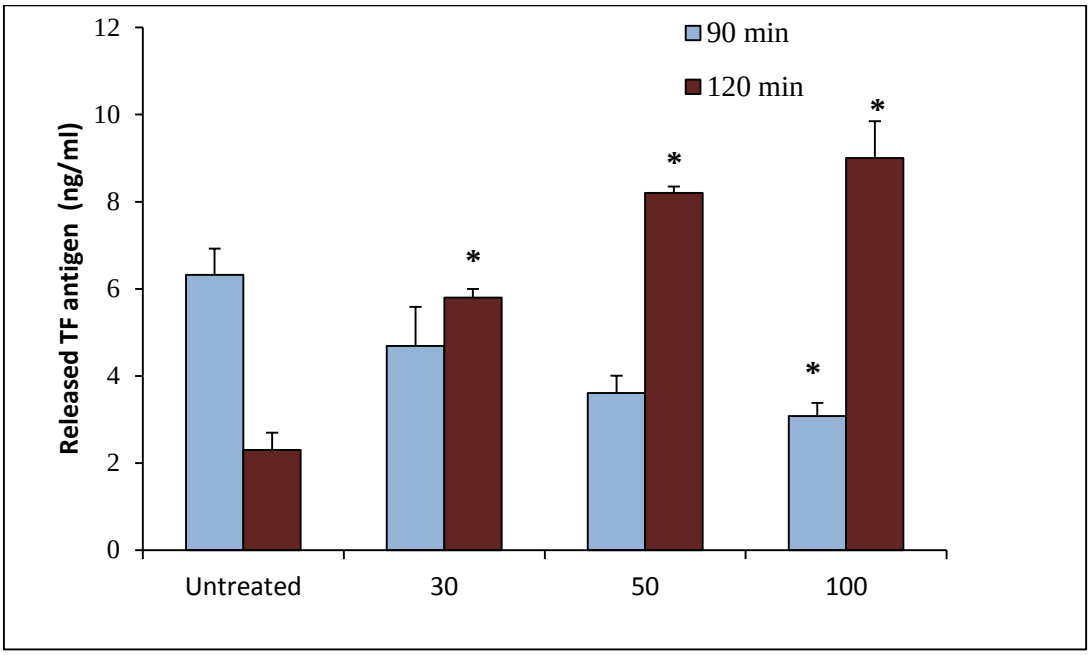

HCAEC (10^5/well) were seeded out into 12 well-plates and transfected with wild-type TF plasmid. The cells were pre-incubated with a range of SB202190 concentrations (0-100 nM) for 30 min prior to activation with PAR2-AP (20 µM). The medium was removed at 90 and 120 min post-activation, the microvesicles were isolated by ultracentrifugation, and microvesicle and microvesicle-associated TF antigen was determined by TF-ELISA. (Data are representative of 3 independent experiments and expressed as means ± sd, *=P<0.05 vs. untreated sample)

Figure 3.20. Effect of PD98059 on the phosphorylation of ERK1/2 by Mek-1

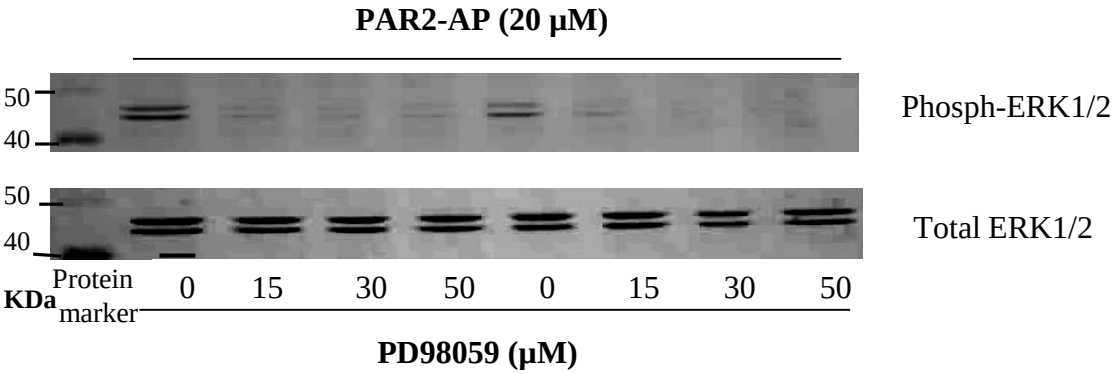

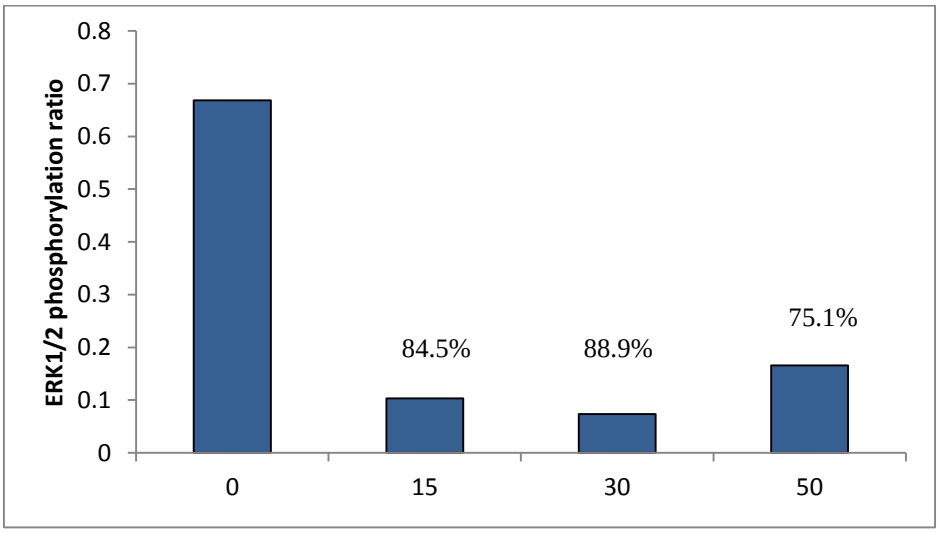

HCAEC (10^5/well) were seeded out into 12-well plates and transfected with wild-type TF plasmid and allowed to express the TF protein over 48 h. The cells were pre-incubated with a range of concentrations of PD98059 (0-50µM) for 30 min prior to activation with PAR2-AP (20 µM). Phosphorylation of ERK1/2 was measured at 40 min post-activation by western blot using an anti-phospho-ERK1/2 antibody and then normalised against the total ERK1/2 antigen, probed with an anti-ERK1/2 antibody. Data are representative of the average of two experiments in duplicate.

The cells were incubated with a range of concentrations of PD98059 (0-50 μM) for 30 min. The cells were then activated with PAR2-AP (20 μM). The microvesicles were isolated at 90 min following activation. Incubation of cells with higher concentrations of PD98059 marginally decreased the level of microvesicles' release at 90 min (Fig 3.21), whereas, incubation of the cells with higher concentrations of PD98059 resulted in not significant increases in the level of TF release (Fig 3.22).

3.4. Discussion

Human endothelium releases microvesicles carrying TF, which are associated with an increased risk of thrombosis. These microvesicles have been shown to induce thrombosis through a TF-dependent mechanism (Combes et al., 1999; Nomura et al., 2008). The role of serine residues within the cytoplasmic domain of TF in incorporation and release of TF as microvesicles has recently been demonstrated (Collier & Ettelaie, 2011). The phosphorylation of Ser253 within TF, together with other PAR2-initiated mechanisms, act as an "on switch" to release TF. Recently, a study by Collier et al., (2013) showed that the binding of the cytoskeletal protein filamin-A to the cytoplasmic domain of TF is crucial for the incorporation of TF into microvesicles. The activation of PAR2 also initiates the activation of a proline-directed kinase that was unidentified at the time of this work, and which was assumed to be capable of phosphorylating Ser258 within the cytoplasmic domain of TF (Dorfleutner & Ruf, 2003). In this study, experiments were focused on the investigation of the role of TF on the phosphorylation state of the MAPK enzymes (p38 and ERK1/2). In addition, an attempt was made to determine the possible role of these enzymes in regulation of TF release through phosphorylation of TF-Ser258.

Figure 3.21. Effect of inhibition of the ERK1/2 pathway on microvesicles' release from HCAEC

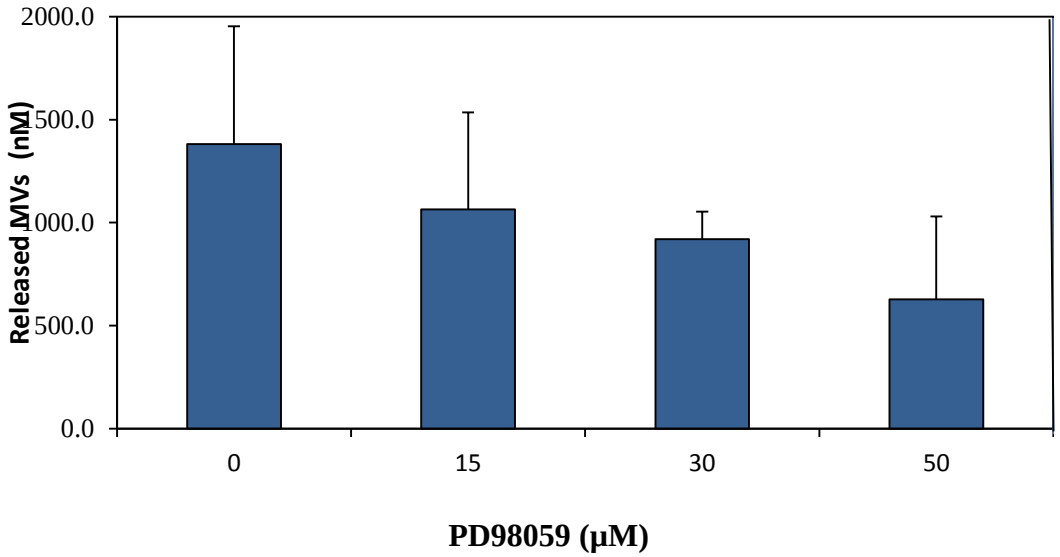

HCAEC (10^5/well) were seeded out into 12-well plates, transfected with wild-type TF plasmid and allowed to express the TF protein over 48 h. The cells were pre-incubated with a range of concentrations of PD98059 (0-50 µM) for 30 min prior to activation with PAR2-AP (20 µM). The medium was removed at 90 min post-activation, the microvesicles were isolated by ultracentrifugation, and microvesicle density measured using a Zymuphen microvesicle assay. (Data are representative of 3 independent experiments and expressed as means ± sd, *=P<0.05 vs. untreated sample)

Figure 3.22. Effect of inhibition of the ERK1/2 pathway on TF release within microvesicles

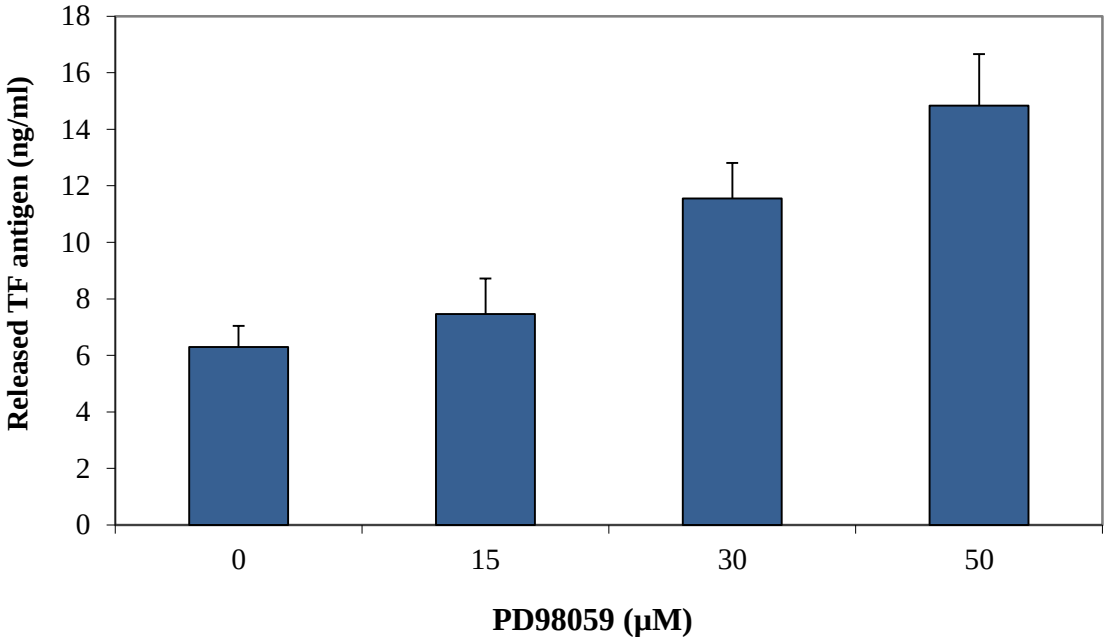

HCAEC (10^5/well) were seeded out into 12-well plates, transfected with wild-type TF plasmid and allowed to express the TF protein over 48 h. The cells were pre-incubated with a range of concentrations of PD98059 (0-50µM) for 30 min prior to activation with PAR2-AP (20 µM). The medium was removed at 90 min post-activation, the microvesicles were isolated by ultracentrifugation, and microvesicle-associated TF antigen was determined by TF-ELISA. (Data are representative of 3 independent experiments and expressed as means ± sd, *=P<0.05 vs. untreated sample)

In this investigation, HCAEC were used as a model for studying the systematic regulation of the phosphorylation and release of TF. This is because HCAEC do not constitutively express TF or readily release microvesicles (Collier & Ettelaie, 2010). Therefore, HCAEC allow the study of mutant forms of TF with minimal interference from the wild-type cellular TF. In addition, it has been shown that HCAEC express PAR2 on the cell surface (Collier & Ettelaie, 2010).

Throughout this study, HCAEC were transfected with wild-type or mutant forms of pCMV-XL5-TF plasmid to express TF in these cells. The TF expression was confirmed by measuring TF mRNA (Fig 3.5) and TF protein expression (Fig 3.7). Initially, the ability of TF to induce p38 and ERK1/2 MAPK phosphorylation was investigated. Both p38 and ERK1/2 phosphorylation were observed in HCAEC expressing TF after PAR2 activation. The initial early peak of p38 phosphorylation at 40 min (Fig 3.8) was concurrent with ERK1/2 phosphorylation (which peaked at 45 min) (Fig 3.10). However, while ERK1/2 activation was diminished beyond 90 min, a second p38 phosphorylation peak was observed at approximately 120 min post-activation. The early activation peaks for p38 and ERK1/2 were probably a consequence of PAR2 activation since these were also present in un-transfected, PAR2-activated cells. This is in agreement with previous studies showing the ability of PAR2 to induce the phosphorylation of ERK and p38 MAPK in a relatively transient manner (Kanke et al., 2001; Ott et al., 2005). The late activation of p38 was, however, absent in un-transfected HCAEC (Fig 3.9). This indicates that the activation of p38 may be promoted by TF itself following activation with PAR2-AP and is in agreement with the suggested role of the cytoplasmic domain of TF in inducing the phosphorylation of p38 (Ott et al., 2005). However, the mechanism whereby TF directly activates p38 remains under investigation. The influence

of TF-Ser253 phosphorylation on the activation of the p38 and ERK was investigated next. p38 phosphorylation was enhanced in the absence of Ser253 phosphorylation (Ala-substituted) while Asp-substitution (to mimic phosphorylation) reduced the level of p38 phosphorylation (Fig 3.11). In contrast, expression of Asp253-substituted TF enhanced the phosphorylation of ERK1/2 (Fig 3.12). These data suggest that prevention of TF release through Ala-substitution of residue 253 enhanced the second phase of p38 activity while acceleration of TF release through Asp-substitution eliminated this peak (Fig. 3.11). Therefore, it was hypothesised that the second wave of activation of p38 is dependent on the presence of TF protein itself, but subsequent to induction of PAR2. This is consistent with a previous report suggesting that the phosphorylation of Ser258 within human TF is both regulated by TF itself and requires the activation of PAR2 (Collier & Ettelaie, 2011). In addition, it has been shown that the de-palmitoylation of Cys245 is a precursor event for the tandem phosphorylation of the two serine residues (Bach et al., 1988; Zioncheck et al., 1992; Dorfleutner & Ruf, 2003). This event may in effect permit the relocation of TF out of cellular regions, or the mobilisation of TF to specific membrane regions, exposing the cytoplasmic domain to target kinases. Prolonged activation of the p38 pathway is thought to be the hallmark of induction of p38-mediated cell apoptosis, while short durations of activity often coincide with cell proliferation (Dolado & Nebreda, 2008). Furthermore, the increase in ERK activity coincided with the first p38 activity peak and preceded the release of TF into microvesicles (90 min) (Collier & Ettelaie, 2011). Therefore, it is possible that the release of TF in effect has an anti-inflammatory/anti-apoptotic influence on the parent cell and is mediated through transient phosphorylation of both ERK and p38 pathways. In contrast, it appears that the persistence of TF in cells, following activation, promotes the prolonged activation of p38, which may lead to inflammatory responses and apoptosis (Dolado & Nebreda, 2008).

In addition to the above, the possibility of p38 being responsible for the phosphorylation of Ser258 within TF and preventing its incorporation into cell-derived microvesicles was explored. SB202190 was shown to be able to decrease CHOP phosphorylation at concentrations as low as 30 nM; however, complete inhibition of CHOP phosphorylation was not achieved (Fig 3.14). This is because CHOP may also be phosphorylated by casein kinase 2 (Ubeda & Habener, 2003). Maximal release of TF is at 90 min and declines by 120 min (Collier & Ettelaie, 2011). Inhibition of p38 pathway by SB202190 resulted in the inhibition of phosphorylation of TF at Ser258 (Fig 3.17). This was concurrent with the maintained level of release of TF within microvesicles at 120 min (Fig 3.19). This is in agreement with data showing that mutation of Ser258 to Ala prevents the inhibition of the release of TF at 120 min, while Asp-substitution of this residue suppresses the release of TF (Collier & Ettelaie, 2011). Therefore, it may be suggested that once sufficient amounts of TF are released, the process is self-regulated by a mechanism that involves p38 activation and is itself activated during the TF release phase (Fig 3.23). Interestingly, at a concentration of 30 nM, SB202190 significantly inhibited the phosphorylation of TF at Ser258 by p38 (Fig 3.17). This suggests that the Ser258 phosphorylation is associated with the activities of p38α kinase, since p38β activity is not affected by this concentration of SB202190 (Davies et al., 2000). However, although the phosphorylation of Ser258 was largely inhibited, complete suppression was not achieved. This is possibly because of activation of other kinases such as ERK1/2, which may also be capable of TF phosphorylation under different cellular conditions. In addition, ERK1/2 was only capable of phosphorylating TF at Ser258 to low extents (Ettelaie et al., 2013). This may explain the marginal increase in the release of TF within microvesicles, following the inhibition of the ERK1/2 pathway (Fig 3.22).

In conclusion, this study has shown that transient short-term activation (first peak) of p38 is induced by PAR2 and the prolonged activation of p38 (second peak) is promoted by TF. In contrast, transient ERK phosphorylation is induced by PAR2 but not by TF. In addition, p38 appears to be the PDK responsible for the phosphorylation of Ser258 within TF and for the regulation of the release of TF in microvesicles.

Figure 3.23. Proposed mechanism for the regulation of TF release into microvesicle by p38

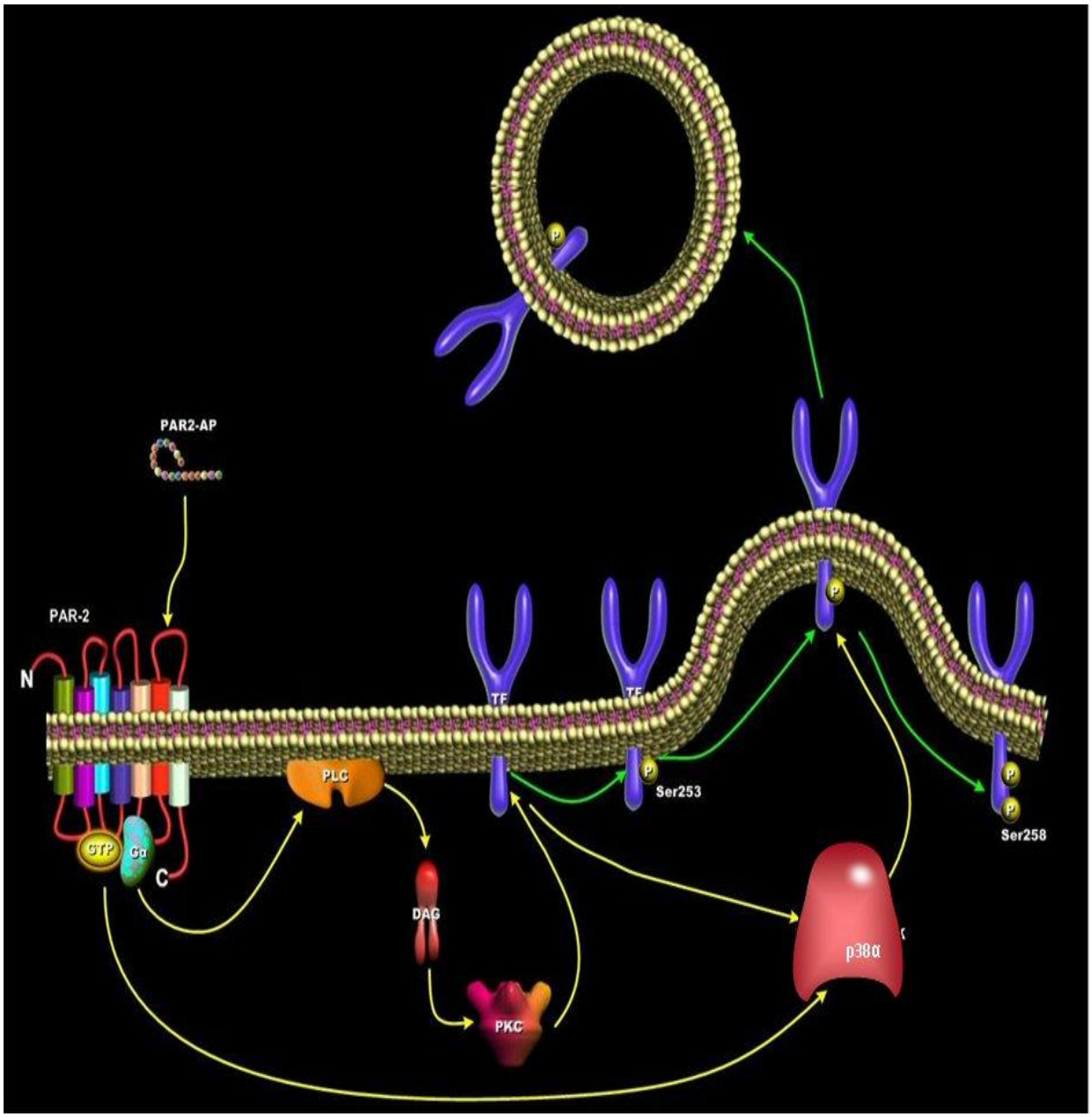

The incorporation of TF into microvesicles is mediated by the phosphorylation of the TF cytoplasmic serine residues. Activation of PAR2 results in phosphorylation of Ser253 within TF, which leads to the release of TF within microvesicles. This process also initiates the activation of p38, which leads to the phosphorylation of Ser258 within TF and the termination of TF release.

CHAPTER 4

The influence of TF accumulation on endothelial cell proliferation and apoptosis

4.1. Introduction

Phosphorylation of the cytoplasmic domain of TF is essential for incorporation and release of TF into microvesicles. The phosphorylation of Ser258 within the cytoplasmic domain of TF terminates the incorporation of TF into microvesicles. Furthermore, the phosphorylation of Ser258 is dependent on the phosphorylation of Ser253 (Collier & Ettelaie, 2011). The results obtained from the previous chapter demonstrate that p38 MAPK is a kinase capable of phosphorylating Ser258 and terminating the release of TF into microvesicles. Moreover, it appears that the prevention of TF release through Ala substitution of residue 253 enhances the late activation of p38. In this part of the investigation, the association of disruption of TF release with cellular proliferation or apoptosis was examined. Furthermore, the outcome of incubation of endothelial cells with high levels of exogenous TF-bearing microvesicles was examined.

4.1.1. The cell cycle and the G1-S transition

The cell cycle consists of four discrete phases (Fig 4.1): the G1 phase, in which the cells prepare for DNA synthesis; the S phase, in which DNA is replicated; the G2 phase, during which the cells prepare for mitosis; and the M phase during which the chromosomes are separated to make two daughter cells. The cell cycle is tightly coordinated by cell cycle checkpoints to ensure the ordered progression of the cell cycle and to detect possible defects during DNA synthesis. There are at least three regulatory checkpoints, of which the most important is the so-called restriction point in the G1 phase (Fig 4.1). At a point late in G1, the cell either exits the cell cycle or, having passed this point, becomes irreversibly committed to division (Sherr, 1994).

Figure 4.1. The Cell Cycle

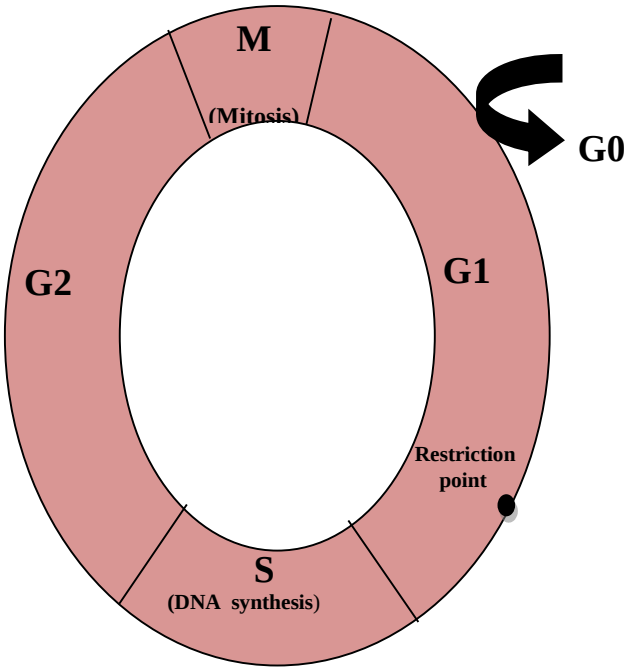

The cell cycle consists of four phases: the G1phase, in which the cell transcribes and expresses the protein required for the S phase; the S phase, during which DNA replication occurs; the G2 phase, in which the cell produces the additional proteins and prepares to divide; and the M phase, in which cell division occurs. The restriction point, in late G1, is the point after which the progression through the cell cycle becomes independent of the extracellular stimulus and the commitment to divide is irreversible.

A variety of cellular proteins control these checkpoints. However, the progression of the cell cycle is centrally controlled by cyclin-dependent kinases (cdks). The activity of cdks themselves is extensively regulated by specific cyclins. Cyclins bind to cdks to make activated kinase complexes and selectively phosphorylate proteins. Different sets of cyclins are active at various phases of the cell cycle. These include Cyclin A, D and E. Cyclin D plays a pivotal role at the transition point between G1 arrest and the S phase of DNA synthesis (Sherr, 1994). There are three Cyclin D sub-types (D1, D2, and D3); Cyclin D1 is the most ubiquitously expressed of the three and also the best studied. The activity of cyclin-dependent kinases is negatively regulated by the cell cycle inhibitory proteins, known as the INK4 and Cip/Kip protein families. These inhibitory proteins can bind to cdk, preventing the interaction of cdk with Cyclin D. Alternatively, these inhibitory proteins bind to the cdk-cyclin complex and suppress the cdk activity (Carnero & Hannon, 1998; Pavletich, 1999). The Cip/Kip family of proteins includes p21, p27 and p57. These function by inhibiting cdk kinase activities at the G1/S and G2/M checkpoints. p21 is a potent inhibitor of most cyclin/cdk complexes and is capable of preventing the transition from the G1 to the S phase (Harper et al., 1993).

4.1.2. The involvement of TF in endothelial cell proliferation

Under resting conditions, the rate of proliferation in endothelial cells and vascular smooth muscle cells is minimal. However, these cells may re-enter the cell cycle in response to a variety of physiological and pathological stimuli. Abnormal vascular smooth muscle cells' proliferation contributes to vascular diseases such as atherosclerosis (Spyridopoulos & Andres, 1998). Abnormal endothelial cell proliferation is also implicated in pulmonary hypertension (Tuder et al., 2009). However, endothelial cell proliferation is essential for angiogenesis (formation of new microvessels) and is pivotal

during embryogenesis (Matsumoto et al., 2001). In contrast, deregulation of this process contributes to tumour growth, diabetic retinopathy, rheumatoid arthritis, and atherosclerosis (Carmeliet & Jain, 2000).

It has been shown that TF induces cell proliferation mediated by TF-FVIIa-dependent signalling pathways (Versteeg & Ruf, 2006). Previous studies have shown that incubation of endothelial cells with recombinant TF alone results in endothelial cell proliferation (Pradier & Ettelaie, 2008; Collier & Ettelaie, 2010). This function is thought to arise from the interaction of TF with integrins (Collier & Ettelaie, 2010; Kocatürk et al., 2013; Kocatürk & Versteeg, 2013), resulting in the activation of proliferative signalling mechanisms including the ERK pathway of MAPK (Collier & Ettelaie, 2010). ERK in turn phosphorylates many proteins involved in cell cycle progression.

4.1.3. Cellular apoptosis

Apoptosis or programmed cell death is a normal process that occurs during development and aging and acts as a homeostatic mechanism to maintain cell populations in multicellular organisms (Green & Reed, 1998; Kwon et al., 2006). However, apoptosis can be induced in response to a variety of stimuli (Norbury et al., 2001) including the withdrawal of survival factors such as hormones or growth factors (Elmore, 2007), cytokines (Martin et al., 1995) or nitric oxide (Brune, 2003). Cells undergoing apoptosis show characteristic morphological changes (Mans et al., 2000) including cell shrinkage, membrane blebbing and chromatin condensation. These events are followed by DNA fragmentation and compartmentalisation into membrane-enclosed vesicles known as apoptotic bodies (Chiu et al., 2006). Two main pathways of induction of apoptosis have been identified and are known as the extrinsic (death receptor) and the intrinsic

(mitochondrial) pathways. Both these pathways lead to the activation of proteases called caspases which degrade cytoskeletal and other cellular proteins (Fig 4.2). The extrinsic pathway is initiated by specific cytokines known as death ligands, which include Fas-ligand and TNF-α. The interaction of these cytokines with their respective cell surface receptors (Locksley et al., 2001) ultimately leads to the activation of pro-caspase-8 which in turn cleaves and activates downstream pro-caspases (Boatright et al., 2003; Bao & Shi, 2007). Activated caspase-8 also proteolytically activates the protein Bid. Activated Bid then relocates to the mitochondria where it induces caspase-9 activation and therefore feeds back onto the intrinsic pathway of apoptosis (Fig 4.2).

The intrinsic pathway can be induced by a variety of stimuli including deficiency of nutrients or growth factors, hypoxia and DNA damage. The apoptotic signals eventually converge at mitochondria, mainly by Bax. The interaction of Bax with the outer membrane of the mitochondria results in the permeabilisation of the membrane, allowing the release of cytochrome c from the mitochondria (Cory & Adams, 2002; Kuwana et al., 2002; Scorrano et al., 2002). Once in the cytosol, cytochrome c interacts with the adaptor protein Apaf-1 (apoptotic protease activating factor-1). This complex utilises ATP to activate pro-caspase-9 (Liu et al., 1996) which in turn activates downstream caspases (Sun et al., 2004). A group of proteins known as the Bcl-2-family of proteins are the main regulators of mitochondrial events and include both pro- and anti-apoptotic members. The main pro-apoptotic members of Bcl-2 are Bad, Bax and Bid, while Bcl-2 and Bcl-XL are anti-apoptotic (Petros et al., 2004).

Figure 4.2. The apoptosis pathways

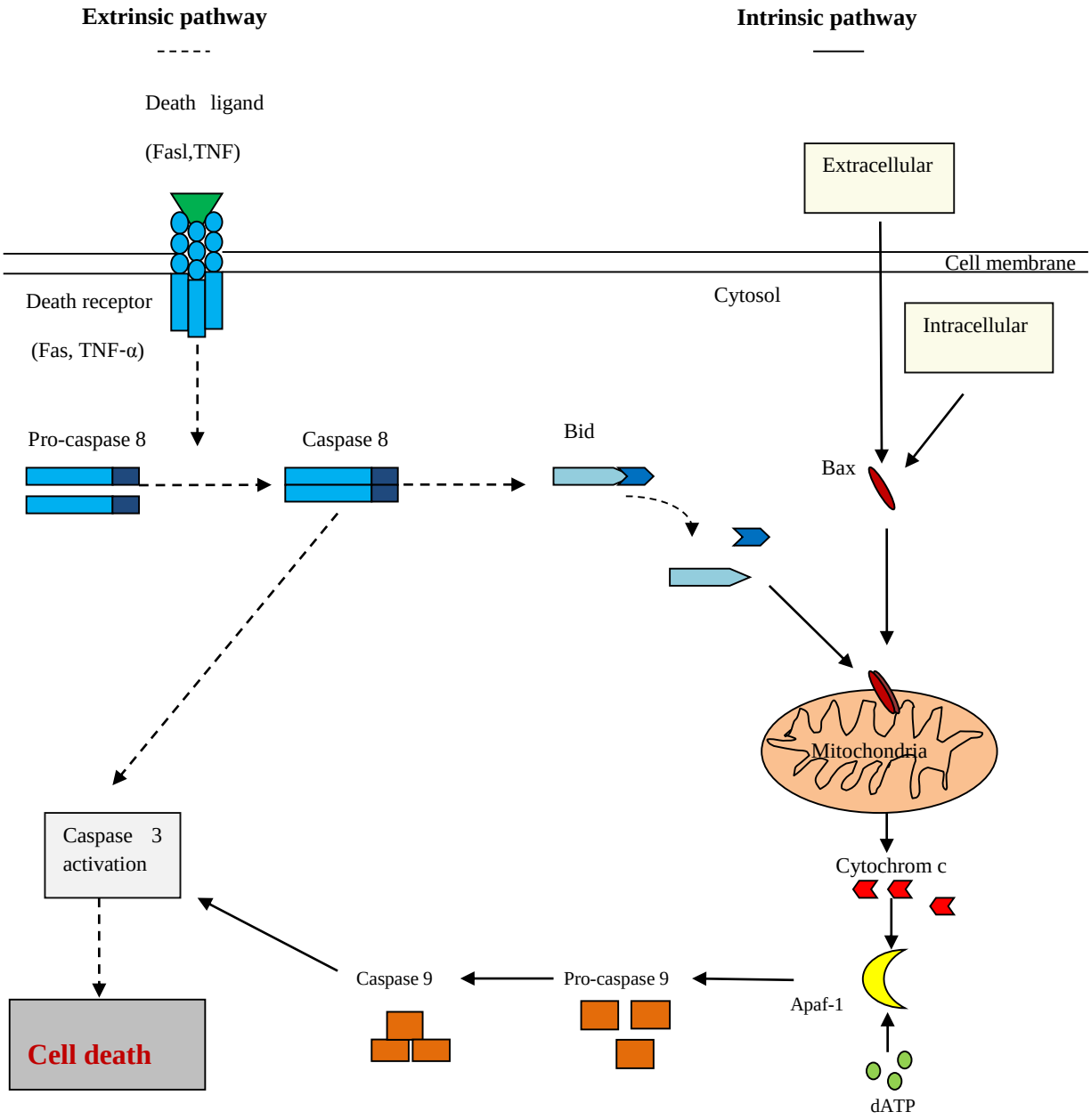

Apoptosis is mediated by two main pathways, the extrinsic and the intrinsic pathways. The extrinsic pathway is activated by binding of a death ligand to its corresponding receptor. This triggers the signal to activate the initiator caspase (caspase 8) which in turn activates the executioner caspase-3. Caspase-8 can also cleave the protein Bid and trigger apoptosis via mitochondrial events. The intrinsic pathway is activated by diverse biological, chemical and physical stimuli. These signals are transmitted to the mitochondria by the proapoptotic proteins, Bax and Bid. These signals trigger the release of cytochrome c from the mitochondria into the cytosol. Cytosolic cytochrome c triggers procaspase-9 activation which then cleaves and activates downstream procaspases. (Adapted from Whelan et al., 2010)

Activated Bax also interacts with the anti-apoptotic proteins and inhibits their protective effect. The expression of the Bcl-2-family of proteins itself is regulated by p53 (Schuler & Green, 2001) and is further covered in chapter 5.

4.1.4. The association of TF and endothelial cell apoptosis

Denudation of the endothelial layer occurs as a consequence of endothelial cell apoptosis and is often associated with chronic inflammatory diseases. Apoptosis is also implicated in the progression of atherosclerosis and plaque formation. Increased level of cellular apoptosis is thought to be responsible for plaque instability and may predispose the subject to plaque rupture. The association of TF with apoptotic vascular endothelial cells has long been established (Greeno et al., 1996; Bombeli et al., 1997). TF activity has been shown to be associated with the procoagulant potential of apoptotic cells. The thrombogenic activity of TF is facilitated by the exposure of PS on the outer layer of apoptotic cells (Bach et al., 1986). In addition to its thrombogenic activity, there is evidence that TF is directly involved in the induction of apoptosis. *In vitro* studies by Pradier and Ettelaie (2008) and Frentzou et al. (2010) have shown that treatment of endothelial cells or cardiomyocytes with high concentrations of TF results in the arrest of the progression through the cell cycle, leading to cell apoptosis. Moreover, endothelial cells may acquire and recycle TF carried by circulating microvesicles (Osterud & Bjorklid, 2012; Collier et al., 2013; Dasgupta et al., 2012). Therefore, high levels of TF accumulated within the cells may overload the physiological release of TF by endothelial cells. Subsequently, activation of the endothelial cells through injury, inflammation or exposure to cytokines may then promote pro-apoptotic mechanisms, leading to endothelial dysfunction associated with disease conditions.

4.1.5 Aims

The main objectives were as follows.

- To examine the influence of expression of wild-type and mutant forms of TF on endothelial cell proliferation
- To examine the influence of p38α pathway inhibition on the expression of the cell cycle regulator, Cyclin D1
- To examine the influence of expression of wild-type and mutant forms of TF on endothelial cell apoptosis as well as the modulators of cell cycle arrest (p21) and apoptosis (Bax)
- To examine the influence of treatment of endothelial cells with high levels of TF-containing microvesicles on cellular apoptosis
- To examine the influence of p38α pathway inhibition on TF-mediated cell apoptosis

4.2. Methods

4.2.1. Examination of the influence of expression of wild-type and mutant forms of TF on endothelial cell proliferation

HCAEC (10^5/well) were seeded out in 12-well plates and transfected with 1 µg of plasmid DNA in order to express wild-type or mutant forms of TF (TF_{Asp253} and TF_{Ala253}) as described in the general methods section. In addition, one set of cells was transfected to express EGFP as a control. Following transfection, the cells were incubated for 48 h to allow the expression of TF or EGFP proteins. HCAEC were then adapted to serum-free medium and activated by incubation with PAR2-AP (20 µM). An un-transfected/non-activated sample was included for comparison. Cell numbers were determined at 24 h post-activation using crystal violet staining (Chiba et al., 1998). The cells were fixed with 3 % (w/v) glutaraldehyde (100 µl) for 15 min and incubated with 1 % (v/v) crystal violet

solution (100 µl) for 30 min at room temperature. The cells were then washed 3 times with de-ionised water and the stain eluted out with 1 % (w/v) SDS solution by incubation for 15 min at room temperature. The absorption was measured at 595 nm using a spectrophotometer**.** A standard curve was prepared using an increasing number of HCAEC (5-100 x 10^3/well). HCAEC were counted in a haemocytometer and diluted with 5 % (v/v) of MV medium to give an appropriate cell density. Samples of cell suspension (5-100 x10^3 cells) were introduced into 12-well plates in 500 µl MV medium and incubated for 2 h to allow the cells to adhere. The cells were then fixed with 3 % (w/v) glutaraldehyde for 15 min and incubated with 1 % (v/v) crystal violet solution for a further 30 min. The number of cells was then determined as above for each sample to construct the standard curve of cell number against absorption at 595 nm (Fig 4.3).

4.2.2. The influence of expression of wild-type and mutant forms of TF on cyclin D1 mRNA expression

4.2.2.1. Time-course analysis of the expression of cyclin D1 mRNA by semi-quantitative real-time RT-PCR in endothelial cells expressing wild-type TF

HCAEC (10^5/well) were seeded out into 12-well plates, transfected to express wild-type TF, and allowed to express the protein over 48 h. The cells were then adapted to serum-free medium and activated by incubation with PAR2-AP (20 µM). The cells were harvested and total RNA was isolated using the TRI-reagent system at 0 h (non-activated), 8 h, 16 h and 24 h post-activation. The concentration and purity of RNA samples were determined as described in the general methods section 2.7.1.

Figure 4.3. Standard curve for the determination of cell numbers

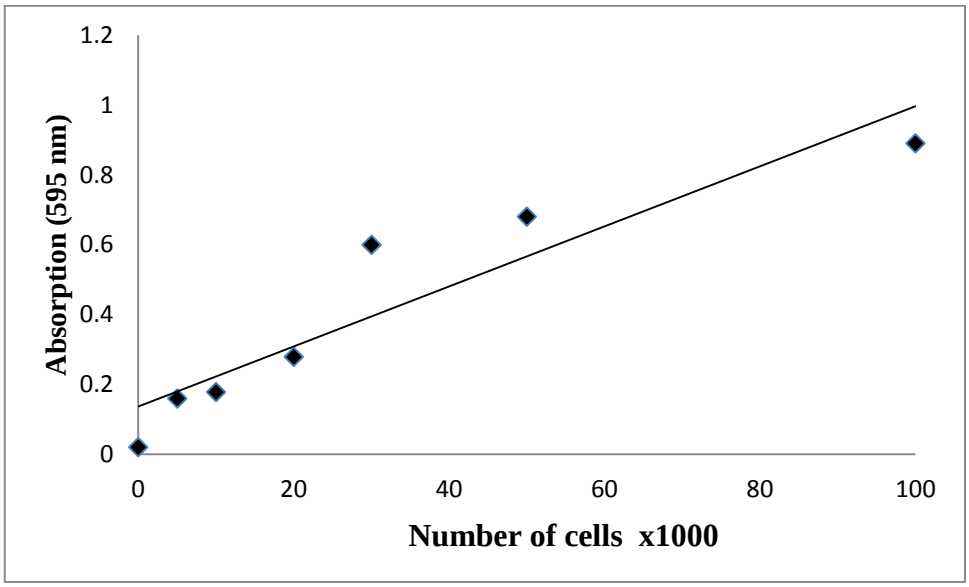

HCAEC (5-100 x10^3 cells) were seeded out into 12-well plates in 500 µl of complete MV medium. Following 2 h incubation, the cells were fixed with 3 % (w/v) glutaraldehyde (100 µl) for 15 min and then incubated with 1 % (v/v) crystal violet solution for a further 30 min. The cells were then washed 3 times with de-ionised water and the stain eluted out with 1 % (w/v) SDS solution by incubation for 15 min at room temperature. The absorption value for each sample was measured at 595 nm and a standard curve of cell number against absorption constructed. Data represent the mean value of three separate experiments carried out as duplicates.

Real-time RT-PCR was performed in triplicate for each time point using 0.1 µg of total RNA samples. Primers were designed to separately amplify cyclin D1 and β-actin as described in the general method section 2.7.3. Following the RT step, PCR was carried out at melting temperatures of 90°C using the GoTaq® 1-Step RT-qPCR System on an iCycler thermal cycler. The Ct values for cyclin D1 mRNA were determined for each sample and then normalised against the values of β-actin the ratios were then compared to untreated sets of samples using the $2^{-\Delta\Delta CT}$ method (Livak et al., 2001).

To ensure the amplification of a single transcript the RT-PCR products were also visualised on a 2 % (w/v) agarose gel, stained with SYBR GreenI; the images were recorded using the GeneSnap program.

The primers used were:

cyclin D1-forward: 5'-CCGTCCATGCGGAAGATC-3'

cyclin D1-reverse: 5'-ATGGCCAGCGGGAAGAC-3'

β-actin-forward 5′-TGATGGTGGGCATGGGTCAGA-3′

β-actin -reverse 5′-GTCGTCCCAGTTGGTGACGAT-3′

4.2.2.2. Analysis of the cyclin D1 mRNA expression in cells expressing the wild-type and mutant forms of TF

HCAEC (10^5) were seeded out into 12-well plates and transfected to express wild-type or mutant forms of TF (TF_{Asp253} and TF_{Asp253}). Following transfection, the cells were incubated for 48 h to allow the expression of TF. The cells were then adapted to serum-free medium and activated by incubation with PAR2-AP (20 µM) for 8 h. Total RNA was isolated from the cell samples as described in the general methods section 2.7.1.

The levels of cyclin D1 mRNA were measured by real-time RT-PCR using cyclin D1 and β-actin primer sets as explained above in section 4.2.4.1. The Ct values for cyclin D1 mRNA were determined for each sample, which were then normalised against the values of β-actin, the ratios were compared to untreated sets of samples using the $2^{-\Delta\Delta CT}$ method (Livak et al., 2001).

4.2.3. Examination of the influence of the expression of wild-type and mutant forms of TF on Cyclin D1 protein expression by western blot

HCAEC (10^5/well) were seeded out into 12-well plates and transfected to express the wild-type or mutant forms of TF (TF_{Asp253} and TF_{Asp253}). Samples of cells were also used untreated. The cells were incubated for 48 h, adapted to serum-free medium and activated with PAR2-AP (20 µM). The cells were then lysed after 8 h incubation in 100 µl of Laemmli's buffer containing a protease inhibitor cocktail. The total concentrations of protein were estimated using Bradford protein-estimation assay as described in the general methods section 2.6.1. The protein samples were then separated by 12 % (w/v) SDS-PAGE and transferred onto nitrocellulose membranes. The amount of Cyclin D1 protein was determined by probing the membranes with a mouse monoclonal anti-human Cyclin D1 antibody according to Table 4.1. The membranes were then washed with TBST and probed with a goat anti-mouse alkaline phosphatase-conjugated antibody. The bands were visualised using Western Blue stabilised alkaline phosphatase-substrate and recorded. As loading controls, the membranes were probed for GAPDH using a goat anti-human GAPDH antibody followed by a donkey anti-goat alkaline phosphatase-conjugated antibody. The bands were then visualised using the Western Blue stabilised alkaline phosphatase-substrate and recorded using the

Table 4.1. Antibody dilutions for western blot

Primary antibodies	Dilution antibodies: TBST (v/v)	Secondary antibodies	Dilution antibodies: TBST (v/v)
Mouse monoclonal anti-human Cyclin D1(DCS6)	1:1000	Goat anti-mouse alkaline phosphatase-conjugated antibody	1:5000
Goat anti-human GAPDH	1:3000	donkey anti-goat alkaline phosphatase-conjugated antibody	1:5000
Mouse monoclonal anti-human p21(WA-1)	1:5000	Goat anti-mouse HRP-conjugated antibody	1:5000
Mouse monoclonal anti-human Bax antibody (2D2)	1:1000	Goat anti-mouse alkaline phosphatase-conjugated antibody	1:5000
Rabbit anti-human p38	1:2000	Goat anti-rabbit HRP-conjugated antibody	1:5000

GeneSnap program. The levels of Cyclin D1 expression were normalised against respective GAPDH, using the ImageJ program.

4.2.4. The influence of p38α silencing on Cyclin D1 expression

4.2.4.1. Optimisation of p38-siRNA concentration

p38α activity was inhibited using the post-transcriptional gene-silencing method as follows. The p38α-specific siRNA consisted of a pool of 4 target-specific 19-25 nt siRNAs designed to knock down gene expression. In order to determine the optimal concentration of p38α-siRNA required for maximal suppression of p38α expression, HCAEC (10^5/well) were transfected with a range of p38α-siRNA (25, 45 and 90 nM) and incubated for 48 h. The levels of p38 protein were analysed by western blot using antibody against p38 according to Table 4.1. As loading controls, the membranes were probed for GAPDH using a goat anti-human GAPDH antibody followed by a donkey anti-goat alkaline phosphatase-conjugated antibody. The bands were then visualised using the Western Blue stabilised alkaline phosphatase-substrate and recorded using the GeneSnap program. The levels of p38 protein expression were normalised against respective GAPDH, using the ImageJ program.

4.2.4.2. Measurement of the efficiency of p38α-siRNA transfection in HCAEC by flow cytometry

HCAEC (10^5/well) were cultured in 12-well plates and incubated for 24 h. The cells were transfected with a siRNA-FITC conjugate (45 nM) using Lipofectin reagent and incubated for 5 h. Un-transfected set of cells were used as a control. Transfected and un-transfected cells were then harvested and re-suspended with PBS (300 µl) and analysed

using a FACSCalibur flow cytometer running CellQuest software, as described in the general methods section 2.5.

4.2.4.3. Examination of the influence of silencing p38α on Cyclin D1 protein expression

HCAEC (10^5/well) were cultured in 12-well culture plates. The cells were transfected with a plasmid to express wild-type TF and co-transfected with either p38α-siRNA or a control siRNA. Control siRNA contains a scrambled sequence that has been shown not to recognise any mRNA. Following 48 h incubation the cells were adapted to serum-free medium and activated with PAR2-AP (20 µM). The cells were then lysed at 8 h post-activation in Laemmli's buffer, and the proteins were separated by 12 % (w/v) SDS-PAGE. The bands were transferred onto nitrocellulose membranes, as described in section 2.6.3. Membranes were probed using a mouse anti-human Cyclin D1 antibody followed by anti-mouse HRP-phosphatase-conjugated antibody diluted in TBST according to Table 4.1. The images were recorded using the GeneSnap image capture system. The membranes were then probed for GAPDH using a goat anti-human GAPDH followed by anti-goat alkaline phosphatase-conjugated antibody diluted in TBST according to Table 4.1. The images were recorded using the GeneSnap image capture system. The amounts of Cyclin D1 protein were then normalised against the respective GAPDH in each sample.

4.2.5. Examination of the influence of the expression of wild-type and mutant forms of TF on endothelial cell apoptosis

To date, various methods have been developed and introduced to measure cellular apoptosis, and each has its advantages and drawbacks. In this study, qualitative DeadEnd

fluorescence-based TUNEL assay was used to measure DNA fragmentation In addition, the extent of DNA fragmentation was quantified using the TiterTACS™ Colorimetric Apoptosis Detection Kit. Other methods of analysis of apoptosis, including measurements of caspase activity and annexin V exposure, were not used since these procedures do not distinguish between cell activation that occurs in response to PAR2 activation and cellular apoptosis.

4.2.5.1. Analysis of apoptosis by confocal microscopy

DeadEnd fluorescence-based TUNEL assay was used to measure DNA fragmentation. The assay is based on labelling the 3'-OH ends of DNA with fluorescein-12-dUTP using Terminal Deoxynucleotidyl Transferase. The extent DNA fragmentation leads to increased incorporation of the fluoresant dUTP and may be visualised by confocal microscopy. HCAEC (10^5) were seeded out into glass-base 35 mm dishes and transfected to express wild-type or mutant forms of TF. In addition, one set of cells was transfected with an empty plasmid (pCMV-EGFP) as a negative control. After incubation for 48 h, the cells were adapted to serum-free medium (500 µl) and stimulated with PAR2-AP (20 µM) for 18 h. For comparison, sets of cells were treated with TNFα (10 ng/ml) and used as a positive control (Robaye et a006C., 1991). The cells were fixed using 4 % (v/v) formaldehyde for 30 min and washed three times with PBS. Subsequently, the cells were permeabilised with Triton X-100 (0.2 %) (v/v) in PBS for 5 min and washed twice for 5 min each with PBS. The cells were then covered with 50 µl of equilibration buffer (200 nM potassium cacodylate, 25 mM Tris-Hcl pH 6.0, 0.2 mM DTT, 0.025 % (w/v) BSA, 2.5 mM $CoCl_2$) for 10 min at room temperature. The equilibration buffer was removed and the cells were incubated with 50 µl of Terminal deoxynucleotidyl Transferase reaction buffer containing 45 µl equilibration buffer, 4 µl flurescein-12-dUTP, and 25

units of TdT enzyme (1 µl). The dishes were covered to protect them from light and incubated at 37°C for 60 min in a humidified incubator. The cells were then incubated with 2x SSC buffer (50 µl) for 15 min at room temperature to stop the reaction. The cells were washed twice with PBS (5 min each), and the nucleus was stained with 5 µg/ml of DAPI for 10 min at room temperature before washing with PBS. Finally 200 µl PBS was added and the cells were analysed by confocal microscopy at room temperature using a Zeiss LSM 710 confocal microscope with a ×20 objective.

4.2.5.2. Analysis of apoptosis using the TiterTACS™ Colorimetric Apoptosis Detection Kit

HCAEC (10^5/well) were seeded out in 12-well plates and transfected to express wild-type or mutant forms of TF, as described in section 2.4.1. In addition, one set of cells was transfected to express EGFP as a control. After 48 h incubation, the cells were adapted to serum-free medium and activated with PAR2-AP (20 µM) for 18 h at 37°C. For comparison, sets of cells were treated with TNFα (10 ng/ml) and used as a positive control. The cells were washed three times with PBS, before being fixed with 4 % formaldehyde (v/v) for 10 min at room temperature. After three washes with PBS the cells were further fixed with pure methanol for 20 min at room temperature. 200 µl of Cytonin solution (provided by the kit) was added to the wells and incubated for 15 min at room temperature to permeabilise the cells, and the cells were then washed twice with distilled water (800 µl). A positive control was generated by adding TACS Nuclease™ Solution (200 µl) to each control well and incubating for 30 min at 37°C. The wells were then washed three times with PBS and incubated with 3 % peroxide: methanol solution (200 µl) for 5 min at room temperature. Following one wash with dH_2O (600 µl), the 1X TdT labelling buffer (600 µl) was added to each well and incubated for a further 5 min.

The labelling buffer was then replaced with 200 µl of labelling reaction solution (1X TdT labelling buffer (200 µl), TdT dNTP Mix (1.4 µl), TdT Enzyme (1.4 µl), and 50X Mn^{2+} (4 µl)) and incubated for 1 h at 37°C. The reaction was stopped by adding 600 µl of 1X TdT stop buffer (provided by the kit) for 5 minutes. After three washes with PBS the cells were incubated with strep-HRP solution (200 µl) for 10 min at room temperature. The cells were washed for the last time with 800 µl PBS containing 0.1 % (v/v) Tween 20. Finally, 400 µl of colorimetric substrate (TACS-Sapphire) was added to each well followed by incubation for 30 min at room temperature in the dark. The reaction in each sample was stopped by adding 5 % (v/v) phosphoric acid (200 µl). The solution in each well was quickly transferred to a 96-well plates and the absorption was measured at 450 nm on a plate-reader. The changes in the level of cell apoptosis were then compared to the untreated (negative control) sample.

4.2.5.3. The influence of TF-containing microvesicles on endothelial cell apoptosis

Cell-derived microvesicles were isolated from MDA-MB-231 cell line by ultracentrifugation as described in section 2.8. The concentrations of microvesicles were determined using the Zymuphen microvesicle determination kit. TF antigen and activity levels were measured using a TF-ELISA kit and TF chromogenic assay, as described in sections 2.8.2 & 2.9. HCAEC (10^5/well) were seeded out in 12-well plates. The cells were incubated with TF-containing microvesicles (100 ng/ml TF) for 24 h, adapted to serum-free medium and activated with PAR2-AP (20 µM) for 18 h. In addition, one set was untreated and used as a negative control. The level of cellular apoptosis was then analysed using the TiterTACS™ Colorimetric Apoptosis Detection Kit as described in the previous section 4.2.5.2.

4.2.5.4. Examination of the role of p38α in TF-mediated endothelial cells apoptosis using the TiterTACS™ Colorimetric Apoptosis Detection Kit

HCAEC (10^5/well) were seeded out in 12-well plates and transfected to express wild-type or mutant form of TF (TF_{Ala253}) or, alternatively, EGFP. Sets of cells were used un-transfected. Following 48 h incubation the cells were adapted to serum-free medium. Sets of cells were then treated with 100 nM of p38 inhibitor (SB202190) for 30 min together with untreated sets used as controls. The cells were then activated with PAR2-AP (20 μM), incubated for 18 h, fixed and analysed using the TiterTACS™ Colorimetric Apoptosis Detection Kit as described before in section 4.2.5.2.

4.2.6. Examination of the influence of the expression of wild-type and mutant forms of TF on p21 and Bax protein expression by western blot

HCAEC (10^5/wells) were seeded out into 12-well plates and transfected to express the wild-type or mutant forms of TF. In addition, a set of cells was transfected to express EGFP and was used as a control. Un-transfected/untreated sets of cells were also used for comparison. The cells were incubated for 48 h, adapted to serum-free medium and activated with PAR2-AP (20 μM) for 4, 8 or 18 h. The cells were then lysed in Laemmli's buffer containing a protease inhibitor cocktail. The total protein was separated by 12 % (w/v) SDS-PAGE and transferred onto nitrocellulose membranes. Total amounts of p21 protein were determined by probing the membranes with a mouse anti-human p21 and then re-probing with an anti-mouse HRP-conjugated antibody according to Table 4.1. The bands were then visualised using TMB-stabilised stabilised substrate for HRP and recorded using the GeneSnap program. Bax proteins were also analysed as above using a mouse anti-human Bax antibody and followed by anti-mouse HRP-conjugated antibody according to the Table 4.1. As loading controls, the membranes were probed for GAPDH

using a goat anti-human GAPDH antibody followed by a donkey anti-goat alkaline phosphatase-conjugated antibody. The bands were then visualised using the Western Blue stabilised alkaline phosphatase-substrate and recorded using the GeneSnap program. The levels of p21 and Bax protein expression were normalised against respective GAPDH, using the ImageJ program.

4.2.7. Examination of the influence of TF-containing microvesicles on Bax protein expression

HCAEC (10^5/well) were incubated with TF-containing microvesicles (20-100 ng/ml TF) for 2 h in serum-free medium. The cells were then activated with PAR2-AP (20 µM) for 18 h and the amounts of cellular Bax protein were measured in comparison to GAPDH as described in section 4.2.6.

4.2.8. Analysis of the influence of the expression of wild-type and mutant forms of TF on p21 and bax mRNA expression by semi-quantitative real-time RT-PCR

HCAEC (10^5/well) were seeded out into 12-well plates and transfected to express the wild-type or mutant forms of TF. Un-transfected/untreated samples of cells were used. The cells were incubated for 48 h, adapted to serum-free medium and activated with PAR2-AP (20 µM) for 4 h. Total RNA was isolated from the cell samples as described in section 2.7.1. The RT-PCR reaction was performed using 100 ng of total RNA from each sample, and the primers to amplify p21, bax, and β-actin were designed as described in the general methods section 2.7.2. The Ct values of p21 and bax cDNA were normalised against respective values of β-actin gene and then compared to un-transfected/untreated sets of samples using the $2^{-\Delta\Delta CT}$ method (Livak et al., 2001).

The primers used were:

p21 forward primer 5'-GGAAGACCATGTGGACCTGT-3'

p21 reverse primer 5'-GGCGTTTGGAGTGGTAGAAA-3'

bax- forward primer 5'-CCATCATGGGCTGGACATTGG-3',

bax- reverse primer 5'-AGCACTCCCGCCACAAAGATG-3'

β-actin-forward 5′-TGATGGTGGGCATGGGTCAGA-3′

β-actin -reverse 5′-GTCGTCCCAGTTGGTGACGAT-3′

4.2.9. Analysis of the influence of TF-containing microvesicles on bax mRNA expression by semi-quantitative real-time RT-PCR

HCAEC (10^5/well) were seeded out into 12-well plates adapted to serum-free medium and treated with TF-containing microvesicles (100 ng/ml TF) for 2 h. The cells were then activated with PAR2-AP (20 μM) for 4 h and the expressions of bax mRNA were analysed by RT-PCR as described in section 4.2.8.

4.3. Results

4.3.1. Examination of the influence of expression of wild-type and mutant forms of TF on endothelial cell proliferation

Sets of human HCAEC (10^5/well) were transfected to express wild-type or mutant forms of TF or EGFP and activated with PAR2-AP (20 μM). Activation of cells with PAR2-AP resulted in increased cell proliferation rate (approximately 11 % within 24 h) in cells expressing TF_{Wt}, TF_{Asp253} and to a lesser extent in EGFP-expressing cells, compared to non-activated cells (Figure 4.4). In contrast, a small reduction in cell numbers was observed in the cells expressing TF_{Ala253} at 24 h following activation.

Figure 4.4. The influence of wild-type and mutant forms of TF on endothelial cell proliferation

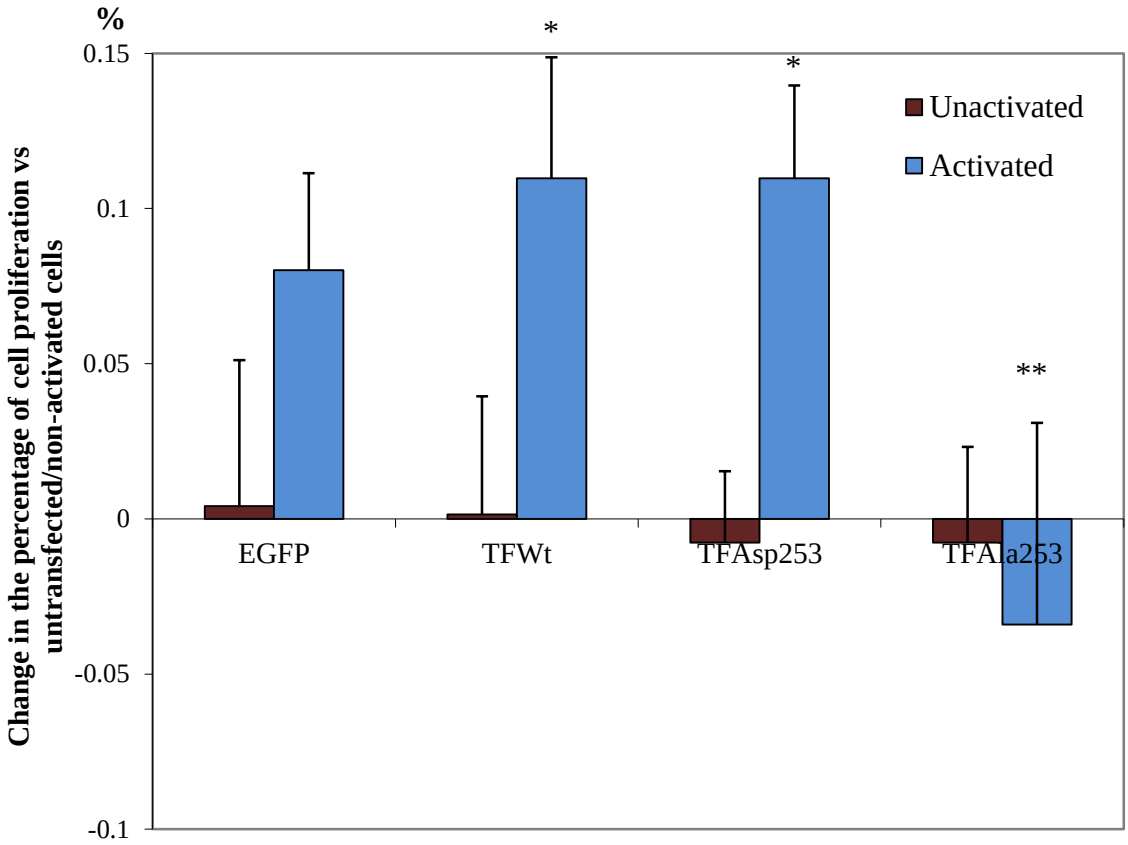

HCAEC (10^5/well) were seeded out in 12-well plates and transfected to express $TF_{Wt,}$ TF_{Asp253}, and TF_{Ala253} or EGFP. The cells were adapted to serum-free medium and activated with PAR2-AP (20 µM). An un-transfected/non-activated sample was included for comparison. Cell numbers were determined as a ratio of control cells, using crystal violet staining. (Data are representative of 3 independent experiments and expressed as means ± sd, *=$p<0.05$ vs un-transfected/non-activated sample; **=$p<0.05$ vs activated cell sample expressing TF_{Wt})

4.3.2. Examination of the influence of expression of wild-type and mutant forms of TF on cyclin D1 expression

Cyclin D1 mRNA expression was analysed using a semi-quantitative RT-PCR procedure. A melting curve analysis showed two peaks for the RT-PCR products representing cyclin D1 and β-actin (Fig 4.5A). The RT-PCR products were also visualised on a 2 % (w/v) agarose gel to further confirm the presence of single bands for cyclin D1 and β-actin (Fig 4.5B). Time-course analysis of samples transfected with wild-type TF and activated with PAR2-AP showed the maximal cyclin D1 expression to be at 8 h post-activation (Fig 4.6). Transfection of endothelial cells with wild-type or mutant forms of TF showed increased expression of cyclin D1 mRNA in cells expressing TF_{Wt} and TF_{Asp253} at 8 h post-activation, compared to non-activated cells. In addition, lower levels of cyclin D1 mRNA were observed in cells expressing TF_{Ala253} (Figure 4.7). Western blot analysis also showed increases in cyclin D1 protein levels in cells expressing TF_{Wt}, TF_{Asp253} following activation with PAR2-AP. In contrast, reduced levels of cyclin D1 protein were observed in cells expressing TF_{Ala253} (Figure 4.8).

4.3.3. Examination of the influence of silencing of p38α on cyclin D1 expression

4.3.3.1. Optimisation of p38-siRNA transfection

HCAEC (10^5/well) were transfected with a range of p38α-siRNA (25, 45 and 90 nM) and incubated for 48 h. The levels of p38 protein were analysed by western blot. The greatest reduction in p38 protein expression, compared to cells transfected with control siRNA transfected cells, was observed using 45 nM of p38α-siRNA (Fig 4.9). In addition, the transfection efficiency was assessed by transfection of HCAEC (10^5) with a siRNA-FITC.

Figure 4.5. RT-PCR analysis of cyclin D1 mRNA expression

(A)

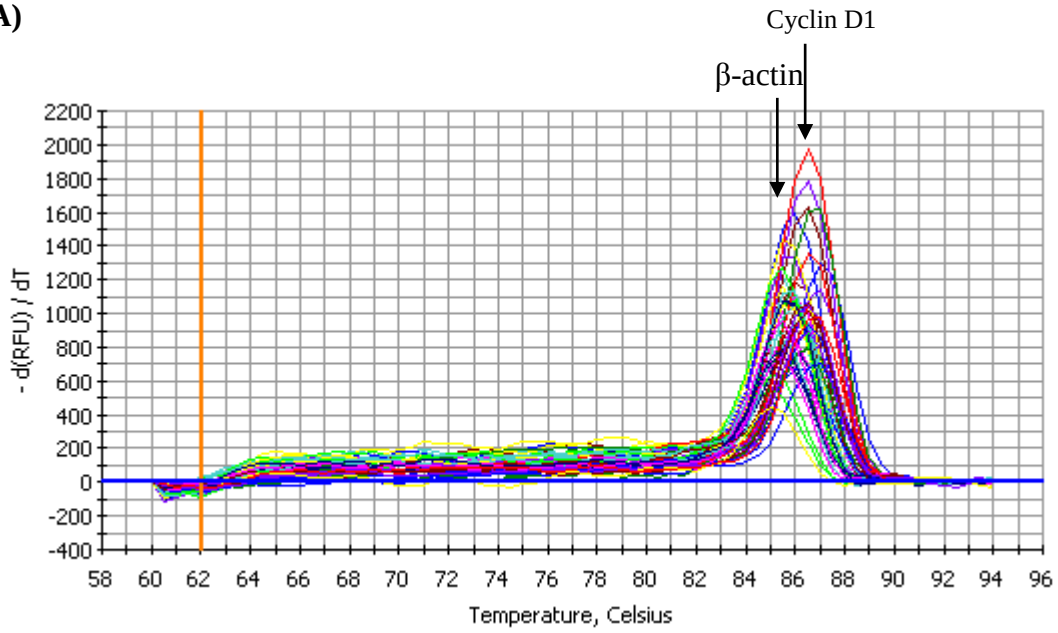

(B)

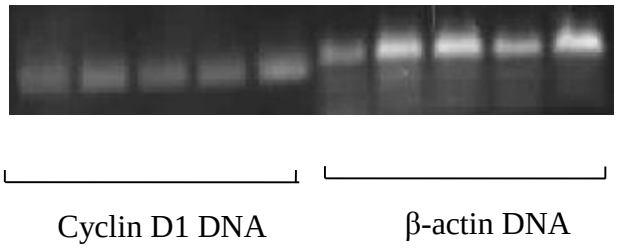

HCAEC (10^5) expressing TF_{Wt}, were adapted to serum-free medium and activated with PAR2-AP (20 µM) for up to 24 h. Total RNA was isolated from the cells and the real-time RT-PCR was carried out to amplify cyclin D1 and β-actin. The melting curves were derived from amplification of cyclin D1 and β-actin (A). Single peak indicates specific amplification of cyclin D1 and β-actin. The RT-PCR products were also visualised on a 2 % (w/v) agarose gel electrophoresis to ensure specificity (B).

Figure 4.6. The influence of TF on cyclin D1 mRNA expression over 24 h in activated HCAEC

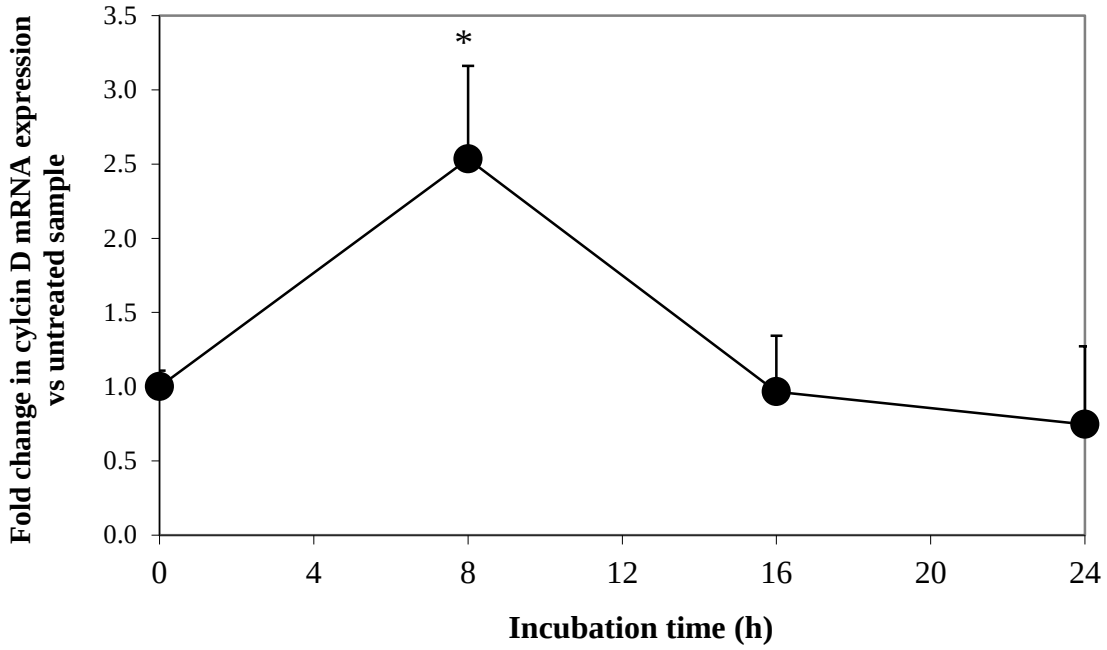

HCAEC (10^5/well) were seeded out in 12-well plates and transfected to express wild-type TF. The cells were adapted to serum-free medium and incubated with PAR2-AP (20 μM). Samples were removed at intervals up to 24 h and RNA was extracted. The expression of cyclin D1 was analysed by RT-PCR. The ratio of cyclin D1 mRNA was determined against the non-activated sample (Data are representative of 3 independent experiments and expressed as means ± sd, *=$p<0.05$. vs non-activated sample)

Figure 4.7. The influence of wild-type and mutant forms of TF on cyclin D1 mRNA expression

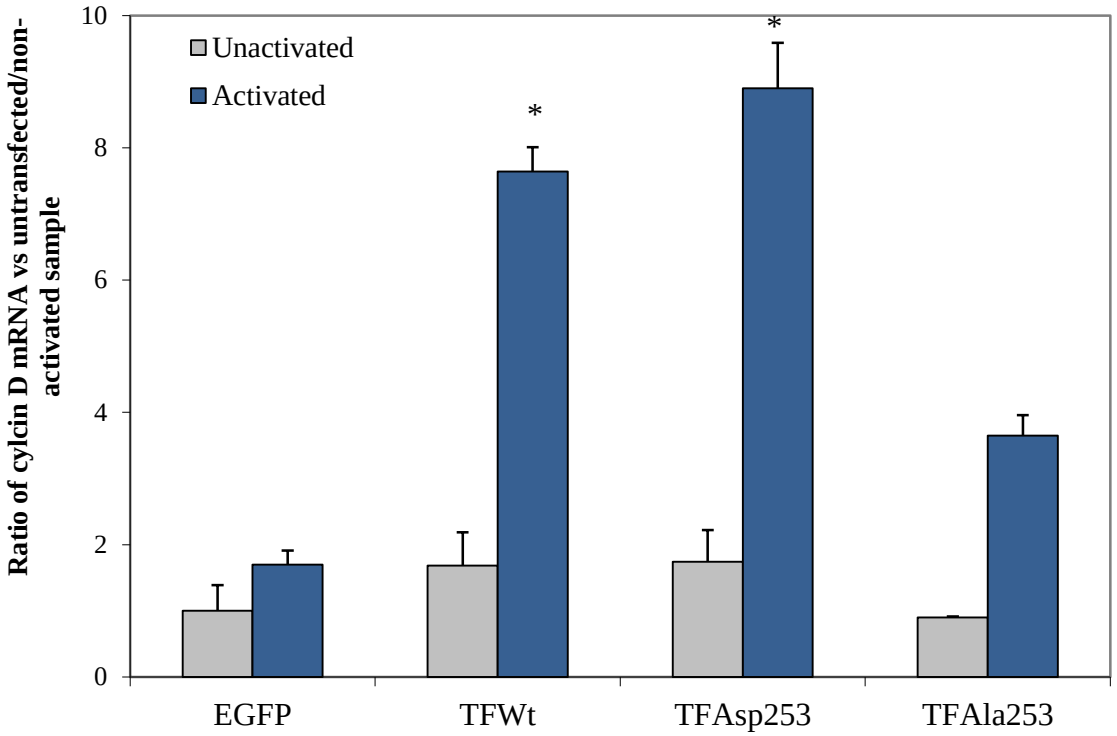

HCAEC (10^5/well) were cultured in 12-well plates and transfected to express $TF_{Wt,}$ TF_{Asp253}, and TF_{Ala253} or EGFP. The cells were adapted to serum-free medium and activated with PAR2-AP (20 µM). Total RNA was isolated from the cells at 8 h post-activation and the relative amount of cyclin D1 mRNA was determined by RT-PCR. (Data are representative of 3 independent experiments and expressed as means ± sd, *=$p<0.05$ vs respective non-activated samples)

Figure 4.8. The influence of wild-type and mutant forms of TF on Cyclin D1 protein expression

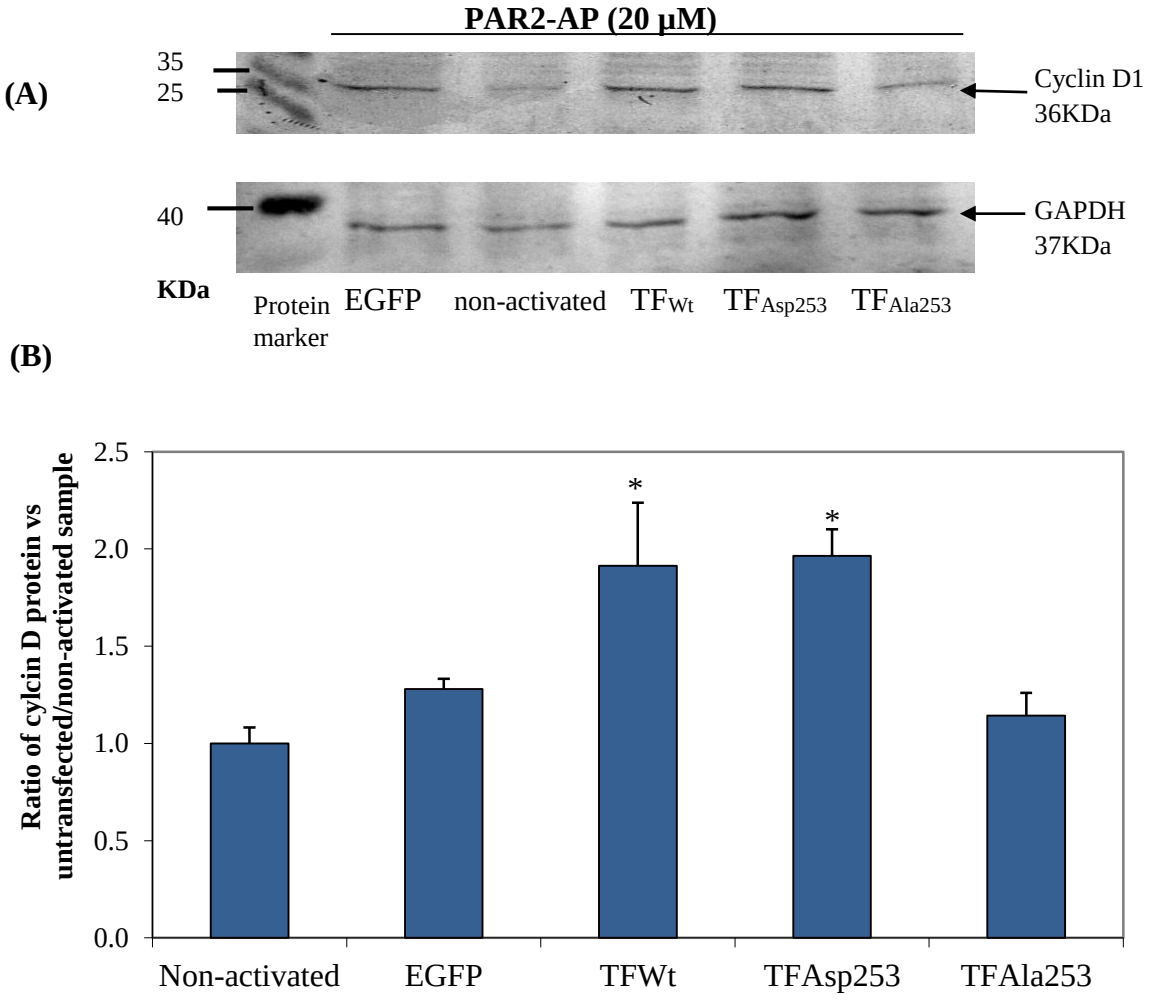

HCAEC (10^5/well) were cultured in 12-well plates and transfected to express $TF_{Wt,}$ TF_{Asp253}, and TF_{Ala253} or EGFP. The cells were adapted to serum-free medium and activated with PAR2-AP (20 µM) for 8 h. The cells were then lysed in Laemmli's buffer and the proteins separated by 12 % (w/v) SDS-PAGE. Proteins were transferred onto nitrocellulose membranes and probed for Cyclin D1 using a mouse monoclonal anti-human Cyclin D1. The membranes were then probed for GAPDH using a goat anti-human GAPDH antibody, and images were recorded using the GeneSnap program (A). The amount of Cyclin D1 protein was determined by western blot analysis and (B) quantified against GAPDH using the ImageJ program. (Data are representative of 3 independent experiments and expressed as means ± sd, *=$p<0.05$ vs un-transfected/non-activated sample).

Figure 4.9. Optimisation of concentration of p38α –siRNA

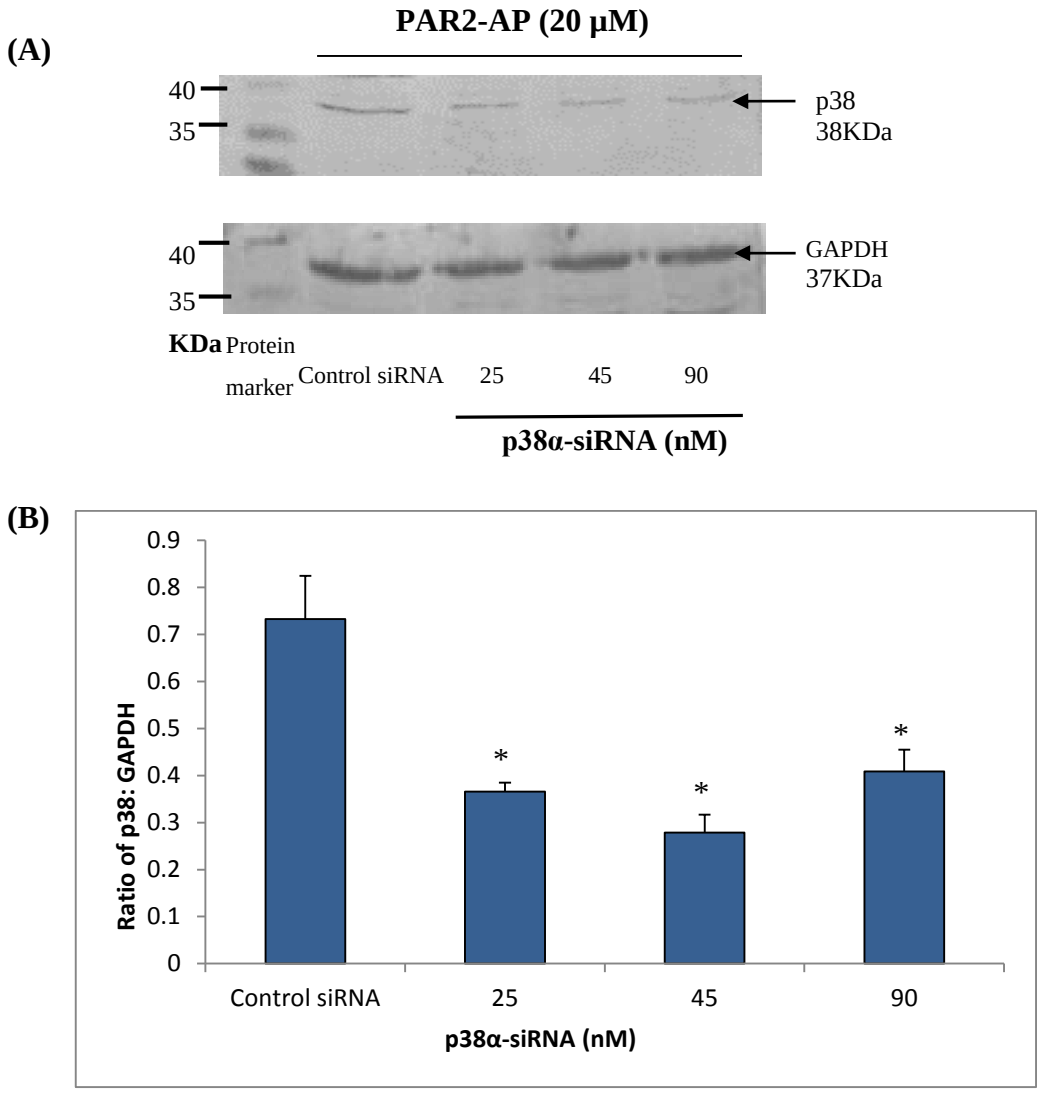

HCAEC (10^5/well) were cultured in 12-well plates and transfected with a range of p38α-siRNA concentrations (25, 45 and 90 nM). Sets of cells were transfected with control siRNA. The cells were incubated for 48 h, adapted to serum-free medium and activated with PAR2-AP (20 µM). The cells were then lysed in Laemmli's buffer and the proteins separated by 12 % (w/v) SDS-PAGE. Proteins were transferred onto nitrocellulose membranes and probed for p38 using a rabbit anti-human p38. The membranes were then probed for GAPDH using a goat anti-human GAPDH antibody, and images were recorded using the GeneSnap program (A). The amounts of p38 protein were normalised against the respective GAPDH in each sample (B) using the ImageJ program. (Data are representative of 3 independent experiments and expressed as means ± sd, *=$p<0.05$ vs control siRNA sample)

The incorporation of the siRNA into the cells was assessed by flow cytometry. Transfection of the cells with 45 nM of siRNA-FITC resulted in an average transfection efficiency percentage of 67 % above that of the un-transfected cells (Fig 4.10). Western blot analysis of the cells co-transfected with wild-type TF plasmid together with p38α-siRNA and activated with PAR2-AP for 8 h showed an increase in cyclin D1 expression compared to the same sample co-transfected with control siRNA (Fig 4.11).

4.3.4. Examination of the influence of the expression of wild-type and mutant forms of TF on endothelial cell apoptosis

In order to assess the influence of the expression of wild-type and mutant forms of TF on the rate of endothelial cell apoptosis, HCAEC (10^5) were transfected to express TF_{Wt}, TF_{Asp253}, TF_{Ala253} or EGFP 48 h prior to testing. DNA fragmentation was measured using a fluorescence-based TUNEL-based apoptosis assay at 24 h following activation with PAR2-AP. In addition, sets of un-transfected cells were treated with TNFα (10 ng/ml) and used as positive controls. Analysis of the cells indicated increased levels of DNA fragmentation in cells expressing TF_{Ala253} (Fig 4.12). This was further confirmed using a quantitative chromogenic TUNEL assay based on HRP-end labelling of fragmented DNA (Fig 4.13). The differences between the rates of apoptosis in cells transfected to express EGFP, TF_{Wt}, TF_{Asp253} and un-transfected cells, or any of the non-activated cells, were not significant. Furthermore, incubation of the cells with high concentrations of TF-containing microvesicles (100 ng/ml TF) increased the observed level of apoptosis significantly (Fig 4.14).

Figure 4.10. Determination of transfection efficiency of p38-siRNA into HCAEC by flow cytometry

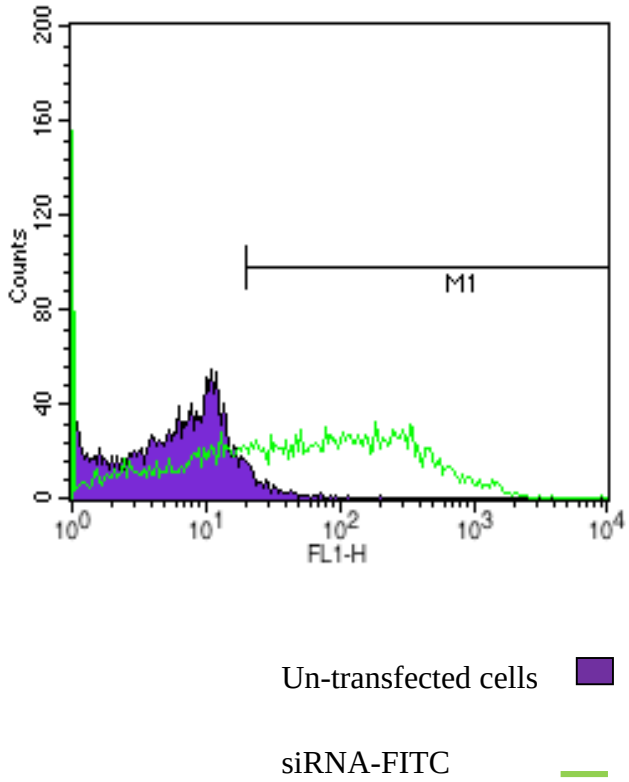

HCAEC (10^5/well) were cultured in 12-well plates in serum-free medium and transfected with siRNA-FITC (45 µl) in order to establish transfection efficiency. Following 5 h incubation, the cells were harvested, washed with PBS and re-suspended in 300 µl PBS. 10,000 cells were analysed by FACSCalibur flow cytometry running Cell Quest software. The marker was set to contain 3 % of un-transfected cells.

Figure 4.11. The influence of silencing of p38α on Cyclin D1 protein expression

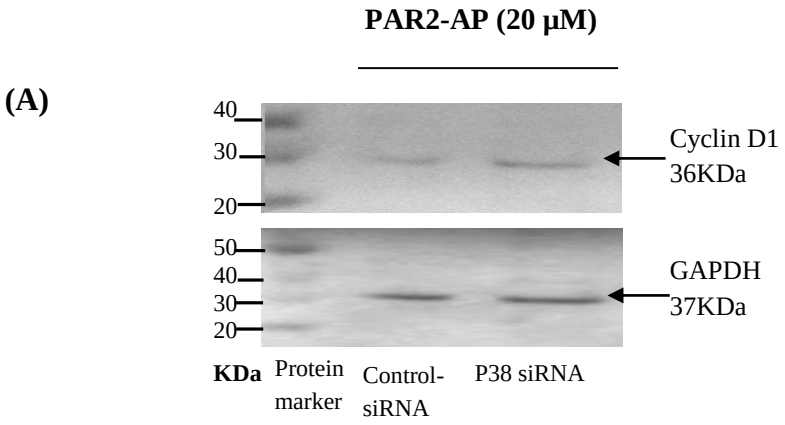

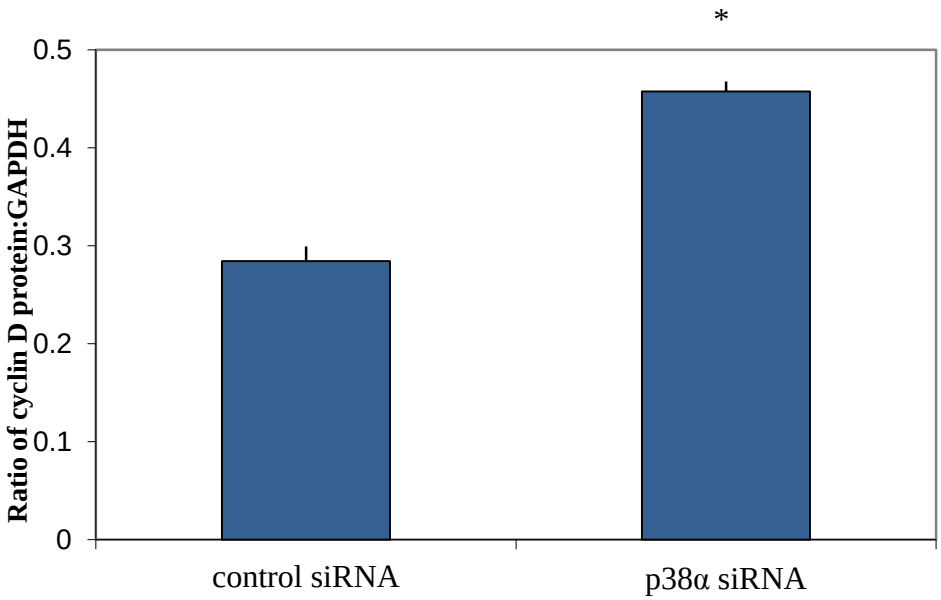

HCAEC (10^5/well) were transfected to express wild-type TF and also co-transfected with either p38α-siRNA or a control siRNA. The cells were then adapted to serum-free medium and activated with PAR2-AP (20 µM). The cells were then lysed in Laemmli's buffer and the proteins separated by 12 % (w/v) SDS-PAGE. Proteins were transferred onto nitrocellulose membranes and probed for Cyclin D1 using a mouse monoclonal anti-human Cyclin D1 antibody. The membranes were then probed for GAPDH using a goat anti-human GAPDH antibody, and images were recorded using the GeneSnap program (A). The amount of Cyclin D1 protein was determined by western blot analysis and quantified against GAPDH (B) using the ImageJ program. (Data are representative of 3 independent experiments and expressed as means ± sd,*=$p<0.05$ vs control sample)

Figure 4.12. The influence of the expression of wild-type and mutant forms of TF on endothelial cell apoptosis using DeadEnd fluorescence-based TUNEL assay

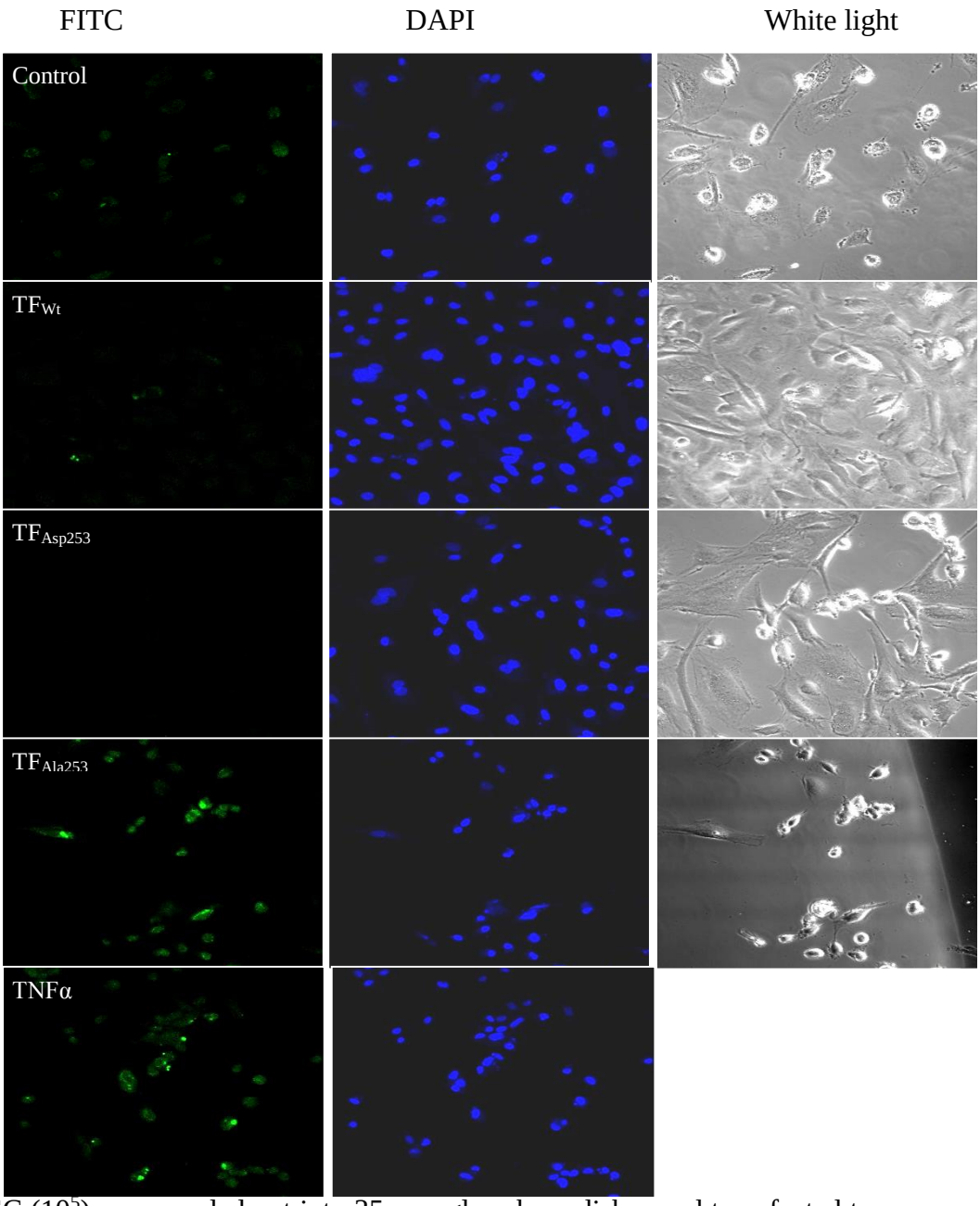

HCAEC (10^5) were seeded out into 35 mm glass-base dishes and transfected to express TF_{Wt}, TF_{Asp253}, and TF_{Ala253} or control plasmid for 48 h. The cells were adapted to serum-free medium and activated with PAR2-AP (20 μM). Sets of cells were activated with TNFα (10 μg/ml) for 18 h. The cells were then fixed, developed using the DeadEnd fluorescence-based TUNEL assay and analysed by confocal microscopy with a ×20 objective. (n=3)

Figure 4.13. The influence of the expression of wild-type and mutant forms of TF on endothelial cell apoptosis using TiterTACS™ Colorimetric Apoptosis Detection Kit

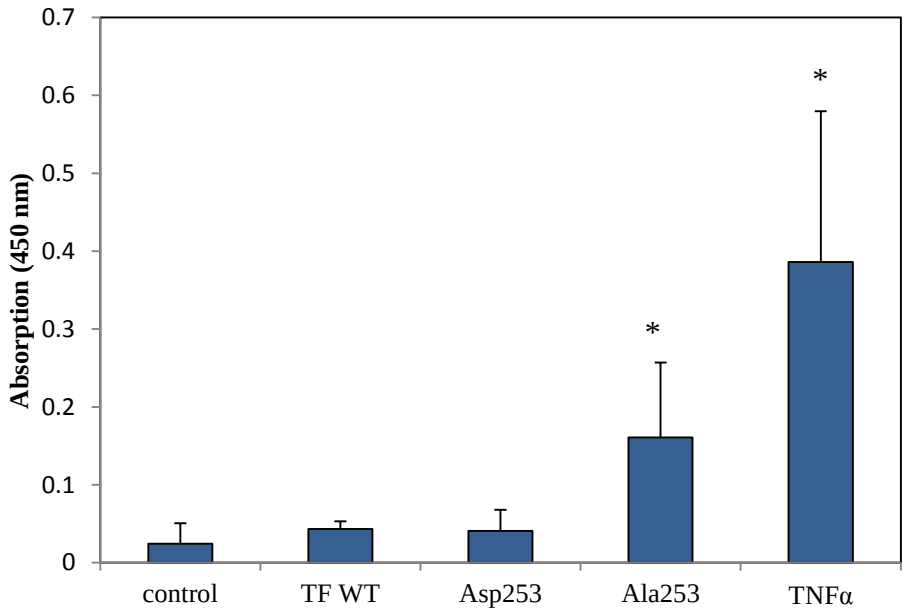

HCAEC (10^5) were seeded out into 35 mm glass-base dishes and transfected to express TF_{Wt}, TF_{Asp253}, and TF_{Ala253} or control plasmid for 48 h. The cells were adapted to serum-free medium and activated with PAR2-AP (20 μM) for 18 h. The cells were then fixed and the level of cell apoptosis was quantified using the TiterTACS™ Colorimetric Apoptosis Detection Kit. (Data are representative of 3 independent experiments and expressed as means ± sd, *=$p<0.05$ vs control plasmid-expressing sample)

Figure 4.14. Examination of the outcome of high concentration of TF-containing microvesicles on endothelial cell apoptosis using TiterTACS™ Colorimetric Apoptosis Detection Kit

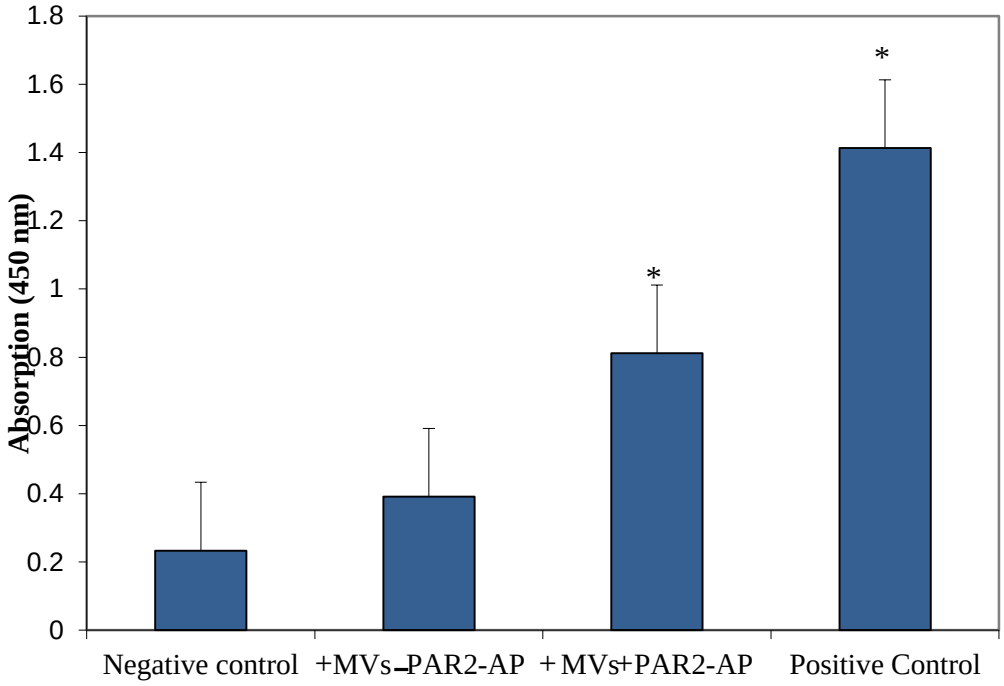

HCAEC (10^5 /well) were incubated with TF-containing microvesicles (100 ng/ml TF) derived from MDA-MB-231 for 24h in serum-free medium, and activated with PAR2-AP (20 µM). In addition, one set was untreated and was used as a negative control. The rate of cellular apoptosis was measured at 18 h post-activation using the apoptosis detection kit. (Data are representative of 3 independent experiments and expressed as means ± sd, *=$p<0.05$ vs non-treated sample)

4.3.5. The influence of inhibition of p38α activity on TF-mediated endothelial cell apoptosis

HCAEC (10^5) were transfected to express TF_{Wt}, TF_{Ala253} or control plasmid and activated with PAR2-AP, pre-incubated with SB202190 (100 nM) to specifically inhibit p38α activity. Cellular apoptosis was measured at 18 h using the TiterTACS™ Colorimetric Apoptosis Detection Kit. Inhibition of p38α activity significantly reduced the rate of cell apoptosis in cells expressing TF_{Ala253} compared to those observed in cells without the inhibitor. Furthermore, inhibition of p38α in cells expressing TF_{Wt} restored the level of apoptosis to levels similar to those observed in the control samples (Fig 4.15).

4.3.6. Analysis of the influence of TF on p21 and Bax expression

In an attempt to elucidate the mechanisms by which TF may induce cell cycle arrest or cellular apoptosis, the expression of Bax and p21 proteins in cells expressing wild-type and mutant forms of TF were examined by western blot. The level of Bax protein peaked at 18 h post-activation (Fig 4.16 A & B) while there was no detectable difference in Bax protein observed at 4 or 8 h post-activation (data not shown). p21 protein bands were too faint to detect accurately. Therefore, the analysis of p21 protein expression was not performed. Incubation of the cells with TF-containing microvesicles (100 ng/ml TF) for 2h also induced Bax protein expression following PAR2-AP activation for 18 h (Fig 4.17).

Figure 4.15. The influence of inhibition of p38 activity on endothelial cell apoptosis

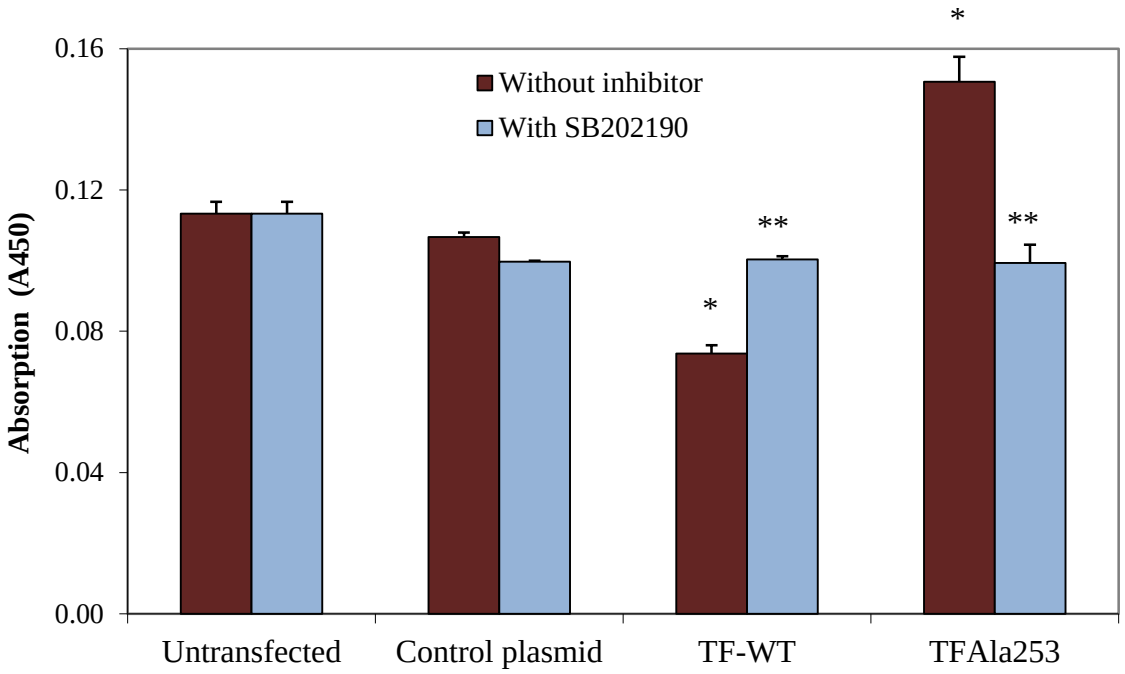

HCAEC (10^5/well) were seeded out in 12-well plates, transfected to express TF_{Wt} and TF_{Ala253} or control plasmid and incubated for 48 h. Sets of cells were un-transfected for comparison. The cells were adapted to serum-free medium and treated with or without SB202190 (100 nM) for 30 min. Both sets of cells were then activated with PAR2-AP (20 µM) and the level of cell apoptosis was measured at 18 h using the TiterTACS™ Colorimetric Apoptosis Detection Kit. (Data are representative of 3 independent experiments and expressed as means ± sd, *=$p<0.05$ vs un-transfected/non-treated sample; **=$p<0.05$ vs respective untreated sample)

Figure 4.16. Analysis of Bax protein expression in cells expressing wild-type and mutant forms of TF

(A)

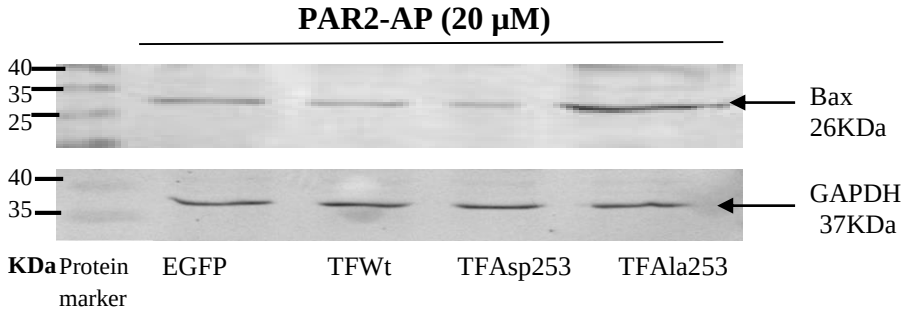

(B)

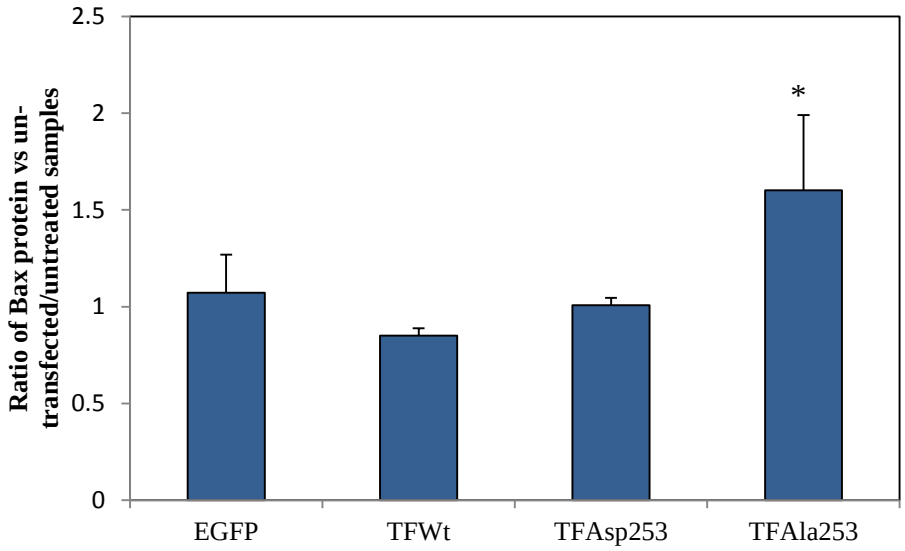

HCAEC (10^5/well) were cultured in 12-well plates and transfected with TF_{Wt}, TF_{Asp253}, and TF_{Ala253} or EGFP. The cells were incubated for 48 h, adapted to serum-free medium and activated with PAR2-AP (20 µM) for 18 h. The cells were then lysed in Laemmli's buffer, and the proteins were separated by 12 % (w/v) SDS-PAGE. Proteins were transferred onto nitrocellulose membranes and probed for Bax using a mouse anti-human Bax. The membranes were then probed for GAPDH using a rabbit anti-human GAPDH antibody and images were recorded using the GeneSnap program (A). The amount of Bax protein was quantified against GAPDH (B). (Data are representative of 3 independent experiments and expressed as means ± sd, *=$p<0.05$ vs non-treated sample)

Figure 4.17. Analysis of Bax protein expression in cells incubated with TF-containing microvesicles

(A)

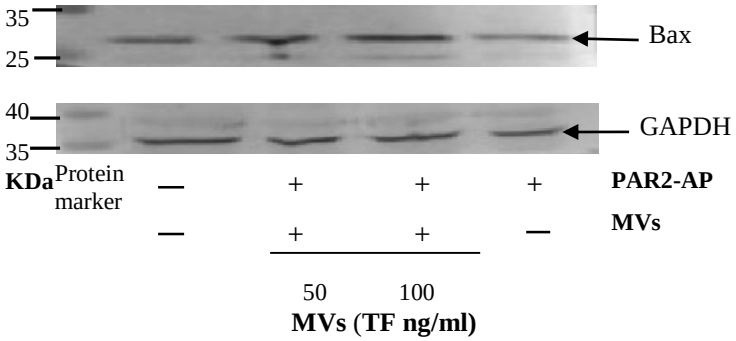

(B)

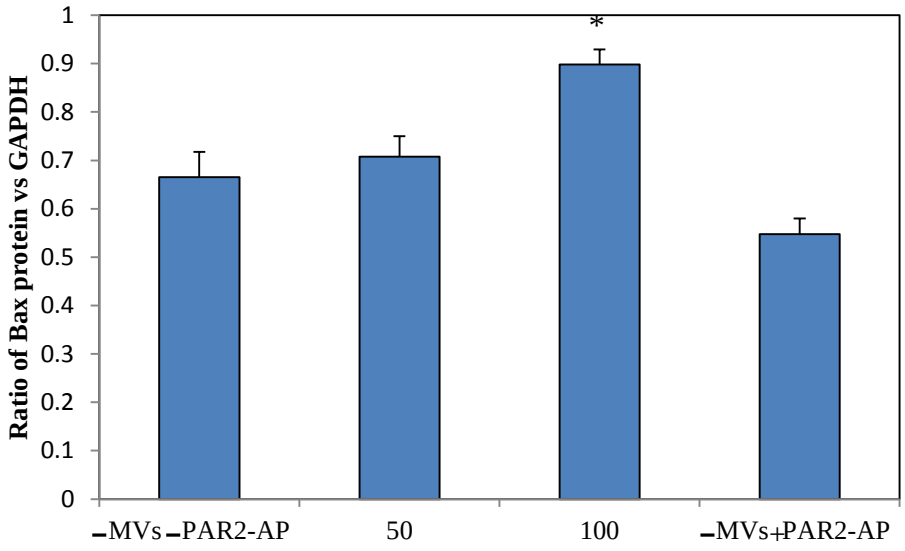

HCAEC (10^5/well) were incubated with microvesicles-TF (50, 100 ng/ml TF) derivded from breast cancer cell line MDA-MB-231 (for 2 h in serum-free medium. The cells were then activated with PAR2-AP (20 µM) for 18 h. The cells were then lysed in Laemmli's buffer and proteins separated by 12 % (w/v) SDS-PAGE. Proteins were transferred onto nitrocellulose membranes and probed for Bax using a mouse anti-human Bax. The membranes were then probed for GAPDH using a rabbit anti-human GAPDH antibody, and images were recorded (A) using the GeneSnap program. The amount of Bax protein was quantified (B) against GAPDH. (Data are representative of 3 independent experiments and expressed as means ± sd, *=$p<0.05$ vs non-treated sample)

In a separate experiment, cells were transfected to express wild-type and mutant forms of TF, activated with PAR2-AP and incubated for 4 h. The expressions of p21 and bax mRNA were investigated. RT-PCR analysis of p21 and bax mRNA in cells expressing TF_{Ala253} and activated with PAR2-AP showed an increase in both p21 and bax mRNA significantly at 4 h post-activation (Fig 4.18 A & B). Furthermore, no significant changes in p21 and bax mRNA levels were observed in cells expressing TF_{Wt} or TF_{Asp253}. The increase in bax mRNA was also observed in cells treated with high concentrations of TF (100 ng/ml TF) (Fig 4.19). In contrast, treatment of the cells with low concentrations of TF (50 ng/ml TF) resulted in a decrease in the bax mRNA level (not shown).

4.4. Discussion

A previous study has shown an association between the phosphorylation of Ser258 and the termination of TF release within cell-derived microvesicles (Collier & Ettelaie, 2011). The data presented in chapter 3 demonstrated that p38α was a main kinase, responsible for the phosphorylation of Ser258 within the cytoplasmic domain of TF. In this part of the study, the hypothesis that TF may also induce endothelial cell proliferation or apoptosis through p38 activation was examined. In order to use a consistent model throughout this study, cells expressing Ala 253-substituted TF were used. This substitution prevents the release of TF from the cell. Comparisons were made with cells expressing wild-type TF and Asp 253-substituted TF. However, the use of transfection systems is artificial, and they may not truly represent the pathophysiological conditions in the human body. Therefore, it was considered that treatment of endothelial cells with TF-containing microvesicles would support and extend the artificial method of introducing the TF into endothelial cells.

Figure 4.18. Analysis of expression of p21 and bax mRNA in cells expressing wild-type and mutant forms of TF

(A)

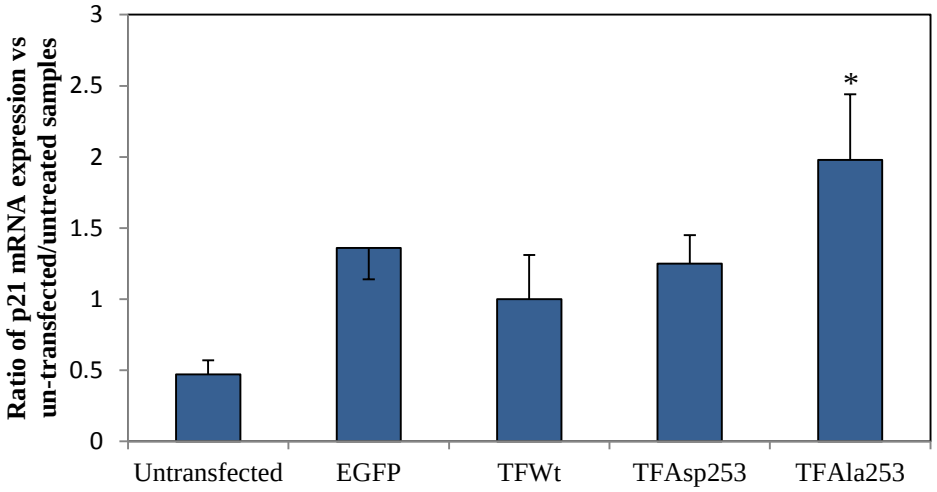

(B)

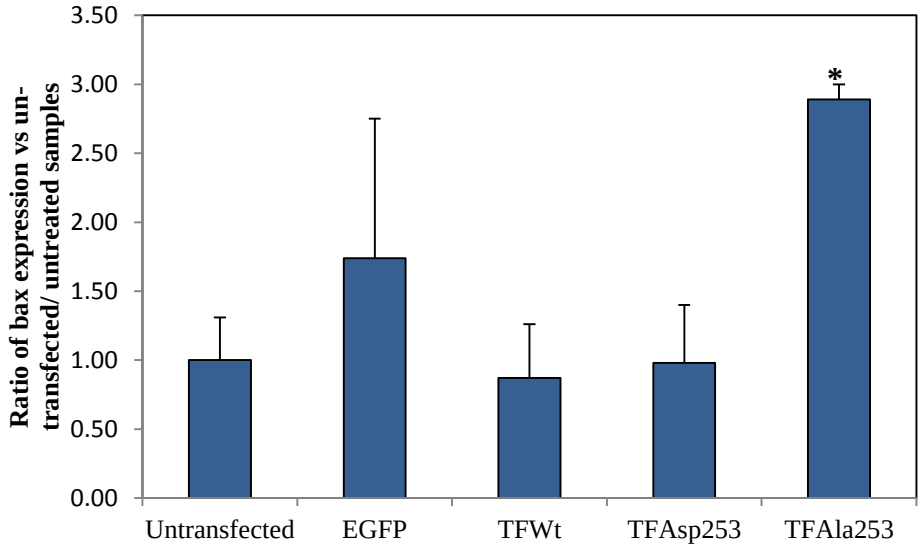

HCAEC (10^5) expressing TF_{Wt}, TF_{Asp253}, and TF_{Ala253} or EGFP were adapted to serum-free medium and activated with PAR2-AP (20 µM). In addition, an un-transfected/non-activated sample was included as a control. Total RNA was isolated from the cells at 4 h post-activation, and the relative amounts of (A) p21 mRNA and (B) bax mRNA were determined by RT-PCR. (Data are representative of 3 independent experiments and expressed as means ± sd, *=$p<0.05$ vs un-transfected/non-treated sample)

Figure 4.19. Analysis of expression of bax mRNA in cells treated with high concentration of microvesicles-TF

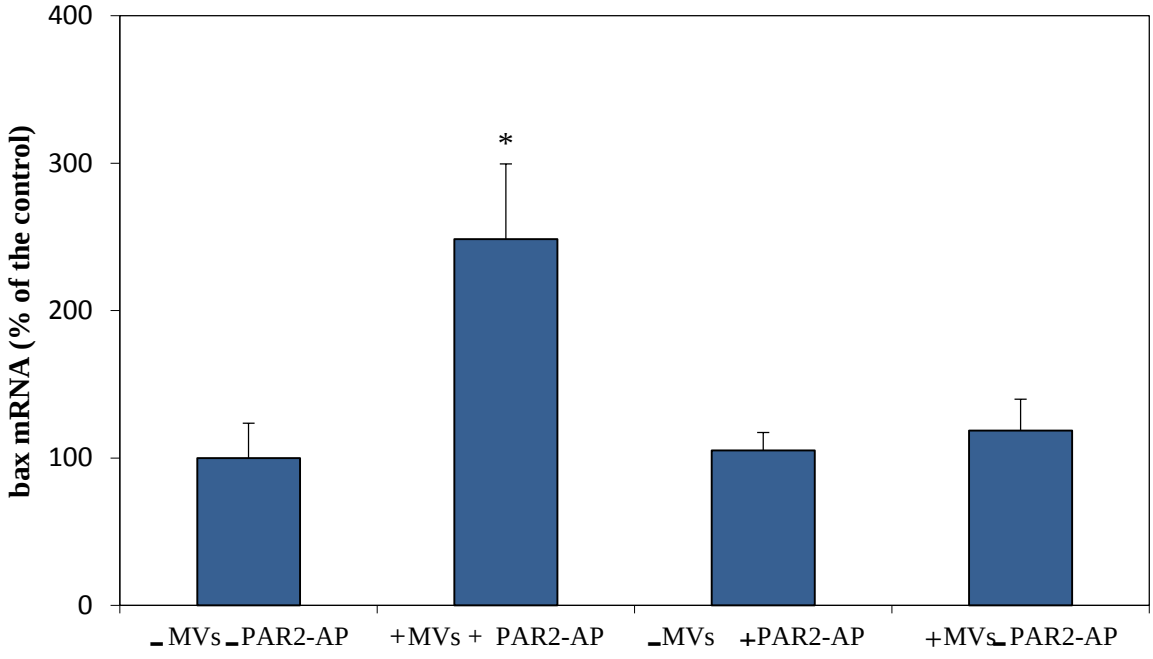

HCAEC (10^5/well) were incubated with microvesicles-TF (100 ng/ml TF) derived from breast cancer cell line MDA-MB-231 for 2 h in serum-free medium. The cells were then activated with PAR2-AP (20 µM) for 4 h. Total RNA was isolated from the cells and the relative amounts of bax mRNA were determined by RT-PCR. (Data are representative of 3 independent experiments and expressed as means ± sd, *=$p<0.05$ vs non-treated sample)

In the first part of this section, an attempt was made to elucidate the role of TF-mediated p38 activation in endothelial cell proliferation and, particularly, the expression of the cell cycle regulator Cyclin D1. Cyclin D1 is the main regulatory element for the progression of cells from the G1 to the S phase and can be regulated in response to diverse stimuli (Guardavaccaro et al., 2000; Ravenhall et al., 2000). Activation of cells expressing TF_{Wt} or TF_{Asp253} with PAR2-AP resulted in increased endothelial cell proliferation (Fig 4.4). This increase was concurrent with upregulation of cyclin D1 mRNA expression (Fig 4.7) and Cyclin D1 protein at 8 h post-activation (Fig 4.8). This increase in Cyclin D1 expression suggests that the entry into the cell cycle following PAR2 activation may be enhanced by the presence of TF. These findings are in agreement with previous reports showing that the incubation of endothelial cells (Pradier & Ettelaie, 2008; Collier & Ettelaie, 2010) and the cardiomyocyte cell line H9c2 (Frentzou et al., 2010) with moderate amounts of recombinant or microvesicle-derived TF results in cell proliferation. Interestingly, although activation of cells expressing TF_{Ala253} induced the upregulation of cyclin D1 mRNA expression (Fig 4.7), this did not lead to increased expression of Cyclin D1 protein (Fig 4.8) or cell proliferation (Fig 4.4). This agrees with the hypothesis that the entry into the cell cycle following PAR2 activation is enhanced by the presence of TF. However, the prolonged presence of TF and/or inability of the cell to release TF within microvesicles results in cell cycle arrest. In addition, in the previous chapter it was shown that PAR2 activation in TF-expressing endothelial cells resulted in the prolonged phosphorylation of p38 in cells expressing TF_{Wt}. Furthermore, this phosphorylation was augmented in cells expressing TF_{Ala253} but was absent in cells expressing TF_{Asp253}. Therefore, it seems possible that the presence of TF in the cells can induce cell proliferation through p38 phosphorylation, while the accumulation of TF in cells by preventing its release can amplify and prolong p38 phosphorylation and lead to cell cycle

arrest. Another possible explanation for these findings is that the presence of TF can activate growth signalling mediated by the ERK1/2 pathway, inducing endothelial cell proliferation (Collier & Ettelaie, 2010). However, prolonged activation of p38 due to accumulation of TF may inhibit the growth signal and suppress the cell cycle progression.

To further investigate the role of p38 in endothelial cell proliferation, the influence of inhibition of p38 on the expression of Cyclin D1 was further examined. p38 activity was specifically inhibited using SB202190. Alternatively, the expression of p38α was suppressed using specific p38α-siRNA. Inhibition of p38 expression in cells expressing wild-type TF using p38α-siRNA resulted in a reduction in Cyclin D1 protein expression after 8 h post-activation (Fig 4.11). This suggests the involvement of p38 in the up-regulation of expression of Cyclin D1 and cell cycle progression in cells expressing TF.

Next, the hypothesis that the prolonged accumulation or retention of TF in cells may induce apoptosis in endothelial cells and the role of p38 was investigated. Prevention of TF release by transfection of endothelial cells with TF_{Ala253} showed a significant increase in cellular apoptosis at 18 h post-activation (Fig 4.12 & Fig 4.13). Furthermore, there was no difference in the level of apoptosis in cells transfected to express TF_{Wt}, TF_{Asp253} or control plasmid compared to un-transfected cells. In addition, treatment of endothelial cells with high concentrations of TF-containing microvesicles also increased cellular apoptosis following PAR2 activation (Fig 4.14). These data suggest that the accumulation of TF in the cells is likely to lead to the activation of apoptotic signals and promote cellular apoptosis. Moreover, the presence of TF in the cells at a low level has no influence on endothelial cell apoptosis. Therefore, cells can prevent apoptosis by releasing TF. These results are in agreement with other studies which have shown that

high concentrations of TF observed in severe disease conditions can cause cellular apoptosis (Pradier & Ettelaie, 2008; Frentzou et al., 2010). In addition, it has been reported that prolonged exposure of HUVEC to microvesicles obtained from activated THP-1 cells can induce apoptosis (Aharon et al., 2008). Interestingly, these alterations in cellular apoptosis were reversed by suppression of the activity of p38. Inhibition of p38 activity using SB202190 (100 nM) reduced the level of apoptosis significantly in the cells expressing TF_{Ala253} compared to untreated cells (Fig 4.15). In addition, inhibition of p38 activity in cells expressing TF_{Wt}, resulted in the suppression of the anti-apoptotic influence of TF_{Wt} restoring this to levels similar to those observed in the control samples (Fig 4.15). Therefore, p38 appears to be a key mediator between TF and the mechanism of cell apoptosis. Therefore, in conclusion, the accumulation of TF in the endothelial cells is capable of inducing apoptosis in these cells. This process appears to be mediated through a p38-dependent mechanism. Although earlier studies have focused on the role of TF on apoptosis, no previous study has investigated the mechanism by which TF induces apoptosis.

Finally, to further identify the mediators of TF-induced cell apoptosis, the influence of wild-type and mutant forms of TF on p21 and Bax expression in endothelial cells was examined. The expression of both Bax and p21 appeared to be increased in cells expressing TF_{Ala253} compared to cells expressing TF_{Wt} and TF_{Asp253} or control cells (Fig 4.16) and (Fig 4.18 A & B) and appeared to be concurrent with cellular apoptosis (Fig 4.11). Therefore, these findings indicate that the accumulation of TF in the endothelial cells can also lead to cell cycle arrest by up-regulating the expression of p21 mRNA (Fig 4.18 A) (and possibly p21 protein) as the initial step. Subsequently, the fate of the cell

can be determined by the regulation of the expression of Bax (Fig 4.16, Fig 4.17, Fig 4.18 A & Fig 4.19).

The activation of cells in response to injury, trauma or inflammatory mediators results in the release of TF as cell-derived microvesicles. At lower concentrations of TF, it is envisaged that cells will be able to release sufficient amounts of the stored TF and therefore respond to the injury in the form of increased proliferation. However, accumulation of large amounts of TF through high levels of pro-inflammatory factors or through the sequestration of microvesicles from the bloodstream may compromise the ability of endothelial cells to respond to cell activation in a positive manner and result in the arrest of the progression through the cell cycle, leading to cell apoptosis. In conclusion, this study has shown that the activity of p38 in TF-bearing cells, following activation of PAR2, may have a bi-functional outcome resulting in the induction of cell proliferation or, alternatively, cell apoptosis, and may depend on the duration and magnitude of p38 activity. These findings seem to be consistent with the current understanding of the p38 function, which is thought to have a dual role, capable of activation or inhibition of cell cycle depending on the stimulus (Dolado & Nebreda, 2008; Tormos et al., 2013).

CHAPTER 5

Investigation of the mechanism of TF-mediated cellular apoptosis

5.1. Introduction

The association between endothelial cell apoptosis and inflammatory diseases is well established. In the previous sections of this study it was shown that the prolonged accumulation or retention of TF in endothelial cells resulted in induction of cellular apoptosis. In this section, the association of TF with the induction of the pro-apoptotic transcription protein p53 is examined.

5.1.1. p53 pathway and cellular apoptosis

p53 is a transcription factor that is activated in response to a range of stress stimuli including DNA damage, oncogene activation and hypoxia. Upon activation of p53, the levels of p53 increase in the nucleus. Accumulation of p53 in the nucleus results in the transcription of genes whose protein products induce cell cycle arrest or apoptosis. One of the first discovered p53 target genes was the cyclin-dependent kinase inhibitor (CDK) p21. p21 induces cell cycle arrest at G1 by inhibiting cyclin/cdk complexes (El-Deiry et al., 1994) (Fig 5.1). This prevents the replication of damaged DNA and allows time for DNA repair (Abbas & Dutta, 2009). Conversely, if the damage is extensive, p53 induces apoptosis by activating genes that promote the apoptotic pathways (Vousden, 2000; Chipuk & Green, 2006). These genes include bax (Toshiyuki & Reed, 1995; Polyak et al., 1997), puma (Nakano & Vousden, 2001), noxa (Sax et al., 2002) and bid (Oda et al., 2000). The balance between cell survival and death also depends on several factors including the level of p53 expression, as well as posttranslational modifications and subcellular localisation of p53 (Murray et al., 2008; Meek et al., 2009).

Figure.5.1. p53 signalling pathway

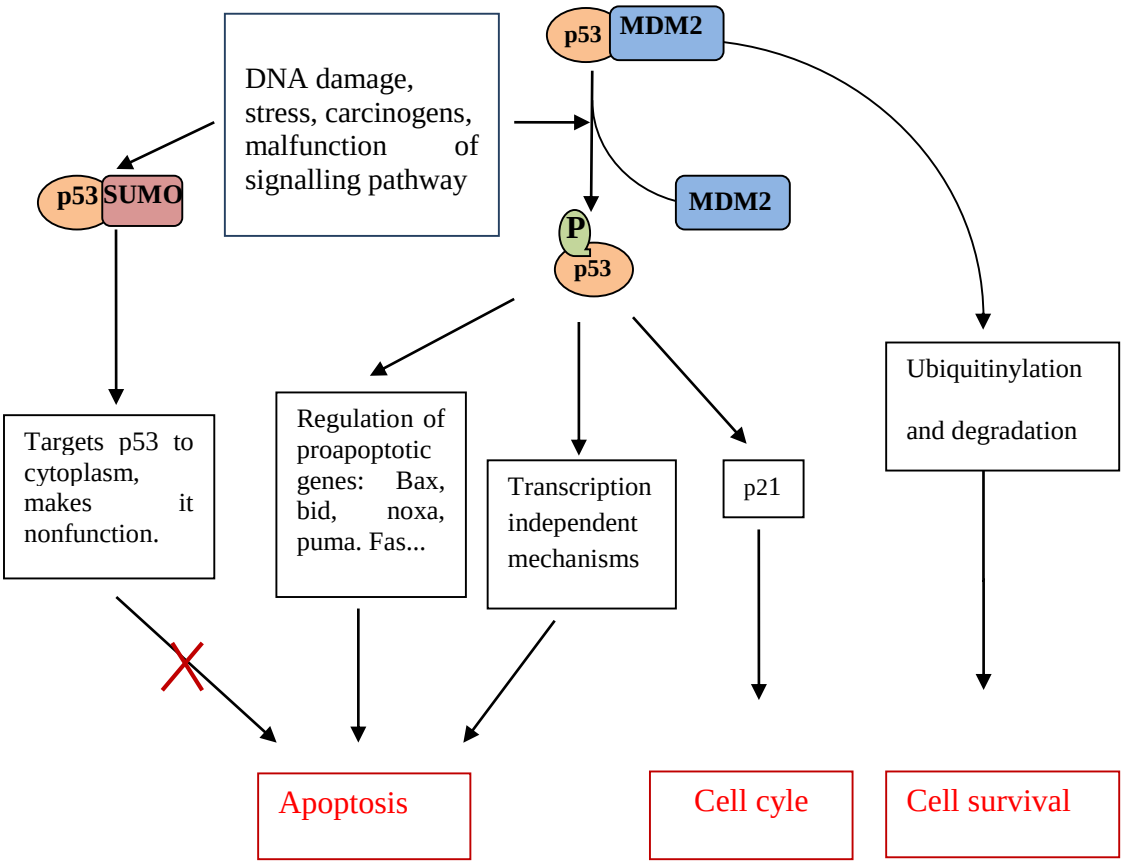

The non-activated p53 is associated with MDM2 ubiquitin ligase leading to p53 degradation and allowing the normal cell cycle to proceed. p53 is activated following DNA damage, stress or aberrant signalling, resulting in dissociation from its negative regulator MDM2. Activated p53 is involved in cell cycle arrest by increasing the expression of p21. Activated p53 also up-regulates a number of genes involved in apoptosis. p53 can also regulate apoptosis via mechanisms independent of transcriptional activation. Sumoylation of p53 targets it to cytoplasm and inhibit apoptosis (Adapted from Fuster et al., 2007)

Even though the apoptotic activity of p53 can also function in a transcription-independent manner (Mihar et al., 2003; Chipuk et al., 2004; Vousden, 2005; Fuster et al., 2007) by regulation of mitochondrial membrane permeabilisation, the main apoptotic activity of p53 has been attributed to its transcriptional activity. In addition, it has been demonstrated that p53 can also influence other biological processes, such as cell motility, cell differentiation, cell survival, autophagy and angiogenesis (Crighton et al., 2006).

5.1.2. p53 structure and stability

Wild-type p53 protein is composed of several functional domains that are crucial for mediating its varied functions: two transactivation domains (TAD1 and TAD2) and a proline-rich domain, at N-terminus, a core domain containing a DNA-specific binding domain, and a C-terminus domain containing an oligomerisation domain and regulatory domain (Fig 5.2). The N-terminus domain is crucial for the transcriptional activation function of p53 and plays an important role in apoptosis (Campbell et al., 2013). The transcriptional activity of p53 is regulated by the association of the N-terminus domain with proteins such as p300, MDM2 and Pin1 (Joerger & Fersht, 2008). In addition, the N-terminus domain contains multiple phosphorylation sites which are phosphorylated by different protein kinases (Walker & Levine, 1996).

p53 protein concentrations are kept at low levels in unstressed cells, allowing the normal cell cycle to proceed. This control is primarily regulated by MDM2 (Yang et al., 2004) and constitutes the main mechanism responsible for keeping the levels of p53 in check. MDM2 inhibits p53 by acting as a p53-specific E3 ubiquitin ligase that conjugates a chain of ubiquitin molecules onto the N-terminus of p53. The interaction of MDM2 with p53

Figure.5.2. Structure of p53 protein

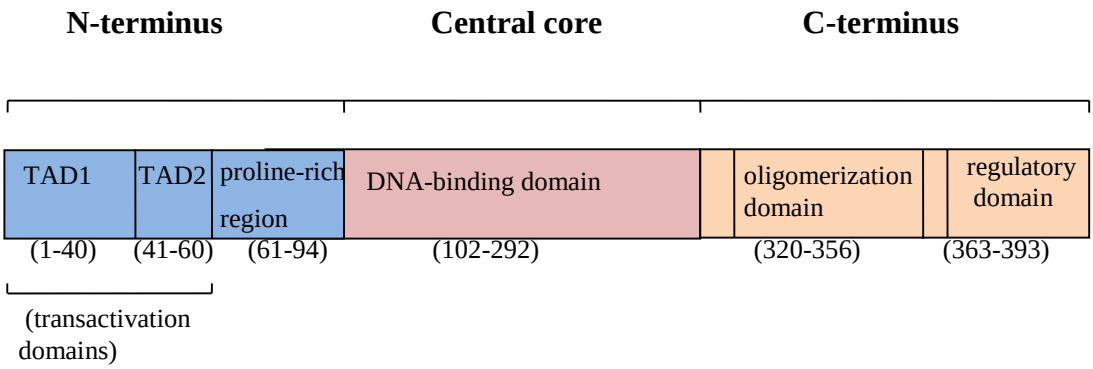

The human p53 protein consists of 393 amino acids, which have been divided into three functional domains; an N-terminal activation domain containing TAD1 and TAD2 domains, a DNA-binding domain, and a C-terminal tetramerisation domain. (Adapted from Loughery & Meek, 2013)

promotes nuclear exportation of p53 and the subsequent proteasomal degradation in the cytoplasm (Haupt et al., 1997; Honda et al., 1997; Kubbutat et al., 1997; Iwakuma & Lozano, 2003). Aside from its ubiquitin ligase function, MDM2 also blocks the transcriptional activity of p53 by binding to its transcriptional-activation domain (Momand et al., 1992). Furthermore, MDM2 is also able to induce conformational changes with the DNA-binding domain of p53, thereby inhibiting the interaction of p53 with DNA (Cross et al., 2011). This regulation occurs through a feedback loop in which p53 stimulates the expression of MDM2 protein and, in turn, MDM2 inhibits p53. In addition to MDM2, p53 is also regulated by other ubiquitin ligases the complement of which is dependent on the cell type (Love & Grossman, 2012).

Exposure of the cell to stress stimuli or DNA-damaging agents leads to enhancement of the stabilisation of p53 by inhibiting its negative regulation by MDM2. This results in the accumulation of p53 within the nucleus where p53 interacts with sequence-specific sites of its target genes (Appella & Anderson, 2001). The activity and function of p53 are regulated by a variety of post-translational changes, including phosphorylation, acetylation, and protein–protein interactions (Appella & Anderson, 2001). These post-translational changes influence the stability, subcellular localisation, and DNA binding ability of p53. However, phosphorylation of p53 is considered the essential step for p53 stabilisation and has also been shown to increase its DNA binding ability (Hupp & Lane, 1994). p53 phosphorylation is brought about by a broad range of kinases, including JNK and p38 (Bulavin & Fornace, 2004; Bradham & McClay, 2006). Phosphorylation of serine residues within the N-terminus of p53 is thought to prevent MDM2 binding as well as promoting interaction with transcription factors and co-activator proteins including p300 (Meek & Anderson, 2009; Jenkins et al., 2012).

5.1.3. Aims

In chapters 3 and 4, prevention of TF release through Ala-substitution of residue 253 was shown to enhance p38 activation and induce apoptosis. Furthermore, inhibition of p38 pathway resulted in inhibition of cell apoptosis in the cells expressing TF_{Ala253}. However, the mechanisms by which accumulation of TF-mediated p38 activation induce cell apoptosis have not been examined. The main objectives of this chapter were as follows.

- To examine the possible role of TF-induced p38 activation on p53 phosphorylation, localisation in nucleus, and transcriptional activity
- To investigate the involvement of p53 in TF-mediated apoptosis and determine whether the accumulation of TF-inducing apoptosis arises from p53 activation

5.2. Methods

5.2.1. Measurement of p53 expression

5.2.1.1. Time-course analysis of the level of p53 protein

In order to determine the changes in the level of p53 protein, HCAEC (10^5 /well) were seeded out in 12-well plates and adapted to serum-free medium. The cells were treated with TNFα (2 μg/ml) for 0, 2, 4, 6 h. The cells were then lysed in Laemmli's buffer (100 μl), and the protein concentration in each sample was estimated using Bradford assay as described in the general method section 2.6.1.The amount of p53 protein was assessed by SDS-PAGE followed by western blot analysis as described in the general method sections 2.6.2. & 2.6.3. The membranes were probed for p53 and GAPDH using rabbit anti-p53 and mouse anti-GAPDH antibodies diluted in TBST according to Table 5.1. The images were recorded using the GeneSnap program and p53 bands were compared to GAPDH using the ImageJ program.

Table 5. 1. Antibodies-TBST dilution for western blot

Primary antibodies	Dilution antibodies: TBST (v/v)	Secondary antibodies	Dilution antibodies: TBST (v/v)
Rabbit anti-phospho-p53 (Ser33) polyclonal	1:1000	Goat anti-rabbit HRP-conjugated antibody	1:5000
Rabbit anti-human phospho-p53 (Ser46) antibody	1:1000	Goat anti-rabbit HRP-conjugated antibody	1:5000
Rabbit anti-human p53 IgG antibody	1:1000	Goat anti-rabbit alkaline phosphatase-conjugated antibody	1:5000
Mouse monoclonal anti-human GAPDH antibody (1D4B)	1:2000	Goat anti-mouse alkaline phosphatase-conjugated antibody	1:5000
Rabbit anti-human GAPDH antibody	1:2000	Goat anti-rabbit alkaline phosphatase-conjugated antibody	1:5000

5.2.1.2. Examination of nuclear localisation of p53 protein

HCAEC (10^5/well) were cultured in 12-well plates and adapted to serum-free medium. The cells were treated with TNFα (2 µg/ml) for 0, 2, 4, 6 h. Cells were harvested and washed with 200 µl cold PBS. For each time point, the cell suspension was divided between two microcentrifuge tubes. One tube was centrifuged at 1200 *g* for 5 min, lysed in 50 µl Laemmli's buffer and used as a total fraction. In order to separate the nuclear fraction from the cytoplasmic fraction the other tube was centrifuged at 1200 *g* for 5 min and the pellet was re-suspended in 40 µl of hypotonic buffer. The samples was then transferred to a pre-chilled microcentrifuge tube and incubated in ice for 15 min. 1 % (w/v) of Triton X100 (2.2 µl) was added and vortexed for 10 s. The nuclear fraction was collected by centrifugation at 12,000 rpm for 30 s. The supernatant (cytoplasmic fraction) was transferred to a pre-chilled microcentrifuge tube and stored at -70°C. The nuclear fraction was re-suspended in 15 µl complete lysis buffer containing 1 mM DTT and 1 % (v/v) protease inhibitor cocktail. The solution was vortexed for 10 s and incubated on ice for 30 min. The solution was then vortexed for 30 s, centrifuged for 10 min at 12,000 rpm and transferred to a pre-chilled microcentrifuge tube. Nuclear and total fractions of p53 protein at each time point were examined by SDS-PAGE and analysed by western blot as in section 5.2.1.1.

5.2.1.3. Examination of the role of TF-mediated p38 activation on the regulation of p53 protein levels

To examine the role of TF on the maintenance of p53 protein levels, HCAEC (10^5/well) were transfected to express (TF_{Wt}) or mutant forms of TF (TF_{Asp253}, TF_{Ala253}) over 48 h. In addition, one set of cells was transfected to express EGFP and used as a control. The cells were then adapted to serum-free medium and activated with PAR2-AP (20 µM) for 4 h. The

cells were then lysed in Laemmli's buffer (100 µl) and the amounts of cellular p53 protein were measured in comparison to GAPDH as described in section 5.2.1.1.

HCAEC (10^5/well) were incubated with microvesicles containing TF (100 ng/ml TF) isolated from MDA-BM-132 cells as described in section 4.2.7. After 2 h incubation, the cells were activated with PAR2-AP (20 µM) for 4 h. The amounts of cellular p53 protein were measured in comparison to GAPDH as described in section 5.2.1.1.

To examine the correlation between TF-mediated p38 activation and p53 protein levels, HCAEC (10^5/well) were co-transfected with p38α specific siRNA or a control siRNA. Similar sets of cells were also co-transfected with either pCMV-XL5-TF or pCMV-EGFP plasmids as described in section 4.2.4. p53 protein levels were examined by SDS-PAGE and western blot for p53 and GAPDH as in section 5.2.1.1.

5.2.1.4. Analysis of the involvement of TF-mediated p38 activation in the expression of p53 mRNA using semi-quantitative real-time RT-PCR

HCAEC (10^5/well) were cultured in 12-well culture plates. The cells were transfected to express wild-type or mutant forms of TF. In addition, one set of cells was transfected to express EGFP and used as a control. The cells were permitted to express the TF or EGFP proteins for 48 h. The cells were then adapted to serum-free medium and activated with PAR2-AP (20 µM) for 4 h. Samples of non-activated/untreated cells were also examined alongside them. Total RNA was extracted from the cells using TRI reagent, as described in the general methods section 2.7.1. RT-PCR was performed in triplicate using 0.1 µg of total RNA samples. Primers were designed to amplify cyclin p53 and β-actin in separate tubes as described in general method sections 2.7.2. Following the RT step, PCR was carried out at

melting temperatures of 90°C using the GoTaq® 1-Step RT-qPCR System on an iCycler thermal cycler as in section 2.7.3.

The primers used were as follows:

p53 forward primer 5'-GTTCCGAGAGCTGAATGAGG-3',

p53 reverse primer 5'-TTATGGCGGGAGGTAGACTG-3';

β-actin forward 5′-TGATGGTGGGCATGGGTCAGA-3′

β-actin reverse 5′-GTCGTCCCAGTTGGTGACGAT-3′

The Ct values of p53 cDNA were normalised against the values for β-actin gene and compared to untreated sets of samples using the $2^{-\Delta\Delta CT}$ method (Livak et al. 2001).

5.2.2. Investigation of the involvement of TF-mediated p38 activation in the phosphorylation of p53

HCAEC (10^5/well) were seeded out into 12-well plates and transfected with pCMV-XL5-TF, pCMV-XL5-TF_{Ala253} or, alternatively, with pCMV-EGFP as a control. The cells were incubated for 48 h to permit TF or EGFP protein expression. The cells were then adapted to serum-free medium and activated with PAR2-AP (20 µM) for 4 h. Untreated samples of cells were also used as control. Other sets of cells were pre-incubated with either SB202190 (100 nM) or equivalent amounts of DMSO-vehicle for 30 min prior to activation. Cells were then lysed in 100 µl of Laemmli's buffer and analysed by western blot using antibodies against p53-phospho-Ser33 and total p53 as described in sections 2.6.2. & 2.6.3. The levels of p53-phosphorylation at Ser46 were also analysed using a specific antibody, as above. In addition, other set of cells were incubated with microvesicles containing TF (100 ng/ml TF)

for 2 h in serum-free medium. The cells were then activated with PAR2-AP (20 µM) for 4 h and the level of p53 phospho-Ser33 was measured as above. To further investigate the role of p38 in the phosphorylation of p53 at Ser33, HCAEC (10^5/well) were co-transfected with p38α-siRNA or a control siRNA in conjunction with pCMV-XL5-TF plasmid as described in section 4.2.4.3. The levels of p53 phosphorylation at Ser33 were analysed as above.

5.2.3. Analysis of the involvement of TF-mediated p38 activation in the nuclear localisation of p53, by confocal microscopy

To examine the role of TF in p53 nuclear localisation, laser scanning confocal image microscopy (LSCIM) was employed. HCAEC (10^5) were seeded out into 35 mm glass-based dishes and transfected to express wild-type or mutant forms of TF. In addition one set was transfected to express EGFP and used as a control. The cells were incubated for 48 h to permit TF or EGFP protein expression. In some experiments, the cells were co-transfected with p38α-siRNA or a control siRNA alone, or in conjunction with pCMV-XL5-TF plasmid. Cells were adapted to serum-free medium and activated with PAR2-AP (20 µM) for 4 h. Samples of cells were also used untreated or, alternatively, activated with TNFα (10 ng/ml) and used as negative and positive controls respectively for 4h. The cells were then washed three times with PBS (2 ml), fixed with 3 % (v/v) formaldehyde for 30 min, permeabilised using 0.2 % (w/v) Triton X-100 for 4 min and blocked with 5 % (v/v) donkey serum for 30 min. The cells were then labelled with a rabbit polyclonal anti-human p53 antibody diluted 1:200 (v/v) in PBS, for 2 h at room temperature and then washed three times with PBS (2 ml). The cells were then re-probed with a NorthernLights donkey anti-rabbit IgG-NL637 diluted 1:200 (v/v) in PBS. After three further washes with PBS the nuclei were then labelled by incubation with DAPI (5 µg/ml) for 15 min. All samples were

analysed by confocal microscopy at room temperature using a Zeiss LSM 710 confocal microscope with a ×20 objective and images were captured using ZEN software. The donkey anti-rabbit IgG secondary antibody was fluorescein isothyocyanate (FITC) conjugated. This antibody binds to the rabbit anti-human p53 antibody and has an emission detectable at 637 nm; therefore, p53 localisation will appear red. The fluorescence emission of DAPI is at 461 nm and is detected as a blue channel. The co-localisation of p53 in the nuclei was subsequently determin using ImagePro Plus software. The correlation of the intensity distributions between the two colors in selected image was measured using Pearson correlation coefficient (R_r) and has range of 1 (perfect correlation) to -1 (perfect but negative correlation) with 0 denoting the absence of a relationship

Rr is given as follows:

$$R_r = \frac{\sum_i \left(S1_i - S1_{aver}\right) \cdot \left(S2_i - S2_{aver}\right)}{\sqrt{\sum_i \left(S1_i - S1_{aver}\right)^2 \cdot \sum_i \left(S2_i - S2_{aver}\right)^2}}$$

$S1_i$ is the intensity of the first (red) flourophore and the $S1_{aver}$ is arthmatic mean, whereas S2i and $S2_{aver}$ are the corresponding intinsities for the second (blue) flourophore.

5.2.4. Examination of the involvement of TF in the transcriptional activity of p53 by measuring bax mRNA expression

Pifithrin-α is known to inhibit the transcriptional activity of p53 (Bulavin et al., 1999) without influencing the non-transcriptional function of p53 (Sanchez-Prieto et al., 2000; Kishi et al., 2001).

Initially, to optimise the pifithrin-α concentration to obtain a maximal p53 inhibition, HCAEC (10^5/well) were adapted to serum-free medium and pre-incubated with a range of pifithrin-α concentrations (0-200 nM) for 30 min. The cells were then activated with TNFα (10 ng/ml) for 4 h. The expression of bax mRNA was measured semi-quantitatively by real-time RT-PCR as described in section 2.7.3. Next, HCAEC (10^5/well) were transfected with pCMV-XL5-TF, pCMV-XL5-TF_{Ala253} or, alternatively, with pCMV-EGFP as a control and incubated for 48 h to permit TF or EGFP protein expression. The cells were adapted to serum-free medium and incubated with pre-optimised pifithrin-α (100 nM) or an equivalent amount of DMSO-vehicle for 30 min prior to activation with PAR2-AP (20 μM). The expression of bax mRNA was measured semi-quantitatively at 4 h post-activation by real-time RT-PCR as above, and the Ct values for bax in each sample were then normalised against the values of β-actin for each sample and compared to untreated sets of samples using the $2^{-\Delta\Delta CT}$ method (Livak et al., 2001).

5.2.5. Examination of the involvement of TF in the transcriptional activity of p53, using the PathDetect® *in vivo* p53 pathway *cis*-reporting system

The PathDetect® luciferase reporter plasmid system was used in this study to investigate the effect of accumulation of TF in the cell on transcriptional activity of p53. The p53-Luc vector is composed of a *cis*-acting enhancer element which contains a specific consensus sequence that is recognised by the transcription factor p53.

These enhancer elements have been inserted upstream of a minimal TA promoter and the TATA box (Fig 5.3). This complete promoter sequence drives the expression of the luciferase gene upon p53 binding. Therefore, the activation of p53 may be monitored by measuring the level of luciferase expressed in mammalian cells.

To assess the influence of TF on p53 activity, HCAEC (10^5/well) were cultured in 12-well plates and co-transfected with pCMV-XL5-TF, pCMV-XL5-TF_{Asp253}, pCMV-XL5-TF_{Ala253} or pCMV-EGFP, together with 1 µg of Pathdetect p53-Luc *cis*-reporting plasmid. The cells were incubated for 48 h to permit expression of the TF or EGFP proteins. The cells were then adapted to serum-free medium and activated with PAR2-AP (20 µM). In a separate experiment, the cells were co-transfected with pCMV-XL5-TF_{Ala253} and 1 µg of Pathdetect p53-Luc *cis*-reporting plasmid as above, but pre-incubated with SB202190 (100 nM) or equivalent amounts of DMSO-vehicle for 30 min prior to activation with PAR2-AP (20 µM). Untransfected sets of cells were activated by TNF (10 ng/ml) and included as positive controls. After 8 h, the cells were washed once with PBS and lysed in luciferase cell culture lysis reagent (450 µl) (the contents are not shown by the manufacturers). The cell lysate was chilled on ice, vortexed for 15 s, and then centrifuged at 12,000 rpm for 15 s to remove any cell debris. The cell extract was transferred to a fresh tube and a 20 µl sample was mixed with 100 µl of luciferase substrate in a luminometer tube. The luciferase activity was then measured by detecting the light produced from oxidation of luciferin into oxyluciferin catalysed by the cells-expressed luciferase. The light intensity produced for each sample was detected using a Junior LB9509 luminometer over a period of 5 min.

Figure 5.3. p53 plasmid vector map

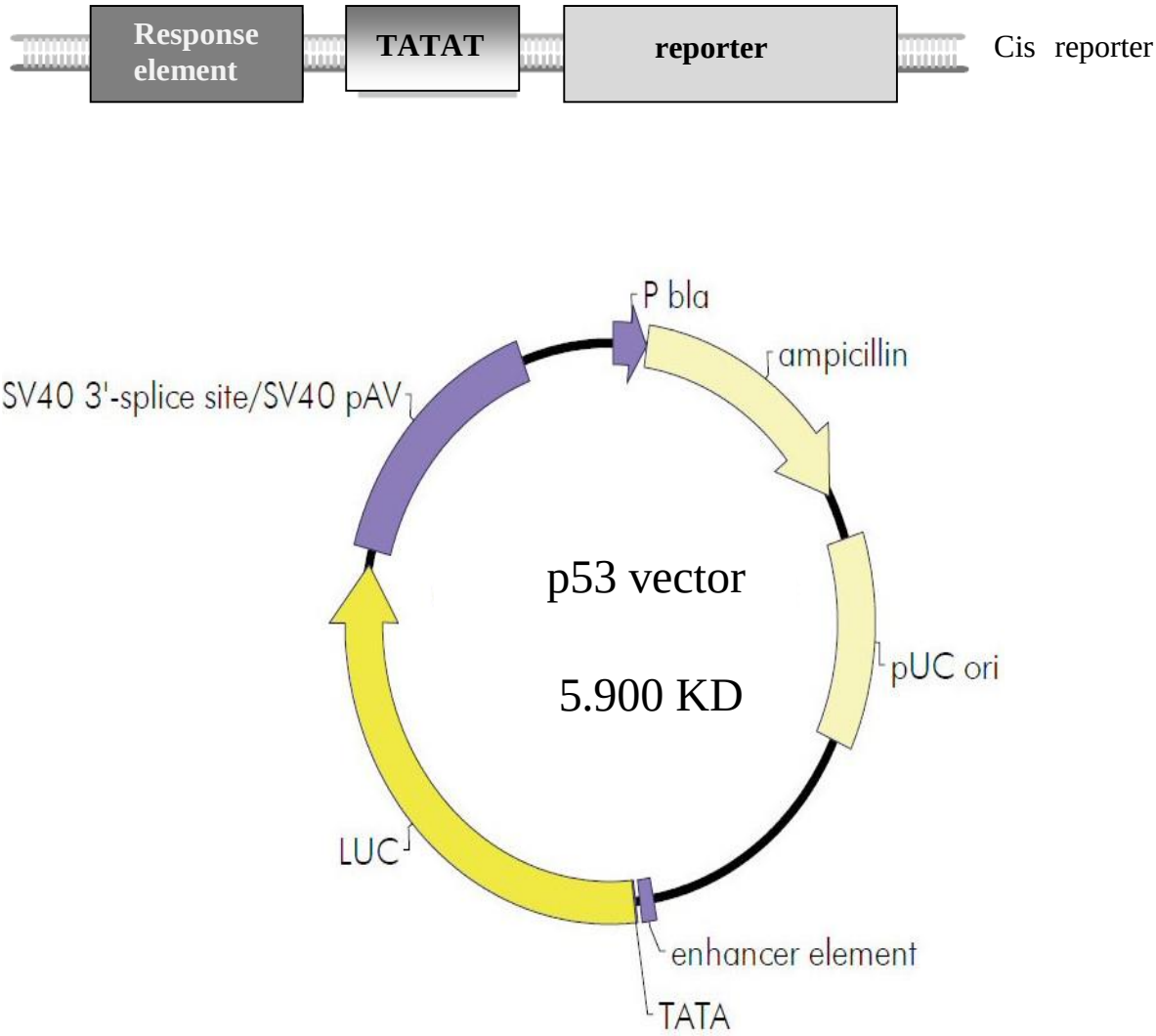

The pathDetect p53 reporter vector is designed to study the activation of the p53 pathway. Activated p53 transcription factor will recognise a specific consensus enhancer element, resulting in the induction of the transcription and expression of the luciferase gene (Luc). p53 transcriptional activity may therefore be monitored by measuring the activity of the expressed luciferase produced. (Obtained from www.chem-agilent.com)

5.2.6. Examination of the involvement of TF in p53-mediated apoptosis using TiterTACS™ Colorimetric Apoptosis Detection Kit and p53 inhibitor

HCAEC (10^5/well) were seeded out into 12-well plates. The cells were transfected with pCMV-XL5-TF, pCMV-XL5-TF_{Ala253} or, alternatively, with pCMV-EGFP as a control, adapted to serum-free medium and incubated for 30 min with either pifithrin-α (100 nM) or equivalent amounts of DMSO-vehicle. The cells were then activated with PAR2-AP (20 µM) and incubated for 18 h. The cells were fixed using 4 % (v/v) formaldehyde and the rate of apoptosis was measured using the TiterTACS™ Colorimetric apoptosis detection kit as described in section 4.2.5.2.

5.3. Results

5.3.1. Investigation of the role of TF-mediated p38 activation on p53 expression and protein levels

Prior to examination of the role of TF-mediated p38 activation in the regulation of p53, the time-point for maximal p53 protein level was determined. Activation of HCAEC with TNFα (2 ng/ml) resulted in maximal levels of the total and nuclear p53 protein at around 4 h post-activation (Fig 5.4. & 5.5). The influence of TF on p53 protein expression was analysed next. Western blot analysis of p53 in cells expressing wild-type or mutant forms of TF or, alternatively, EGFP indicated significantly higher levels of p53 protein at 4 h post-activation

Figure 5.4. Time-course of p53 protein level by western blot

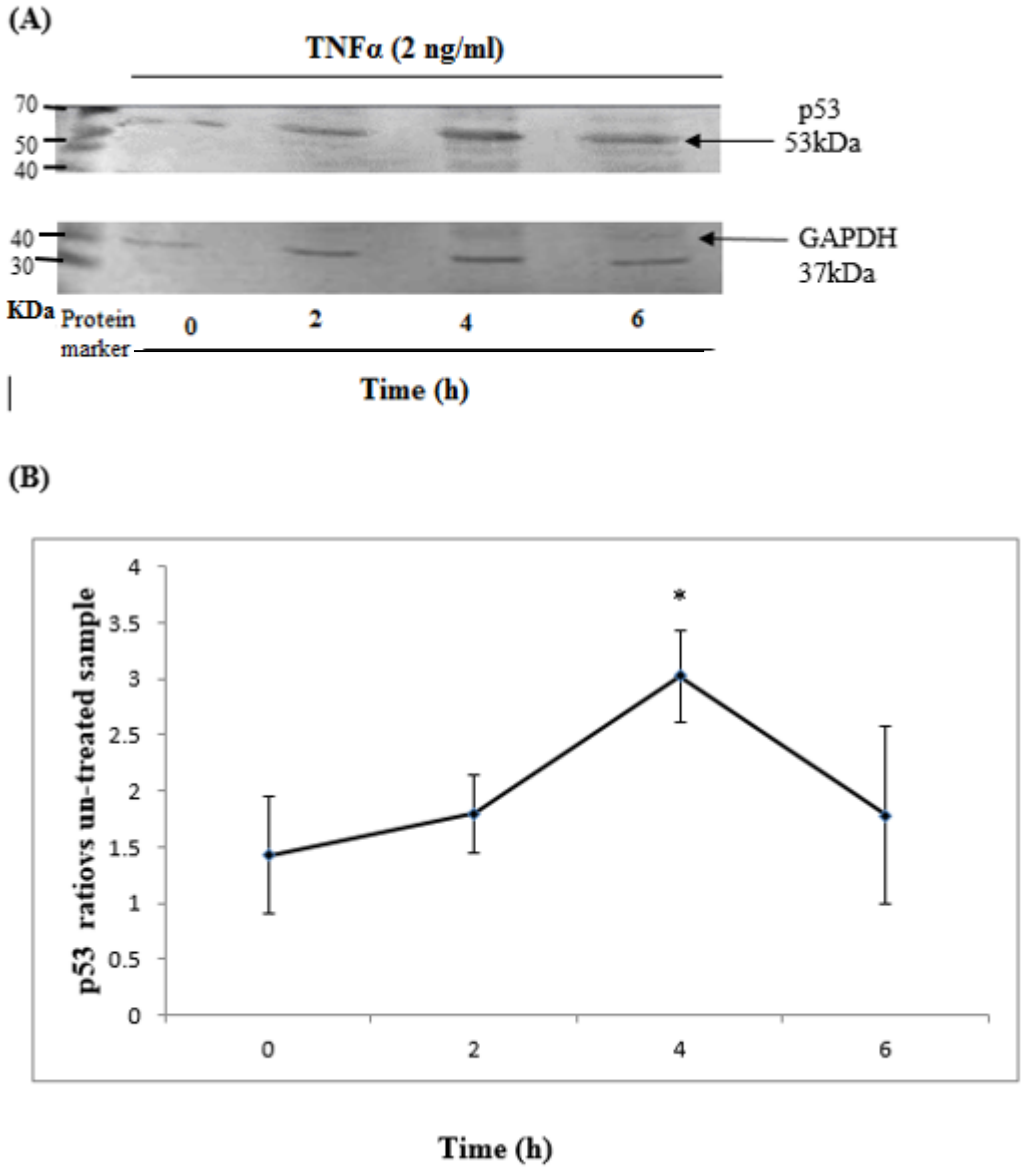

HCAEC (10^5/well) were adapted to serum-free medium activated with TNFα (2 ng/ml) and incubated as indicated on the graph. The cells were then lysed in Laemmli's buffer, and proteins were separated by 12 % (w/v) SDS-PAGE. Proteins were transferred into nitrocellulose membranes and probed for p53 using a rabbit anti-human p53 antibody. The membranes were then probed for GAPDH using a goat anti-human GAPDH antibody, and images were recorded using the GeneSnap program. The amounts of p53 protein were normalised against the respective GAPDH in each sample using the ImageJ program. (Data are representative of 3 independent experiments and expressed as means ± sd, *=$p<0.05$ vs untreated sample)

Figure 5.5. Time-course of nuclear p53 protein

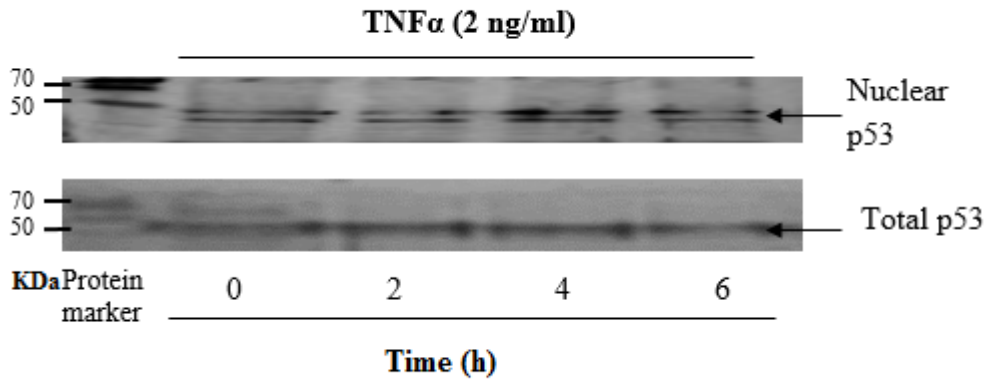

HCAEC (10^5/well) were adapted to serum-free medium, activated with TNFα (2 ng/ml) and incubated as indicated on the graph. The cells were harvested and nuclear and total fractions were isolated using the nuclear extract kit. Nuclear and total proteins from each sample were analysed on a 12 % (w/v) SDS-PAGE. Proteins were transferred onto nitrocellulose membranes and probed for p53 using a rabbit anti-human p53 antibody. Images were recorded using the GeneSnap program. (The gel is representatives of 2 independent experiments)

with PAR2-AP (20 µM) in cells expressing wild-type and mutant forms of TF compared to un-transfected cells and was particularly high in cells expressing TF_{Ala253} (Fig 5.6). In contrast, semi-quantitative RT-PCR analysis of p53 mRNA at 4 h post-activation with PAR2-AP (20 µM) showed no significant changes in the level of p53 mRNA expression in cells expressing wild-type TF or EGFP compared to non-activated samples (Fig 5.7 A). Furthermore, transfection of HCAEC to express either the TF_{wt} or TF_{Ala253} or control EGFP showed no significant alteration in p53 mRNA between any of the activated-transfected cell samples (Fig 5.7 B). To determine whether the increase in the level of p53 protein following PAR2 activation was dependent on p38 activity, HCAEC were co-transfected with p38α-siRNA together with pCMV-XL5-TF or pCMV-EGFP plasmid. Co-transfection of HCAEC with p38α-siRNA in conjunction with pCMV-XL5-TF plasmid followed by activation with PAR2-AP (20 µM) for 4 h significantly reduced the amount of p53 protein compared to samples co-transfected with the control siRNA and pCMV-XL5-TF (Fig 5.8). The addition of microvesicles containing high concentrations of TF (100 ng/ml) resulted in significant increases in p53 protein levels following activation of PAR2, whereas corresponding concentrations of control microvesicles had little influence (Fig 5.9).

5.3.2. Investigation of the role of TF-mediated p38 activation on p53 phosphorylation

Measurement of the degree of p53 phosphorylation by western blot analysis in cells transfected to express TF_{Wt} or TF_{Ala253} and activated with PAR2-AP for 4 h showed an increase in phosphorylation of Ser33 within p53, in cells expressing TF_{Ala253}, and to a lesser extent in cells expressing TF_{Wt}. Furthermore, this increase in p53 phosphorylation at Ser33 was reduced by inhibition of p38 using SB202190 compared to similar samples

Figure 5.6. Analysis of p53 protein levels in cells expressing the wild-type and mutant forms of TF

(A)

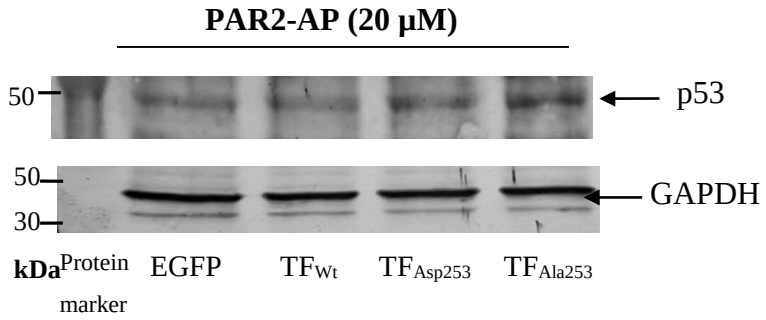

(B)

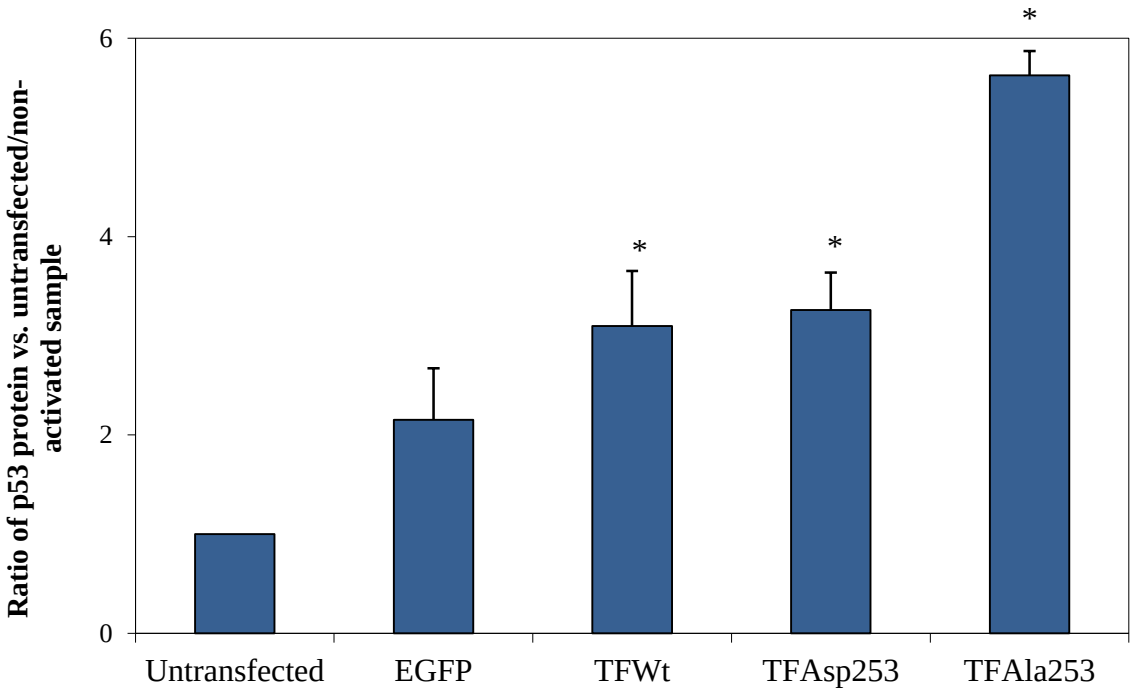

HCAEC (10^5/well) were transfected to express TF_{Wt}, TF_{Asp253}, TF_{Ala253} or EGFP. The cells were incubated for 48 h, adapted to serum-free medium and activated with PAR2-AP (20 µM) for 4 h. The cells were then lysed in Laemmli's buffer and proteins were separated by 12 % (w/v) SDS-PAGE. Proteins were transferred into nitrocellulose membranes and probed for p53 using a rabbit anti-human p53 antibody. The membranes were then probed for GAPDH using a rabbit anti-human GAPDH antibody, and images were recorded (A) using the GeneSnap program. The amounts of p53 protein were normalised against the respective GAPDH in each sample (B) using the ImageJ program. (Data are representative of 3 independent experiments and expressed as means ± sd, *=$p<0.05$ vs an un-transfected/untreated sample)

Figure 5.7. Analysis of p53 mRNA expression in HCAEC expressing wild-type and mutant forms of TF by semi-quantitative real-time RT-PCR

(A)

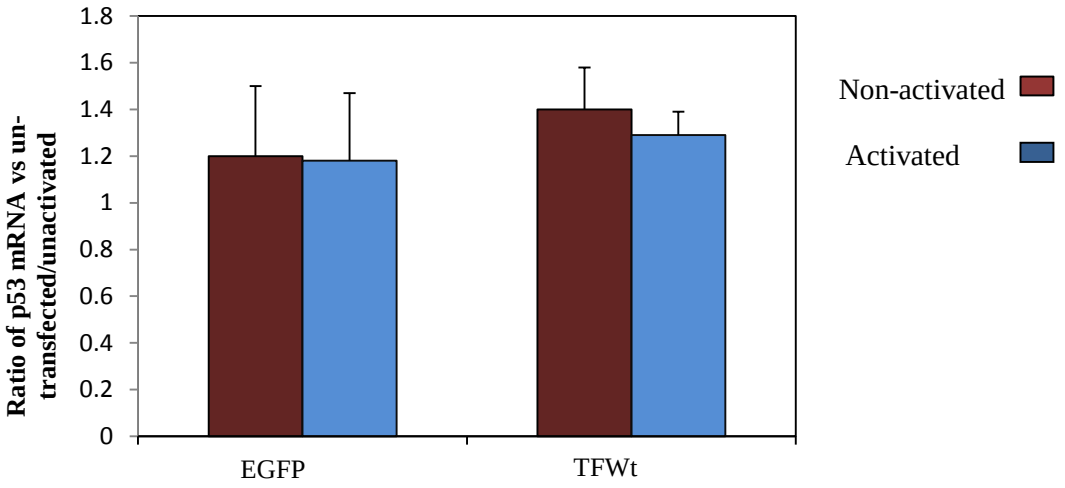

(B)

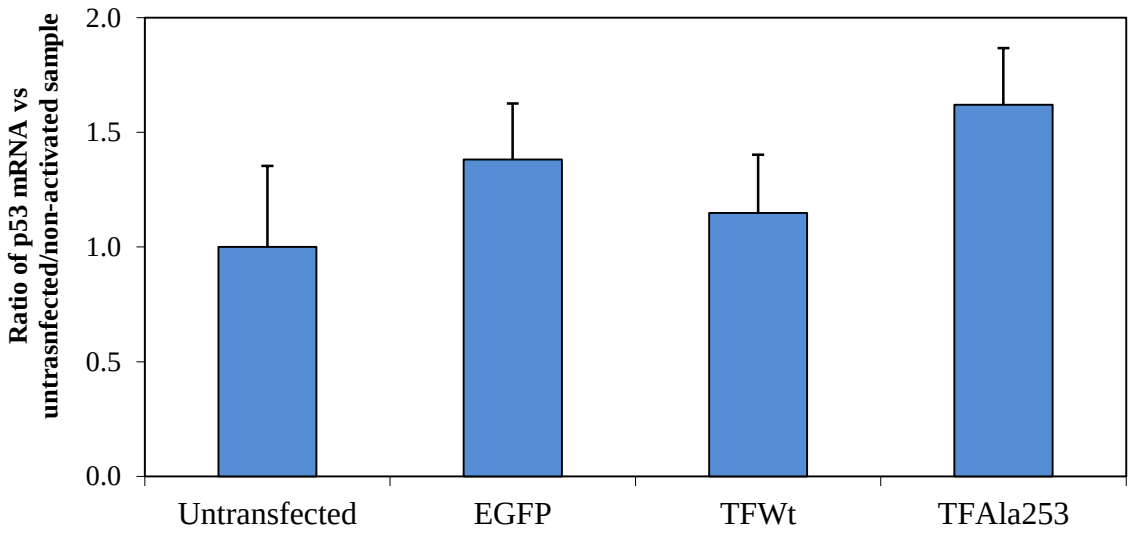

HCAEC (10^5/well) expressing TF_{Wt}, TF_{Ala253} or EGFP were adapted to serum-free medium and activated with PAR2-AP (20 µM). Total RNA was isolated at 4 h post-activation and real-time RT-PCR analysis was carried out to determine the Ct values for p53 mRNA against respective β-actin for each sample. The calculated ratios were then compared to the un-transfected/non-activated sample (A) in activated cells expressing TF_{Wt} or EGFP, and (B) in activated cells expressing TF_{Wt}, TF_{Ala253} or EGFP. (Data are representative of 3 independent experiments and expressed as means ± sd)

Figure 5.8. Analysis of p53 protein expression in cells lacking p38α

(A)

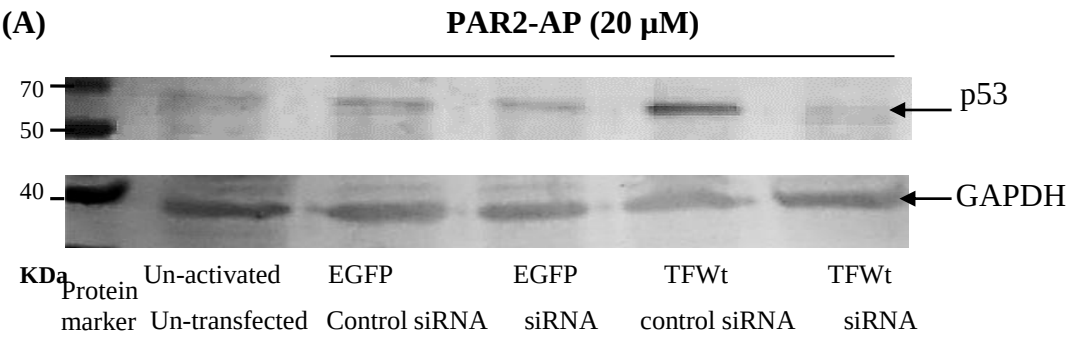

(B)

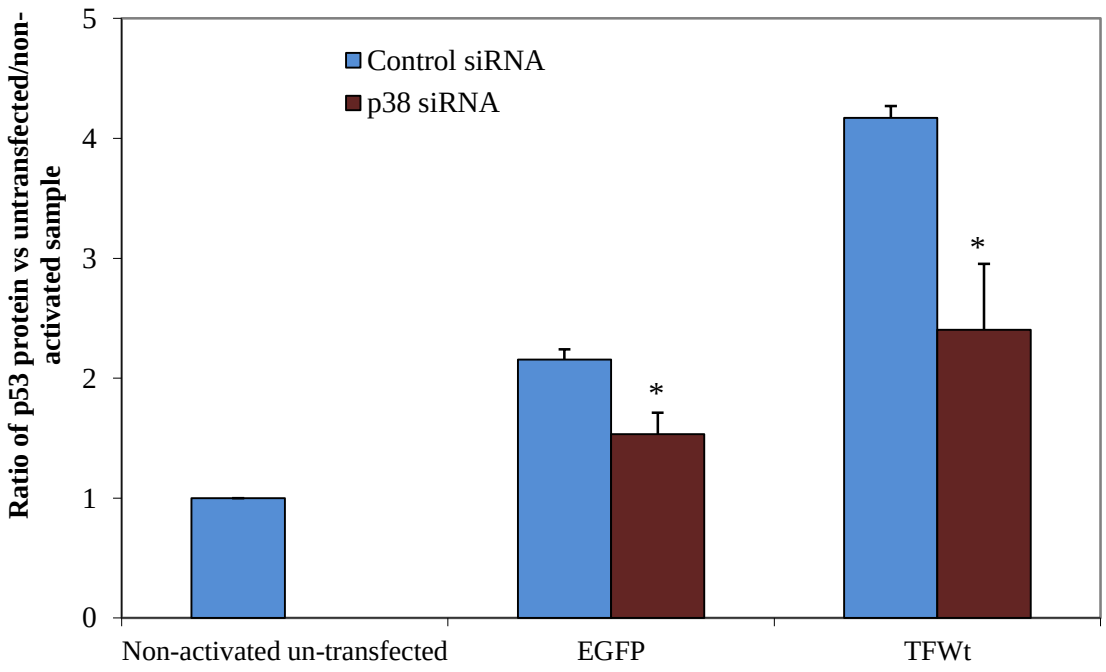

HCAEC (10^5/well) were co-transfected to express TF_{Wt} or EGFP, together with either p38α siRNA or a control siRNA. The cells were then adapted to serum-free medium and activated with PAR2-AP (20 µM). An un-transfected/non-activated sample was included for comparison. The cells were then lysed in Laemmli's buffer (100 µl) and proteins were separated by 12 % (w/v) SDS-PAGE. The proteins were transferred onto nitrocellulose membranes and probed for p53 using a rabbit anti-human p53 antibody. The membranes were then probed for GAPDH using a mouse anti-human GAPDH antibody and images were recorded (A) using the GeneSnap program. The amounts of p53 protein were normalised against the respective GAPDH in each sample (B) using the ImageJ program. (Data are representative of 3 independent experiments and expressed as means ± sd, *=$p<0.05$ vs a respective control-siRNA sample)

Figure 5.9. Analysis of p53 protein levels in cells treated with microvesicles-TF

(A)

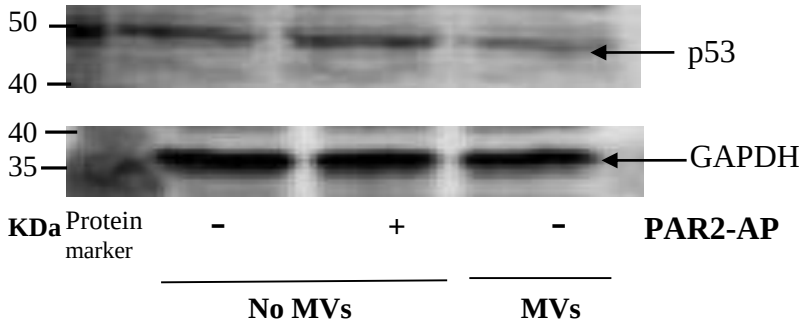

(B)

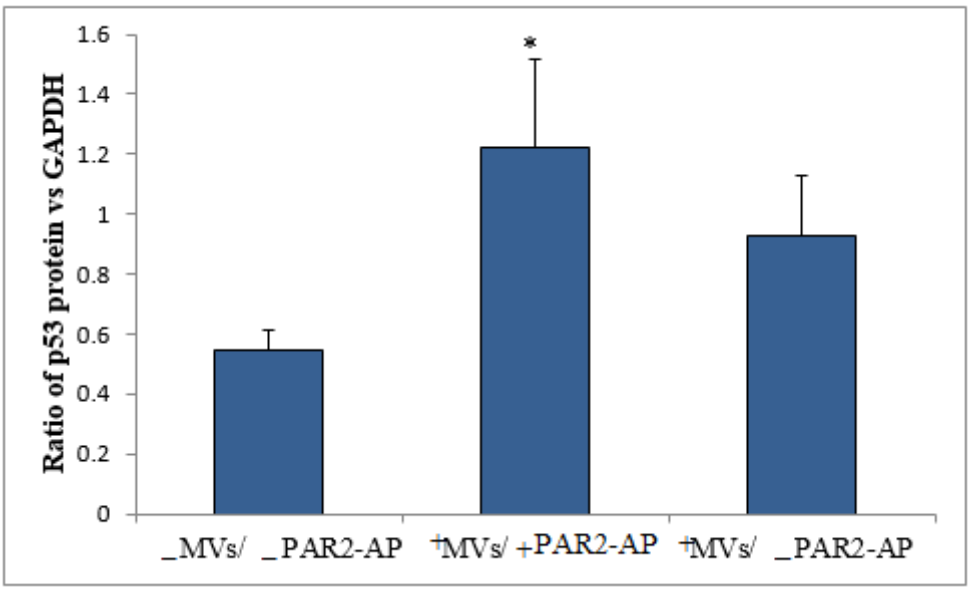

HCAEC (10^5/well) were incubated with TF-containing microvesicles (100 ng/ml TF) isolated from MDA-MB-231 cells line for 2 h in serum-free medium. The cells were activated with PAR2-AP (20 µM) for 4 h. The cells were then lysed in Laemmli's buffer and proteins were separated by 12 % (w/v) SDS-PAGE. Proteins were transferred into nitrocellulose membranes and probed for p53 using a rabbit anti-human p53 antibody. The membranes were then probed for GAPDH using a rabbit anti-human GAPDH antibody and images were recorded (A) using the GeneSnap program. The amounts of p53 protein were normalised against the respective GAPDH in each sample (B) using the ImageJ program. (Data are representative of 3 independent experiments and expressed as means ± sd, *=$p<0.05$ vs an untreated sample)

treated with equivalent amounts of DMSO-vehicle (Fig 5.10 A & B). The increase in p53 phosphorylation was also observed by the treatment of the cells with microvesicles derived from MDA-MB-231 cells, containing high concentrations of TF (100 ng/ml) (Fig 5.11). Moreover, the phosphorylation of Ser46 was barely detectable in any of the samples (Fig 5.12). In addition, co-transfection of the cells with p38α-siRNA in conjunction with pCMV-XL5-TF plasmid followed by PAR2-AP activation resulted in a significant inhibition of p53 phosphorylation at Ser33 (Fig 5.13).

5.3.3. Analysis of the effect of TF-mediated p38 activation on p53 nuclear localisation

The level of p53 localisation within the nucleus was examined by confocal microscopy. HCAEC transfected to express wild-type or mutant forms of TF showed a significant accumulation of p53 within the nucleus in cells expressing TF_{Wt} and TF_{Ala253} following activation of PAR2 for 4 h (Fig 5.14). In addition, co-transfection of cells with pCMV-XL5-TF, together with p38α-siRNA, reduced the level of p53 nuclear localisation upon PAR2 activation compared to the sample co-transfected with control siRNA (Fig 5.15).

5.3.4. Examination of the role of TF in the regulation of p53 transcriptional function by measuring bax mRNA expression

Pifithrin-α may be used to inhibit the transcriptional activity of p53 (Bulavin et al., 1999) without affecting non-p53-dependent apoptosis (Sanchez-Prieto et al., 2000; Kishi et al., 2001). Pre-incubation of HCAEC with a range of pifithrin-α (0-200 nM) for 30 min prior to activation with TNFα (10 ng/ml) resulted in a significant decrease in bax mRNA expression at 4 h. This inhibition was concentration-dependent and observed at

Figure 5.10. Analysis of the role of p38 on the phosphorylation of p53 in HCAEC expressing TF_{Wt} or TF_{Ala253}

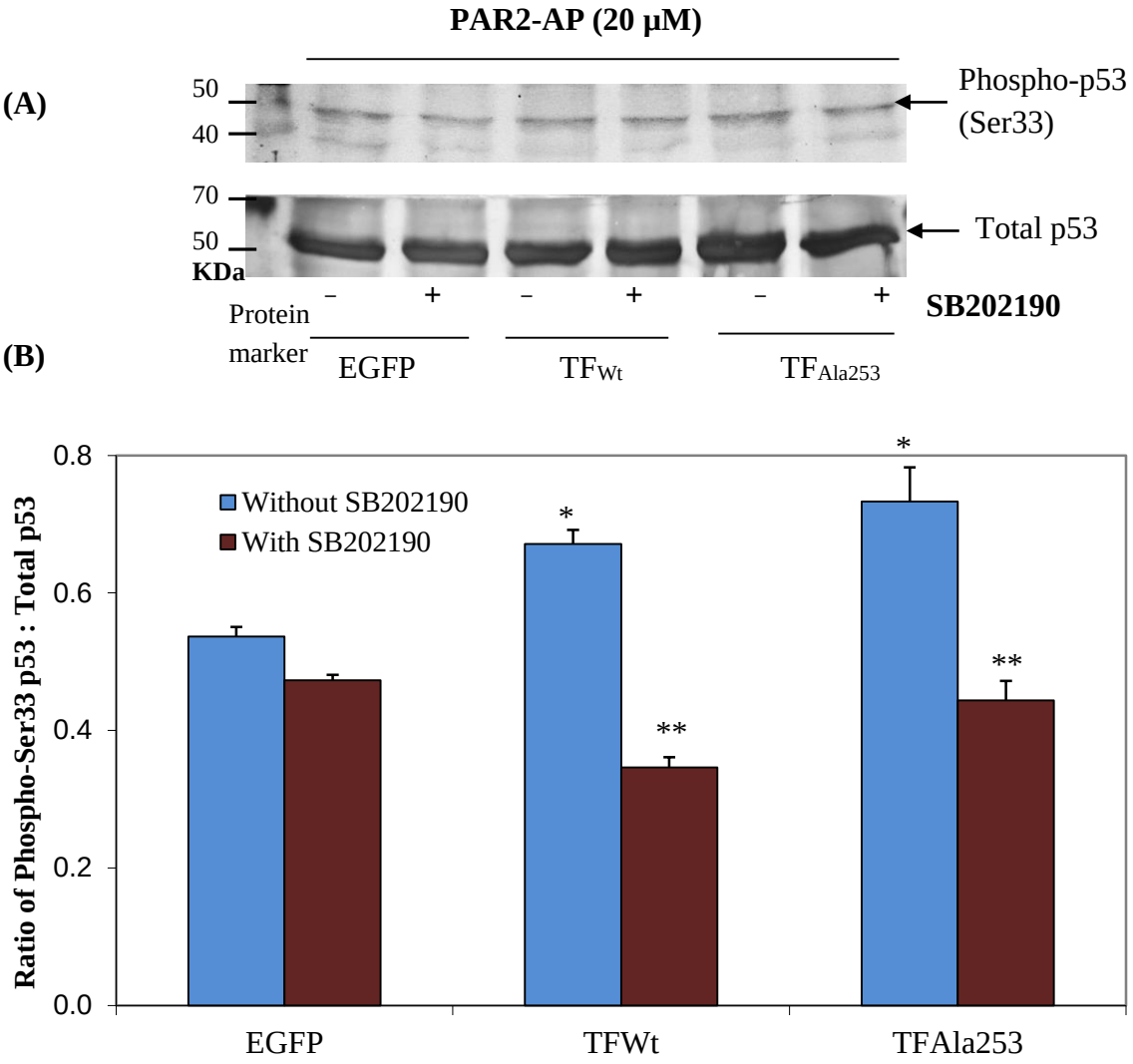

HCAEC (10^5/well) expressing TF_{Wt}, TF_{Ala253} or EGFP were adapted to serum-free medium and treated with SB202190 (100 nM) or DMSO vehicle for 30 min. The cells were then activated with PAR2-AP (20 µM), incubated for 4 h and then lysed in Laemmli's buffer (100 µl). The proteins were separated by 12 % (w/v) SDS-PAGE, transferred onto nitrocellulose membranes and probed for phosphorylated Ser33-p53 using a rabbit anti-human p53 phospho-Ser33 antibody. The membranes were then probed for total p53 using a rabbit anti-human p53 antibody and images were recorded (A) using the GeneSnap program. The ratio of phosphorylated p53 to total p53 was calculated (B) using the ImageJ program. (Data are representative of 3 independent experiments and expressed as means ± sd, *=$p<0.05$ vs an untreated EGFP sample; **=$p<0.05$ vs a respective untreated sample)

Figure 5.11. Analysis of p53 phosphorylation at Ser33 in cells treated with microvesicles containing high concentration of TF

(A)

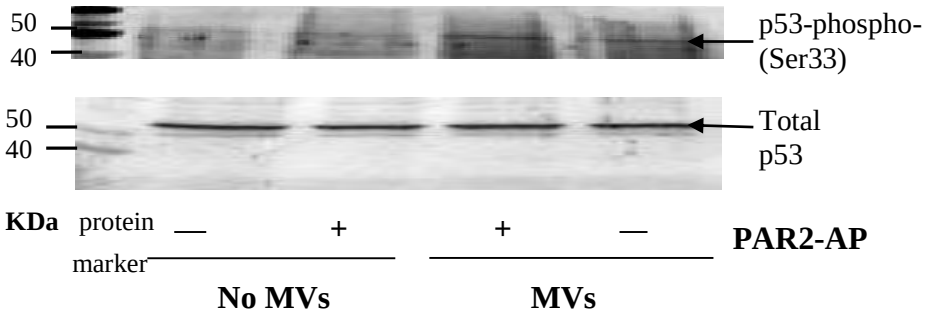

(B)

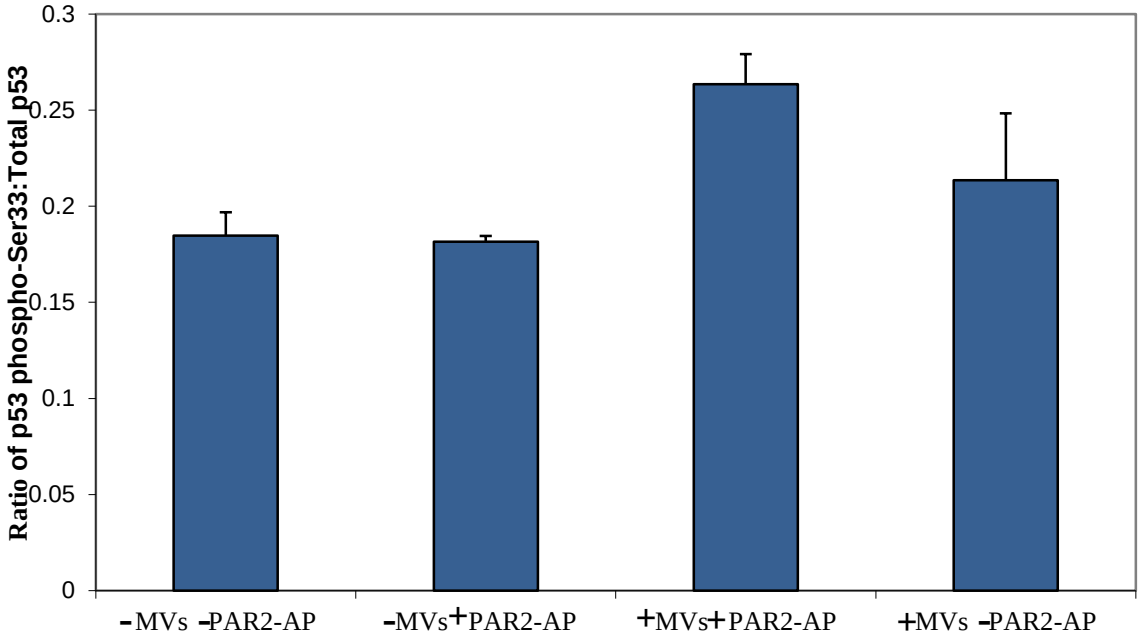

HCAEC (10^5/well) were incubated with TF-containing microvesicles (100 ng/ml TF) derived from MDA-BM-231 cells and incubated for 2 h in serum free medium. The cells were activated with PAR2-AP (20 µM) for 4 h. The cells were then lysed in Laemmli's buffer and proteins were separated by 12 % (w/v) SDS-PAGE, transferred onto nitrocellulose membranes and probed for phosphorylated Ser33-p53 using a rabbit anti-human p53 phospho-Ser33 antibody. The membranes were then probed for total p53 using a rabbit anti-human p53 antibody and images were recorded (A) using the GeneSnap program. The ratio of phosphorylated p53 to total p53 was calculated (B) using the ImageJ program. (Data are representative of 3 independent experiments and expressed as means ± sd)

Figure 5.12. Analysis of the phosphorylation of p53 at Ser46 in HCAEC expressing TF_{Wt} or TFA_{Ala253}

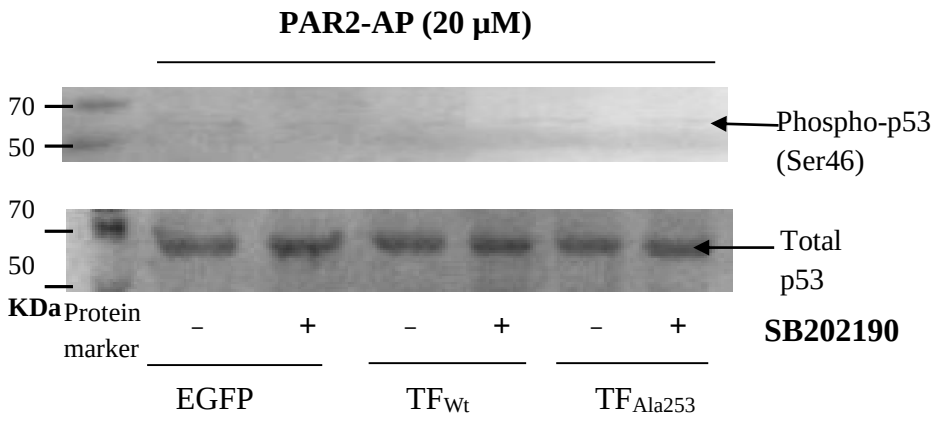

HCAEC (10^5/well) expressing TF_{Wt}, TF_{Ala253} or EGFP were adapted to serum-free medium and treated with SB202190 (100 nM) or DMSO-vehicle for 30 min. The cells were then activated with PAR2-AP (20 µM), incubated for 4 h and then lysed in Laemmli's buffer (100 µl). The proteins were separated by 12 % (w/v) SDS-PAGE, transferred onto nitrocellulose membranes and probed for phosphorylated Ser46-p53 using a rabbit anti-human p53 phospho-Ser46 p53 antibody. The membranes were then probed for total p53 using a rabbit anti-human p53 antibody and images were recorded using the GeneSnap program. (The gel is representatives of 3 independent experiments)

Figure 5.13. Analysis of p53 phosphorylation at Ser33 following silencing of p38α expression

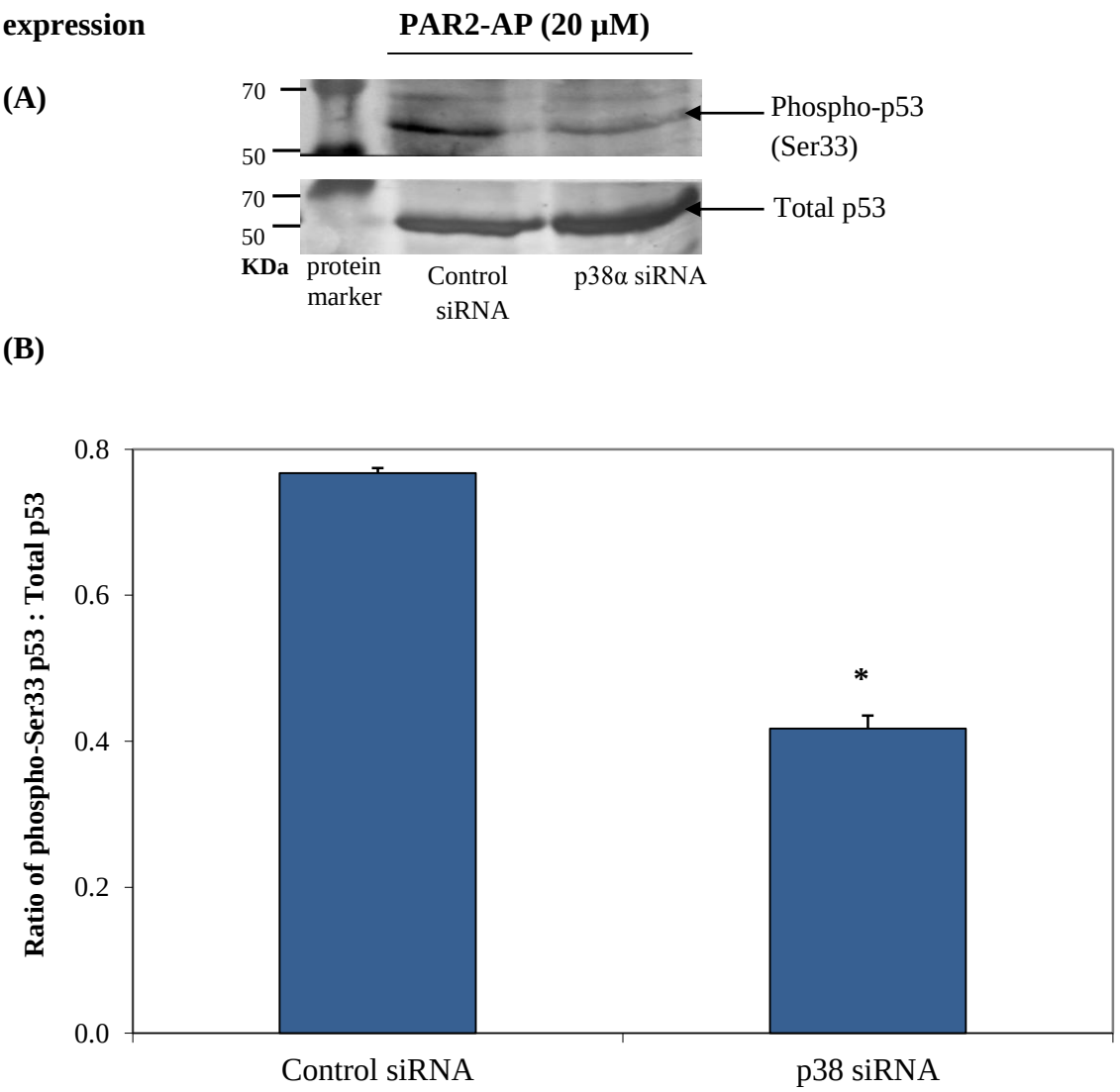

HCAEC (10^5/well) were co-transfected with pCMV-XL5-TF and either p38 siRNA or a control siRNA and incubated for 48 h. The cells were adapted to serum-free medium and activated with PAR2-AP (20 µM) for 4 h. The cells were then lysed in Laemmli's buffer (100 µl) and proteins were separated by 12 % (w/v) SDS-PAGE. The proteins were transferred onto nitrocellulose membranes and probed for phosphorylated Ser33-p53 using a rabbit anti-human p53 phospho-Ser33 antibody. The membranes were then probed for total p53 using a rabbit anti-human p53 antibody and images were recorded (A) using the GeneSnap program. The ratio of phosphorylated p53 to total p53 was calculated (B) using the ImageJ program. (Data are representative of 3 independent experiments and expressed as means ± sd, *=$p<0.05$ vs a sample with control siRNA).

Figure 5.14. The role of wild-type and mutant forms of TF on p53 nuclear localisation

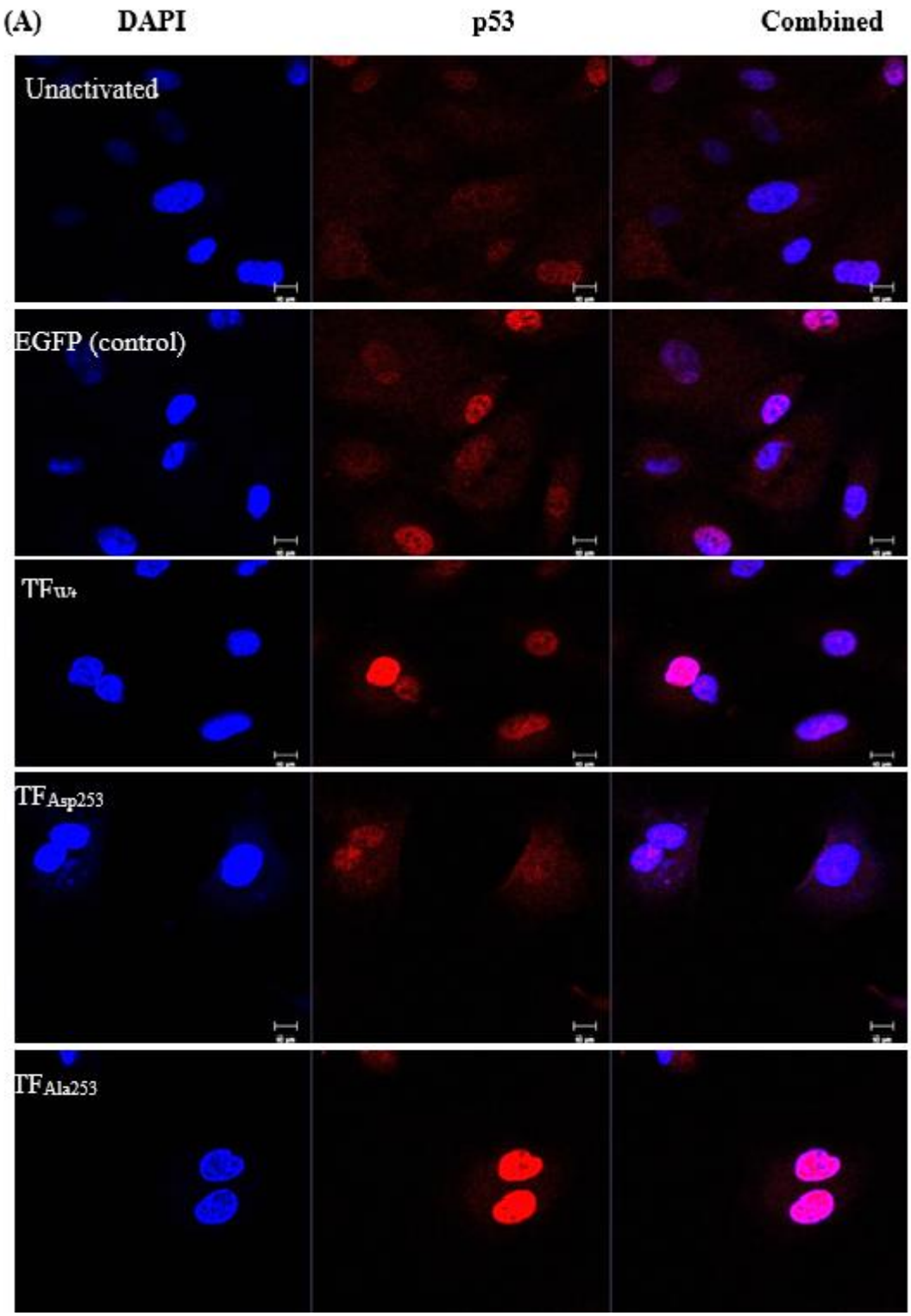

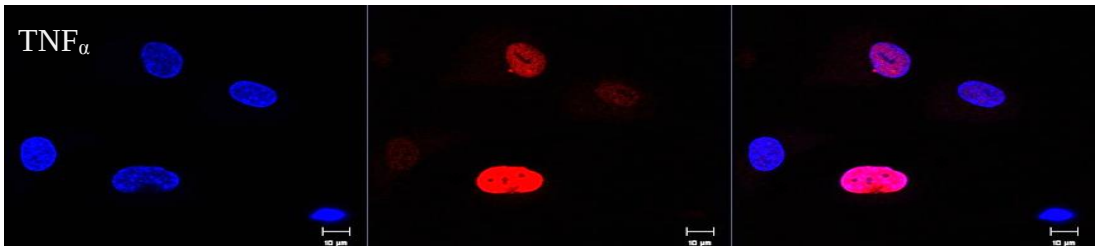

(B)

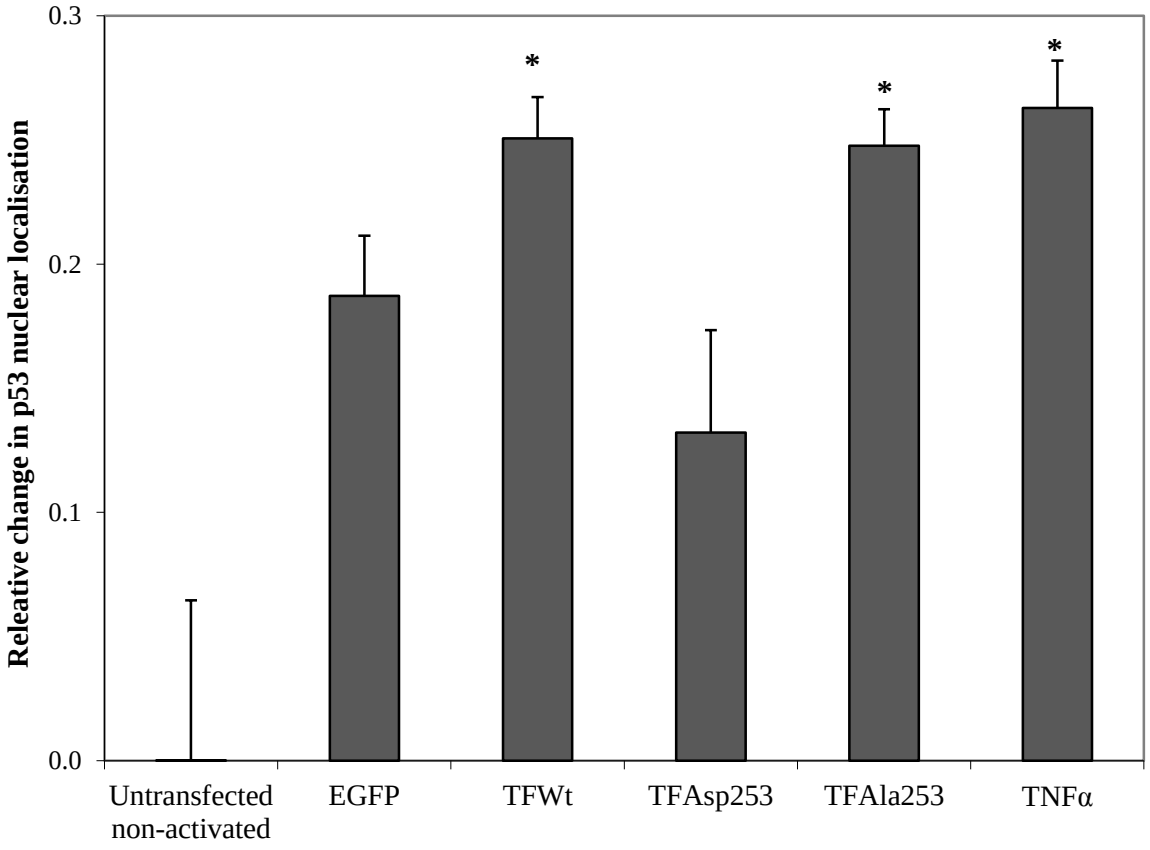

HCAEC (10^5) were seeded out into 35 mm glass base dishes, transfected to express $TF_{Wt,}$ TF_{Asp253}, TF_{Ala253} or EGFP (control) and incubated to express the TF/EGFP proteins for 48 h. The cells were adapted to serum-free medium and activated with PAR2-AP (20 µM) for 4 h. Un-transfected sets were used either unactivated (negative control) or alternatively incubated with TNF (10 ng/ml) used as a positive control. The cells were then fixed, permeabilised, labelled with a rabbit anti-human p53 antibody and probed with a NorthernLights donkey anti-rabbit IgG-NL637. The nuclei were labelled with DAPI and analysed by confocal microscopy with a ×20 objective (A). Co-localisation coefficients were determined (B) using ImagePro Plus software. (Data are representative of 3 independent experiments and expressed as means ± sd, *=$p<0.05$ vs an un-transfected/untreated sample)

Figure 5.15. Analysis of the involvement of p38 activation on p53 nuclear localisation by confocal microscopy

(A)

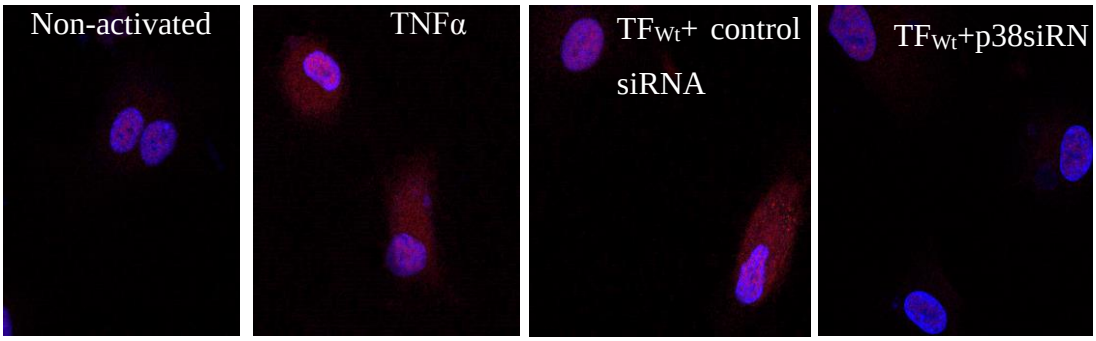

(B)

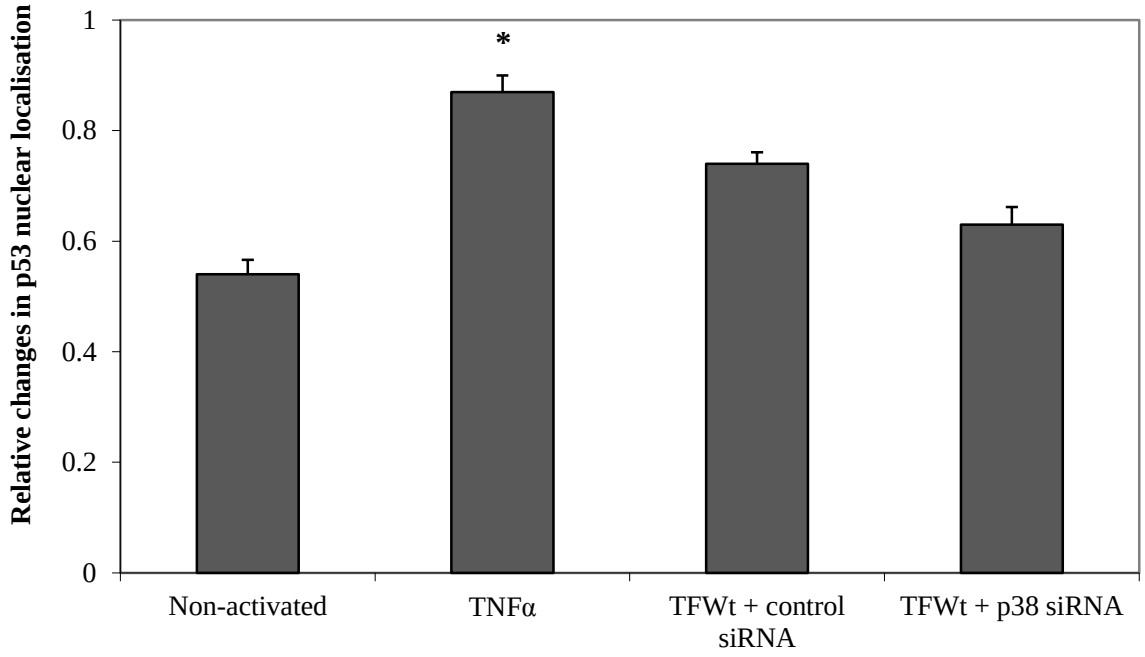

HCAEC (10^5) were seeded out into 35 mm glass base dishes and transfected to express TF_{Wt} together with either p38 siRNA or a control siRNA. Cells were adapted to serum-free medium and activated with PAR2-AP (20 µM) for 4 h. An un-transfected set of cells was activated with TNFα (10 ng/ml) and used as a positive control. The cells were then fixed, permeabilised and labelled with rabbit anti-human p53 antibody developed with a NorthernLights donkey anti-rabbit IgG-NL637. The nuclei were then labelled with DAPI and analysed by confocal microscopy (A) with a ×20 objective. Co-localisation coefficients were determined using (B) ImagePro Plus software. (Data are representative of 3 independent experiments and expressed as means ± sd, *=$p<0.05$ vs an un-transfected/untreated sample)

concentrations as low as 50 nM (Fig 5.16). Furthermore, transfection of the cells to express TF_{Ala253} prior to activation with PAR2-AP resulted in a significant up-regulation of bax mRNA at 4 h post-activation. Moreover, this up-regulation of bax mRNA was completely suppressed in cells pre-incubated with 100 nM of pifithrin-α (Fig 5.17).

5.3.5. Examination of the involvement of TF in p53-mediated apoptosis

Transfection of HCAEC to express TF_{Wt}, TF_{Ala253} or EGFP followed by activation with PAR2-AP (20 µM) showed a significant increase in the rate of apoptosis in cells expressing TF_{Ala253} after 18 h incubation. However, this increase in the rate of apoptosis was significantly reduced by pre-incubation of the cells with pifithrin-α (100 nM) for 30 min, prior to activation (Fig 5.18).

5.3.6. Investigation of the influence of TF-mediated p38 activation on the transcriptional activity of p53

To investigate the signalling pathways activated by TF-mediated p38 activation leading to cellular apoptosis, a luciferase reporter assay utilising the p53 luciferase-reporter vector was used. The p53 reporter plasmid was extracted from bacteria *E. coli* strain TB-1 using a midi-prep kit as described in the general methods section 2.3.1. The plasmid was analysed by agarose gel electrophoresis (Fig 5.19). Co-transfection of cells with pCMV-XL5-TF_{Ala253} together with 1 µg of Pathdetect p53-Luc *cis*-reporting plasmid significantly enhanced the transcriptional activity of p53 following 18 h activation of PAR2 (Fig 5.20). In contrast, cells expressing TF_{Asp253} did not induce the transcriptional activity of p53. Furthermore, inhibition of the activity of p38 using SB202190 in cells expressing TF_{Ala253} resulted in a significant reduction in the transcriptional activity of p53 (Fig 5.21).

Figure 5.16. Optimisation of p53 inhibitor (pifithrin-α) by measuring Bax mRNA using real-time RT-PCR

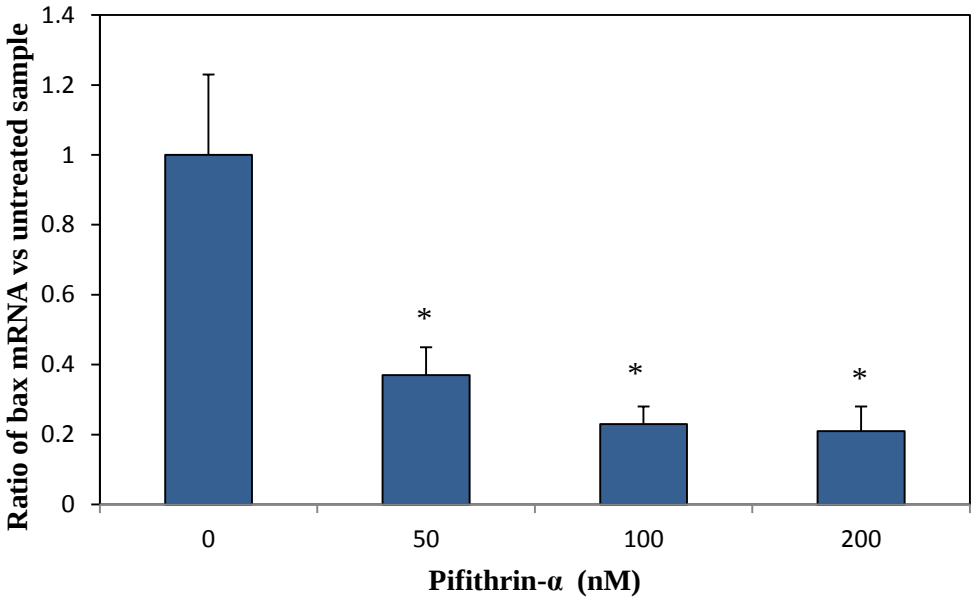

HCAEC (10^5/well) were adapted to serum-free medium and treated with a range of Pifithrin-α (0- 200 nM) 30 min before activation with TNFα (10 ng/ml). Total RNA was isolated at 4 h post-activation and the relative amounts of bax mRNA in untreated and treated cell samples were determined by real-time RT-PCR. The Ct values were normalised against the respective β-actin mRNA in each sample. (Data are representative of 3 independent experiments and expressed as means ± sd, *=$p<0.05$ vs untreated sample)

Figure 5.17. Analysis of bax mRNA expression in the presence and absence of p53 inhibitor

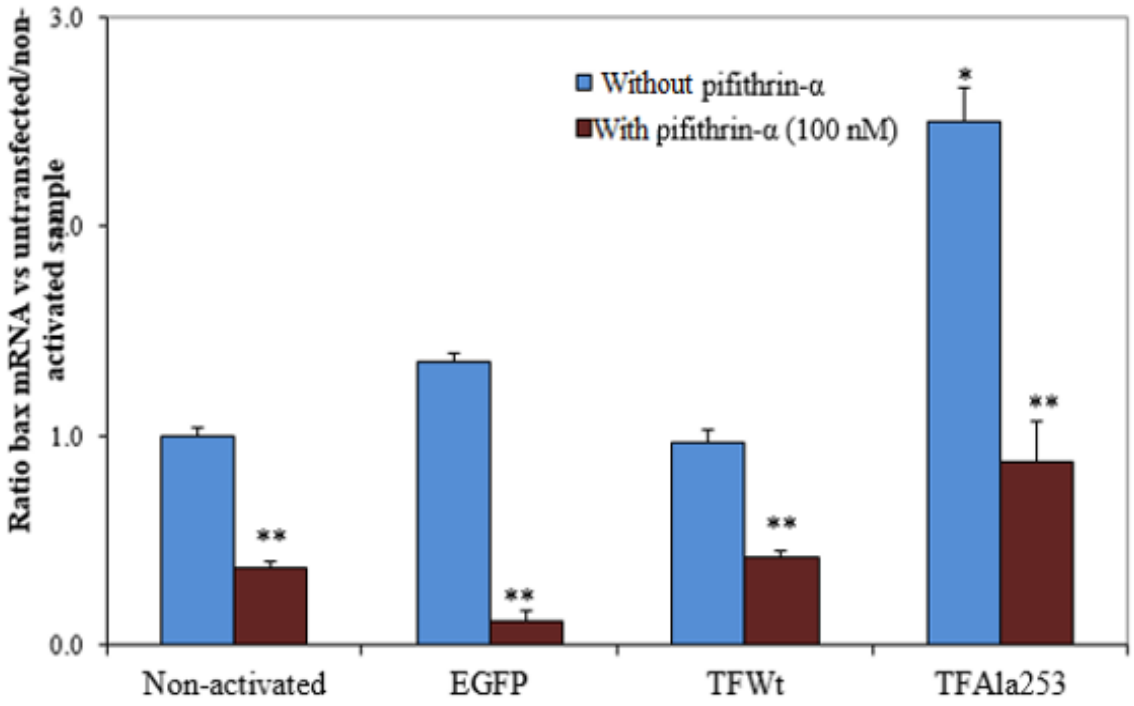

HCAEC were transfected to express TF_{Wt}, TF_{Ala253} or EGFP. The cells were incubated for 48 h, adapted to serum-free medium and treated with 100 nM of pifithrin-α or equivalent amounts of DMSO for 30 min prior to activation with PAR2-AP (20 µM). Total RNA was isolated at 4 h post-activation and the relative amount of Bax mRNA was determined by real-time RT-PCR. (Data are representative of 3 independent experiments and expressed as means ± sd, *=$p<0.05$ vs an un-transfected/untreated sample; **=$p<0.05$ vs a respective sample without pifithrin-α)

Figure 5.18. Examination of the outcome of accumulation of TF on p53-mediated apoptosis

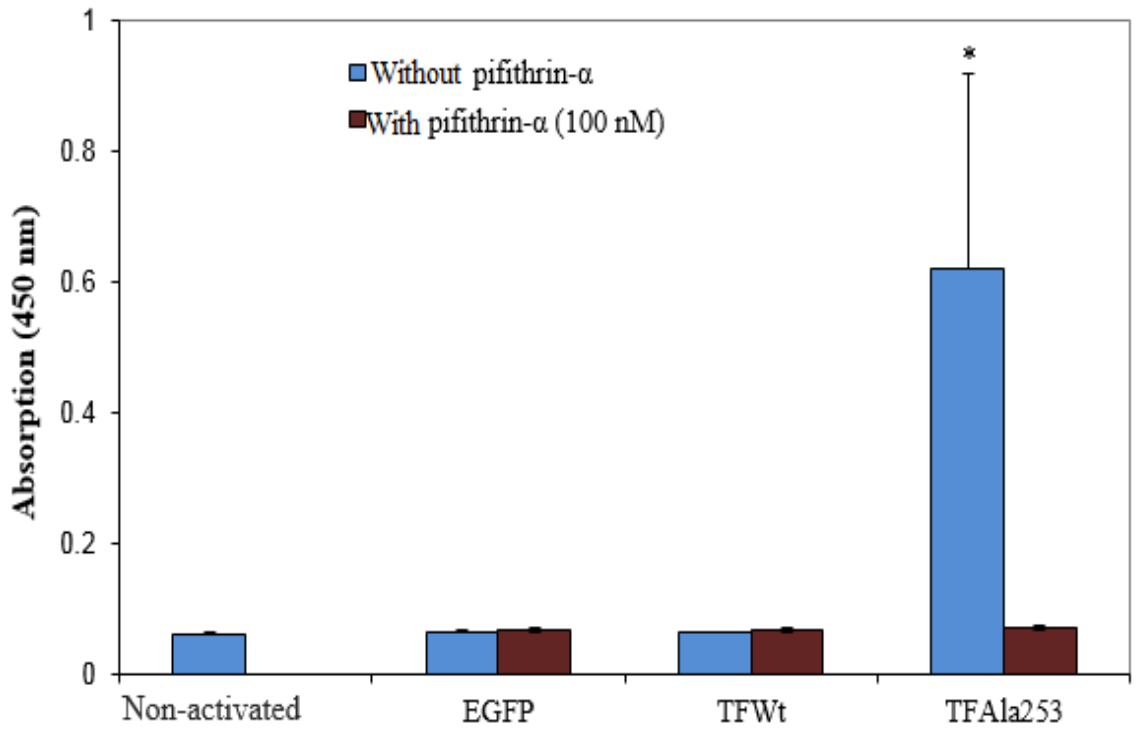

HCAEC (10^5/well) were transfected to express TF_{Wt}, TF_{Ala253} or EGFP for 48 h, adapted to serum-free medium and pre-incubated with pifithrin-α (100 nM) or equivalent amount of DMSO for 30 min prior to activation with PAR2-AP (20μM). The rate of cellular apoptosis was measured at 18 h using the apoptosis detection kit. (Data are representative of 3 independent experiments and expressed as means ± sd, *=$p<0.05$ vs an un-transfected/un-treated sample)

Figure 5.19. Confirmation of the purity of the p53-luc plasmid using agarose gel electrophoresis

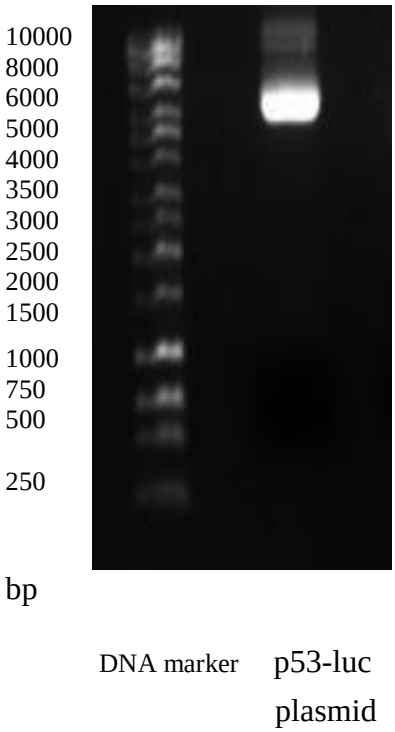

The plasmid DNA was extracted from *E. coli* strain TB-1 using a midi-prep kit and analysed by 0.5 % (w/v) agarose gel electrophoresis. A band representing p53-luc plasmid DNA was observed at the expected size of approximately 5900 bp.

Figure 5.20. Analysis of the involvement of TF retention on the transcriptional activity of p53 using a luciferase reporter assay

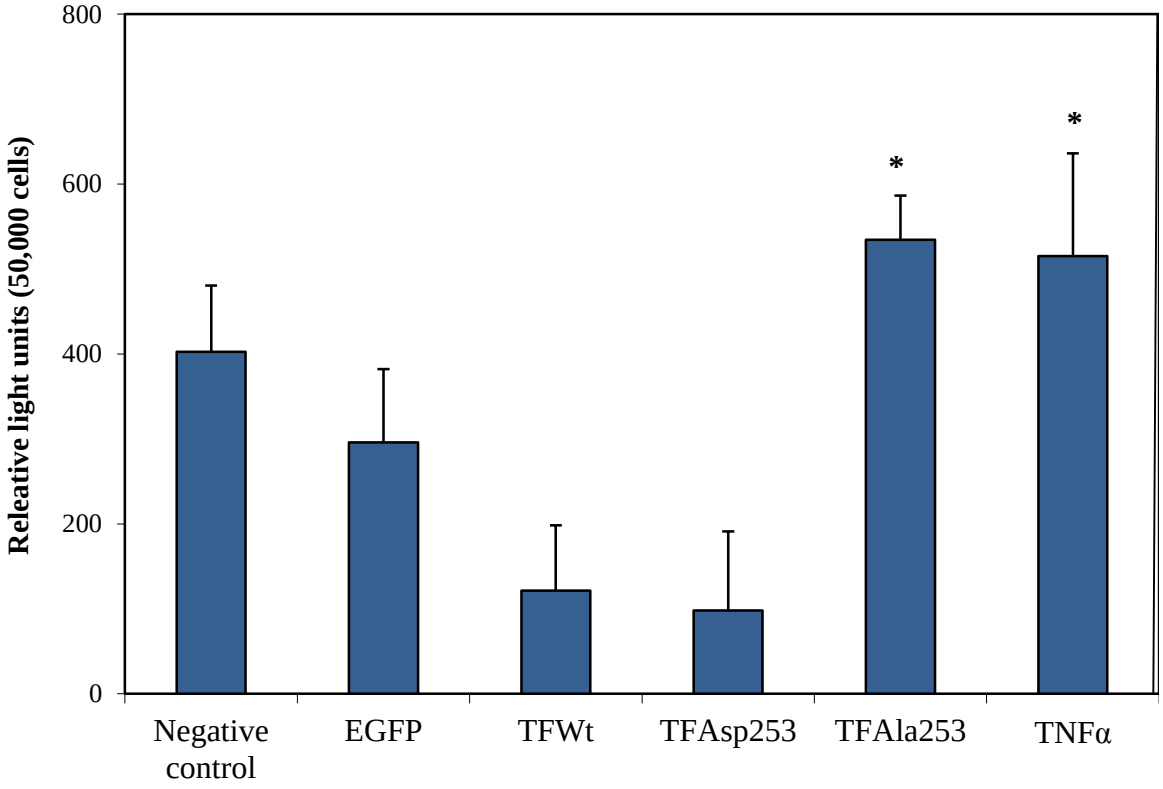

HCAEC (10^5/well) were co-transfected to express TF_{Wt}, TF_{Asp253}, TF_{Ala253} or EGFP together with 1 µg of Pathdetect p53-Luc *cis*-reporting plasmid or just Pathdetect p53-Luc *cis*-reporting plasmid as a control. The cells were adapted to serum-free medium and activated with PAR2-AP (20 µM). In addition, one set of cells was treated with TNFα (10 ng/ml) as a positive control and the another set was left untreated as a negative control. The cells were harvested at 8 h, and the luciferase activity was measured. (Data are representative of 3 independent experiments and expressed as means ± sd, *=$p<0.05$ vs a cell sample expressing TF_{Wt})

Figure 5.21. Analysis of the transcriptional activity of p53 in the presence of SB202190

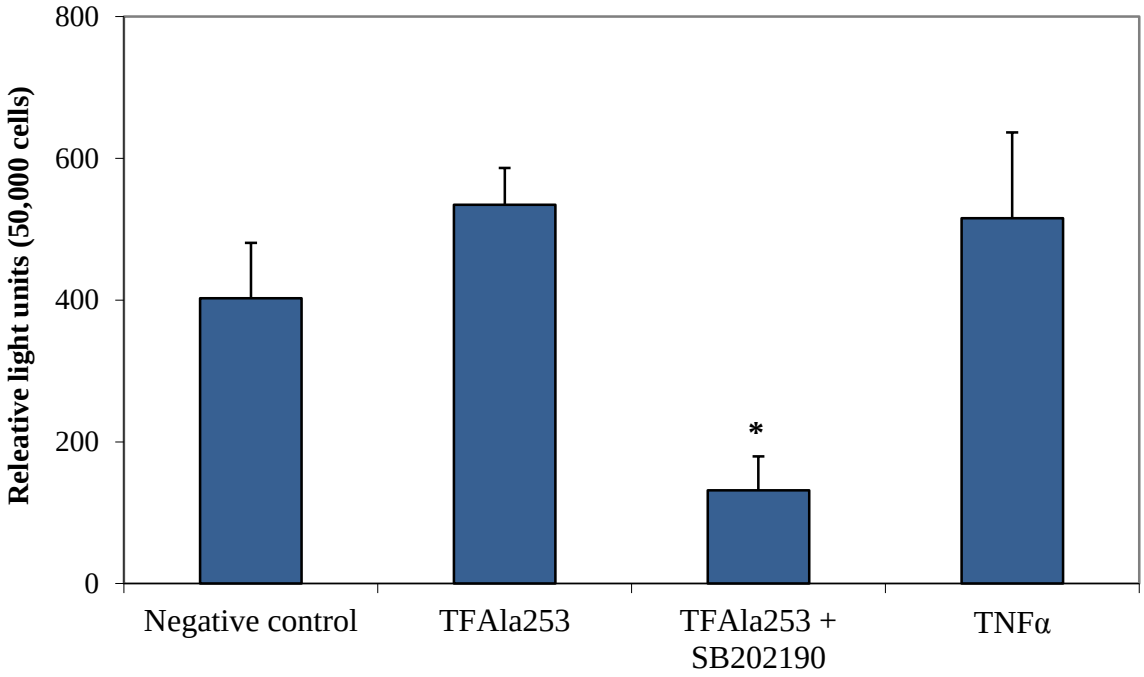

HCAEC (10^5/well) were co-transfected to express TF_{Ala253} together with p53-Luc plasmid or just Pathdetect p53-Luc *cis*-reporting plasmid as a control. The cells were adapted to serum-free medium and pre-incubated with SB202190 (100 nM) or equivalent amounts of DMSO prior to activation with PAR2-AP (20 µM). In addition, one set of cells was treated with TNFα (10 ng/ml) as a positive control and the another set was left untreated as a negative control. The cells were harvested at 8 h and luciferase activity was measured. (Data are representative of 3 independent experiments and expressed as means ± sd, *=$p<0.05$ vs an untreated sample expressing TF_{Ala253})

5.4. Discussion

In the previous chapters it was shown that the accumulation of TF in HCAEC leads to prolonged activation of p38 and is associated with apoptosis in these cells. It is known that, upon DNA damage or other stress stimuli, p53 protein regulates apoptosis by up-regulating genes involved in both the intrinsic and extrinsic pathways of apoptosis (Chipuk & Green, 2006). The aim of this section was to determine the mechanisms by which the accumulation of TF-mediates p38 activation and induces cell apoptosis. It has been shown that, following various stress signals to the cell, p38 is capable of phosphorylating Ser33 and Ser46 within the trans-activation domain of p53 protein (Bulavin et al., 1999; Sanchez-Prieto et al., 2000; Kishi et al., 2001). Phosphorylation of these residues is a prerequisite for the stabilisation of p53 within the nucleus by dissociating its negative regulator, MDM2. The resultant increase in the transcriptional activity of p53 mediates the up-regulation of the expression of a number of genes including p21 (Levine, 1997) and bax (El-Deiry et al., 1993). These proteins in turn promote cell cycle arrest and apoptosis, respectively.

Initially, the influence of wild-type and mutant forms of TF on the expression of p53 was examined. Western blot analysis of p53 protein in transfected HCAEC express showed a significant increase in the p53 protein levels in both the wild-type and mutant forms of TF (particularly in cells expressing TF_{Ala253}) within 4 h of activation with PAR2-AP (20 µM) (Fig 5.6). However, no increase in p53 mRNA was detected in any of the transfected cells (Fig 5.7 A & B), suggesting that the observed increase was due to stabilisation of p53 rather than *de novo* synthesis of the protein. Moreover, the activation of TF-expressing cells appeared to stabilise p53 via p38 activation. This was confirmed by lower p53 protein levels in cells co-transfected with pCMV-XL TF and p38α siRNA (Fig 5.8). In addition, accumulation of TF in cells expressing TF_{Ala253} was associated with increased

phosphorylation of p53 at Ser33 but not Ser46 (Fig 5.10 & 5.12). Inhibition of p38 activity either by using SB202190 or by siRNA silencing was sufficient to inhibit TF-induced phosphorylation of p53 at Ser33 (Fig 5.10 & 5.13). The regulation of p53 activity can vary according to cell type and the nature of the stimulus (Gottlieb et al., 1996). Therefore, phosphorylation of Ser33 and Ser46 within p53 may occur via different mechanisms (Yoshida et al., 2006) and may be independent (Kishi et al., 2001; Saito et al., 2003). For example, while the phosphorylation of Ser33 is mediated by p38 (Bulavin et al., 1999; Kishi et al., 2001) Ser46 may also be phosphorylated by protein kinase Cδ (Kurihara et al., 2007). These data using transfection were also observed in incubation of the cells with high levels of TF-containing microvesicles (Fig 5.9 & 5.11).

Nuclear localisation is critical for the transcriptional activity of p53 where p53 transactivates a number of pro-apoptotic genes. The ability of TF and p38 to promote nuclear localisation of p53 was examined next by confocal microscopy. Activation of HCAEC expressing TF_{Wt} or TF_{Ala253} resulted in significant nuclear localisation of p53, but this was absent in cells expressing TF_{Asp253} (Fig 5.14). The increased p53 nuclear localisation was suppressed by suppressing the expression of p38 using siRNA (Fig 5.15). Furthermore, the increased p53 nuclear localisation was concurrent with the up-regulation of bax mRNA in cells expressing TF_{Ala253} (Fig 5.16). However, despite the increased nuclear localisation in both cell samples expressing TF_{Wt} and TF_{Ala253}, p53 transcriptional activity was only observed in cells expressing TF_{Ala253} (Fig 5.18). Moreover, incubation of cells with pifithrin-α reduced the observed p53 activity. Pifithrin-α is known to prevent cell apoptosis specifically by inhibiting the transcriptional activity of p53 (Bulavin et al., 1999) and without affecting other mechanisms involved in apoptosis (Sanchez-Prieto et al., 2000; Kishi et al., 2001). Therefore, the TF-mediated up-regulation of Bax and the induction of cell apoptosis appear

to be solely dependent on the transcriptional activity of p53 and subsequently abrogated by pre-incubation of cells with pifithrin-α in cells expressing TF_{Ala253} (Fig 5.16 and 5.17). These data indicate that the pro-apoptotic effect of TF is mediated by p53, which is part of the intrinsic pathway of apoptosis (Chipuk et al., 2004), although previous data appear to suggest some cross-talk to the extrinsic pathway of apoptosis (Frentzou et al., 2010).

From the data presented (Fig 5.8, 5.10, 5.13, 5.15 & 5.21), p38 appears to be a key connection between TF and the mechanism of cell apoptosis. Inhibition of p38 using SB20190, or the siRNA-mediated suppression of p38 expression, prevented p53 up-regulation, and phosphorylation of Ser33 within p53; it also suppressed the transcriptional activity of p53 (Fig 5.21). Moreover, these observations point to a mechanism by which the transcriptional activity of p53 is restrained in samples able to release TF.

Prevention of apoptosis through the down-regulation of p53 activity by serine/threonine-phosphatases has previously been demonstrated (Takekawa et al., 2000; Bulavin et al., 2002; Ueda et al., 2003). Moreover, it is known that, following the phosphorylation of Ser33, the action of prolyl isolmerase 1 (Pin1) protects p53 from de-phosphorylation, acting as a delay mechanism and enhancing the promotion of cell apoptosis (Zacchi et al., 2002; Cohen et al., 2008). Interestingly, this protection does not alter the amount of p53 protein but preserves the transcriptional activity of p53 (Zheng et al., 2002). Therefore, the lack of protection may explain why, despite the increased levels of p53 in cells expressing TF_{Wt} and TF_{Asp253}, and increased nuclear localisation observed in cells expressing TF_{Wt}, no increase in Bax protein or cell apoptosis was observed in these cells.

In summary, transfection of HCAEC to express wild-type or, alternatively, Ala253-substituted TF was shown to increase p53 protein level and localisation to the nucleus. However, an increase in cell apoptosis was observed only in cells expressing TF_{Ala253}. This increase in cell apoptosis was concurrent with an increase in p53 phosphorylation at Ser33 and an increase in p53 transcriptional activity with subsequent up-regulation in the expression of bax, through a mechanism that appears to be dependent on p38 activity. Therefore, p38 appears to be a key mediator between TF and the mechanism of cell apoptosis.

CHAPTER 6

General discussion

6. General discussion

The principal aim of this thesis was to examine the mechanism associating the increased circulating TF-containing microvesicles with endothelial cell apoptosis which is often observed during chronic inflammatory diseases (Dimmeler et al., 1999; Gardner et al., 2014). Endothelial cells express and release TF-containing microvesicles in response to injury, trauma or inflammatory mediators (Napoleone et al., 1997; Steffel et al., 2005). Furthermore, endothelial cells may acquire TF carried by circulating microvesicles (Dasgupta et al., 2012; Osterud & Bjorklid, 2012; Collier et al., 2013) and can cause endothelial dysfunction (Widlansky et al., 2003). In addition to the role of TF in haemostasis, it has become evident that TF is also capable of inducing signalling mechanisms. Signalling via TF has been shown to be associated with cell proliferation (Versteeg & Ruf, 2006; Ettelaie et al., 2008; Collier & Ettelaie, 2010; Kocaturk et al., 2013). However, the involvement of TF in cell apoptosis has also been demonstrated (Pradier & Ettelaie, 2008; Frentzou et al., 2010). The ability of TF to induce cellular effects may arise from its signalling activity via phosphorylation of the two serine residues (Ser253 and Ser258) within the TF cytoplasmic domain. The role of serine residues within the cytoplasmic domain of TF in the incorporation and release of TF as microvesicles has recently been demonstrated (Collier & Ettelaie, 2011).

The first part of this study aimed to assess the role of phosphorylation of the cytoplasmic domain of TF on the activation of ERK1/2 and p38 pathways, their contribution to the regulation of TF release as microvesicles, and the termination of this process. TF was shown to be capable of inducing both p38 and ERK1/2 phosphorylation following PAR2 activation. Preventing the release of TF by Ala253-substitution of TF enhanced the phosphorylation of p38. In addition, inhibition of the p38 pathway by SB202190 was shown

to inhibit the phosphorylation of Ser258. The inhibition of p38 was concurrent with the increased level of release of TF within microvesicles. Next, the influence of disruption of TF release on cell proliferation and apoptosis and the role of p38 pathway in these processes were examined. Expression of wild-type or Asp253-substituted TF increased the rate of proliferation in endothelial cells. In contrast, the expression of Ala253-substituted TF did not lead to cell proliferation. Furthermore, the expression of Ala253-substituted TF promoted cellular apoptosis in activated cells but was suppressed by the inhibition of p38 activity. In contrast, no endothelial cell apoptosis was observed in cells expressing wild-type or Asp253-substituted TF. Finally, the mechanisms by which accumulation of TF induces cellular apoptosis were examined. It was demonstrated that accumulation of TF in the cells leads to an increase in cell apoptosis. This effect seems to be dependent on p38 activity and on the transcriptional activity of p53. In order to ensure that the model of the endothelial cells in which the cells transfected to express TF were representative of the pathophysiological conditions in the human body, in some experiments the endothelial cells were also incubated with TF-containing microvesicles. However, despite testing different types of transfection reagent, it was not possible to transfect human coronary artery endothelial efficiently. The highest transfection efficiency (29 %) was achieved using Lipofectin. Therefore, the observations were based on the fraction of population of cells rather than all the cells in the sample. In addition, the endothelial cells can be influenced by other factors including; medications, smoking and other inflammatory conditions, *in vivo*. Therefore, to be cautious when interpreting the *in vitro* results to the condition of vascular disease observed *in vivo* since the *in vitro* experiments cannot replicate the precise physiological conditions within the human body.

This study has demonstrated that the prolonged activation of p38α results in the phosphorylation of Ser258 within the cytoplasmic domain of TF. This feedback mechanism results in the termination of the release of TF within microvesicles. Therefore, it may be suggested that once sufficient amounts of TF are released by the cells, the process is self-regulated by a mechanism which is itself activated during the TF release phase (Fig 3.23). Prolonged activation of the p38 pathway is thought to be the hallmark of induction of p38-mediated cell apoptosis, while short durations of activity appear to coincide with cell proliferation (Dolado & Nebreda, 2008). Moreover, the transient activation of p38 was concurrent with the induction of the ERK pathway. p38 is involved in inflammatory responses implicated in a variety of vascular diseases (Force et al., 1996; Ono & Han, 2000; Behr et al., 2003; Kumar et al., 2003). Therefore, the inability to release TF may result in inflammatory signalling mediated by p38, leading to cell apoptosis**.** The mechanism by which TF activates p38 is still unknown and is thought to be mediated via Src (Versteeg et al., 2000). In addition, the activation of p38 by TF may also involve receptors such as the integrins which also require the presence of scaffolding proteins (Kocaturk et al., 2013). However, the mechanisms of p38 activation require further investigation.

A number of studies have demonstrated the mechanisms of TF-mediated cell proliferation. This function appears to arise from the interaction of TF with β1-integrins (Dorfleutner et al., 2004; Collier & Ettelaie, 2010; Kocaturk et al., 2013), resulting in the activation of proliferative signalling mechanisms including the ERK pathway (Collier & Ettelaie, 2010). However, no previous study has investigated the mechanisms of TF-mediated cell apoptosis. In this study it was demonstrated that the release of TF by the cells has a proliferative influence on the parent cell, mediated through the activation of ERK and the transient activation of p38 pathways. Furthermore, it appears that cells able to release TF

showed an increase in cell proliferation through increased Cyclin D1 expression and entry into the cell cycle. In contrast, the persistence of TF within the cells following activation, promotes the prolonged activation of p38, which may lead to inflammatory responses giving rise to apoptosis. These results agree with the findings of other studies, in which Cyclin D1 expression is shown to be positively regulated by the ERK, and negatively by the p38 **(**Lavoie et al., 1996; Ravenhall et al., 2000**).** Accumulation of TF within the cells resulted in up-regulation of p21 and Bax expression and, subsequently, apoptosis. Therefore, it is possible that the entry into the cell cycle, following PAR2 activation, is enhanced by the presence of TF. However, the prolonged presence of TF and/or inability of the cell to release TF within microvesicles results in cell cycle arrest and, subsequently, apoptosis. This suggests that activation of the endothelial cells through injury or inflammatory mediators may in turn promote the pro-apoptotic mechanisms which manifest themselves as endothelial dysfunction associated with disease conditions. A trend was observed in which accumulation of TF within the endothelial cells was shown to increase p53 protein levels, phosphorylation of p53 at Ser33, its localisation to the nucleus and increased transcriptional activity. p53 is known to induce cell cycle arrest and apoptosis by up-regulation of the expression of p21 (Levine, 1997) and bax (El-Deiry et al., 1994) respectively. In addition, p38 has been shown to be capable of phosphorylating Ser33 within the trans-activation domain of p53 protein following various stress signals to the cell (Kishi et al., 2001). Therefore**,** it is possible that the accumulation of TF within the cells can induce p53 phosphorylation at Ser33 by p38 resulting in the stabilisation of p53 within the nucleus. This leads to increased expression of p21, which promotes cell cycle arrest. At this point, the cells may release TF and the cell cycle may proceed; alternatively, if the cells are unable to release TF then the apoptotic mechanisms are activated by increased expression of Bax. Moreover, it is known that, following the phosphorylation of Ser33, the action of prolyl

isolmerase 1 (Pin1) protects p53 from de-phosphorylation, acting as a delay mechanism and enhancing the promotion of cell apoptosis (Zacchi et al., 2002; Cohen et al., 2008). Interestingly, this protection does not alter the amount of p53 protein but preserves the transcriptional activity of p53 (Zheng et al., 2002). The lack of p53 protection in cells expressing wild-type and Asp253-substituted TF, provides an explanation of why, despite the increased levels of p53 and increased nuclear localisation observed in these cells, no increase in Bax or cell apoptosis was observed. Interestingly, the serine-proline-leucine motif is present around both Ser258 within TF (KENSPLNVS) and Ser33 within p53 (NVLSPLPSQ), which agree with the finding that the phosphorylation of Ser258 within TF is mediated by p38α. Therefore, due to the similarity between the sequences surrounding Ser33 in p53 and Ser258 in TF, it is likely that Pin1 also protects the phosphorylation state of TF at Ser258 against phosphatase activity. This feedback mechanism may in turn enhance the activation of p38 and also regulate the termination of TF release from cells. Further investigation to confirm the role of Pin1 on the stabilisation of Ser258 phosphorylation within TF could be carried out using siRNA targeting Pin1 mRNA and measuring the phosphorylation of Ser258, TF release and cell apoptosis.

It has been demonstrated that the levels of circulating TF are increased during cancer, infection and cardiovascular disease. The released TF may be taken up by the endothelium and may eventually alter the function of the endothelium within the vasculature and the heart, rise to cardiovascular disease. During early pathological conditions, low levels of TF can induce endothelial cell proliferation, leading to the remodelling of the endothelium. Such remodelling of the endothelium could initially be beneficial in supplying the tissues with oxygen. In contrast, during severe progressive disease states, high amounts of TF cause

the death of the cells. This may also partly explain the phenomenon of endothelial denudation observed during cardiovascular disease.

In summary, elevated levels of TF-associated microvesicles originating from endothelial cells have been found in various disease states and may contribute to a hypercoagulable state. In addition to its role in coagulation, TF influences a number of cellular processes by initiating intracellular signalling pathways. Endothelial cells may express TF in response to inflammatory modulators or acquire and recycle TF carried by circulating microvesicles. Activation of endothelial cells in response to injury or inflammatory mediators would be capable of releasing sufficient amounts of stored TF to prevent apoptosis. However, accumulation of large amounts of TF representative of those observed in severe disease, through high levels of pro-inflammatory factors or through the sequestration of microvesicles from the bloodstream, may compromise the ability of endothelial cells to respond to cell activation in a positive manner and result in cellular apoptosis. In conclusion, this study has shown that induction of cellular apoptosis by TF is mediated through the prolonged activation of p38, leading to the phosphorylation of Ser33 and stabilisation of the transcriptional activity of p53, localised within the nucleus. This in turn results in the expression of Bax and induction of cell apoptosis.

Figure 6.1. Schematic representation of a proposed mechanism for TF-mediated apoptosis

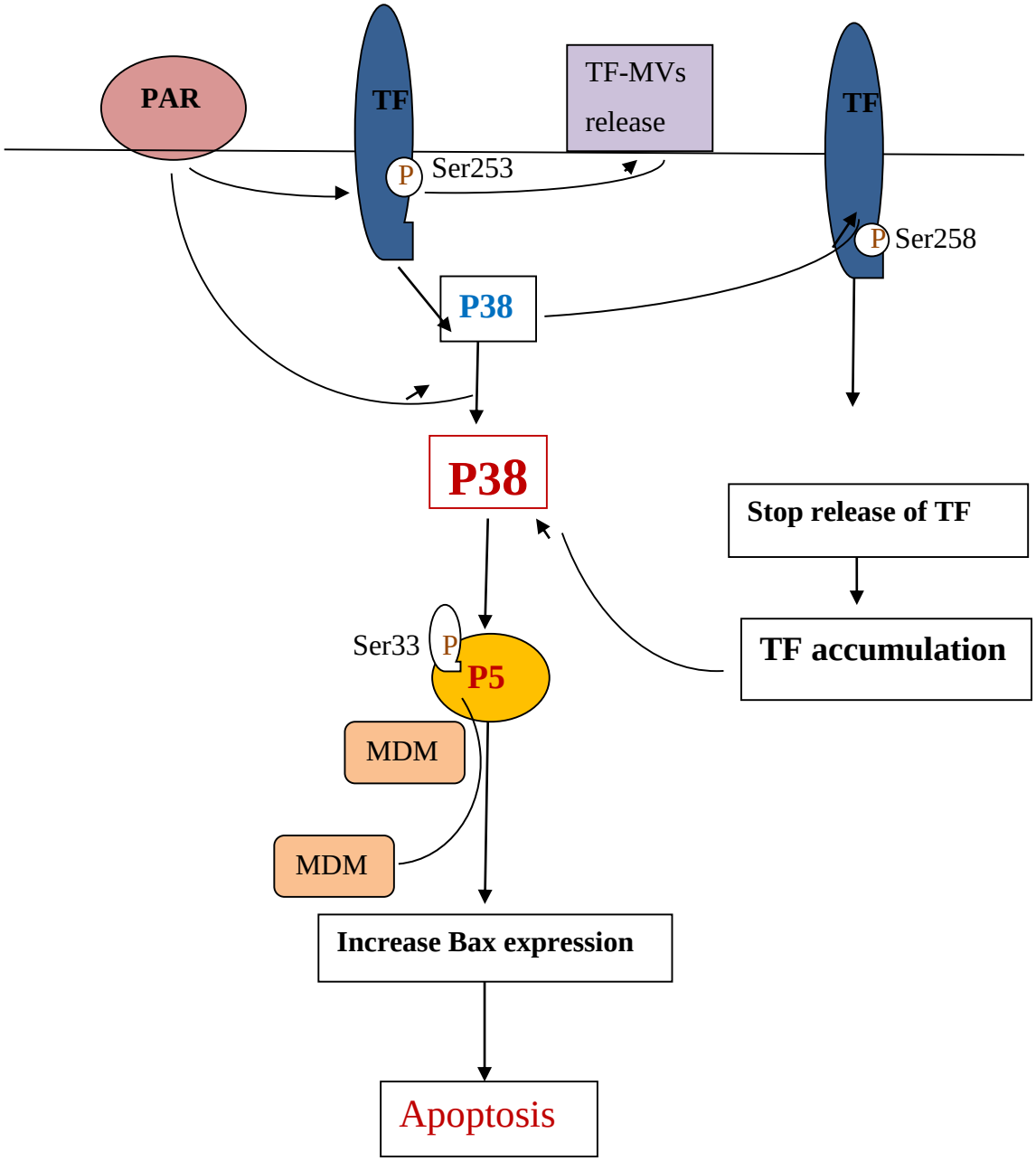

It is proposed that the activation of TF by PAR2-AP results in activation of p38 and termination of TF release via phosphorylation of Ser258. The suggested hypothesis is that accumulation of TF in the cells results in enhancement of p38 activation which phosphorylate p53 at Ser33 and dissociate it from MDM2. p53 in turn upregulates Bax expression which induces cellular apoptosis.

References

Abbas T, Dutta A. (2009) p21 in cancer: intricate networks and multiple activities. *Nat. Rev. Cancer*. **9**:400–414.

Abe K, Shoji M, Chen J, , Bierhaus A, Danave I, Micko C, Casper K, Dillehay DL, Nawroth PP, Rickles FR. (1999) Regulation of vascular endothelial growth factor production and angiogenesis by the cytoplasmic tail of tissue factor. *Proceedings of the National Academy of Sciences of the United States of America.* **96** (15):8663-8668.

Aberg M, Siegbahn A. (2013) Tissue factor non-coagulant signaling-molecular mechanisms and biological consequences with a focus on cell migration and apoptosis. *Journal of Thrombosis and Haemostasis.* **11** (5):817-825.

Aguirre-Ghiso JA, Estrada Y, Liu D, Ossowski L. (2003) ERKMAPK activity as a determinant of tumor growth and dormancy; Regulation by p38(SAPK). *Cancer Research.* **63** (7):1684-1695.

Ahamed J, Niessen F, Kurokawa T, Lee YK, Bhattacharjee G, Morrissey JH, Ruf W. (2007) Regulation of macrophage procoagulant responses by the tissue factor cytoplasmic domain in endotoxemia. *Blood.* **109** (12): 5251-5259.

Ahamed J, Ruf W. (2004) Protease-activated receptor 2-dependent phosphorylation of the tissue factor cytoplasmic domain. *Journal of Biological Chemistry.* **279** (22):23038-23044.

Aharon A, Tamari T, Brenner B. 2008. Monocyte-derived microparticles and exosomes induce procoagulant and apoptotic effects on endothelial cells. *Thromb Haemost.* **100** (5):878-885.

Ahn YS. (2005) Cell-derived microparticles: 'Miniature envoys with many faces'. *Journal of Thrombosis and Haemostasis.* **3** (5):884-887.

Albrecht S, Kotzsch M, Siegert G, Luther T, Grossmann H, Grosser M, Müller M. (1996) Detection of circulating tissue factor and factor VII in a normal population. *Thrombosis and haemostasis*. **75** (5):772-777.

Alessi DR, Gomez N, Moorhead G, Lewis T, Keyse SM, Cohen P. (1995) Inactivation of p42 MAP kinase by protein phosphatase 2A and a protein tyrosine phosphatase, but not CL100, in various cell lines. *Current Biology*. **5** (3):283-295.

Amabile N, Boulanger CM, Guerin AP, Tedgui A, London GM. (2011) Measurement of circulating endothelial microparticles levels is superior to pulse wave velocity for prediction of global and cardiovascular mortality in end-stage renal disease. *European Heart Journal*. **31**:827-827.

Annex BH, Denning SM, Channon KM, Sketch MH, Stack RS, Morrissey JH, Peters KG. (1995) Differential expression of tissue factor protein in directional atherectomy specimens from patients with stable and unstable coronary syndromes. *Circulation.* **91** (3): 619-622.

Appella E, Anderson CW. (2001) Post-translational modifications and activation of p53 by genotoxic stresses. *European Journal of Biochemistry*. **268** (10):2764-2772.

Archipoff G, Beretz A, Freyssinet JM, Klein-Soyer C, Brisson C, Cazenave JP. (1991) Heterogeneous regulation of constitutive thrombomodulin or inducible tissue-factor activities on the surface of human saphenous-vein endothelial cells in culture following stimulation by interleukin-1, tumour necrosis factor, thrombin or phorbol ester. *Biochem.* **273**:679-684.

Bach R, Gentry R. Nemerson Y. (1986) Factor-vii binding to tissue factor in reconstituted phospholipid-vesicles - induction of cooperativity by phosphatidylserine. *Biochemistry.* **25** (14):4007-4020.

Bach R, Konigsberg WH, Nemerson Y. (1988) Human-tissue factor contains thioester-linked palmitate and stearate on the cytoplasmichalf-cystine. *Biochemistry*. **27** (12):4227-4231.

Ballif BA, Blenis J. (2001) Molecular mechanisms mediating mammalian mitogen-activated protein kinase (MAPK) kinase (MEK)-MAPK cell survival signals. *Cell growth and differentiation*. **12** (8):397-408.

Bao, Q. Shi Y. (2007) Apoptosome: a platform for the activation of initiator caspases. *Cell Death and Differentiation.* **14** (1):56-65.

Batteiger B, Newhall V WJ, Jones RB. (1982) The use of Tween 20 as a blocking agent in the immunological detection of proteins transferred to nitrocellulose membranes. *Journal of immunological methods.* **55** (3):297-307.

Bazan JF. (1990) Structural design and molecular evolution of a cytokine receptor superfamily. *Proceedings of the National Academy of Sciences of the United States of America.* **87** (18):6934-6938.

Behn-Krappa A, Newton AC. (1999) The hydrophobic phosphorylation motif of conventional protein kinase C is regulated by autophosphorylation. *Current Biology*. **9** (14):728-737.

Behr TM, Berova M, Doe CP, Ju H, Angermann CE, Boehm J, Willette RN. (2003) p38 mitogen-activated protein kinase inhibitors for the treatment of chronic cardiovascular disease. *Current opinion in investigational drugs.* (London, England: 2000) **4** (9):1059-1064.

Berckmans RJ, Nieuwland R, Boing AN, Romijn F, Hack CE, Sturk A. (2001) Cell-derived microparticles circulate in healthy humans and support low grade thrombin generation. *Thrombosis and Haemostasis.* **85** (4):639-646.

Bevilacqua MP, Schleef RR, Gimbrone Jr MA, Loskutoff DJ. (1986) Regulation of the fibrinolytic system of cultured human vascular endothelium by interleukin 1. *Journal of Clinical Investigation.* **78** (2):587.

Boatright, K. M., M. Renatus, et al. (2003) A unified model for apical caspase activation. *Molecular Cell*. **11** (2):529-541.

Bogdanov VY, Balasubramanian V, Hathcock J, Vele O, Lieb M, Nemerson Y. (2003) Alternatively spliced human tissue factor: a circulating, soluble, thrombogenic protein. *Nature Medicine*. **9** (4):458-462.

Bohgaki M, Atsumi T, Yamashita Y, Yasuda S, Sakai Y, Furusaki A, Bohgaki T, Amengual O, Amasaki Y, Koike T. (2004) The p38 mitogen-activated protein kinase (MAPK) pathway mediates induction of the tissue factor gene in monocytes stimulated with human monoclonal anti-beta(2)Glycoprotein I antibodies. *International Immunology*. **16** (11):1633-1641.

Bolton TG, Nye SH, Robbins DJ, Ip NY, Radziejewska E, Morgenbesser SD, Depinho RA, Panayotatos N, Cobb MH, Yancopoulos GD. 1991. ERKS a family of protein-serine-threonine kinases that are activated and tyrosine phosphorylated in response to insulin and NGF. *Cell*. **65** (4):663-676.

Bombeli, T., A. Karsan et al. (1997) Apoptotic vascular endothelial cells become procoagulant. *Blood*. **89** (7):2429-2442.

Bradham C, McClay DR. (2006) p38 MAPK in development and cancer. *Cell Cycle*. **5** (8):824-828.

Bromberg ME, Konigsberg WH, Madison JF, Pawashe A, Garen A. (1995) Tissue Factor promotes melanoma metastasis by a pathway independent of blood-coagulation. *Proceedings of the National Academy of Sciences of the United States of America.* **92** (18), 8205-8209.

Brune B. (2003) Nitric oxide: NO apoptosis or turning it ON? *Cell Death and Differentiation.* **10** (8):864-869.

Bulavin DV, Demidov ON, Saito Si, Kauraniemi P, Phillips C, Amundson SA, Ambrosino C, Sauter G, Nebreda AR, Anderson CW. (2002) Amplification of PPM1D in human tumors abrogates p53 tumor-suppressor activity. *Nature genetics*. **31** (2):210-215.

Bulavin DV, Fornace Jr AJ. (2004) p38 MAP kinase's emerging role as a tumor suppressor. *Advances in cancer research*. **92**:95-118.

Bulavin DV, Saito S, Hollander MC, Sakaguchi K, Anderson CW, Appella E, Fornace AJ,Jr. (1999) Phosphorylation of human p53 by p38 kinase coordinates N-terminal phosphorylation and apoptosis in response to UV radiation. *The EMBO journal.* **18** (23):6845-6854.

Burnier L, Fontana P, Kwak BR, Angelillo-Scherrer A. (2009) Cell-derived microparticles in haemostasis and vascular medicine. *Thrombosis and Haemostasis*. **101** (3):439-451.

Butenas S, Bouchard BA, Brummel-Ziedins KE, Parhami-Seren B, Mann KG. (2005) Tissue factor activity in whole blood. *Blood.* **105** (7):2764-2770.

Camerer E, Gjernes E, Wiiger M, Pringle S, Prydz H. (2000) Binding of factor VIIa to tissue factor on keratinocytes induces gene expression. *Journal of Biological Chemistry*. **275** (9):6580-6585.

Campbell HG, Mehta R, Neumann AA, Rubio C, Baird M, Slatter TL, Braithwaite AW. (2013) Activation of p53 following ionizing radiation, but not other stressors, is dependent on the proline-rich domain (PRD). *Oncogene*. **32** (7):827-836.

Carmeliet P, Jain R K. (2000) Angiogenesis in cancer and other diseases. *Nature*. **407** (6801): 249-257.

Carnero A, Hannon G J. (1998) The INK4 family of CDK inhibitors. *Curr Top Microbiol Immunol.* **227**:43–55.

Chen J, Kasper M, Heck T, Nakagawa K, Humpert PM, Bai L, Wu G, Zhang YM, Luther T, Andrassy M. (2005) Tissue factor as a link between wounding and tissue repair. *Diabetes.* **54** (7):2143-2154.

Chen Z, Gibson TB, Robinson F, Silvestro L, Pearson G, Xu BE, Wright A, Vanderbilt C, Cobb MH. (2001) MAP kinases. *Chemical Reviews*. **101** (8):2449-2476.

Chiba K, Kawakami K, Tohyama K. (1998) Simultaneous evaluation of cell viability by neutral red, MTT and crystal violet staining assays of the same cells. *Toxicology in vitro.* **12** (3):251-258.

Chipuk JE, Green DR. (2006) Dissecting p53-dependent apoptosis. *Cell Death & Differentiation.* **13** (6):994-1002.

Chipuk JE, Kuwana T, Bouchier-Hayes L, Droin NM, Newmeyer DD, Schuler M, Green DR. (2004) Direct activation of Bax by p53 mediates mitochondrial membrane permeabilization and apoptosis. *Science*. **303** (5660):1010-1014.

Chiu LCM, Ho TS, Wong EYL, Ooi VEC. (2006) Ethyl acetate extract of Patrinia scabiosaefolia downregulates anti-apoptotic Bcl-2/BCI-X-L expression, and induces apoptosis in human breast carcinoma MCF-7 cells independent of caspase-9 activation. *Journal of Ethnopharmacology.* **105** (1-2):263-268.

Chu AJ. (2011) Tissue factor, blood coagulation, and beyond: an overview. *International journal of inflammation.* **2011:**367284

Cohen M, Wuillemin C, Bischof P. (2008) Trophoblastic p53 is stabilised by a cis–trans isomerisation necessary for the formation of high molecular weight complexes involving the N-terminus of p53. *Biochimie.* 90 (6):855-862.

Cohen P. (1997). The search for physiological substrates of MAP and SAP kinases in mammalian cells. *Trends in Cell Biology*. **7** (9):353-361.

Collier MEW, Ettelaie C. (2010) Induction of Endothelial Cell Proliferation by Recombinant and Microparticle-Tissue Factor Involves beta 1-Integrin and Extracellular

Signal Regulated Kinase Activation. *Arteriosclerosis Thrombosis and Vascular Biology*. **30** (9):1810-U297.

Collier MEW, Ettelaie C. (2011) Regulation of the Incorporation of Tissue Factor into Microparticles by Serine Phosphorylation of the Cytoplasmic Domain of Tissue Factor. *Journal of Biological Chemistry*. **286** (14).

Collier MEW, Mah PM, Xiao Y, Maraveyas A, Ettelaie C. (2013) Microparticle-associated tissue factor is recycled by endothelial cells resulting in enhanced surface tissue factor activity. *Thrombosis and haemostasis.* **110** (5):966-76.

Combes V, Simon AC, Grau GE, Arnoux D, Camoin L, Sabatier F, Mutin M, Sanmarco M, Sampol J, Dignat-George Fo. (1999) In vitro generation of endothelial microparticles and possible prothrombotic activity in patients with lupus anticoagulant. *Journal of Clinical Investigation.* **104** (1):93-102.

Cory S, Adams JM. (2002) The BCL2 family: Regulators of the cellular life-or-death switch. *Nature Reviews Cancer.* **2** (9):647-656.

Coughlin SR, Camerer E. (2003) Participation in inflammation. *Journal of Clinical Investigation.* **111** (1):25-27.

Crighton D, Wilkinson S, O'Prey J, Syed N, Smith P, Harrison PR, Gasco M, Garrone O, Crook T, Ryan KM. (2006) DRAM, a p53-induced modulator of autophagy, is critical for apoptosis. *Cell.* **126** (1):121-134.

Cross B, Chen L, Cheng Q, Li B, Yuan Z-M, Chen J. (2011) Inhibition of p53 DNA binding function by the MDM2 protein acidic domain. *Journal of Biological Chemistry*. **286** (18):16018-16029.

Cuadrado A, Nebreda AR. (2010) Mechanisms and functions of p38 MAPK signalling. *Biochemical Journal*. **429**:403-417.

Cuenda A, Rousseau S. (2007) p38 MAP-kinases pathway regulation, function and role in human diseases. *Biochimica et Biophysica Acta (BBA)-Molecular Cell Research.* **1773** (8):1358-1375.

Cuevas BD, Abell AN, Johnson GL. (2007) Role of mitogen-activated protein kinase kinase kinases in signal integration. *Oncogene*. **26** (22):3159-3171.

Cunningham MA, Romas P, Hutchinson P, Holdsworth SR, Tipping PG. (1999) Tissue factor and factor VIIa receptor/ligand interactions induce proinflammatory effects in macrophages. *Blood.* **94** (10):3413-3420.

Dasgupta SK, Le A, Chavakis T, Rumbaut RE, Thiagarajan P. (2012) Developmental Endothelial Locus-1 (Del-1) Mediates Clearance of Platelet Microparticles by the Endothelium. *Circulation*. **125** (13):1664-1672.

Davies SP, Reddy H, Caivano M, Cohen P. (2000) Specificity and mechanism of action of some commonly used protein kinase inhibitors. *Biochemical Journal.* **351**:95-105.

Deregibus MC, Cantaluppi V, Calogero R, Lo Iacono M, Tetta C, Biancone L, Bruno S, Bussolati B, Camussi G. (2007) Endothelial progenitor cell-derived microvesicles activate an angiogenic program in endothelial cells by a horizontal transfer of mRNA. *Blood*. **110** (7):2440-2448.

Diamant M, Tushuizen ME, et al. (2004) Cellular microparticles: new players in the field of vascular disease? *European Journal of Clinical Investigation.* **34** (6):392-401.

Dimmeler S, Hermann C, Zeiher AM. (1999) Apoptosis of endothelial cells. Contribution to the pathophysiology of atherosclerosis? *European cytokine network.* **9** (4):697-8.

Dolado I, Nebreda AR. (2008). Regulation of tumorigenesis by p38 alpha MAP kinase. *Topics in Current Genetics*. **20**:99-128.

Dorfleutner A, Hintermann E, Tarui T, Takada Y, Ruf W. (2004) Cross-talk of integrin α3β1 and tissue factor in cell migration. *Mol Biol Cell*. **2004** (15):4416–4425.

Dorfleutner A, Ruf W. (2003) Regulation of tissue factor cytoplasmic domain phosphorylation by palmitoylation. *Blood*. **102** (12):3998-4005.

Doyle K. (1996) *Promega protocols and applications guide* / 3rd ed. Madison: Promega Corporation.

Drake TA, Morrissey JH, Edgington TS. (1989) Selective cellular expression of tissue factor in human tissues. Implications for disorders of hemostasis and thrombosis. *The American journal of pathology.* **134** (5):1087.

Dudley DT, Pang L, Decker SJ, Bridges AJ, and Saltiel AR. (1995) A synthetic inhibitor of the mitogen-activated protein kinase cascade. *Proc Natl Acad Sci USA.* **92:**7686–7689.

Efimova T, Broome AM, Eckert RL. (2003) A regulatory role for p38 delta MAPK in keratinocyte differentiation-Evidence for p38 delta-ERK1/2 complex formation. *Journal of Biological Chemistry.* **278** (36):34277-34285.

El-Deiry WS, Harper JW, O'Connor PM, Velculescu VE, Canman CE, Jackman J, Pietenpol JA, Burrell M, Hill DE, Wang Y. (1994) WAF1/CIP1 is induced in p53-mediated G1 arrest and apoptosis. *Cancer research*. **54** (5):1169-1174.

El-Deiry WS, Tokino T, Velculescu VE, Levy DB, Parsons R, Trent JM, Lin D, Mercer WE, Kinzler KW, Vogelstein B. (1993) *WAF1*, a potential mediator of p53 tumor suppression. *Cell*. **75** (4):817-825.

Elmore S. (2007) Apoptosis: a review of programmed cell death. *Toxicologic pathology*. **35** (4):495-516.

Eto M, Kozai T, Cosentino F, Joch H, LÃ¼scher TF. (2002) Statin prevents tissue factor expression in human endothelial cells role of Rho/Rho-kinase and Akt pathways. *Circulation.* **105** (15):1756-1759.

Ettelaie C, ElKeeb AM, Maraveyas A, Collier MEW. (2013) p38 alpha phosphorylates serine 258 within the cytoplasmic domain of tissue factor and prevents its incorporation into cell-derived microparticles. *Biochimica Et Biophysica Acta-Molecular Cell Research.* **1833** (3):613-621.

Ettelaie C, Su S, Li C, Collier ME. (2008) Tissue factor-containing microparticles released from mesangial cells in response to high glucose and AGE induce tube formation in microvascular cells. *Microvasc Res*. **76**:152–60.

Force T, Pombo CM, Avruch JA, Bonventre JV, Kyriakis JM. (1996) Stress-activated protein kinases in cardiovascular disease. *Circulation research*. **78** (6):947-953.

Frentzou GA, Collier MEW, Seymour A-ML, Ettelaie C. (2010) Differential induction of cellular proliferation, hypertrophy and apoptosis in H9c2 cardiomyocytes by exogenous tissue factor. *Molecular and cellular biochemistry.* **345** (1-2):119-130.

Freyssinet JM. 2003. Cellular microparticles: what are they bad or good for? *Journal of Thrombosis and Haemostasis.* **1** (7):1655-1662.

Funderburg NT, Mayne E, Sieg SF, Asaad R, Jiang W, Kalinowska M, Luciano AA, Stevens W, Rodriguez B, Brenchley JM. (2010) Increased tissue factor expression on circulating monocytes in chronic HIV infection: relationship to in vivo coagulation and immune activation. *Blood*. **115** (2):161-167.

Fuster JJ, Sanz-Gonzalez SM, Moll UM, Andres V. (2007) Classic and novel roles of p53: prospects for anticancer therapy. *Trends in Molecular Medicine*. **13** (5):192-199.

Galley HF, Webster NR. (2004) Physiology of the endothelium. *British Journal of Anaesthesia*. **93** (1):105-113.

Gardner AW, Parker DE, Montgomery PS, Sosnowska D, Casanegra AI, Ungvari Z, Csiszar A, Sonntag WE. (2014) Greater Endothelial Apoptosis and Oxidative Stress in Patients with Peripheral Artery Disease. *International Journal of Vascular Medicine.* **2014**, Article ID 160534, 8 pages

Gottlieb TM, Oren M. (1996) p53 in growth control and neoplasia. *Biochimica et Biophysica Acta.* (BBA)-Reviews on Cancer **1287** (2):77-102.

Green DR, Reed JC. (1998) Mitochondria and apoptosis. *Science.* **281** (5381):1309-1312.

Greeno EW, Bach RR, Moldow CF. (1996) Apoptosis is associated with increased cell surface tissue factor procoagulant activity. *Laboratory Investigation.* **75** (2):281-289.

Grethe S, Ares MPS, Andersson T, Porn-Ares MI. (2004) p38 MAPK mediates TNF-induced apoptosis in endothelial cells via phosphorylation and downregulation of Bcl-x(L). *Experimental Cell Research.* **298** (2):632-642.

Grethe S, Porn-Ares MI. (2006) p38 MAPK regulates phosphorylation of Bad via MA-dependent suppression of the MEK1/2-ERK1/2 survival pathway in TNF-alpha induced endothelial apoptosis. *Cellular Signalling*. **18** (4):531-540.

Guan ZH, Buckman SY, Pentland AP, Templeton DJ, Morrison AR. (1998). Induction of cyclooxygenase-2 by the activated MEKK1 -> SEK1/MKK4 -> p38 mitogen-activated protein kinase pathway. *Journal of Biological Chemistry*. **273** (21):12901-12908.

Guardavaccaro D, Corrente G, Covone F, Micheli L, D'Agnano I, Starace G, Caruso M, Tirone F. (2000) Arrest of G1-S progression by the p53-inducible gene PC3 is Rb dependent and relies on the inhibition of cyclin D1 transcription. *Molecular and cellular biology.* **20** (5):1797-1815.

Gupta, S., et al. (1995) Transcription factor ATF2 regulation by the JNK signal transduction pathway. *Science.* **267** (5196):389-393.

Habersberger J, Strang F, Scheichl A, Htun N, Bassler N, Merivirta RM, Krippner G, Meikle P, Eisenhardt, SU, Meredith I, Peter K. (2012) Circulating microparticles generate and transport monomeric C-reactive protein in patients with myocardial infarction. *Cardiovascular research.* **96** (1):64-72.

Han J, Lee JD, Bibbs L, Ulevitch RJ. (1994) A MAP kinase targeted by endotoxin and hyperosmolarity in mammalian-cells. *Science*. **265** (5173):808-811.

Hanks SK, Hunter T. (1995) Protein kinases 6. The eukaryotic protein kinase superfamily: kinase (catalytic) domain structure and classification. *The FASEB journal*. **9** (8):576-596.

Harper JW, Adami GR, Wei N, Keyomarsi K, Elledge SJ. (1993) The p21 cdk-interacting protein cip1 is a potent inhibitor of g1 cyclin-dependent kinases. *Cell*. **75** (4): 805-816.

Haupt S, Berger M, Goldberg Z, Haupt Y. (2003) Apoptosis - the p53 network. *Journal of Cell Science.* **116** (20):4077-4085.

Haupt Y, Maya R, Kazaz A, Oren M. 1997. Mdm2 promotes the rapid degradation of p53. *Nature*. **387** (6630):296-299.

Hjortoe GM, Petersen LC, Albrektsen T, Sorensen BB, Norby PL, Mandal SK, Pendurthi UR, Rao LVM. (2004) Tissue factor-factor VIIa-specific up-regulation of IL-8 expression in MDA-MB-231 cells is mediated by PAR-2 and results in increased cell migration. *Blood*. **103** (8):3029-3037.

Hornberg JJ, Bruggeman FJ, Binder B, Geest CR, de Vaate A, Lankelma J, Heinrich R, Westerhoff HV. (2005) Principles behind the multifarious control of signal transduction-ERK phosphorylation and kinase/phosphatase control. *Febs Journal*. **272** (1):244-258.

Honda R, Tanaka H, Yasuda H. (1997) Oncoprotein MDM2 is a ubiquitin ligase E3 for tumor suppressor p53. *Febs Letters.* **420** (1):25-27.

Hron G, Kollars M, Weber H, Sagaster V, Quehenberger P, Eichinger S, Kyrle PA, Weltermann A. (2007) Tissue factor-positive microparticles: Cellular origin and association with coagulation activation in patients with colorectal cancer. *Thrombosis and Haemostasis*. **97** (1):119-123.

Hugel Bnd, MartÃnez MC, Kunzelmann C, Freyssinet J-M. (2005) Membrane microparticles: two sides of the coin. *Physiology.* **20** (1):22-27.

Hupp TR, Lane DP. (1994) Allosteric activation of latent p53 tetramers. *Current biology.* **4** (10):865-875.

Hussein A, Böing A N, Biró É, Hoek F J, Vogel G M, Meuleman D G, Nieuwland R. (2008) Phospholipid composition of in vitro endothelial microparticles and their in vivo thrombogenic properties. *Thromb Res.***121** (6):865–871.

Imajo M, Tsuchiya Y, Nishida E. (2006) Regulatory mechanisms and functions of MAP kinase signaling pathways. *Iubmb Life*. **58** (5-6):312-317.

Iwakuma T, Lozano G. (2003) MDM2, an introduction. *Molecular Cancer Research.* **1** (14):993-1000.

Jenkins LMM, Durell SR, Mazur SJ, Appella E. (2012) p53 N-terminal phosphorylation: a defining layer of complex regulation. *Carcinogenesis.* **33** (8):1441-1449.

Jiang X, Bailly MA, Panetti TS, Cappello M, Konigsberg WH, Bromberg ME. (2004) Formation of tissue factor-factor VIIa-factor Xa complex promotes cellular signaling and migration of human breast cancer cells. *Journal of Thrombosis and Haemostasis*. **2** (1):93-101.

Jiang Y, Chen CH, Li ZJ, Guo W, Gegner JA, Lin SC, Han JH. (1996) Characterization of the structure and function of a new mitogen-activated protein kinase (p38 beta). *Journal of Biological Chemistry.* **271** (30):17920-17926.

Jiang Y, Gram H, Zhao M, New LG, Gu J, Feng LL, DiPadova F, Ulevitch RJ, Han JH. (1997) Characterization of the structure and function of the fourth member of p38 group mitogen-activated protein kinases, p38 delta. *Journal of Biological Chemistry*. **272** (48):30122-30128.

Jimenez JJ, Jy W, Mauro LM, Horstman LL, Bidot CJ, Ahn YS. (2005) Endothelial microparticles (EMP) as vascular disease markers. *Advances in clinical chemistry*. **39**:131-159.

Joerger AC, Fersht AR. (2008) Structural biology of the tumor suppressor p53. *Annu. Rev. Biochem.* **77**:557-582.

Jung K-H, Chu K, Lee S-T, Park H-K, Bahn J-J, Kim D-H, Kim J-H, Kim M, Lee SK, Roh J-K. (2009) Circulating Endothelial Microparticles as a Marker of Cerebrovascular Disease. *Annals of Neurology.* **66** (2):191-199.

Junttila MR, Li S-P, Westermarck J. (2008). Phosphatase-mediated crosstalk between MAPK signaling pathways in the regulation of cell survival. *The FASEB Journal*. **22** (4):954-965.

Kanke T, Macfarlane SR, Seatter MJ, Davenport E, Paul A, McKenzie RC, Plevin R. (2001) Proteinase-activated receptor-2-mediated activation of stress-activated protein kinases and inhibitory kappa B kinases in NCTC 2544 keratinocytes. *Journal of Biological Chemistry*. **276** (34):31657-31666.

Kishi H, Nakagawa K, Matsumoto M, Suga M, Ando M, Taya Y, Yamaizumi M. (2001) Osmotic shock induces G (1) arrest through p53 phosphorylation at Ser(33) by activated p38(MAPK) without phosphorylation at Ser(15) and Ser(20). *Journal of Biological Chemistry*. **276** (42):39115-39122.

Kocaturk B, Van den Berg YW, Tiekena C, Mieog JSD, de Kruijf EM, Engels CC, van der Ent MA, Kuppen PJ, Van de Velde CJ, Ruf W and others. (2013) Alternatively spliced tissue factor promotes breast cancer growth in a beta 1 integrin-dependent manner. *Proceedings of the National Academy of Sciences of the United States of America.* **110** (28):11517-11522.

Kocaturk B, Versteeg HH. (2013) Tissue factor-integrin interactions in cancer and thrombosis: every Jack has his Jill. *Journal of thrombosis and haemostasis*:*JTH* 11Suppl **1**:285-93.

Kubbutat MHG, Jones SN, Vousden KH. (1997) Regulation of p53 stability by Mdm2. *Nature.* **387** (6630):299-303.

Kumar S, Boehm J, Lee JC. (2003) p38 MAP kinases: key signalling molecules as therapeutic targets for inflammatory diseases. *Nature Reviews Drug Discovery*. **2** (9):717-726.

Kurihara A, Nagoshi H, Yabuki M, Okuyama R, Obinata M, Ikawa S. (2007) Ser46 phosphorylation of p53 is not always sufficient to induce apoptosis: multiple mechanisms of regulation of p53-dependent apoptosis. *Genes to Cells*. **12** (7):853-861.

Kuwana T, Mackey M R. et al. (2002). Bid, Bax, and lipids cooperate to form supramolecular openings in the outer mitochondrial membrane. *Cell*. **111** (3): 331-342.

Kyriakis JM, Avruch J. (2001) Mammalian mitogen-activated protein kinase signal transduction pathways activated by stress and inflammation. *Physiological Reviews*. **81** (2):807-869.

Lafarga V, Cuadrado A, de Silanes IL, Bengoechea R, Fernandez-Capetillo O, Nebreda AR. (2009) p38 Mitogen-Activated Protein Kinase- and HuR-Dependent Stabilization of p21(Cip1) mRNA Mediates the G(1)/S Checkpoint. *Molecular and Cellular Biology*. **29** (16):4341-4351.

Lavoie JeN, L'Allemain G, Brunet A, MÃ¼ller R, PouyssÃ©gur J. (1996) Cyclin D1 expression is regulated positively by the p42/p44MAPK and negatively by the p38/HOGMAPK pathway. *Journal of Biological Chemistry*. **271** (34):20608-20616.

Lechner C, Zahalka MA, Giot JF, Moller NPH, Ullrich A. (1996) ERK6, a mitogen-activated protein kinase involved in C2C12 myoblast differentiation. *Proceedings of the National Academy of Sciences of the United States of America.* **93** (9):4355-4359.

Lee T, Kim SJ, Sumpio BE. (2003) Role of PP2A in the regulation of p38-MAPK activation in bovine aortic endothelial cells exposed to cyclic strain. *Journal of Cellular Physiology*. **194** (3):349-355.

Levine AJ. (1997) p53, the cellular gatekeeper for growth and division. *Cell*. **88** (3):323-331.

Liu XS, Kim CN, Yang J, Jemmerson R, Wang XD. (1996) Induction of apoptotic program in cell-free extracts: Requirement for dATP and cytochrome c. *Cell*. **86** (1):147-157.

Livak KJ, Schmittgen TD. (2001) Analysis of relative gene expression data using real-time quantitative PCR and the 2(T) (-Delta Delta C) method. *Methods*. **25** (4):402-408.

Locksley RM, Killeen N, Lenardo MJ. (2001) The TNF and TNF receptor superfamilies: Integrating mammalian biology. *Cell*. **104** (4): 487-501.

Lopez-Pedrera C, Buendia P, Cuadrado MJ, Siendones E, Aguirre MA, Barbarroja N, Montiel-Duarte C, Torres A, Khamashta M, Velasco F. (2006) Antiphospholipid antibodies from patients with the antiphospholipid syndrome induce monocyte tissue factor expression through the simultaneous activation of NF-kappa B/Rel proteins via the p38 mitogen-

activated protein kinase pathway, and of the MEK-1/ERK pathway. *Arthritis and Rheumatism.* **54** (1):301-311.

Loughery J, Meek D. (2013). Switching on p53: an essential role for protein phosphorylation? *BioDiscovery* **8.**

Lowes VL, Ip NY, Wong YH. (2002) Integration of signals from receptor tyrosine kinases and G protein-coupled receptors. *Neurosignals.* **11** (1):5-19.

Love IM, Grossman SR. (2012) It Takes 15 to Tango Making Sense of the Many Ubiquitin Ligases of p53. *Genes & cancer*. **3** (3-4):249-263.

Mack M, Kleinschmidt A, Bruehl H, Klier C, Nelson PJ, Erfle V, Schlondorff D. (2000) Transfer of CCR5 between different cells by membrane derived microparticles: A potential mechanism for HIV-1 infection in the kidney. *Journal of the American Society of Nephrology*. **11** (Program and Abstract Issue):477A.

Mackman N. (1996) Regulation of tissue factor gene expression in human monocytic and endothelial cells. *Pathophysiology of Haemostasis and Thrombosis.* **26**:17-19.

Mackman N. (2009) The Role of Tissue Factor and Factor VIIa in Hemostasis. *International Anesthesia Research Society.* **108** (5):1447–52.

Maier W, Altwegg LA, Corti R, Gay S, Hersberger M, Maly FE, Sütsch G, Roffi M, Neidhart M, Eberli FR, Tanner FC, Gobbi S, von Eckardstein A, Lüscher TF. (2005).

Inflammatory markers at the site of ruptured plaque in acute myocardial infarction locally increased interleukin-6 and serum amyloid A but decreased C-reactive protein. *Circulation.* **111** (11):1355-1361.

Mans DR, da Rocha AB, Schwartsmann G. (2000) Anti-cancer drug discovery and development in Brazil: targeted plant collection as a rational strategy to acquire candidate anti-cancer compounds. *The Oncologist*. **5** (3):185-98.

Manthey CL, Wang S-W, Kinney SD, Yao Z. (1998) SB202190, a selective inhibitor of p38 mitogen-activated protein kinase, is a powerful regulator of LPS-induced mRNAs in monocytes. *Journal of leukocyte biology*. **64** (3):409-417.

Mantovani A, Dejana E. (1989). Cytokines as communication signals between leukocytes and endothelial cells. *Immunology today*. **10** (11):370-375.

Marinissen MT, Chiariello M, Gutkind JS. (2001) Regulation of gene expression by the small GTPase Rho through the ERK6 (p38 gamma) MAP kinase pathway. *Genes & Development.* **15** (5):535-553.

Martin SJ, Reutelingsperger CP, McGahon AJ, Rader JA, van Schie RC, LaFace DM, Green DR.. (1995) Early redistribution of plasma-membrane phosphatidylserine is a general feature of apoptosis regardless of the initiating stimulus - inhibition by overexpression of BCL-2 AND ABL. *Journal of Experimental Medicine*. **182** (5):1545-1556.

Matsumoto K, Yoshitomi H, Rossant J, Zaret KS. (2001) Liver organogenesis promoted by endothelial cells prior to vascular function. *Science.* **294** (5542):559-563.

Mechtcheriakova D, Schabbauer G, Lucerna M, Clauss M, De Martin R, Binder BR, Hofer E. (2001) Specificity, diversity, and convergence in VEGF and TNF-α signaling events leading to tissue factor up-regulation via EGR-1 in endothelial cells. *The FASEB Journal.* **15** (1):230-242.

Meek DW, Anderson CW. (2009) Posttranslational Modification of p53: Cooperative Integrators of Function. *Cold Spring Harbor Perspectives in Biology*. **1** (6).

Meloche S, Pouyssegur J. (2007) The ERK1/2 mitogen-activated protein kinase pathway as a master regulator of the G1-to S-phase transition. *Oncogene.* **26** (22):3227-3239.

Mesri M, Altieri DC. (1999) Leukocyte microparticles stimulate endothelial cell cytokine release and tissue factor induction in a JNK1 signaling pathway. *Journal of Biological Chemistry*. **274** (33):23111-23118.

Michiels C. (2003) Endothelial cell functions. *Journal of Cellular Physiology*. **196** (3):430-443.

Mihara M, Erster S, Zaika A, Petrenko O, Chittenden T, Pancoska P, Moll UM. 2003. p53 has a direct apoptogenic role at the mitochondria. *Molecular cell.* **11** (3):577-590.

Mody RS, Carson SD. (1997) Tissue factor cytoplasmic domain peptide is multiply phosphorylated in vitro. *Biochemistry*. **36** (25):7869-7875.

Molostvov G, Morris A, Rose P, Basu S. (2002) Modulation of Bcl-2 family proteins in primary endothelial cells during apoptosis. *Pathophysiology of Haemostasis and Thrombosis*. **32** (2):85-91.

Momand J, Zambetti GP, Olson DC, George D, Levine AJ. (1992) The MDM-2 oncogene product forms a complex with the p53 protein and inhibits p53-mediated transactivation. *Cell.* **69** (7):1237-1245.

Montagut C, Settleman J. (2009) Targeting the RAF-MEK-ERK pathway in cancer therapy. *Cancer letters.* **283** (2):125-134.

Morel O, Ohlmann P, Epailly E, Bakouboula B, Zobairi F, Jesel L, Meyer N, Chenard M-P, Freyssinet J-M, Bareiss P and others. (2008) Endothelial cell activation contributes to the release of procoagulant microparticles during acute cardiac allograft rejection. *Journal of Heart and Lung Transplantation.* **27** (1):38-45.

Morel O, Toti F, Hugel B, Freyssinet JM. (2004) Cellular microparticles: a disseminated storage pool of bioactive vascular effectors. *Current Opinion in Hematology.* **11** (3):156-164.

Morris DR, Ding Y, Ricks TK, Gullapalli A, Wolfe BL, Trejo J. (2006) Protease-activated receptor-2 is essential for factor VIIa and Xa-induced signaling, migration, and invasion of breast cancer cells. *Cancer Research*. **66** (1):307-314.

Morrissey JH, Fakhrai H, Edgington TS. (1987) Molecular-cloning of the cdna for tissue factor, the cellular receptor for the initiation of the coagulation protease cascade. *Cell*. **50** (1):129-135.

Morrissey JH. (2001) Tissue factor: An enzyme cofactor and a true receptor. *Thrombosis and Haemostasis.* **86** (1):66-74.

Mueller BM, Ruf W. (1998) Requirement for binding of catalytically active factor VIIa in tissue factor-dependent experimental metastasis. *Journal of Clinical Investigation.* **101** (7):1372-1378.

Muller I, Klocke A, Alex M, Kotzsch M, Luther T, Morgenstern E, Zieseniss S, Zahler S, Preissner K, Engelmann B. (2003) Intravascular tissue factor initiates coagulation via circulating microvesicles and platelets. *Faseb Journal.* **17** (1):476-+

Murray-Zmijewski F, Slee EA, Lu X. (2008) A complex barcode underlies the heterogeneous response of p53 to stress. *Nat. Rev. Mol. Cell Biol.* **9**:702–712.

Nakano K. Vousden KH. (2001) *PUMA*, a novel proapoptotic gene, is induced by p53. *Mol. Cell.* **7**:683–694

Napoleone E, Di Santo A, Lorenzet R. (1997) Monocytes upregulate endothelial cell expression of tissue factor: a role for cell-cell contact and cross-talk. *Blood.* **89** (2):541-549.

Nawroth PP, Stern DM. (1986) Modulation of endothelial cell hemostatic properties by tumor necrosis factor. *The Journal of experimental medicine.* **163** (3):740-745.

Nieuwland R, Berckmans RJ, McGregor S, Boing AN, Romijn F, Westendorp RGJ, Hack CE, Sturk A. (2000) Cellular origin and procoagulant properties of microparticles in meningococcal sepsis. *Blood.* **95** (3):930-935.

Nieuwland R, Berckmans RJ, Rotteveel-Eijkman RC, Maquelin KN, Roozendaal KJ, Jansen PGM, ten Have K, Eijsman Ln, Hack CE, Sturk A. (1997) Cell-derived microparticles generated in patients during cardiopulmonary bypass are highly procoagulant. *Circulation.* **96** (10):3534-3541.

Noguchi M, Sakai T, Kisiel W. (1989) Correlation between antigenic and functional expression of tissue factor on the surface of cultured human endothelial cells following stimulation by lipopolysaccharide endotoxin. *Thrombosis research.* **55** (1):87-97.

Nomura S, Ozaki Y, Ikeda Y. (2008) Function and role of microparticles in various clinical settings. *Thrombosis research*. **123** (1):8-23.

Norbury CJ, Hickson ID. (2001) Cellular responses to DNA damage. *Annual review of pharmacology and toxicology.* **41** (1):367-401.

Nystedt S, Ramakrishnan V, Sundelin J. (1996) The Proteinase-activated Receptor 2 Is Induced by Inflammatory Mediators in Human Endothelial Cells comparison with the thrombin receptor. *Journal of Biological Chemistry*. **271** (25):14910-14915.

Oda E, Ohki R, Murasawa H, Nemoto J, Shibue T, Yamashita T, Tokino T, Taniguchi T. and Tanaka N. (2000) Noxa, a BH3-only member of the Bcl-2 family and candidate mediator of p53-induced apoptosis. *Science.* **288**:1053–1058.

Oku K, Amengual O, Zigon P, Horita T, Yasuda S, Atsumi T. (2013) Essential role of the p38 mitogen-activated protein kinase pathway in tissue factor gene expression mediated by the phosphatidylserine-dependent antiprothrombin antibody. *Rheumatology.* **52** (10):1775-1784.

Ono K, Han JH. (2000) The p38 signal transduction pathway - Activation and function. *Cellular Signalling*. **12** (1):1-13.

Osterud B, Bjorklid E. (2012) Tissue factor in blood cells and endothelial cells. *Frontiers in bioscience.* (Elite edition) **4**:289-99.

Ott I, Fischer EG, Miyagi Y, Mueller BM, Ruf W. (1998) A role for tissue factor in cell adhesion and migration mediated by interaction with actin-binding protein 280. *The Journal of cell biology.* **140** (5):1241-1253.

Ott I, Weigand B, Michl R, Seitz I, Sabbari-Erfani N, Neumann F-J, Schömig A. (2005) Tissue factor cytoplasmic domain stimulates migration by activation of the GTPase Rac1 and the mitogen-activated protein kinase p38. *Circulation.* **111** (3):349-355.

Paborsky LR, Caras IW, Fisher KL, Gorman CM. (1991) Lipid association, but not the transmembrane domain, is required for tissue factor activity. Substitution of the transmembrane domain with a phosphatidylinositol anchor. *Journal of Biological Chemistry.* **266** (32):21911-21916.

Park JM, Greten FR, Li ZW, Karin M. (2002). Macrophage apoptosis by anthrax lethal factor through p38 MAP kinase inhibition. *Science*. **297** (5589):2048-2051.

Parry GCN, Mackman N. (1995) Transcriptional regulation of tissue factor expression in human endothelial cells. *Arteriosclerosis, thrombosis, and vascular biology.* **15** (5):612-621.

Pavletich NP. (1999) Mechanisms of cyclin-dependent kinase regulation: structures of Cdks, their cyclin activators, and Cip and 1NK4 inhibitors. *J Mol Biol*. **287**:821–829.

Payne DM, Rossomando AJ, Martino P, Erickson AK, Her JH, Shabanowitz J, Hunt DF, Weber MJ, Sturgill TW. (1991) Identification of the regulatory phosphorylation sites in pp42/mitogen-activated protein-kinase (MAP KINASE). *Embo Journal*. **10** (4):885-892.

Pearson G RF, Beer Gibson T, Xu BE, Karandikar M, Berman K. (2001) Mitogen activated protein (MAPK) kinase pathways: regulation and physiological functions. *Endocr Rev.* **22**:153-83.

Peterson DB, Sander T, Kaul S, Wakim BT, Halligan B, Twigger S, Pritchard KA, Jr., Oldham KT, Ou J-S. (2008) Comparative proteomic analysis of PAI-1 and TNF-alpha-derived endothelial microparticles. *Proteomics.* **8** (12):2430-2446.

Petros, AM, Olejniczak ET, Fesik SW. (2004). Structural biology of the Bcl-2 family of proteins. *Biochimica et Biophysica Acta-Molecular Cell Research.* **1644** (2-3):83-94.

Pilzer D, Gasser O, Moskovich O, Schifferli JA, Fishelson Z. (2005) Emission of membrane vesicles: roles in complement resistance, immunity and cancer. *Springer Seminars in Immunopathology*. **27** (3):375-387.

Polyak K, Xia Y, Zweier JL, Kinzler KW, Vogelstein B. (1997) A model for p53-induced apoptosis. *Nature.* **389** (6648):300-305.

Poulsen LK, Jacobsen N, SÃrensen BB, Bergenhem NCH, Kelly JD, Foster DC, Thastrup O, Ezban M, Petersen LC. (1998) Signal transduction via the mitogen-activated protein kinase pathway induced by binding of coagulation factor VIIa to tissue factor. *Journal of Biological Chemistry.* **273** (11):6228-6232.

Pradier A, Ettelaie C. (2008) The influence of exogenous tissue factor on the regulators of proliferation and apoptosis in endothelial cells. *Journal of Vascular Research*. **45** (1):19-32.

Pyo RT, Sato Y, Mackman N, Taubman MB. (2004) Mice deficient in tissue factor demonstrate attenuated intimal hyperplasia in response to vascular injury and decreased smooth muscle cell migration. *Thrombosis and Haemostasis.* **92** (3):451-458.

Raingeaud, J., Joël Gupta, Shashi Rogers, Jeffrey S Dickens, Martin Han, Jiahuai Ulevitch, Richard J Davis, Roger J. (1995) Pro-inflammatory cytokines and environmental stress cause p38 mitogen-activated protein kinase activation by dual phosphorylation on tyrosine and threonine. *Journal of Biological Chemistry*. **270** (13):7420-7426.

Rauch U, Bonderman D, Bohrmann B, Badimon JJ, Himber J, Riederer MA, Nemerson Y. (2000) Transfer of tissue factor from leukocytes to platelets is mediated by CD15 and tissue factor. *Blood*. **96** (1):170-175.

Rautou P-E, Vion A-C, Amabile N, Chironi G, Simon A, Tedgui A, Boulanger CM. (2011) Microparticles, Vascular Function, and Atherothrombosis. *Circulation Research.* **109** (5):593-606.

Ravenhall C, Guida E, Harris T, Koutsoubos V, Stewart A. (2000) The importance of ERK activity in the regulation of cyclin D1 levels and DNA synthesis in human cultured airway smooth muscle. *British journal of pharmacology*. **131** (1):17-28.

Rickles FR, Patierno S, Fernandez PM. (2003) Tissue factor, thrombin, and cancer. *Chest* **124** (3):58S-68S.

Riewald M, Ruf W. (2003) Science review: Role of coagulation protease cascades in sepsis. *Critical Care*. **7** (2):123-129.

Robaye B, Mosselmans R, Fiers W, Dumont JE, Galand P. (1991) Tumor necrosis factor induces apoptosis (programmed cell death) in normal endothelial cells in vitro. *The American journal of pathology*, ***138*** (2), 447.

Rothmeier AS, Ruf W. (2012) Protease-activated receptor 2 signaling in inflammation. *Springer*. p 133-149.

Rouse J, Cohen P, Trigon S, Morange M, Alonso-Llamazares A, Zamanillo D, Hunt T, Nebreda AR. (1994) A novel kinase cascade triggered by stress and heat shock that stimulates MAPKAP kinase-2 and phosphorylation of the small heat shock proteins. *Cell*. **78** (6):1027-1037.

Ruf W. (1999) Tissue factor signaling in hemostasis. *Blood.* **94** (10):54-55.

Ryden L, Grabau D, Schaffner F, Jonsson P-E, Ruf W, Belting M. (2010) Evidence for tissue factor phosphorylation and its correlation with protease-activated receptor expression and the prognosis of primary breast cancer. *International Journal of Cancer*. **126** (10):2330-2340.

Sabatier F, Camoin-Jau L, Anfosso F, Sampol J, Dignat-George F. (2009) Circulating endothelial cells, microparticles and progenitors: key players towards the definition of vascular competence. *Journal of Cellular and Molecular Medicine.* **13** (3):454-471.

Sabatier F, Darmon P, Hugel B, Combes V, Sanmarco M, Velut JG, Arnoux D, Charpiot P, Freyssinet JM, Oliver C and others. (2002) Type 1 and type 2 diabetic patients display different patterns of cellular microparticles. *Diabetes*. **51** (9):2840-2845.

Saito S, Yamaguchi H, Higashimoto Y, Chao C, Xu Y, Fornace AJ, Appella E, Anderson CW. (2003) Phosphorylation site interdependence of human p53 post-translational modifications in response to stress. *Journal of Biological Chemistry*. **278** (39):37536-37544.

Sakabe K, Teramoto H, Zohar M, Behbahani B, Miyazaki H, Chikumi H, Gutkind JS. (2002) Potent transforming activity of the small GTP-binding protein Rit in NIH 3T3 cells: evidence for a role of a p38 gamma-dependent signaling pathway. *Febs Letters.* **511** (1-3):15-20.

Sanchez-Prieto R, Rojas JM, Taya Y, Gutkind JS. (2000). A role for the p38 mitogen-activated protein kinase pathway in the transcriptional activation of p53 on genotoxic stress by chemotherapeutic agents. *Cancer Research*. **60** (9):2464-2472.

Sax JK, Fei P, Murphy ME, Bernhard E, Korsmeyer SJ, El-Deiry WS. (2002) BID regulation by p53 contributes to chemosensitivity. *Nat. Cell Biol.* **4**:842–849.

Schecter AD, Spirn B, Rossikhina M, Giesen PLA, Bogdanov V, Fallon JT, Fisher EA, Schnapp LM, Nemerson Y, Taubman MB. (2004) Release of active tissue factor by human arterial smooth muscle cells. *Circulation Research.* **87** (2):126-132.

Scholz T, Temmler U, Krause S, Heptinstall S, Losche W. (2002) Transfer of tissue factor from platelets to monocytes: Role of platelet-derived microvesicles and CD62P. *Thrombosis and Haemostasis.* **88** (6):1033-1038.

Schuler M, Green DR. (2001) Mechanisms of p53-dependent apoptosis. *Biochemical Society Transactions.* **29** (6):684-687.

Scorrano L, Ashiya M, Buttle K, Weiler S, Oakes SA, Mannella CA, Korsmeyer SJ. (2002). A distinct pathway remodels mitochondrial cristae and mobilizes cytochrome c during apoptosis. Developmental. *Cell.* **2** (1):55-67.

Shaul YD, Seger R. (2007) The MEK/ERK cascade: From signaling specificity to diverse functions. *Biochimica et Biophysica Acta-Molecular Cell Research*. **1773** (8):1213-1226.

Sherr CJ. (1994). G1 phase progression: cycling on cue. *Cell.* **79**:551-555.

Shet AS. (2008) Characterizing blood microparticles: technical aspects and challenges. *Vascular health and risk management*. **4** (4):769-74.

Shet AS, Aras O, Gupta K, Hass MJ, Rausch DJ, Saba N, Koopmeiners L, Key NS, Hebbel RP. 2003. Sickle blood contains tissue factor-positive microparticles derived from endothelial cells and monocytes. *Blood*. **102** (7):2678-2683.

Siegbahn A. (2004) Cellular consequences upon factor VIIa binding to tissue factor. *Pathophysiology of Haemostasis and Thrombosis*. **30** (Suppl. 2): 41-47.

Siegbahn A, Johnell M, Sorensen BB, Petersen LC, Heldin C-H. (2005) Regulation of chemotaxis by the cytoplasmic domain of tissue factor. *Thrombosis and Haemostasis.* **93** (1):27-34.

Simak J, Gelderman MP, Yu H, Wright V, Baird AE. (2006) Circulating endothelial microparticles in acute ischemic stroke: a link to severity, lesion volume and outcome. *Journal of Thrombosis and Haemostasis.* **4** (6):1296-1302.

Spyridopoulos I, Andres V. (1998) Control of vascular smooth muscle and endothelial cell proliferation and its implication in cardiovascular disease. *Frontiers in Bioscience* **3**: 269-287.

Steffel J, Hermann M, Greutert H, Gay S, Luscher TF, Ruschitzka F, Tanner FC. (2005) Celecoxib decreases endothelial tissue factor expression through inhibition of c-jun terminal NH2 kinase phosphorylation. *Circulation*. **111** (13):1685-1689.

Sun H, Charles CH, Lau LF, Tonks NK. (1993) MKP-1 (3CH134), an immediate-early gene-product, is a dual-specificity phosphatase that dephosphorylates map kinase in-vivo. *Cell.* **75** (3):487-493.

Sun SY, Hail N, Lotan R. (2004). Apoptosis as a novel target for cancer chemoprevention. *Journal of the National Cancer Institute.* **96** (9):662-672.

Takekawa M, Adachi M, Nakahata A, Nakayama I, Itoh F, Tsukuda H, Taya Y, Imai K. (2000) p53-inducible Wip1 phosphatase mediates a negative feedback regulation of p38 MAPK-p53 signaling in response to UV radiation. *The EMBO journal.* **19** (23):6517-6526.

Tanoue T, Adachi M, Moriguchi T, Nishida E. (2000) A conserved docking motif in MAP kinases common to substrates, activators and regulators. *Nature Cell Biology*. **2** (2):110-116.

Taubman MB, Fallon JT, Schecter AD, Giesen P, Mendlowitz M, Fyfe BS, Marmur JD, Nemerson Y. (1997) Tissue factor in the pathogenesis of atherosclerosis. *Thrombosis and Haemostasis.* **78** (1):200-204.

Tormos AM, TalÃ©ns-Visconti R, Nebreda AR, Sastre J. (2013) p38 MAPK: A dual role in hepatocyte proliferation through reactive oxygen species. *Free radical research.* **47** (11):905-916.

Toshiyuki M, Reed JC. (1995) Tumor suppressor p53 is a direct transcriptional activator of the human bax gene. *Cell.* **80** (2):293-299.

Tremoli E, Camera M, Toschi V, Colli S. (1999) Tissue factor in atherosclerosis. *Atherosclerosis.* **144** (2):273-283.

Tseng J-C, Chang L-C, Jiang B-Y, Liu Y-C, Chen H-J, Yu C-T, Hua C-C. (2014) Elevated circulating levels of tissue factor-positive microvesicles are associated with distant metastasis in lung cancer. *Journal of cancer research and clinical oncology*. **140** (1):61-67.

Tuder RM, Abman SH, Braun T, Capron Fdr, Stevens T, Thistlethwaite PA, Haworth SG. (2009) Development and pathology of pulmonary hypertension. *Journal of the American College of Cardiology*. **54** (1):S3-S9.

Ubeda M, Habener JF. (2003) CHOP transcription factor phosphorylation by casein kinase 2 inhibits transcriptional activation. *Journal of Biological Chemistry*. **278** (42):40514-40520.

Ueda K, Arakawa H, Nakamura Y. (2003.) Dual-specificity phosphatase 5 (DUSP5) as a direct transcriptional target of tumor suppressor p53. *Oncogene.* **22** (36):5586-5591.

Valladares, A., Alvarez, A. M., Ventura, S. J., Roncero, C., Benito, M., Porras, A. (2000) p38 mitogen-activated protein kinase mediates tumor necrosis factor-alpha-induced apoptosis in rat fetal brown adipocytes. *Endocrinology.* **141** (12):4383-4395.

Vega-Ostertag M, Casper K, Swerlick R, Ferrara D, Harris EN, Pierangeli SS. (2005) Involvement of p38 MAPK in the up-regulation of tissue factor on endothelial cells by antiphospholipid antibodies. *Arthritis and Rheumatism.* **52** (5):1545-1554.

Vergnolle N, Hollenberg MD, Sharkey KA, Wallace JL. (1999) Characterization of the inflammatory response to proteinase-activated receptor-2 (PAR(2))-activating peptides in the rat paw. *British Journal of Pharmacology*. **127** (5):1083-1090.

Versteeg HH, Hoedemaeker I, Diks SH, Stam JC, Spaargaren M, en Henegouwen PMPvB, van Deventer SJH, Peppelenbosch MP. (2000) Factor VIIa/tissue factor-induced signaling via activation of Src-like kinases, phosphatidylinositol 3-kinase, and Rac. *Journal of Biological Chemistry*. **275** (37):28750-28756.

Versteeg H, Ruf W. (2006) Emerging insights in tissue factor-dependent signaling events. *Seminars in Thrombosis and Hemostasis.* **32** (1):24-32.

Vousden KH. (2000) p53: Death star. *Cell.* **103** (5):691-694.

Vousden KH. (2005) p53 and PUMA: A deadly duo. *Science*. **309** (5741):1685-1686.

Walker KK, Levine AJ. (1996) Identification of a novel p53 functional domain that is necessary for efficient growth suppression. *Proceedings of the National Academy of Sciences*. **93** (26):15335-15340.

Wang X, Lau C, Wiehler S, Pow A, Mazzulli T, Gutierrez C, Proud D, Chow C-W. (2006) Syk is downstream of intercellular adhesion molecule-1 and mediates human rhinovirus activation of p38 MAPK in airway epithelial cells. *Journal of Immunology*. **177** (10):6859-6870.

Wang, X, Ron D. (1996) Stress-induced phosphorylation and activation of the transcription factor CHOP (GADD153) by p38 MAP kinase. *Science.* **272** (5266):1347-1349.

Whelan, RS, Kaplinskiy V, Kitsis RN. (2010) Cell Death in the Pathogenesis of Heart Disease: Mechanisms and Significance. Annual Review of Physiology. **72:**19-44.

Widlansky ME, Gokce N, Keaney JF, Vita JA. (2003) The clinical implications of endothelial dysfunction. *Journal of the American College of Cardiology*. **42** (7):1149-1160.

Wilcox JN, et al. (1989) Localization of tissue factor in the normal vessel wall and in the atherosclerotic plaque. *Proceedings of the National Academy of Sciences.* **86** (8):2839-2843.

Yang YL, Li CCH, Weissman AM. (2004) Regulating the p53 system through ubiquitination. *Oncogene.* **23** (11):2096-2106.

Yin YX, Liu YX, Jin YJ, Hall EJ, Barrett JC. (2003) PAC1 phosphatase is a transcription target of p53 in signalling apoptosis and growth suppression. *Nature.* **422** (6931):527-531.

Yoshida K, Liu HS, Miki Y. (2006) Protein kinase C delta regulates Ser(46) phosphorylation of p53 tumor suppressor in the apoptotic response to DNA damage. *Journal of Biological Chemistry.* **281** (9):5734-5740.

Yu JL, Rak JW. (2004) Shedding of tissue factor (TF)-containing microparticles rather than alternatively spliced TF is the main source of TF activity released from human cancer cells. *Journal of Thrombosis and Haemostasis*. **2** (11):2065-2067.

Zacchi P, Gostissa M, Uchida T, Salvagno C, Avolio F, Volinia S, Ronai Ze, Blandino G, Schneider C, Del Sal G. (2002) The prolyl isomerase Pin1 reveals a mechanism to control p53 functions after genotoxic insults. *Nature.* **419** (6909):853-857.

Zechner D, Craig R, Hanford DS, McDonough PM, Sabbadini RA, Glembotski CC. (1998) MKK6 activates myocardial cell NF-kappa B and inhibits apoptosis in a p38 mitogen-activated protein kinase-dependent manner. *Journal of Biological Chemistry*. **273** (14):8232-8239.

Zhang S, Han J, Sells MA, Chernoff J, Knaus UG, Ulevitch RJ, Bokoch GM. (1995). Rho family GTPases regulate p38 mitogen-activated protein kinase through the downstream mediator Pak1. *Journal of Biological Chemistry*. **270** (41):23934-23936.

Zheng H, You H, Zhou XZ, Murray SA, Uchida T, Wulf G, Gu L, Tang X, Lu KP, Xiao Z-XJ. (2002) The prolyl isomerase Pin1 is a regulator of p53 in genotoxic response. *Nature.* **419** (6909):849-853.

Zhu T, Lobie PE. (2000) Janus kinase 2-dependent activation of p38 mitogen-activated protein kinase by growth hormone Resultant transcriptional activation of ATF-2 and CHOP, cytoskeletal re-organization and mitogenesis. *Journal of Biological Chemistry*. **275** (3):2103-2114.

Zioncheck TF, Roy S, Vehar GA. (1992) The cytoplasmic domain of tissue factor is phosphorylated by a protein kinase-c-dependent mechanism. *Journal of Biological Chemistry*. **267** (6):3561-3564.

Zwaal RFA, Schroit AJ. 1997. Pathophysiologic implications of membrane phospholipid asymmetry in blood cells. *Blood*. **89** (4):1121-1132.